Ehsan Houshfar

Experimental and Numerical Studies on Two-Stage Combustion of Biomass

Thesis for the degree of Philosophiae Doctor

Trondheim, June 2012

Norwegian University of Science and Technology
Faculty of Engineering Science and Technology
Department of Energy and Process Engineering

NTNU – Trondheim
Norwegian University of
Science and Technology

NTNU
Norwegian University of Science and Technology

Thesis for the degree of Philosophiae Doctor

Faculty of Engineering Science and Technology
Department of Energy and Process Engineering

ISBN 978-82-471-3449-8 (printed ver.)
ISBN 978-82-471-3450-4 (electronic ver.)
ISSN 1503-8181

Doctoral theses at NTNU, 2012:87

Printed by NTNU-trykk

This thesis is dedicated to
my parents,
my wife, Atefeh,
and my daughter, Hania,
for their love, endless support
and encouragement during this work.

Abstract

In this thesis, two-stage combustion of biomass was experimentally/numerically investigated in a multifuel reactor. The following emissions issues have been the main focus of the work:

1- NO_x and N_2O

2- Unburnt species (CO and C_xH_y)

3- Corrosion related emissions

The study had a focus on two-stage combustion in order to reduce pollutant emissions (primarily NO_x emissions). It is well known that pollutant emissions are very dependent on the process conditions such as temperature, reactant concentrations and residence times. On the other hand, emissions are also dependent on the fuel properties (moisture content, volatiles, alkali content, etc.). A detailed study of the important parameters with suitable biomass fuels in order to optimize the various process conditions was performed.

Different experimental studies were carried out on biomass fuels in order to study the effect of fuel properties and combustion parameters on pollutant emissions. Process conditions typical for biomass combustion processes were studied. Advanced experimental equipment was used in these studies. The experiments showed the effects of staged air combustion, compared to non-staged combustion, on the emission levels clearly. A NO_x reduction of up to 85% was reached with staged air combustion using demolition wood as fuel. An optimum primary excess air ratio of 0.8−0.95 was found as a minimizing parameter for the NO_x emissions for staged air combustion. Air staging had, however, a negative effect on N_2O emissions. Even though the trends showed a very small reduction in the NO_x level as temperature increased for non-staged combustion, the effect of temperature was not significant for NO_x and C_xH_y, neither in staged air combustion or non-staged combustion, while it had a great influence on the N_2O and CO emissions, with decreasing levels with increasing temperature. Furthermore, flue gas recirculation (FGR) was used in combination with staged combustion to obtain an enhanced NO_x reduction.

The fate of the main corrosive compounds, in particular chlorine, was determined in an experimental campaign using fuel mixtures. The corrosion risk associated with three fuel mixtures was quite different. Grot (Norwegian term used for tree's tops and branches) was found to be a poor corrosion-reduction additive and could not serve as an alternative fuel for co-firing with straw. Peat was found to reduce the corrosive compounds only at high peat additions (50 wt%). Sewage sludge was the best alternative for corrosion reduction as 10 wt% addition almost eliminated chlorine from the fly ash.

Numerical studies were also performed to estimate the emission level in the flue gas using a comprehensive mechanism in a configuration which simulated two-stage combustion of biomass. Furthermore, a reduction of the comprehensive chemical mechanism was performed since the mechanism is still complex and needs very long computational time and powerful hardware resources. The selected detailed mechanism in this study contains 81 species and 703 elementary reactions. Necessity analysis was used to determine which species and reactions that are of less importance for the predictability of the final result and, hence, can be discarded. For validation, numerical results using the derived reduced mechanism were compared with the results obtained with the original detailed mechanism. The reduced mechanism contains 35 species and 198 reactions, corresponding to 72% reduction in the number of reactions and, therefore, improving the computational time considerably. Yet the model based on the reduced mechanism predicts correctly concentrations of NO_x and CO that are essentially identical to those of the complete mechanism in the range of reaction conditions of interest. The modeling conditions are selected in a way to mimic values in the different ranges of temperature, excess air ratio and residence time, since these variables are the main affecting parameters on NO_x emission.

Preface

This thesis is submitted to the Norwegian University of Science and Technology (NTNU) for partial fulfillment of the requirements for the degree of philosophiae doctor.

This doctoral work has been performed at the Department of Energy and Process Engineering, NTNU, Trondheim, with Prof. Terese Løvås as main supervisor and with co-supervisor Dr. Øyvind Skreiberg.

This doctoral work was performed as part of the KRAV project (Enabling Small Scale Biomass CHP in Norway) financed by The Research Council of Norway, SINTEF Energy Research, Agder Energi, Eidsiva Bioenergi, Solør Bioenergi Holding, Statkraft Varme (former Trondheim Energi Fjernvarme), and Vardar. Some parts of this research work were also performed under the financial support of the Bioenergy Innovation Centre (CenBio), which is funded by the Research Council of Norway, a number of industry partners, and 7 R&D institutes.

Author's Contribution

The papers are co-authored. The author of the thesis has performed the following work for the presented papers:

Paper I. Performing the experiments, fuel analysis, calibration, data collection, data treatment and analysis (except for ELPI measurements), writing paper with interpretation of the results and discussion.

Paper II. Performing the experiments, calibration, data collection, data treatment of the experimental results and analysis, writing paper with interpretation of the results and discussion.

Paper III. Participating in performing the experiments, data treatment and analysis, co-authoring the paper and revision of the paper with interpretation of the results and discussion.

Paper IV. Performing the experiments, calibration, data collection, data treatment and analysis, writing paper with interpretation of the results and discussion.

Paper V. Performing the experiments, fuel analysis, calibration, data collection, data treatment and analysis, writing paper with interpretation of the results and discussion.

Paper VI. Modeling, data treatment, analysis and writing paper with interpretation of the results and discussion.

Paper VII. Modeling, data treatment, analysis and writing paper with interpretation of the results and discussion, presented the paper at the 18th European Biomass Conference and Exhibition 2010 in Lyon, France.

Paper VIII. Performing the experiments, sampling device calibration, data treatment and analysis, co-authoring the paper and revision of the paper with interpretation of the results and discussion.

Paper IX. Co-writing the paper and revision of the paper, participate on the modeling.

The contribution of co-authors in papers I-VII was mainly in the form of supervising and quality control of the papers. Wilson Musinguzi and Franziska Goile were participating on the experimental setup for Paper I and VIII. Dušan Todorović and Alexandra Skreiberg were helping to perform the experiments for Paper III. Paper VIII writing part is performed jointly with Roger Khalil. The last paper is mainly written by Michaël Becidan.

Acknowledgements

I want first to thank my main supervisor, Professor Terese Løvås, for all the hope she has put on me. She has always encouraged me. She has enlightened me through her wide knowledge of combustion and chemical mechanisms and her deep intuitions about where it should go and what is necessary to get there. It was a great pleasure for me to conduct this thesis under her supervision.

I also want to thank warmly my co-supervisor, Dr. Øyvind Skreiberg, for all the delightful discussions and for sharing his vast knowledge of research work. He has taught me how good experimental combustion work is done. I appreciate all his contributions of time, ideas, and funding to make my PhD experience productive and stimulating.

I thank Professor Johan Einar Hustad for giving me the opportunity to start my PhD at NTNU. Thanks also to Professor Ivar Ståle Ertesvåg for his lectures in 2009, which gave me tools that turned out to be essential in my research. Thanks also to Roger A. Khalil, Willy G. Horrigmo, Dušan Todorović, Judit Sandquist, and Michaël Becidan for their contribution to different parts of this thesis.

I would also like to thank my office-mates and colleagues from the Department of Energy and Process Engineering; Behrouz, Hamid, Dhruv, Dhandapani, Amlaku, and Alexis. In addition, I thank the administrative staff in our department for being so helpful.

Thanks also to my family in Tabas-Iran, especially my mother and my father.

Last but not least, I wish to express my special appreciation to my wife, Atefeh. Without her I would be a very different person today, and it would have been certainly much harder to finish a PhD. I thank her for spiritual support and her patience in taking care of our daughter, Hania.

Trondheim, Norway

June 2012

Ehsan Houshfar

Table of Contents

List of Figures

List of Tables

Nomenclature

Latin letters

A_R	Arrhenius coefficient
B_i	Binary value for necessity of species i (0 or 1)
c_i	Concentration of species i
$c^a_{i,j}$	Flow rate of element a by consumption from species i to species j
I_i	Necessity of species i
$I_{i,0}$	Initial necessity value
N_a	Number of atoms
N_R	Total number of reactions involving element a
N_s	Number of species
n^a_i	Number of a atoms in species i
$p^a_{i,j}$	Flow rate of element a by production of species i from species j
R	Reaction number
$r_R(t)$	Reaction rate
S^r	Sensitivity of reaction
S^s	Sensitivity of species
$S^s_{j,i}$	Species sensitivity of species i
t	Time
t_f	Final reaction time
v'_{iR}	Left hand side coefficient of species i in reaction R
v''_{iR}	Right hand side coefficient of species i in reaction R
Y	Target variable

Greek letters

α_i	Error term for species concentration
Δn^a_R	Total flow of atom a in reaction R
λ	Excess air ratio
ω_i	Concentration source term for species i
φ	Equivalence ratio

Abbreviations

AS	Air staging
BFB	Bubbling fluidized bed
CCS	Carbon capture and storage
CEMS	Continuous emissions monitoring system
CFB	Circulating fluidized bed
CFD	Computational fluid dynamics
CHP	Combined heat and power
CS	Combined staged
CW	Coffee waste
DME	Dimethyl ether
DW	Demolition wood
ELPI	Electrical low pressure impactor
FB	Fluidized bed
FC	Fixed carbon
FGR	Flue gas recirculation
FS	Fuel staging
FTIR	Fourier Transform Infra-Red
GC	Gas chromatograph
GDP	Gross domestic products
GG	Branches and tops (grot)
GHG	Greenhouse gas
HHV	High heating value
IC	Internal combustion
IEA	International Energy Agency
IPCC	Intergovernmental Panel on Climate Change
LCA	Life cycle assessment
LPG	Liquefied petroleum gas
MSW	Municipal solid waste
NDIR	Non-dispersive infrared
NO_x	Nitrogen oxides ($NO+NO_2$)
PAH	Polycyclic aromatic hydrocarbons

PCCD	Polychlorinated dibenzo-p-dioxins
PCDF	Polychlorinated dibenzofurans
PFR	Plug flow reactor
PLS	Partial least square
PM	Particulate matter
PSR	Perfectly stirred reactor
SCR	Selective catalytic reduction
SNCR	Selective non-catalytic reduction
SS	Sewage sludge
TCD	Thermal conductivity detectors
TFN	Total fixed nitrogen
UNDP	United Nations Development Programme
VM	Volatile matters
WCOT	Wall-coated open-tubular
WEC	World Energy Council
WGS	Water-gas-shift
WP	Wood pellets

Chapter 1

Overview of the Thesis

This chapter provides an introduction to the research work presented in this thesis. It begins with a description of the research background and explains the motivation for pursuing this work. In addition, it provides an overview of the approach taken as well as of the results obtained. Finally, it introduces the structure of the thesis and a list of publications.

1.1 Motivation and methodology

Since 1950, world population has more than doubled and is believed to increase by 40% by 2050 [Royal Dutch Shell plc 2008]. It is also known that increase in population and GDP will directly affect energy demand, i.e. more population and GDP, more energy needed. Therefore, the world needs more energy resources while at the same time environmental problems should be resolved in the energy production systems.

On the other hand, global warming as a result of carbon dioxide release to the atmosphere caused considerable interest to investigate renewable energies instead of using fossil fuels. One of the most interesting energy carriers in this regard is solid biomass

fuels, as a comparably quick response to the problem, while nuclear and solar energy are more long term solutions.

However, the combustion of biomass is associated with some environmental problems such as nitrogen oxides emissions (NO_x=NO+NO_2), nitrous oxide (N_2O), ash related problems, PAH, etc. NO_x emissions, which are one of the main reasons of acid rain, photochemical smog, global warming and depletion of stratospheric ozone, should be studied carefully in order to be lowered.

The main contribution of this thesis is the application of two-stage combustion of biomass in a one of a kind multifuel reactor in order to study the effects on two important processes; 1) NO_x and N_2O formation and reduction, 2) ash related issues in biomass fired boilers. This has been done by identification of the optimal combustion process variables to minimize NO_x formation; and reduce ash deposition and corrosion on boiler tubes by selection of the best fuel mixtures. Advanced measurement and sampling devices were used to monitor the mentioned emissions.

For the NO_x reduction case, as the main focus of this work, different operational conditions and a wide range of biomass fuels were studied. Fuels with very low nitrogen content, e.g. wood, and fuels with high nitrogen content, like sewage sludge, were pelletized and fed to the reactor in original type or mixed with each other. Excess air ratio was optimized to reach a minimum NO_x emission. Temperature was also varied in the desired range of industrial plants. The effect of fuel mixtures on corrosion related problems and alkali release was also studied simultaneously. Implementation of the obtained optimum parameters is recommended in practice.

An idealized model of the case was also simulated using ideal reactors in DARS©. The effects of temperature, residence time and excess air ratio were studied. Finally, a reduced mechanism was developed from the detailed chemistry by means of necessity analysis which combines sensitivity analysis and reaction flow analysis.

1.2 Thesis organization

An introduction to the subject is given in Chapter 2. Biomass, conversion processes, emissions and other environmental problems are briefly described. In addition, NO_x emissions and techniques for reduction of pollutants, especially NO_x, are introduced.

A critical and extensive literature review is included in Chapter 3 to support the work.

In Chapter 4, the experimental section of the thesis, including the multifuel reactor setup, test procedure, fuels composition, experimental matrix, and sampling devices are described in detail. Pellet preparation and blending are also described in this chapter. The experiments are presented in two parts: NO_x reduction and corrosion abatement.

Chapter 5 contains a brief introduction to the modeling part of the thesis. The model for two-stage combustion is described in more detail. The mechanism reduction methods, particularly necessity analysis, are introduced and the conditions, under which the mechanisms were developed, are introduced.

In the last chapter (Chapter 6), conclusions of the thesis and recommendations for future work are given.

1.3 Publications

1.3.1 Journal publications

1. **Ehsan Houshfar**, Judit Sandquist, Wilson Musinguzi, Roger Antoine Khalil, Michaël Becidan, Øyvind Skreiberg, Franziska Goile, Terese Løvås, Lars Sørum.
   COMBUSTION PROPERTIES OF NORWEGIAN BIOMASS: WOOD CHIPS AND FOREST RESIDUES.
   Applied Mechanics and Materials, 110−116, pp. 4564−4568, 2012.
   [DOI: 10.4028/www.scientific.net/AMM.110-116.4564]

2. **Ehsan Houshfar**, Øyvind Skreiberg, Terese Løvås, Dušan Todorović, Lars Sørum.
   EFFECT OF EXCESS AIR RATIO AND TEMPERATURE ON NO_x EMISSION FROM GRATE COMBUSTION OF BIOMASS IN THE STAGED AIR COMBUSTION SCENARIO.
   Energy & Fuels, 25 (10), pp. 4643–4654, 2011.
   [DOI: 10.1021/ef200714d]

3. **Ehsan Houshfar**, Øyvind Skreiberg, Dušan Todorović, Alexandra Skreiberg, Terese Løvås, Aleksandar Jović, Lars Sørum.
   NO_x EMISSION REDUCTION BY STAGED COMBUSTION IN GRATE COMBUSTION OF BIOMASS FUELS AND FUEL MIXTURES.
   Fuel, In Press, 2012.
   [DOI: 10.1016/j.fuel.2012.03.044]

4. **Ehsan Houshfar**, Terese Løvås, Øyvind Skreiberg.
   EXPERIMENTAL INVESTIGATION ON NO_x REDUCTION BY PRIMARY MEASURES IN BIOMASS COMBUSTION: STRAW, PEAT, SEWAGE SLUDGE, FOREST RESIDUES, AND WOOD PELLETS
   Energies, 5 (2), pp. 270−290, 2012.
   [DOI: 10.3390/en5020270]

5. **Ehsan Houshfar**, Roger Antoine Khalil, Terese Løvås, Øyvind Skreiberg.
ENHANCED NO_x REDUCTION BY COMBINED STAGED AIR AND FLUE GAS RECIRCULATION IN BIOMASS GRATE COMBUSTION.
Energy & Fuels, 26 (5), pp. 3003–3011, 2012.
[DOI: 10.1021/ef300199g]

6. **Ehsan Houshfar**, Øyvind Skreiberg, Peter Glarborg, Terese Løvås.
REDUCED CHEMICAL KINETICS MECHANISMS FOR NO_x EMISSION PREDICTION IN BIOMASS COMBUSTION.
International Journal of Chemical Kinetics, 44 (4), pp. 219–231, 2012.
[DOI: 10.1002/kin.20716]

7. Roger Antoine Khalil, **Ehsan Houshfar**, Wilson Musinguzi, Michaël Becidan, Øyvind Skreiberg, Franziska Goile, Terese Løvås, Lars Sørum.
EXPERIMENTAL INVESTIGATION ON CORROSION ABATEMENT IN STRAW COMBUSTION BY FUEL-MIXING.
Energy & Fuels, 25 (6), pp. 2687–2695, 2011.
[DOI: 10.1021/ef200232r]

8. Michaël Becidan, **Ehsan Houshfar**, Roger Antoine Khalil, Øyvind Skreiberg, Terese Løvås, Lars Sørum.
OPTIMAL MIXTURES TO REDUCE THE FORMATION OF CORROSIVE COMPOUNDS DURING STRAW COMBUSTION: A THERMODYNAMIC ANALYSIS.
Energy & Fuels, 25 (7), pp. 3223–3234, 2011.
[DOI: 10.1021/ef2002475]

1.3.2 Conference papers

1. **Ehsan Houshfar**, Terese Løvås, Øyvind Skreiberg.
DETAILED CHEMICAL KINETICS MODELING OF NO_x REDUCTION IN COMBINED STAGED FUEL AND STAGED AIR COMBUSTION OF BIOMASS.
18th European Biomass Conference & Exhibition (EU BC&E), Lyon, France, May 3−7, 2010.
[DOI: 10.5071/18thEUBCE2010-VP2.4.4]

2. **Ehsan Houshfar**, Øyvind Skreiberg, Peter Glarborg, Terese Løvås.
A REDUCED CHEMICAL KINETICS MECHANISM FOR NO_x EMISSION PREDICTION IN BIOMASS COMBUSTION.
7th International Conference on Chemical Kinetics (ICCK 2011), MIT, Cambridge, Massachusetts, USA, July 10−14, 2011.

1.3.3 Conference presentations

1. **Ehsan Houshfar**, Øyvind Skreiberg, Terese Løvås.
   EMISSION CONTROL THROUGH PRIMARY MEASURES IN BIOMASS COMBUSTION.
   The Renewable Energy Research Conference (RERC 2010), Trondheim, Norway, June 7−8, 2010.

2. **Ehsan Houshfar**, Terese Løvås, Øyvind Skreiberg.
   TWO STAGE COMBUSTION OF BIOMASS AND THE EFFECTS ON NO_x EMISSIONS.
   The CenBio Days, January 17−18, 2011, Trondheim, Norway.

3. **Ehsan Houshfar**, Øyvind Skreiberg, Terese Løvås.
   NO_x EMISSION REDUCTION BY STAGED COMBUSTION IN A GRATE FIRED MULTI-FUEL REACTOR.
   General Section Meeting of the Scandinavian-Nordic Section of the Combustion Institute (SNCI 2011), Trondheim, 28−29 November, 2011.

Chapter 2

Introduction

2.1 Background

There is an increasing demand for energy production and energy consumers want it to be secure and affordable, while at the same time the energy producer should think about climate change. This is one of the greatest challenges in the world for the 21st century, and is called the energy challenge. According to different studies, almost a third of the world population do not have access to a clean and convenient energy service, while the population growth and need for more energy due to development, will make the case worse, as shown in Figure 2-1 [UNDP 2000]. This figure shows that the global population is expected to be doubled by 2100. Hence, supplying a reliable and sustainable energy is essential for global growth and development in the coming decades. The three scenarios shown in Figure 2-1 are known as Case A, B, and C. Case A is a scenario with high economic growth throughout the world. A middle-course reference case (B) is based on the direction in which the world is headed. Case C is the ecologically driven scenario with high growth in developing countries (towards being rich and 'green'). Driving forces for energy production are supply security, demand pressure, environmental problems, and political issues. According to the mentioned concerns, the World Energy Council introduced 3-A's for the future energy policy [WEC 2007]:

- *Accessibility* to modern and affordable energy for all;

- *Availability* in terms of continuity of supply and quality and reliability of service;
- *Acceptability* in terms of social and environmental goals.

The increasing demand for energy in the world increases the consumption of fuels. As a result, access to the conventional fossil fuels is becoming more and more difficult and an increasing trend for the price of oil would be a disaster for the economic recovery. The peaks in oil price are generally related to the countries' concern for energy availability. Apart from economic aspects, the main problem is that fossil fuels are non-renewable. They are limited in supply and will one day be depleted.

The global interest in "alternative energy" or "renewable energy" sources is due to the mentioned problems in addition to the environmental issues of fossil fuels. Alternative energy is basically a type of energy produced from a source other than our conventional fossil fuels, i.e., oil, natural gas, and coal. Renewable energy is by now known as: solar energy, wind power, bioenergy, tidal and wave power, geothermal energy, and hydropower. Hence, not all alternative energy sources are renewable.

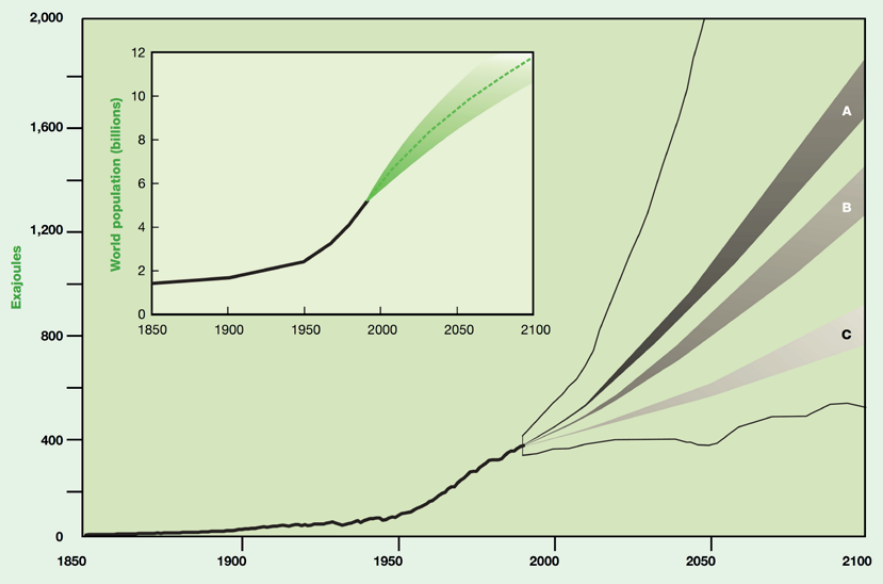

FIGURE 2-1: World population growth and global primary energy requirements (three scenarios).

According to the IEA's world energy outlook, the total energy consumption in the world will increase by a rate of 1.5% per year until 2030. Figure 2-2 shows the share of different types of energy resources in this scenario [IEA report 2009]. Fossil fuels such as coal, oil and gas produce huge amounts of CO_2, the major greenhouse gas, when they are

used in electricity or heat production processes. The best alternative energy resources to replace the fossil fuels are renewable energy carriers such as zero-carbon fuels. When renewable energy sources are used to produce heat and power they produce little or no carbon dioxide. For this reason they are often referred to as being 'zero carbon'. Nuclear power is another zero carbon source of electricity, but it is not a source of renewable energy as there are finite resources of the uranium and plutonium that are used as the fuel. Figure 2-2 demonstrates that in the IEA scenario, the demand for fossil fuels peaks by 2020, and zero-carbon fuels make up a third of the world's primary sources of energy by 2030. Biomass, which already has a large percentage of the total renewable energy sources, is expected to have a strong growth in the coming decades within three key sectors: heat and power generation, transportation biofuels, and other bio-products.

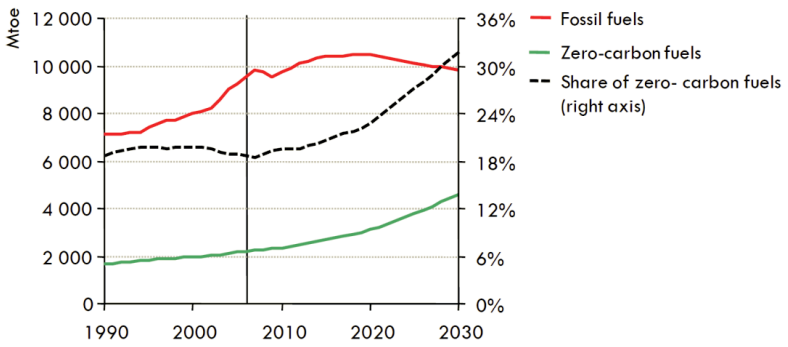

Figure 2-2: World primary energy demand by fuel type [IEA report 2009].

The term “bioenergy” is generally used for the energy extracted from biomass resources for the industrial or residential applications, or the extracted liquid fuel, biofuel, to be used in the transportation sector.

2.2 What is biomass?

Biomass is a collective term used for materials obtained from plant sources or biological materials. It should be noted that fossil fuels such as coal, oil and natural gas are also derived from biological materials; however, these materials absorbed CO_2 from the atmosphere many millions of years ago. Therefore, the difference between biomass and e.g. coal comes from the formation time scale, and this is the reason why some fuels, e.g. peat, are hardly regarded as biomass since they are formed in a medium time scale, in between biomass formation and fossil fuels formation.

Biomass is a carbon based fuel and contains mainly carbon, hydrogen, and oxygen. Small amounts of nitrogen, sulphur, alkali, chlorine, and heavy metals can also be found in the biomass structure. Commonly, the rough chemical formula of biomass is CH_mO_n, where m $\approx$1.2−1.7 and n$\approx$0.5−0.7, typically. Since the term biomass covers an extremely broad range of materials, different characteristics and behaviour are also expected for different types.

Environmentally, biomass fuels are known as almost CO_2-neutral, even though in the conversion process, the carbon will be converted mainly to CO_2. It is known that many issues should be considered in order to call a fuel CO_2 neutral. However, for biomass, many LCA assessments show that biomass can be regarded as an almost CO_2-neutral fuel. The reason is that the carbon cycle for plants is a closed cycle and there is no net addition to the carbon cycle and the total free carbon is constant in the process. The released carbon from the conversion process is needed for the photosynthesis process for plant growth and, hence, the carbon comes back to the plant structure. The photosynthesis reaction illustrated in Figure 2-4 can be simply shown as:

$$H_2O + CO_2 + \text{“sunlight energy”} \rightarrow CH_mO_n \text{ (wood structure)} + O_2 \qquad \textit{(2-1)}$$

All biomass fuels are basically categorized in four groups:

1. Wood and agricultural products: including material taken from forest and farm, energy crops which are low cost, high yield and low maintenance crops grown for energy applications activities or from wood processing, residues from agriculture harvesting or processing, etc.
2. Solid waste: including industrial waste, municipal solid waste (MSW), …
3. Landfill gas and biogas: based on fungi and bacteria activities,
4. Alcohol fuels: obtained from the fermentation of sugars, cellulose and starches found in plants or any organic material.

The chemical elements in the biomass structures, as shown in Figure 2-3, are found in different components, mainly cellulose, hemicellulose and lignin. This complex structure makes the chemical reactions and related kinetics very complicated.

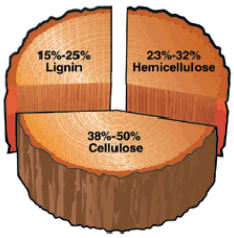

FIGURE 2-3: Biomass structure.

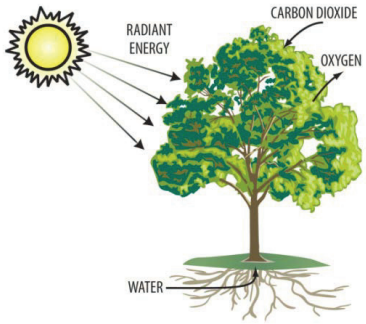

Figure 2-4: Photosynthesis process and CO_2 absorption by plants.

There are many advantages using biomass as an energy source. Apart from the economic and business aspects, it contains less carbon compared to coal and the produced CO_2 also comes back to the plant growth cycle, as mentioned earlier. Use of biomass is largely accepted since it has been used for heating purposes by humans for thousands of years. Additionally, almost all over the world some sources of biomass are available and easily accessible at relatively cheap prices. Table 2-1 shows typical energy prices for wood compared to conventional fossil fuels [Biomass Energy Centre 2012].

Table 2-1: Typical prices for bulk purchase of fuels at domestic or small commercial scale (prices as of February 2012)

Fuel	Price per unit	kWh per unit	pence per kWh
Wood chips (30% MC)	£100 per tonne	3,500 kWh/t	2.9p/kWh
Wood pellets	£200 per tonne	4,800 kWh/t	4.2p/kWh
Natural gas	7.6p/kWh	1	4.8p/kWh
Heating oil	60p per liter	10 kWh/L	6.0p/kWh
LPG (bulk)	50p per liter	6.6 kWh/L	7.6p/kWh
Electricity	14.5p/kWh	1	14.5p/kWh

2.3 Biomass conversion

Three main conversion pathways are known for biomass conversion: biological, thermal, and physical. All these techniques are designed to produce fuels, heat and power, or useful chemical components. Biological conversion includes anaerobic digestion and fermentation in order to produce methane or ethanol. These processes are generally slow

and it takes very long time to convert the biomass to the final fuel. Physical processes are done subject to heating and at high pressure to convert solid fuel to gas/liquid fuels by breaking the bonds of biomass organic matters and reform the intermediates into syngas or hydrocarbon fuels.

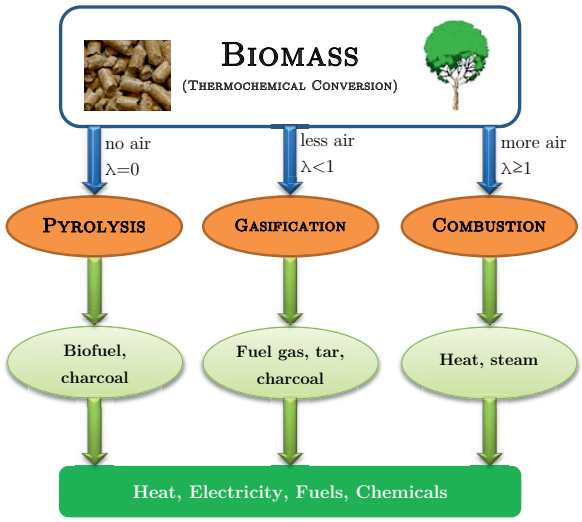

FIGURE 2-5: Thermochemical conversion of biomass.

Thermal conversion, or thermochemical conversion, is the most common biomass conversion path. It is basically categorized into three groups: pyrolysis, gasification, and combustion (see Figure 2-5). The process is mainly regulated by the amount of air needed for the process, i.e. the amount of air or oxidant introduced to the process versus the stoichiometric condition. All these processes are fast compared to biological conversion. In the next section, each of the mentioned thermal conversion processes is explained in more detail.

2.3.1 Pyrolysis

The first process is pyrolysis, which happens in an atmosphere without externally supplied oxygen. It means that the excess air ratio in the reaction zone is zero.

Two types of pyrolysis are generally used: fast pyrolysis and slow pyrolysis. The term is defined based on heating rate, even though the definition of heating range for slow and fast pyrolysis is rather arbitrary in the literature. Sometimes a third type is also introduced as intermediate pyrolysis where the heating rate is somewhere between fast and slow pyrolysis. Each of these has different chemical and physical characteristics, which finally results in various product distributions, i.e. yield of bio-oil, biochar and

gases. Table 2-2 shows typical product distributions for pyrolysis of wood in different modes [IEA task 2012]. Furthermore, changing biomass type, temperature, heating rate, and residence time make it difficult to define general process characteristics for pyrolysis [Mohan *et al.* 2006].

Fast pyrolysis is also known as flash pyrolysis. The hot vapour residence time in this process is a few seconds or less. Fast pyrolysis is a high-temperature process. This process needs a very high heating rate, e.g. 1000 °C/s or even 10,000 °C/s. Valuable fuels, chemicals, and petrochemicals can be produced from this process if a carbon-based fuel is used.

Products of a fast pyrolysis process are mainly vapours, aerosols, and char. The vapours and aerosols are cooled and condensed to be converted to a dark liquid, called bio-oil. The heating value of this liquid is around half of conventional fuel oil [IEA task 2012]. Derived fuel from fast pyrolysis can substitute for diesel and fuel oil in many applications such as boilers and furnaces, in order to produce electricity and heat.

The gas residence time in slow pyrolysis is around 5−30 min [Bridgwater 1990]. Since the residence time is higher compared to flash pyrolysis, gas phase species or volatiles react with each other while tar and char particles are being formed.

The conventional way of biomass pyrolysis over thousands of years has been slow pyrolysis and the main goal has been to produce charcoal. The temperature in this process is in the order of ~500 °C. However, slow pyrolysis produces more solid char which has lower value than valuable chemicals and fuels that can be used in industrial or transportation sectors. Therefore, for higher yield of liquid or gas fuels, usually, fast pyrolysis is suggested.

Table 2-2: Typical product yields from pyrolysis of dry wood.

Mode	Temperature	Heating rate	Vapour residence time	Yield		
				Char	Liquid	Gas
Slow (conventional)	~400−600 °C	5-80 K/min	5−30 min	35%	30%	35%
Intermediate	~500 °C		~ 10−30 s	25%	50%	25%
Fast	~500 °C	10^3-10^4 K/s	~ 1 s	12%	75%	13%

2.3.2 Gasification

Gasification can be considered a subsequent process to pyrolysis. Likewise, there is a complicated chemistry and reaction kinetics behind a gasification process. The excess air ratio in gasification is kept lower than the stoichiometric condition to prevent complete burnout of intermediate species. Figure 2-6 shows a simplified diagram of biomass

gasification. Gasification is done in two different ways: with steam or pure oxygen which results in a medium heating value gas; and with air that produces a low heating value gas [Fossum 2002; Bridgwater 2003]. Almost $1/3$ of the stoichiometric air is needed for a gasification process, i.e. $\lambda \approx 0.33$. The process starts with thermal decomposition of biomass particles through pyrolysis reactions into gas species, liquid tar, and solid char. Subsequently the vapor phase is thermally converted to gas and char. Afterwards char particles are being gasified by means of steam or CO_2. Finally, all the three phases (gas, vapor, and char) are oxidized partially to obtain producer gas. The final product gas, producer gas, is composed of valuable and non-valuable gases.

1. Combustible gases: CO, H_2, CH_4
2. Byproducts: H_2O (steam), CO_2, N_2

Combustible product gases from the gasification process are comparable to the syngas (synthesis gas) produced from steam reforming of natural gas, coal, and other hydrocarbon fuels. Hence, it can be implemented in a Fischer–Tropsch process to produce diesel. By using other catalytic processes, producer gas can be converted to methane, methanol, or dimethyl ether (DME).

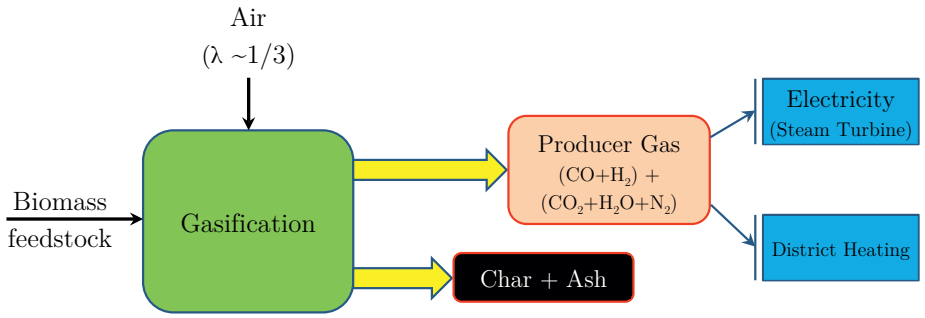

FIGURE 2-6: Simplified schematic of the gasification process.

The reaction sequence for a gasification process can be summarized as below:

Oxidation
The oxidation reactions for the carbon and hydrogen content of biomass in presence of oxidant (O_2, air, O_2/CO_2, etc.) takes place at a temperature of 700−2000 °C.

$$C + O_2 \rightarrow CO_2 + \underline{\text{heat}} \qquad (2\text{-}2)$$

$$C + \tfrac{1}{2}\, O_2 \rightarrow CO + \underline{\text{heat}} \qquad (2\text{-}3)$$

Steam is also formed by reaction of fuel hydrogen content with oxygen:

$$H_2 + ½\ O_2 \rightarrow H_2O + \underline{\text{heat}} \qquad (2\text{-}4)$$

All the oxidation reactions are exothermic and provide the necessary energy for drying and other endothermic processes.

Reduction

In absence of oxygen, reduction reactions take place and valuable gases are produced according to the following reactions. These reactions are endothermic, or slightly exothermic.

$$CO_2 + C + \underline{\text{heat}} \rightarrow 2\ CO \qquad (2\text{-}5)$$

$$H_2O + C + \underline{\text{heat}} \rightarrow CO + H_2 \qquad (2\text{-}6)$$

Reaction (2-5) is known as the Boudouard reaction and is the most important reaction in the reduction process. The next reaction, (2-6), is the water-gas reaction and is important in formation of producer gas.

The last two reactions in the reduction step are the well-known water-gas-shift (WGS) reaction,

$$CO_2 + H_2 \rightarrow CO + H_2O + \underline{\text{heat}} \qquad (2\text{-}7)$$

And the methanisation reaction:

$$C + 2\ H_2 \rightarrow CH_4 + \underline{\text{heat}} \qquad (2\text{-}8)$$

The concentration of the final desirable products, CO and H_2, is controlled by the abovementioned reactions. For instance, the water-gas reaction and water-gas shift reaction are closely linked and play an important role for the CO/H_2 ratio, an important parameter for further processing of the producer gas.

Side reactions

Since oxygen is available in the gasification zone, some part of the producer gas may react with non-reacted oxygen and form final combustion products. This is unavoidable in a real system; however, the goal is to minimize these reactions, even though the released heat from these reactions is beneficial for the reduction process.

$$CO + ½\ O_2 \rightarrow CO_2 + \underline{\text{heat}} \qquad (2\text{-}9)$$

$$H_2 + ½\ O_2 \rightarrow H_2O + \underline{\text{heat}} \qquad (2\text{-}10)$$

2.3.3 Combustion

Millions of years ago, humans started to make fire in order to produce heat to stay warm, cook, and make light. Later, the same technology and concept led to power production from a combustion process. Combustion is the chemical reaction between a fuel and an oxidant resulting in complete burnout, i.e. heat production. Hence, the process is an overall exothermic set of reactions. The energy stored in the chemical bonds of a fuel are converted to heat energy and can be used in a power plant to produce steam needed for a turbine that finally produce electricity and heat.

In case of biomass, combustion means burning of organic materials. Wood is the most widely used fuel for burning, however, there is an increasing interest in other biomass types such as bark, tops and branches, straw, sawdust, waste wood or demolition wood, and energy crops (such as poplar and willow) to be used as feedstock.

The products from the biomass combustion are formed from the reaction of oxygen in the oxidant and fuel elements. Carbon forms carbon dioxide and hydrogen reacts with O_2 to form water vapor. The combustion of a typical biomass fuel with air as oxidant can be written as:

$$CH_mO_n + \lambda\Psi\,(0.21\ O_2 + 0.79\ N_2) \rightarrow CO_2 + a\ H_2O + b\ O_2 + c\ N_2 \qquad (2\text{-}11)$$

where λ is the excess air ratio and Ψ is the stoichiometric coefficient, calculated based on the full burnout condition, i.e. λ=1 and b=0. It should be noted that minor elements, such as nitrogen, sulfur, and chlorine are not listed in the above reaction. The stoichiometric coefficient is given by:

$$\Psi = \frac{1 + \frac{m}{4} - \frac{n}{2}}{0.21} \qquad (2\text{-}12)$$

The constants a, b, and c are also calculated based on the biomass composition:

$$a = \frac{m}{2},\ b = \left(\lambda - 1\right)\left(1 + \frac{m}{4} - \frac{n}{2}\right),\ c = 0.79\lambda\left(\frac{1 + \frac{m}{4} - \frac{n}{2}}{0.21}\right) \qquad (2\text{-}13)$$

Reaction (2-11) is valid for $\lambda \geq 1$, since for lower excess air ratios unburnt species like CO, CH_4, and H_2 will be formed in high quantities.

Use of combustion technology is especially economical near the biomass source, e.g. for farms or cities with simple access to forest resources. Having access to the resources along with adequate storage place can make biomass combustion very attractive. However, continuous feeding which is a challenge in small scale applications is required for a stove. Additionally, many combustion systems need the feed to be in a special size and

specification, meaning that a pretreatment of the feedstock is also required. With newer technologies the challenge of feeding system in conventional wood stoves can be avoided. For example new "pellet stoves" [Boman *et al.* 2011] with an electrically driven auger can be fed with raw feedstock in large size and work for a whole day without being tended.

2.3.4 Biomass in CHP systems

There are large quantities of waste heat in the operation of a conventional power plant or generator. The waste heat recovery can be applied to the cooling circuits and the exhaust gases. This waste heat is useful for industrial processes or space heating, and increases the overall efficiency of the process. Combined heat and power (CHP) or co-generation is the production of useful thermal energy and electricity from the same primary fuel. Different technologies are known for CHP systems, but all are based upon an efficient, integrated system that combines electricity production and heat recovery to increase the plant efficiency. CHP plants generally convert 75-80% of the fuel energy into useful energy, by using the heat output from the electricity production for heating or industrial applications. In the most modern CHP plants, efficiencies of 90% or more can be reached [IPCC 2007]. Another benefit of CHP plants is that they reduce network losses due to being located near the end user, especially in case of small scale applications.

Small scale CHP applications are generally defined as small power plants not using steam turbines as a driver technology, for instance power plants using internal combustion engines with typically less than 1 MW electrical capacity, and emerging technologies as fuel cells, micro-turbines and Stirling engines [ClimateTechWiki 2012]. Research on small scale CHP aims to produce modular units, which can be installed and relocated easily. This is beneficial in places with limited technical support.

Research on small scale CHP applications in Norway is started to enable utilizing biomass as the feedstock in CHP systems with the least environmental impact [KRAV 2008]. Research is required on feasibility studies, optimum reactor designs, minimized emission levels, and higher efficiencies working at the lowest possible cost.

2.3.4.1 Norwegian resources

Application of biomass CHP in Norway, due to the availability of resources all over the country, is of high importance. The current energy production based on biomass in Norway is about 14 TWh, which is almost 10% of the stationary energy consumption [Trømborg *et al.* 2008]. Out of this, about one-half is produced and used in forest industries.

Electricity prices have been relatively low in Norway and central heating facilities are almost nonexistent over the country. This is probably the reason why energy from biomass has a significantly lower share in Norway compared to Sweden and Finland. Wood stoves are the main application of bioenergy in households. However, low end-user prices of electricity prevent the use of refined, solid biofuels in heat production. On the

other hand, harvest levels in Norwegian forests are much below annual growth, implying that forest biomass resources steadily accumulate. Decreasing wood prices combined with increasing prices of oil have improved the interest for solid biofuels in the heat market.

2.3.5 Reactor types

Even though combustion of biomass is clearly a proven technology, the reactor setup and design issues related to solid fuels combustion systems need special attention. Different technologies have been developed over the last decades for biomass combustion, aiming for a better efficiency and lower cost. At the same time, new regulations on emissions have forced the reactors to work with a certain pollutants limit, along with a higher standard regulation on safety issues.

There are three main technologies for performing combustion: over a grate, by fluidization, and in a pulverized fuel system. Below each of the reactor types are briefly introduced.

2.3.5.1 Grate combustion

Fixed bed reactors are the very early design and the most common type among other reactor configurations. However, they are seldom being used any more in new large-scale boilers, due to higher investment costs, higher emissions and limited availability for multifuel use. On the other hand, for small and medium size boilers, <20 MW fuel input, grate combustion is yet a competitive solution with small investment and low emission levels. In addition, grate combustion can be used in a CHP system where excess heat can be sold to a district heating network or utilized as process steam. They operate with generally a long residence time on the grate and due to low gas velocity, which results in high carbon conversion. The fuel is fed to the reactor and remains on the grate which can be fixed or even moving.

Normally, a complete combustion process includes a reactor, gas cooling, and gas cleaning. Solid fuel particles or pellets fall onto the grate/fuel bed and the gas moves either up or down. The reactor is commonly composed of a main section where the air and burned gases flows through, a fuel feeding system, and an ash removal unit.

According to the grate design in the reactor, grate furnaces are categorized in different groups: fixed grate, moving grate, travelling grate, vibrating grate, and rotating grate [Berndes *et al.* 2008].

Air staging or two-stage combustion, is generally described as the introduction of overfire air into the furnace. Internal air staging is generally one of the design features of low NO_x burners. In an air staged combustion system, a portion of the combustion air is diverted from the burners to overfire air ports above the burners. The objective is to form a fuel rich flame zone followed by a region where the residual char is burned out. The effect of fuel rich conditions on NO_x formation is very sensitive to the air amount. After fuel is fed

to the reactor, volatiles and char are formed, each containing bound nitrogen. Oxygen rich conditions drive the competition towards NO_x formation, while fuel rich conditions, e.g. staged combustion, drive the reactions to form N_2 [Cremer *et al.* 2003]. Application of air staging to a grate furnace needs small modifications to the reactor and hence is an effective technique for NO_x reduction. To obtain a maximum reduction, however, it is very important to have separate primary and secondary combustion zones and effectively control gasification and oxidation or final burnout processes of fuel gases. Furthermore, good mixing of air and fuel is important in staged combustion. This is due to the fact that if the mixing condition is not effective, higher amount of excess air will be required for a complete combustion. Higher excess air ratio in the reactor, on the other hand, is proportional to lower overall efficiency of the plant. Therefore, design of the air injection nozzles, especially in the secondary zone where the final burnout should be taking place, is very important to achieve a high turbulence inside the reactor, giving higher efficiency. This can be achieved through higher air feed velocity, using air nozzles, or by modifying the flue gas path inside the reactor.

Grate combustion is in general inexpensive regarding operating cost and has low level of particulates in the flue gas. Additionally, slagging problems are easier to control compared to fluidized bed combustion. However, the fuel and air mixture is not as homogenous as in fluidized bed combustion, resulting in inhomogeneous combustion conditions at some parts of the grate.

2.3.5.2 Fluidized bed reactor

Fluidization is an important technology for many chemical engineering applications since it gives very good heat and mass transfer characteristics. The bed in the fluidized bed (FB) is generally composed of non-reactive materials such as sand. Air is blown from the bottom of the reactor, under the sand particles, and it lifts the bed material. This creates a two-phase flow pattern. Biomass is fed from a place above the sand bed and when it falls down to the bed, it mixes with sand materials and again is being lifted. This gives a high heat transfer rate because of good mixing conditions. These reactors were first used for coal applications and later biomass was successfully applied as a feedstock.

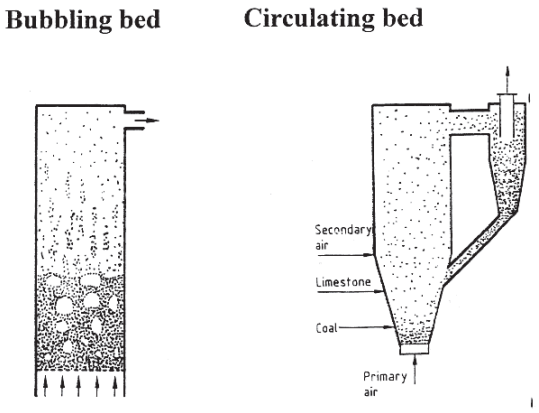

FIGURE 2-7: Fluidized bed reactors [Warnecke 2000].

Figure 2-7 shows two main configurations of fluidized bed reactors: bubbling fluidized bed (BFB), and circulating fluidized bed (CFB). The air flow velocity and gas path is different in BFB and CFB. The gas velocity in BFB is generally lower than in CFB; hence the solid particles are not being transferred out of the bubbling reactor. However, in CFB reactors, due to higher gas velocity, recycling of bed materials is necessary. This implies that CFB requires huge mechanical cyclones to capture and recycle the large amount of bed material, which requires a tall boiler. BFB boilers are offered up to 100 MW and CFB units up to 400-600 MW. Two-stage combustion is also a common measure of emission reduction in FB combustion.
There are a lot of advantages for fluidized bed compared to fixed bed reactors. FB reactors have a very wide operating range regarding fuel composition, e.g. fuels with high ash content can be fed to FB reactors, if the ash is not getting sticky at low temperatures. In addition, due to the good mixing conditions, the temperature profiles along the reactor are uniform and hence the formation of hot spots with high temperatures is generally avoided. Since the temperature is relatively lower than in a grate reactor, use of problematic fuels with low ash melting temperatures, e.g. straw, are also allowed in advanced BFB reactors. The operation cost of a FB reactor is in general high, while necessary maintenance is lower than for fixed bed reactors because there are not too many mechanical parts inside the reactor [Berndes *et al.* 2008].

2.3.5.3 Pulverized fuel combustion

Pulverized fuel (PF) combustion was invented in 1920 and has been a universal choice for coal power plants until 1990. It is mainly used for large scale industrial applications, since in small scale applications PF combustion is not feasible. Still, a majority of coal-fired power station boilers and many large industrial water-tube boilers use pulverized fuel technology. Nowadays, PF combustion technology is well developed and over 90% of

the total power production from coal is obtained in pulverized fuel plants. PF reactors have many advantages over other reactor types, e.g., ability to use various types of fuels with different qualities (multifuel), quick responses to changes in load, use of high pre-heat air temperatures etc. However, using 100% biomass as the feedstock may result in some problems in the pulverized systems if biomass contains a substantial amount of moisture. Also, the alkali content of biomass is responsible for corrosion issues. Due to these problems, co-firing plants have been introduced to burn biomass and coal together and prevent disadvantages of both fuels. Normally 10-25% biomass is used as the supplementary fuel in PF combustion plants.

The size of fuel particles needs to be very fine. The solid fuel (coal, biomass, or peat) is ground (pulverized) to a fine powder, so that less than 2% is +300 micrometer (µm) and 70-75% is below 75 micrometer. The size distribution is very important and quite important for the combustion conditions. Very fine particles are wasting grinding mill power, while too coarse particles do not burn out completely in the combustion chamber and results in higher levels of unburnt species.

The pulverized fuel together with the combustion air is fed into the combustion chamber via burner nozzles. Necessary air may be divided in primary, secondary, and tertiary air (staged air combustion). By proper air staging, low NO_x emissions can be achieved. Combustion takes place at temperatures from 1300-1700 °C, depending largely on fuel composition [IEA Clean Coal Centre 2012]. Fuel residence time is typically 2-5 s inside the reactor, and the particles must be small enough for complete combustion.

2.4 Emissions and environmental problems

Global warming as a result of greenhouse gases (GHG) is one of the major concerns among researchers, politicians, and the public in general. The main emission for global warming is carbon dioxide (CO_2), while other emission gases like CH_4 and N_2O also contribute. The major source of CO_2 is related to power production, i.e. combustion of fossil fuels in power plants.

Approximately 130% increase is expected for the CO_2 level in the atmosphere by the end of 2050, which will increase the earth temperature with about 6 °C [IEA report 2008]. United Nations Intergovernmental Panel on Climate Change (IPCC) concluded that if energy demand/production continues with the current trend, global CO_2 emissions in 2050 should be reduced at least 50% compared to the base year, 2000 [IEA report 2010], in order to keep the temperature rise between 2.0 °C and 2.4 °C.

Having fossil fuels as the dominant source of energy, we should try to reduce the CO_2 level at the same time. This can be achieved with e.g.:

1. CO_2 capturing technologies (CCS)

2. Renewable energy such as hydropower, wind, and bioenergy
3. CO_2 negative technologies; e.g. biomass combustion combined with CCS

Biomass as a renewable source of energy has a lot of environmental advantages over other solid fuels. However, almost all biomass fuels contain some amount of sulfur, nitrogen, and chlorine. Growing plants for use as biomass fuels may also help keep carbon dioxide levels balanced. Plants remove carbon dioxide from the atmosphere when they grow, store carbon in their structure and release oxygen.

As mentioned earlier, combustion of biomass results in formation of CO_2, which is necessary for plants growth. Hence, biomass is also known as almost CO_2-free or carbon neutral fuel. If carbon capture and storage technology is implemented in a biomass combustion plant, the net CO_2 level for the cycle will be negative. Biomass combustion is the only energy system capable of doing this, i.e. provide a carbon negative system.

Although having a CO_2 neutral cycle, burning biomass will result in different types of other pollutants, mainly classified into two groups:

1. unburnt emissions; and
2. combustion related pollutants.

Unburnt emissions are a result of incomplete combustion, due to temperature effects, mixing and residence time; forming CO, HC, tar, PAH, and unburnt char particles [Khan *et al.* 2009]. The second type of pollutants originates from the initial fuel composition such as nitrogen, sulfur and ash elements. It includes PM, NO_x, N_2O, SO_x, HCl and heavy metals [Khan *et al.* 2009]. Ash deposition and corrosion is also influenced directly by fuel composition.

Different reviews have been carried out on aspects of biomass environmental problems [Berndes *et al.* 2008]. Below different emissions based on the relevant elements in biomass are introduced.

2.4.1 CO

Emission of CO is due to incomplete combustion, affected by different parameters. Therefore, in general, an excess air ratio of less than one, or supply of too little oxygen to the combustion zone will be a condition for the formation of carbon monoxide. When air and fuel are not perfectly mixed, zones with low concentration of oxygen will be present, resulting in formation of CO instead of complete burnout of CO. In addition, a sufficient residence time is needed for complete combustion, otherwise CO formation rather than CO_2 [Laryea-Goldsmith 2010] will result.

Since CO is an intermediate species for CO_2 formation, and temperature is an important parameter in this reaction chemistry, zones with low temperatures favor formation of CO, while at higher temperatures the reactions proceed faster toward complete oxidation.

On the other hand, reaction of CO with other gaseous species is an important factor. For example, HCl in the flue gas has a direct relation with the CO emission level, affected by the presence of radicals and catalytic reactions in presence of those species [Wei *et al.* 2004]. Higher NO_x emissions also gives a higher CO level, while combined NO_x and HCl result in a higher CO due to a considerable decrease in CO oxidation in presence of these gases [Roesler *et al.* 1995]. Likewise, it has also been shown that SO_2 in the presence of NO prevents CO oxidation by reducing the concentration of free radicals [Glarborg *et al.* 1996].

2.4.2 Nitrogen: N

2.4.2.1 NO_x

Nitrogen oxides (NO_x=NO+NO_2) are a minor part of the combustion products in the combustion of all biomass fuels containing nitrogen. NO_x has both a negative effect on the climate (indirect effect on greenhouse gas through ozone formation, acid rain, vegetation damage, smog formation, etc.) and human health (to respiratory system, when reacting with ammonia and other compounds to form small particles which can penetrate deeply into sensitive parts of the lungs). The major part of NO_x emissions is coming from fuel-N content and the share of other mechanisms, mainly thermal NO_x, which originate from air nitrogen content, is very low, as the temperature in biomass combustion systems is not so high. Different classes of biomass have a range of nitrogen content of 0−2.5 wt% while special types such as sewage sludge may contain up to 7 wt%. Primary measures (fuel staging, air staging, fuel mixing) can be used to lower the NO_x emissions from fuels with low nitrogen content [Houshfar *et al.* 2010b; Houshfar *et al.* 2012d], while from fuels with high nitrogen content, secondary measures such as SNCR or SCR should also be applied to satisfy local or international regulations. This will be discussed in more detail in the next chapter.

2.4.2.2 N_2O

Nitrous oxide is also a minor product from combustion of biomass, from nitrogen in the fuel. This emission is a greenhouse gas and was recently shown to be the most important ozone-depleting substance [Ravishankara *et al.* 2009]. N_2O has an indirect effect on health through O_3 depletion. However, the emission level of N_2O is usually very low in biomass combustion systems.

A detailed discussion on N-emissions will be given in the following chapters.

2.4.3 Chlorine: Cl

Each biomass having Cl in the composition will produce hydrogen chloride (HCl) in the combustion process, which is toxic and has negative effects on the human respiratory system. HCl is a strong acid, therefore contributing to acid rain and vegetation damage,

but has not high corrosion risk in pipes and other materials in boilers and reactors. Fuel leaching [Dayton *et al.* 1999], automatic cleaning of parts, tubes coating and change of reactor materials are methods to reduce the effect of corrosion from Cl. To regulate the environmental effect of HCl, sorption (dry or in activated carbon) and scrubbers can also be applied. The major part of Cl in the fuel may be converted to salts such as KCl and NaCl for alkali-rich fuels, which are highly corrosive when condensing on superheater tubes or on fly ash particles depositing on superheater tubes. Some Cl can also remain in the bottom ash or will be released as fly ash, which is discussed later.

2.4.4 Sulfur: S

The sulfur content of biomass is relatively low compared to other fuels. However, sulfur oxides (SO_x, mainly SO_2) and alkali sulfates are formed from biomass fuel sulfur oxidation, and contribute to aerosol and smog formation, vegetation damage, acid rain and corrosion; in addition to the dangerous effect on humans by asthmatic effect and damage to the respiratory system. The sulfur retention in ash or release to the gas phase highly depends on the temperature and presence of other mineral compounds [Knudsen *et al.* 2004; Lang *et al.* 2006]. Sulfur containing components may enhance chlorine corrosion at high temperatures and some methods as described for Cl should be applied to avoid corrosion from sulfur. Injection of lime or limestone is a technique to reduce the SO_2 emission, while co-combustion of biomass and coal is an alternative for coal fired boilers.

2.4.5 Calcium: Ca

Ca has a relatively high melting point which increases the melting temperature of ash, and therefore reduces ash sintering on the grate or in the reactor. However, the ratio between Ca and potassium is more important where a low Ca/K ratio can lead to a reduced melting point [Steenari *et al.* 2009]. In such cases, necessary control equipment should be used to reduce the temperature in the combustion system.

2.4.6 Potassium: K and Sodium: Na

K is the major alkali metal in biomass fuels and Na is an important element with respect to corrosion. Due to their low melting point, formation of components from K and Na cause problems in the combustion systems such as sintering in addition to aerosol formation, agglomeration, deposition, corrosion, slagging and fouling. To avoid such problems, it is important to use dust precipitation, fuel leaching, coatings and cleaning. As mentioned before, alkali chlorides (KCl and NaCl) are corrosive components formed by reaction of Cl and K or Na. Sulfation of gaseous KCl is one of the methods to reduce the corrosion problems from KCl [Kassman *et al.* 2010]. A recent study shows that sewage sludge can act as a controller for corrosion when co-combusted with high potassium content biomass fuels [Elled *et al.* 2010].

2.4.7 Silicon: Si

This element is commonly the main ash forming element and deserves special attention in biomass combustion. Fuels such as straw contain more silicon, which is a problematic element causing ash deposition in the system at high or moderate temperatures. In case of high concentration of alkali, formation of alkali silicates will lead to ash melting at low temperatures, e.g. less than 700 °C, hence resulting in deposition problems [Khan *et al.* 2009]. Agglomeration in fluidized bed boilers is also a result of silica, alkali and chlorine.

2.4.8 Zinc: Zn and Cadmium: Cd

Zn and Cd are important heavy metals in the ash composition due to sustainability of ash (ash utilization and recycling) and particulate emissions. Heavy metals are toxic and accumulate in the food chain. Ash treatment and fractional heavy metal separation is used to regulate the amount of these elements in the ash composition while dust precipitation and treatment of condensates reduce the particulates.

2.4.9 Other problems

Emissions such as PM are affected by a series of the discussed elements in the fuel. PM contains normally alkali salts like potassium chloride and potassium sulfates; thus the initial fuel composition, especially the percentage of potassium, chloride and sulfur is very important for creation of PM emissions.

2.5 Emission reduction measures

To control and reduce the mentioned emissions, two different methods are normally being applied to combustion systems:

- primary measures and
- secondary measures,

where primary measures look for the reduction or prevention of these pollutants formation before the fuel is fed to the reactor or in the combustion chamber, while secondary measures reduce emissions with methods such as SCR after creation of the pollutants.

In the previous section, some reduction techniques were presented for different elements. For example, a well-known primary measure to reduce NO_x in biomass combustion reactors is staged combustion; either staged air or staged fuel. Another primary measure is to change the elemental composition of biomass by mixing different kinds of biomass together to make it unproblematic [Salour *et al.* 1993; Steenari and Lindqvist 1999; Pettersson *et al.* 2008] or co-firing of risky biomass with non-problematic fuels to reduce

corrosion [Spliethoff *et al.* 2000; Lundholm *et al.* 2005; Davidsson *et al.* 2007a; Aho *et al.* 2010; Munir *et al.* 2010]. Fuel mixing can also result in a reduction in the fuel cost [Obernberger 1998].

Chapter 3

Literature Review

3.1 Introduction

In this chapter, a comprehensive review is offered to give an overview of the relevant and important literature in the main research area, two-stage combustion of biomass and NO_x emissions. First the important points of current knowledge on NO_x reduction are reviewed. Thereafter, relevant works on ash related problems for combustion of problematic fuels are presented. This review is a survey of articles, books, conference papers, reports, and theses.

3.2 NO_x emissions

For energy production, the most common energy carriers are solid fuels (coal, biomass, wastes, etc.). However, it is a concern that combustion of biomass will lead to high levels of nitrogen oxides emissions (NO_x; collective term for NO and NO_2) from oxidation of nitrogen in the fuel (fuel nitrogen) or potentially oxidation of air nitrogen content. NO_x emissions are contributing to environmental problems such as acid rain, photochemical smog formation and ozone formation in urban areas [Seinfeld 1986; Tariq and Purvis 1996]. Additionally NO_x participate in the chain reactions of ozone removal from the

stratosphere, which in turn results in more ultraviolet radiation to the earth [Johnston 1992; Warnatz *et al.* 2006]. Also nitrous oxide (N_2O) may be formed, having a strong greenhouse gas effect.

3.2.1 NO_x formation mechanisms

The formation of NO_x happens through four main routes:

1. Thermal mechanism (Zeldovich)
2. Prompt mechanism (Fenimore)
3. Nitrous oxide mechanism (N_2O intermediate)
4. Fuel nitrogen conversion (Fuel-N mechanism)

The first three mechanisms are mainly contributing to the conversion of air nitrogen to NO_x. Theoretical and experimental studies have shown that these three mechanisms are contributing much less to NO_x formation in biomass combustion than fuel-N conversion.

3.2.1.1 Thermal NO_x

NO_x emission formation from the thermal or Zeldovich mechanism is dominant at high temperatures and at a wide range of excess air ratios. The set of chemical reactions for this highly temperature dependent mechanism can be written as:

$$O + N_2 \rightarrow NO + N \qquad (3\text{-}1)$$

$$N + O_2 \rightarrow NO + O \qquad (3\text{-}2)$$

At fuel rich conditions and an excess air ratio of close to one, a third reaction is also important, which in combination with the above two reactions is known as the extended Zeldovich mechanism.

$$N + OH \rightarrow NO + H \qquad (3\text{-}3)$$

The Zeldovich mechanism is predominant at temperatures higher than 1500 °C [Tariq and Purvis 1996; Wünning and Wünning 1997], while the temperatures during biomass combustion are typically lower.

The temperature limit for thermal NO_x formation to be important is dependent on the O, O_2 and OH levels and the residence time and in practice means thus typically temperatures above 1400 °C, and is independent of the combustion system and fuel type. According to the literature, thermal NO_x formation in different biomass combustion systems starts at temperatures above 1400 °C and in circulating fluidized bed combustors it becomes relevant at temperatures above 1500 K [Salzmann and Nussbaumer 2001; Mahmoudi *et al.* 2010].

Paper II [Houshfar *et al.* 2011b] investigated the effect of temperature on NO_x formation in biomass combustion. A very small effect of temperature demonstrates that at the investigated temperature range, thermal NO_x has still a minor share to the total NO_x in biomass reactor.

3.2.1.2 Prompt NO_x

The second NO_x formation mechanism was first identified by Fenimore [Fenimore 1971] and was termed "prompt NO_x". It is well known that prompt NO_x formation is significant at special combustion conditions and is almost independent of temperature:

- fuel-rich conditions,
- short residence times.

The abovementioned conditions may happen in surface burners, gas turbines, and staged combustion systems [Barnes *et al.* 1988]. Since the reaction chain is connected to hydrocarbons, the Fenimore mechanism is generally relevant for hydrocarbon fuels. However, in biomass combustion prompt NO_x contribution to the total NO_x is very low due to fuel lean conditions, relatively long residence times and less CH radicals production.

The chemical reactions for prompt NO_x are very complex, but a simple reaction chain can be introduced as below [Turns 1996]:

$$CH + N_2 \rightarrow HCN + N \qquad (3\text{-}4)$$

$$N + O_2 \rightarrow NO + O \qquad (3\text{-}5)$$

$$HCN + OH \rightarrow CN + H_2O \qquad (3\text{-}6)$$

$$CN + O_2 \rightarrow NO + CO \qquad (3\text{-}7)$$

The major hydrocarbon radical contribute to prompt NO_x is CH (Equation (3-4)), and also CH_2, via

$$CH_2 + N_2 \rightarrow HCN + NH \qquad (3\text{-}8)$$

Amine and cyano compounds formed from the above reactions can react to form NO [Strahle 1993].

In conclusion, contributions from the prompt mechanism are mainly found for fuel rich conditions and depend on the CH radicals concentration. These conditions are favored in fossil fuels combustion applications but not in biomass combustion.

3.2.1.3 N_2O intermediate mechanism

The nitrous oxide mechanism was first proposed by Malte *et al.* [Malte and Pratt 1975]. It is of relative importance in very fuel lean, high pressure, and low temperature conditions [Turns 1996]. Therefore, this mechanism can be dominant in gas turbines, compression-ignition engines, and systems operated in flameless mode (where fuel and oxygen are highly diluted in inert gases to prevent peak temperatures in the combustion zone). The elementary reactions involved are:

$$O + N_2 + M \rightarrow N_2O + M \qquad (3\text{-}9)$$

$$H + N_2O \rightarrow NO + NH \qquad (3\text{-}10)$$

$$O + N_2O \rightarrow 2\,NO \qquad (3\text{-}11)$$

where N_2O formed in the first reaction (involving a third body) react with O and H radicals to form NO. Due to the presence of a third body in reaction (3-9), elevated pressures are needed for this mechanism and therefore, this mechanism is not very important in common biomass combustion systems that normally work at atmospheric pressure.

3.2.1.4 Fuel-N conversion

It has been shown that more than 80–90% of NO_x emissions in pulverized coal combustion systems are coming from fuel-N conversion, the remaining emissions being a result of the thermal mechanism [Glarborg *et al.* 2003]. In biomass combustion systems, fuel-N conversion is even more dominant due to the unfavorable temperature conditions in typical biomass furnaces for other than fuel-N conversion. A simplified reaction path diagram for NO_x formation and reduction in biomass combustion is presented in Figure 3-1.

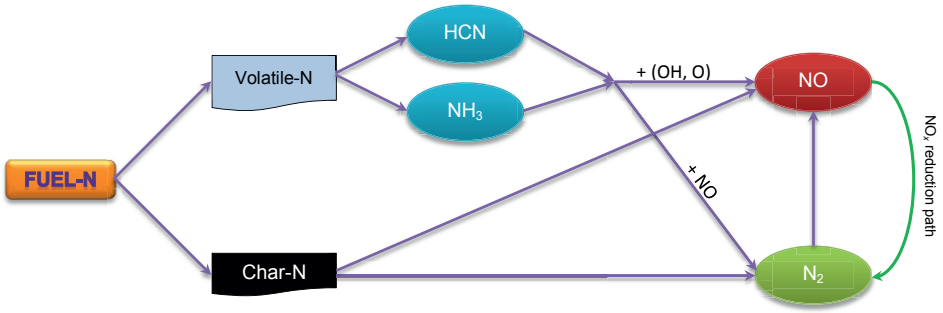

FIGURE 3-1: Simplified fuel nitrogen conversion diagram.

The combustion of biomass is normally carried out in grate or fluidized bed combustors, with relatively low temperature, which increase the importance of fuel-NO_x, while pressurized combustion and high temperature in coal combustion can enhance the other NO_x formation mechanisms. Hence, the other mechanisms can be neglected from further studies of such biomass fired systems. As a conclusion, one should concentrate on fuel-N conversion in order to effectively control NO_x formation in biomass combustion.

3.2.2 Staged combustion

In general, the parameters that affect NO_x formation and reduction are residence time, temperature, excess air ratio, fuel-N content, and mixing condition [Kolb *et al.* 1989; Skreiberg *et al.* 1997; Jenkins *et al.* 1998; Houshfar *et al.* 2011b]. Temperature has the least influence on NO_x formation as mentioned earlier due to the relatively low temperature range of typical biomass combustion [Houshfar *et al.* 2011b]. Note that it is proved that reburning during oxy-combustion is more sensitive to temperature [Normann *et al.* 2011].

Important species and intermediates for NO_x formation and reduction are ammonia (NH_3), hydrogen cyanide (HCN), NO and HNCO in biomass combustion systems [Hämäläinen *et al.* 1994; Sørum *et al.* 2001; Hansson *et al.* 2004; Skreiberg *et al.* 2004b; Becidan *et al.* 2007a]. Also, NO_x precursors, i.e. NH_3 and HCN, are very sensitive to temperature and the HCN/NH_3 ratio increases with increasing temperature [Hansson *et al.* 2004; Becidan *et al.* 2007a; Ren *et al.* 2010].

One of the most important and widely used measures to reduce NO_x in solid fuels combustion is staged combustion. The concepts of air staging, fuel staging, advanced reburning and combined staging originate from the 1970's and 1980's by the groups involving, e.g., Wendt and Pershing [Wendt *et al.* 1973; Pershing and Berkau 1974; Wendt *et al.* 1979; Kramlich *et al.* 1982; Wendt *et al.* 1987; Chen *et al.* 1988; Mereb and Wendt 1994]. Staged combustion, including staged air combustion and staged fuel combustion, can give a NO_x reduction in the range of 50−80% [Kicherer *et al.* 1994; Salzmann and Nussbaumer 2001; Nussbaumer 2003; Zabetta *et al.* 2005; Houshfar *et al.* 2010a; Houshfar *et al.* 2011a; Houshfar *et al.* 2011b; Houshfar *et al.* 2012a; Houshfar *et al.* 2012b; Houshfar *et al.* 2012c; Houshfar *et al.* 2012d].

A principal diagram of staged air combustion is shown in Figure 3-2. The purpose of staged air combustion is to add primary air at a less than stoichiometric ratio, in order to devolatilize the volatile fraction of the fuel, resulting in a fuel gas consisting mainly of CO, H_2, C_xH_y, H_2O, CO_2 and N_2; and also small amounts of NH_3, HCN and NO_x from the fuel nitrogen content. If sufficient oxygen exists in the first stage, the fuel nitrogen intermediates will be converted to NO_x (mainly NO) but shortage of oxygen will cause NO to act as an oxidant for CO, CH_4, HCN and NH_i (with i=0, 1, 2, 3) in the reduction zone, hence reduce the nitrogen in NO and NH_i to molecular nitrogen, i.e. N_2, in reactions

such as [Kilpinen and Hupa 1991; Kilpinen *et al.* 1992; Nussbaumer 2003; Skreiberg *et al.* 2004b]:

$$NO + NH_2 \rightarrow N_2 + H_2O \qquad (3\text{-}12)$$

$$NO + CO \rightarrow \tfrac{1}{2}\, N_2 + CO_2 \qquad (3\text{-}13)$$

The effects of CO, CH_4, and H_2 on HCN and NH_3 oxidation have been studied at 600−1000 °C, showing that CO significantly promotes the NO and N_2O formation through HCN oxidation [Wargadalam *et al.* 2000].

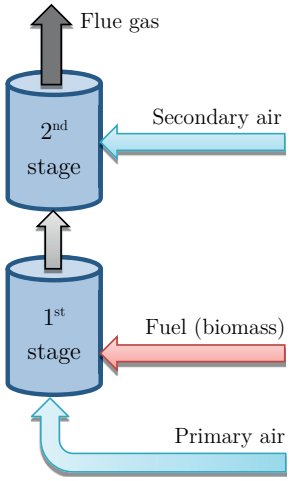

FIGURE 3-2: Sketch of the staged air combustion concept.

NH_3 and HCN form in the pyrolysis stage of combustion depending on the temperature and fuel type, where ammonia is believed to be the most important N-species in the combustion of biomass, while HCN is more important for high-rank coals [Hämäläinen *et al.* 1994; Hansson *et al.* 2004; Becidan *et al.* 2007a]. Ammonia that is formed in this stage is converted to NH_i radicals. At fuel lean combustion, these radicals will be converted to NO, while at fuel rich conditions, N_2 will be the main product [Nussbaumer 1996]. Thereafter sufficient air is added in the second stage to ensure a good burnout and low emission levels from incomplete combustion.

The effect of excess air ratio, residence time and temperature has previously been studied for a single wood particle in batch combustion, showing dependency of the NO level with excess air ratio and temperature simultaneously [Skreiberg *et al.* 1997]. Also, previous work showed the effect of fuel type and co-combustion of biomass with natural gas on NO emissions when using two-stage combustion [Lin *et al.* 2009]. Fuel-N content and the

conversion rate of NO_x precursors (NH_3 and HCN) to NO_x have been experimentally and numerically investigated for different solid biomass [Sørum *et al.* 2001; Johansson *et al.* 2004; Dagaut *et al.* 2008; Stubenberger *et al.* 2008].

Skreiberg *et al.* [Skreiberg *et al.* 1997; Skreiberg *et al.* 2004a] showed that the primary excess air ratio, number of air stages, temperature, and residence time all affect the NO_x reduction level. However, the most important variable is the primary excess air ratio. Generally, increasing the excess air ratio increases the NO_x emission level. Yet an optimum primary excess air ratio exists. Increasing the number of air stages will decrease the potential fuel-N to NO_x conversion, but the effect of additional air stages may be very small. Temperature can decrease, increase, or has no effect on the NO_x emission level, depending on the temperature range applied to the reactor, and finally there is an optimum/sufficient residence time for optimum fuel-N conversion to N_2. Large and modern grate fired boilers are generally operated with an appropriate excess air ratio, and consequently under favorable combustion conditions, which result in low levels of unburnt emissions [Johansson *et al.* 2004].

Fuel staging (and reburning) uses the principal of NO reduction in the second stage by adding more fuel or even a different fuel, e.g., more of the same solid fuel for fuel staging or hydrocarbons, such as natural gas, for reburning. In the first stage, NO_x is formed because of lean combustion. In the second fuel stage, NO reduction occurs at reducing conditions, where air is added for complete combustion. Low NO_x levels can be achieved by fuel staging at lower temperatures than what is needed for air staging and the secondary fuel properties affect the NO_x emission level (better efficiency with smaller particle size and higher amount of volatile matter) [Kicherer *et al.* 1994; Salzmann and Nussbaumer 2001].

Combined staged (CS) technology [Zabetta *et al.* 2005] is a method of NO_x reduction including reburning, staged air combustion (AS), staged fuel combustion (FS) and selective non-catalytic reduction (SNCR) [Wendt *et al.* 1973; Pershing and Berkau 1974; Chen *et al.* 1988]. Combined staged technology starts to reduce NO_x emissions where the other methods are not sufficient. Studies showed that CS is more effective for NO_x reduction, especially in the temperature range of 1000−1400 °C [Zabetta *et al.* 2005]. For temperatures below 850 °C, higher N_2O, lower NO_x and slightly higher CO emissions are reported for co-combustion of coal and woody biomass [Svoboda *et al.* 2003].

3.2.3 Flue gas recirculation

Another technique of primary measures for NO_x reduction in biomass combustion is flue gas recirculation (FGR) which basically increases the total mass flux of the gases and decreases the temperature and the partial pressure of oxygen in the mixture [Bauer *et al.* 2010]. It is proposed that in fixed-bed combustion of straw, the effect of FGR on NO reduction could be considerable [Zhou *et al.*].

The NO_x reduction through FGR is achieved in three steps:

1. the recirculated flue gas acts as an inert gas, containing mainly CO_2, H_2O, a low level of O_2, and N_2. When mixed with the combustion air, it lowers the temperature in the flame region and hence reduces the thermal NO_x formation;
2. by mixing the flue gas with the combustion air, the oxygen availability in the reaction zone is reduced, which consequently affects the NO_x formation chemistry;
3. by increasing the residence time as a result of recirculating NO_x emissions to the reactor and let it go through the combustion zone for a second time.

In a real FGR process, the high concentration of CO_2 affect the formation of H/O/OH radicals, which are critical for NO_x emissions [Normann *et al.* 2010]. In addition to the FGR effects on actual residence time and the radical formation mechanisms, higher CO_2 concentration in the inlet oxidant may result in enhanced char nitrogen conversion [Hosoda *et al.* 1998]. The primary source of NO_x formation from oil and natural gas combustion is thermal NO_x since these fuels have lower or no nitrogen content and higher combustion temperature. Biomass, on the other hand, contains considerable amounts of fuel nitrogen which promotes the formation of fuel NO_x during combustion. It is, therefore, important to understand that, in general, FGR in biomass combustion systems may not be as effective as in technologies applying natural gas or oil burners. However, it has been proven that air staging and flue gas recirculation are effective NO_x reduction methods for high N-content fuels [Anuar and Keener 1995].

Oxygen enrichment in the inlet air is studied mostly in coal combustion and co-combustion systems [Luo *et al.* 2009; Nimmo *et al.* 2010; Kazanc *et al.* 2011]. Recent investigations have also been carried out for O_2/CO_2 as oxidant rather than using oxygen enriched air [Liu *et al.* 2011]. This study showed that in coal combustion, the fuel-N to NO conversion factor decreased with an increasing CO_2 concentration in the presence of coal. They also stated that due to the interaction of fuel-N with recycled NO, the conversion ratio decreased with an increasing NO concentration in the recycled gas and the global conversion factor depends on the excess air ratio, findings which are consistent with the present investigation. Reburning of recirculated NO from the flue gas is also studied using propane in a burner to avoid fuel-N and heterogeneous effects [Kühnemuth *et al.* 2011]. Those experiments showed that the reduction by reburning is lower in oxy-fuel (high O_2 concentration in the inlet oxidant) compared to air combustion, and applying FGR in oxy-fuel combustion increased the total NO reduction. Combustion of different types of coal in an electrically heated combustor under a recycling ratio of 0−0.4 showed a recycled-NO reduction of 60−80% at excess air ratio of <0.7 while the reduction was less at low recycling ratio [Hayashi *et al.* 2002; Hu *et al.* 2003]. Effects of CO_2 concentration, recycled NO_x, and interaction between fuel-N and recycled NO_x on NO_x emission are studied in coal combustion with recycled CO_2 showing 50−80% reduction of recycled NO in the furnace [Okazaki and Ando 1997].

Due to the higher nitrogen content of waste fuels, many studies have also been done in waste combustion plants. [Bianchini *et al.* 2009] performed a study in a fluidized bed reactor with 60% recirculation of hot flue gas. Their study included temperature effect and showed that NO_x emissions can be reduced up to 30% in waste-to-energy plants using FGR. A NO_x reduction of up to 20% was also achieved for a waste incineration plant using about 25% FGR ratio [Liuzzo *et al.* 2007]. Investigations on high temperature air combustion in incineration of solid waste also showed that NO_x emission significantly decreased as a result of decreased oxygen concentration by FGR, with an overall range of NO_x reduction of 28−38% [Suvarnakuta *et al.* 2010].

3.3 Ash related problems

Although concerns for climate change and global warming are of great importance for the world, the economics of bioenergy plants pushes the energy producers to look for cheaper alternatives as feedstock. Therefore, use of herbaceous and agricultural biomass, energy crops, waste wood, municipal solid waste, etc. instead of wood has increased recently; since the price of virgin wood may be so high, making the energy production unfeasible, especially if the plant is located far from the biomass source which imply high transportation cost (taking into account the low energy density of biomass). However, cheap biomass fuels result in serious difficulties in the combustion system. Herbaceous biomass and wastes normally have higher ash content and higher amount of problematic elements compared to wood. Straw has lower carbon content and higher Cl and N content. Potassium, that is a low melting alkali is significantly higher in straw, which intensify problems such as fouling, agglomeration, slagging and corrosion [Nielsen *et al.* 1999]. The combination of chlorine and potassium in a herbaceous fuel decrease the ash melting temperature considerably, making the combustion condition worse [Yin *et al.* 2008]. The chlorine content in biomass is in the range of 0.01−0.9% and normally is highest in animal biomass and straw and decreases in the order: grass, herbaceous and agricultural biomass, residues and wood [Vassilev *et al.* 2010]. Sewage sludge and MSW have high amounts of ash, up to 50 wt%, which causes problems for ash collecting. In addition, existence of large amounts of heavy metals in the ash composition makes ash problematic due to sustainability (ash utilization and recycling) and particulate emissions. Figure 3-3 shows the flow of main ash elements in a combustor. Heavy metals are toxic and accumulate in the food chain. Ash treatment and fractional heavy metal separation is used to regulate the amount of these elements in the ash composition while dust precipitation and treatment of condensates can reduce the particulates [Van Gerven *et al.* 2007].

Formation of hydrogen chloride (HCl), Cl_2 or alkali chlorides (KCl and NaCl) in the combustion process [Nielsen *et al.* 2000] is unavoidable from any biomass having Cl in

the composition. During the combustion of straw, almost 80% of the total Cl released is retained in the ash, while in the case of wood combustion it is lower. Alkali metals and Si contents of the biomass can react with Cl, therefore the higher amount of those elements, the higher the integration of Cl in the ash. Hence, straw combustion will lead to higher levels of HCl and salts, i.e. alkali chlorides.

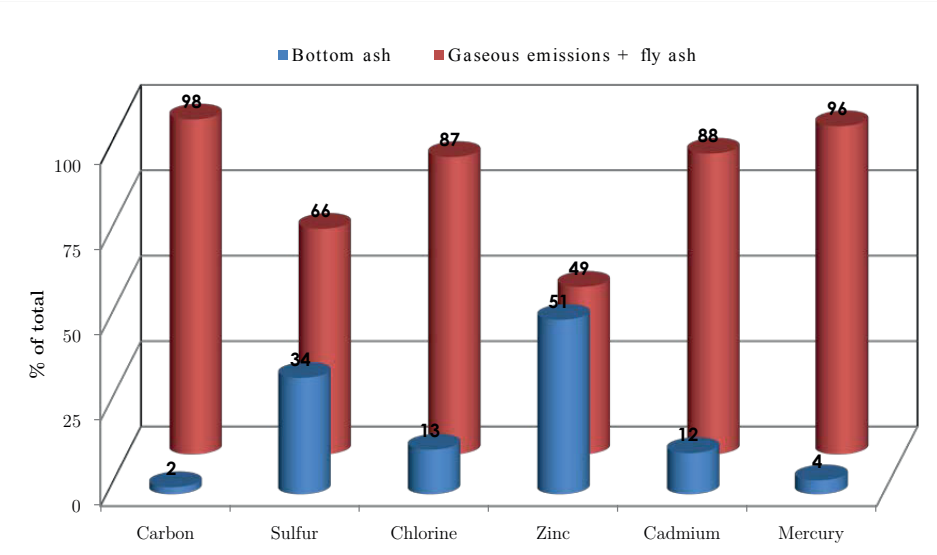

FIGURE 3-3: Flow of selected elements through an MSW combustor.

Red columns represent gaseous emissions including fly ash material, and blue columns represent share of elements in bottom ash. Adapted from [Brunner and Mönch 1986].

The most important issue of Cl is the corrosive behavior of HCl, NaCl and KCl on the metal parts of the boiler and furnace. However, environmental effects of HCl emission and chlorine containing particulates (alkali chlorides: KCl, NaCl and Zn-Pb chlorides: $ZnCl_2$, $PbCl_2$) should be taken into account as well as the effect of HCl on the formation of polychlorinated dibenzo-p-dioxins (PCCDs) and polychlorinated dibenzofurans (PCDFs) which are toxic environmental pollutants [Riedl *et al.* 1999]. The importance of Zn and Pb is because of their effect in the promotion of corrosion by Cl components. Zn and Pb chlorides increase the formation of low-temperature eutectics and, therefore, speed up corrosive reactions [Becidan *et al.* 2010]. In the boiler section of the biomass combustion plants, especially in the heating tubes, the corrosion problem is more due to the subsequent cooling of the flue gas; a large part of the Cl condenses at lower temperatures as alkali chloride salts on the heat exchanger surfaces or on fly ash particles in the flue gas [Davidsson *et al.* 2008]. Particulate matters, PM emissions, are affected by

a series of elements in the fuel. PM contain normally alkali salts like potassium chloride and potassium sulfates; thus the initial fuel composition, especially the percentage of potassium, chloride and sulfur is really important for creation of dust emissions.

The mechanism for the corrosion process of Cl containing species can be explained by different reaction chains. The alkali chlorides condense on the surfaces and react with the sulfur dioxide of the flue gas to form alkali sulfates and gaseous chlorine according to the following sulfation reactions [Nielsen *et al.* 2000].

$$2\ NaCl + SO_2 + O_2 \rightarrow Na_2SO_4 + Cl_2\ (g) \qquad (3\text{-}14)$$

$$2\ KCl + SO_2 \rightarrow K_2SO_4 + Cl_2\ (g) \qquad (3\text{-}15)$$

On the iron surface, Cl_2 can diffuse to the interface to react with Fe and form ferrous chloride. For the stability of $FeCl_2$, the oxygen partial pressure should be close to zero. However, $FeCl_2$ has a high steam pressure, and therefore, will partly evaporate in the flue gas direction due to the higher oxygen partial pressure. The ferrous chloride will react with oxygen and form iron oxides according to oxidation reactions such as ($3\ FeCl_2 + 2O_2 = Fe_3O_4 + 3Cl_2$). The formed Cl_2 can again react with the iron surface to intensify the corrosion cycle [Riedl *et al.* 1999]. A simple schematic illustration of the mechanism is shown in Figure 3-4.

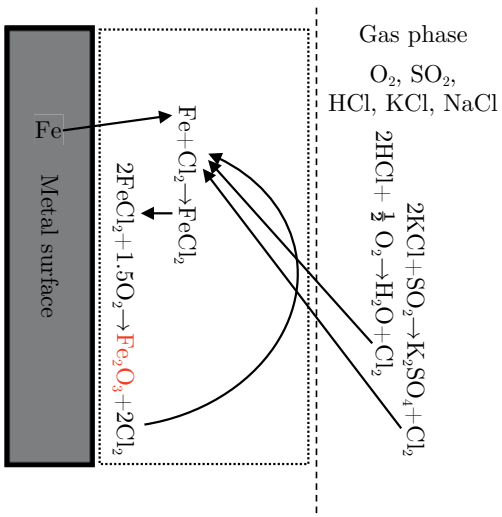

FIGURE 3-4: Corrosion mechanism by alkali chlorides and HCl.

Fuel leaching (washing of biomass to decrease the Cl content) [Dayton *et al.* 1999], automatic cleaning of boiler parts, tubes coating and modification to the reactor

materials are different methods to reduce the effect of corrosion from Cl. To regulate the environmental effect of HCl, sorption (dry or in activated carbon) and scrubbers (using limestone) can also be applied [Obernberger *et al.* 2006].

In addition, a simple primary measure is to change the elemental composition of biomass by mixing different kinds of biomass together to make it unproblematic [Salour *et al.* 1993; Steenari and Lindqvist 1999; Pettersson *et al.* 2008] or co-firing of risky biomass with the non-problematic fuels [Spliethoff *et al.* 2000; Lundholm *et al.* 2005; Davidsson *et al.* 2007a; Aho *et al.* 2010; Munir *et al.* 2010]. Blending can also result in a reduction to the price [Obernberger 1998]. Fuel mixing is normally used for the capture of alkalis in the bottom ash. The other approach is to capture the alkali chlorides in the combustion reactor using additives. Capturing of alkali metals with additives to form species with high melting points will decrease the risk of agglomeration and deposition, hence reduce corrosion problems. Different ash elements are able to capture alkalis. A series of additives has been suggested and studied by researchers, mainly including Al and Si in the structure. Bauxite, kaolinite, calcite, emathlite, dolomite, diatomaceous earth, fly ash from coal, kaolin, limestone and calcium oxide are some well-known additives to capture alkalis in biomass combustion reactors, and kaolin is proposed to be the best absorbent to capture potassium [Davidsson *et al.* 2007b; Bartels *et al.* 2008; Vamvuka *et al.* 2008; Boström *et al.* 2009]. Kaolin ($Al_2O_3 \cdot 2SiO_2 \cdot H_2O$) reacts with the potassium in the deposits and forms silicate minerals like potash mica or potassium aluminum silicates which all have high melting point. However, it should be noted that reactions between alkali chlorides and additives like aluminum silicates may result in the release of HCl from solid material in the bed and freeboard [Coda *et al.* 2001]. The reaction mechanism is according the following reactions:

$$Al_2O_3 \cdot 2SiO_2 \cdot 2H_2O_{(s)} \rightarrow Al_2O_3 \cdot 2SiO_{2(s)} + 2H_2O_{(g)} \qquad (3\text{-}16)$$

$$Al_2O_3 \cdot 2SiO_{2(s)} + 2MCl + H_2O_{(g)} \rightarrow M_2O \cdot Al_2O_3 \cdot 2SiO_{2(s)} + 2HCl_{(g)} \qquad (3\text{-}17)$$

Addition of S to the combustion process has a positive effect on capturing alkali chlorides, and therefore, to decrease corrosion effects. In fact, sulfur as an additive to the furnace shifts alkalis from chlorides to sulfates. The reaction between SO_2 and alkali chlorides is too slow while the sulfation reaction of alkali chlorides with SO_3 is fast enough in the gas phase, and produces alkali sulfates and HCl. Anyhow HCl is less corrosive and is not sticky. Therefore, it can be removed from the flue gas by secondary measures in the gas cleaning step using equipment like scrubbers. The formation rate of SO_3 in the oxidation reaction of SO_2 and decomposition of aluminum sulfate is the limiting parameter for the sulfation reactions [Davidsson *et al.* 2008; Kassman *et al.* 2010].

Phosphorus can also be a helpful agent by capturing potassium in ash and formation of phosphates. During straw combustion, potassium has been found to be taken up by mono

calcium phosphate. High concentration of phosphorus in biomass fuels such as sewage sludge, in turn, promotes the formation of phosphates and prevents formation of corrosive deposit [Elled *et al.* 2010]. However, a high amount of P in the biomass composition will interfere with the sulfur capture, if the aim is to decrease the amount of SO_x emissions in the combustion process [Elled *et al.* 2006].

Several chemical elements are known to prevent Cl from reaching and depositing on heat-exchange surfaces. The main known beneficial elements include Al and Si (mainly as aluminosilicates) and S (mainly as sulfates). The main modes of action of aluminosilicates and sulfur are presented in reactions (3-18) and (3-19) where M represents Na or K [Aho *et al.* 2010; Elled *et al.* 2010].

$$Al_2O_3 \cdot x\,SiO_2(s) + 2\,MCl(g) + H_2O(g) \rightarrow M_2O \cdot Al_2O_3 \cdot x\,SiO_2(s) + 2\,HCl(g)\ \text{(chemisorption)} \quad \textit{(3-18)}$$

$$SO_3(g) + 2\,MCl(g) + H_2O(g) \rightarrow 2\,HCl(g) + M_2SO_4(s)\ \text{(sulfation)} \quad \textit{(3-19)}$$

Reaction (3-19) requires the formation of SO_3, the key component of fast sulfation. SO_3 can originate from the oxidation of sulfur or the decomposition of sulfates, with the latter being more effective.

A third (physical and not chemical) route is also possible, where alkali and/or Cl are bound to the additive ash by van der Waals forces (i.e., absorption).

Furthermore, compounds such as Al, Si, Ca, P, Fe, and more generally "reactive" (i.e., available for reactions) ash compounds [Pommer *et al.* 2009] are expected to affect alkali chemistries, but the mechanisms involved, either physical or chemical, are not clear [Pettersson 2008]. The overall picture of corrosion reduction in real systems is therefore complex to describe in detail.

The corrosion reduction processes are either sequestrating alkali or alkali chlorides or forming alkali sulfates. Cl is either physically (by capture) or chemically (by forming HCl) prevented from depositing (by condensation as vapor or impaction as part of particles/aerosols).

The aforementioned elements may be introduced in the combustion system using dedicated additives, but an innovative solution is co-combustion of biomasses with high corrosion propensities with additional biomass fuels containing high concentrations of aluminosilicates and/or sulfur and/or other ash compounds. This will often be cheaper and allows for safe and sound disposal of the secondary fuels. Such materials include peat, sludge (sewage, pulp, digested, raw, etc.), and coal ash.

Different indicators have been used in the literature to quantify corrosion and deposition potential in biomass fired systems. For example having a high S/Cl ratio, results in sulfates domination and low amount of KCl in deposits. When the S/Cl ratio is low, KCl

dominates. An S/Cl ratio of about 4−6 may decrease the mass flow of Cl in the fine fly ash to about one fourth of the original value, and strongly decrease Cl deposition and risk of corrosion, whereas values lower than 2 are considered as high corrosion risk [Aho *et al.* 2010; Kassman *et al.* 2010]. The excess of sulfur compared to alkalis is illustrated by the ratio 2S/(K+Na), where the higher values are proposed to give lower corrosion due to alkali sulfation. The importance of the (Al+Si)/(K+Na) ratio is connected to the reactions of alkali with aluminum silicates; e.g. addition of sewage sludge increases this ratio [Åmand *et al.* 2006; Davidsson *et al.* 2007a]. Chloride–sulfate molar ratio (Cl+2S)/(K+Na), 2S/(2Ca+K+Na), Cl/(K+Na), (Al+Si)/Cl and 2Ca/(2S+Cl) are also among the commonly used deposition indices [Yin *et al.* 2008]. At high (Cl+2S)/(K+Na) ratio, higher amount of gaseous HCl and SO_2 emissions will be produced, thereby the chlorine content will go towards HCl production instead of alkali chloride species [Tissari *et al.* 2008]. The minimum suggested value for the (Al+Si)/Cl molar ratio is 8−10 to avoid chlorine in deposits where $Al_2(SiO_3)_3$ formation becomes more important than sulfation for the reduction of Cl concentration in deposits and fouling rate [Aho and Silvennoinen 2004].

Straw is an agricultural byproduct from grains and oilseed crops. Straw is a high chlorine-, high potassium-, and high silica-containing biomass. The composition of straw makes it a fuel with both high corrosion and high deposition propensities. Extensive experience from Denmark confirms these challenges, but it does not prevent this country from combusting more than 1 million tons of straw annually in large straw-fired boilers and also farm plants, to produce about 5 TWh bioenergy [FVM 2008]. In the meantime, straw is almost completely unused for energy purposes in Norway and is often considered a waste. The annual potential for bioenergy from straw in Norway has been evaluated to 2.5 TWh [KanEnergi 2007]. Despite its challenges, straw is of interest because it is readily available and cheap because it is considered a largely useless residue today.

Sludge is a semi-solid mixture of particles and water left from industrial wastewater (in the pulp and paper industry, for example) or sewage treatment. About 100,000 tons of sewage sludge (total solids) recovered from treatment plants were reported as “disposed of” in 2008 in Norway [Berge and Mellem 2009; Climate and Pollution Agency 2011]. While more than 80% are used for soil improvement, it is unclear how much (if any) is used to produce energy in thermal systems today. Even though biogas collection from the anaerobic fermentation of sewage sludge and its further use for energy production (CHP) is currently happening, no sewage sludge was combusted in Norway as of 2005 because of high costs and because the authorities have been restrictive in authorizing sewage sludge combustion because it is considered to be a valuable fertilizing agent (especially concerning the recycling of phosphorus) [Nedland 2005]. However, the current fate of the remaining 20% (given as unknown, other, landfilling, or cover material in landfill sites) may be considered less sound than combustion with energy recovery, especially when sewage sludge is considered a valuable corrosion-fighting additive.

Peat is an accumulation of partially decayed vegetal matter rich in humus and carbon [Uhlig and Fjelldal 2005; Teknisk Ukeblad 2011]. Its formation rate is slow, but it may still be exploited in a sustainable manner. Peat briquettes and pellets can be combusted in wood-burning stoves. The total Norwegian resources are evaluated to 5000 million cubic meters of raw peat [Uhlig and Fjelldal 2005; Teknisk Ukeblad 2011], equivalent to 700 million tons of crude oil or 300 million tons of coal. This corresponds to a total energetic value of 8000 TWh (for comparison, the net domestic end-use of energy in Norway in 2005 was 225 TWh, with half of it being electricity). Its annual growth (in Norway) is evaluated to an energy potential of 4–8 TWh. Contrary to countries such as Finland, these peat resources are almost completely unexploited today and, hence, offer a large energetic reservoir.

Peat, sludge, and straw are used in the present study in mixture form to investigate alkali release and the effect of blending with regard to the alkali content. This is reported in Paper VIII and Paper IX. The sewage sludge addition was very effective at reducing the alkali chlorides. The grot addition was deemed to have an insignificant effect on reducing the alkali chloride concentration in the flue gas. Peat was found to contribute to a reduced corrosion environment only when highly supplemented to straw.

Chapter 4

Experimental Approach

This chapter describes how the experiments were carried out. The measurement and sampling devices are introduced.

Experimental procedure, the composition of fuels (ultimate and proximate analyses), and the relevant standards for characterization are explained thereafter.

4.1 Multifuel reactor setup

Multifuel reactors are flexible reactors for fuel testing. They are designed to be as flexible as possible with respect both to fuels and reaction conditions. The features of the reactor used in this study are as follows, and will be explained further:

- Gas type and amount selection
- Gas mixing
- Gas preheating to desired temperature (up to 1300 °C)
- Preheated secondary (tertiary) gas addition
- Combustion, gasification or pyrolysis
- 4 temperature zones in the reactor
- Computer regulated temperature programs both in the reactors and preheaters

- Continuous fuel feed
- Continuous ash removal from the grate
- Bottom ash sampling
- Fly ash sampling
- Flue gas analysis: GC, FTIR, conventional analyzers
- Data logging: temperatures, gas flows, flue gas composition
- Inspection hole

The reactor is shown in Figure 4-1. It is installed vertically and has a total height of 2 m. The inner diameter is 100 mm. The reactor is made of ceramic material (alumina based) and has two reactor tube sections, each 1 m high.

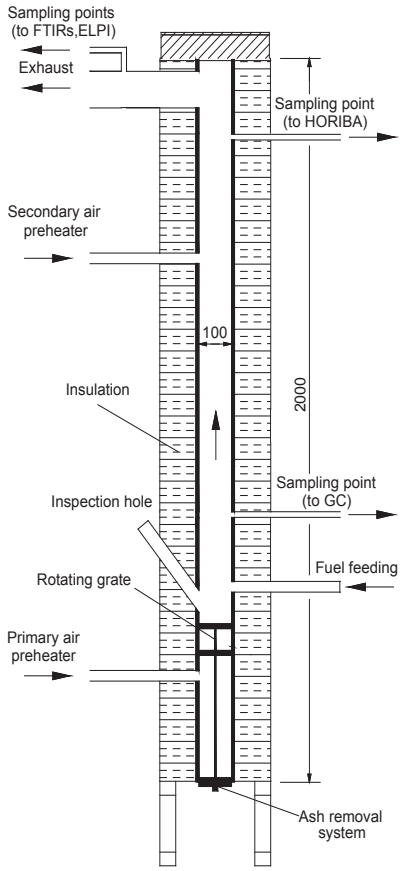

FIGURE 4-1: Schematic drawing of the multifuel reactor (the sizes are given in mm).

A rotating grate, with two grate levels, is placed 0.4 m from the bottom of the reactor, which means that the combustion zone is 1.6 m high. The two grate levels are 10 cm apart and there are rotating blades on each level that moves the unburnt fuel particles on the grates and from the upper grate to the second grate and from the second grate to the ash bin, through a slot in the grates. The rotational speed of the blades is about 3 min per revolution. This means that the residence time of each pellet on the grates is up to about 6 minutes, totally. This ensures complete burnout of the particles/char at the lower grate and that the ashes can be collected in the bottom of the reactor, i.e. in the ash bin. The grates and the ash bin are shown in Figure 4-2.

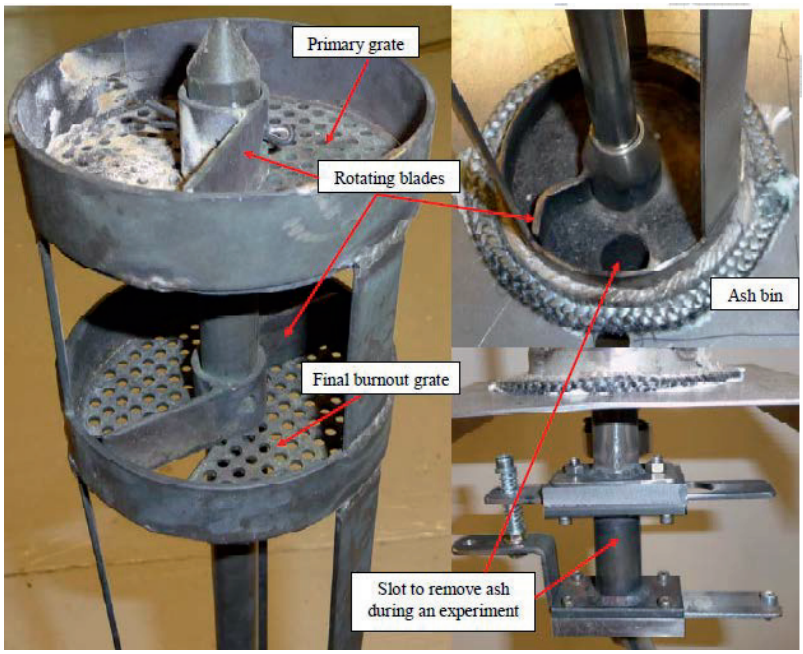

FIGURE 4-2: The design of two grates and ash bin.

A view glass is located just above of the upper grate to be able to see the combustion zone from the outside. The residence time of the fuel in the reactor is high and the gas in the reactor has very low flow velocity (0.04–0.07 m/s). The secondary combustion zone ensures a residence time of several seconds, and is therefore in fact comparable to conventional combustion systems. According to the given reactor dimensions and velocity, the residence time for the primary zone (90 cm) is 13–23 sec and for the secondary zone (70 cm) 10–18 s, giving a total residence time of 23–41 sec. The outer surface of the reactor is insulated, and the reactor heating system has an effect of 16 kW, composed of four identical electric heaters with a height of 0.5 m.

FIGURE 4-3: The multifuel reactor.

The reactor can be heated up to 1300 °C, and the fuel feeding rate can be up to 500 g/h. A pneumatic-vibration based feeding system is installed to ensure automatic fuel feeding at a set rate. Pellets are fed by a water-cooled moving piston into the reactor and immediately fall down on the upper grate. Air can be fed to the reactor in three stages (below the lower grate, above the upper grate (two inlets) and at one level higher up (two inlets)), up to 120 Nl/min, totally. Five preheaters are installed, one for each air inlet stream, to heat the feeding air to the reactor temperature before entering the reactor. The air flow rate is controlled by mass flow controllers via a PC.

4.2 Sampling and measurements

As shown in Figure 4-4, gas is extracted in four places to carry out analysis and further measurements. The flue gas composition is measured by means of three gas analyzers. In case of staged air combustion, a gas chromatograph (GC) is used to measure the gases in the primary section. The GC is sampling between the first and the second combustion stage and is a Varian CP-4900 Micro-GC. Sampling for the GC is made through an 8

mm diameter stainless steel probe and the gas is passed through an ice bath to ensure removal of water, particles and tars, in addition to reducing the temperature to an acceptable level for the GC. The sampling condition is non-condensing gas of 0−40 °C and the maximum sample pressure is 200 kPa. The GC is equipped with two dual-channel micro-machined thermal conductivity detectors (TCD), with a detection limit of 1 ppm for WCOT (wall-coated open-tubular) columns. The WCOT column is a column in which the liquid stationary phase is coated on the essentially unmodified smooth inner wall of the tube. The sample flow rate is 1 l/min and the sampling time interval is 2 minutes. Argon and helium are used in two columns, 10 m and 20 m long, respectively. The first column measures CH_4, CO_2, C_2H_2+C_2H_4 and C_2H_6 while the second column measures H_2, O_2, N_2, CH_4 and CO.

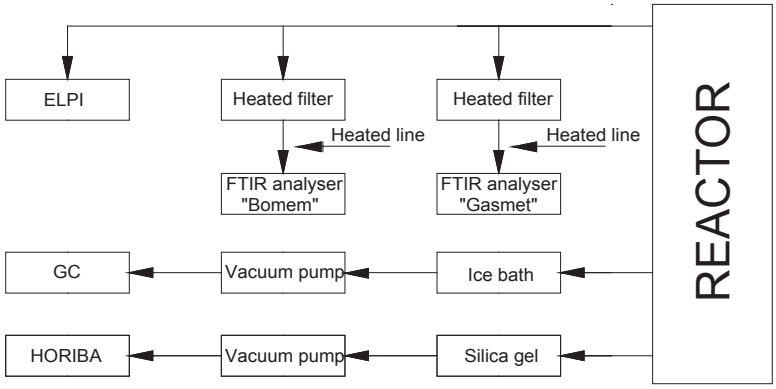

Figure 4-4: Schematic diagram of the sampling line.

A Horiba multi-species gas analyzer PG-250 is sampling from the top of the reactor. It is capable of measuring five components; NO_x, SO_2, CO, CO_2 and O_2, with the same methods used by permanent CEMS (continuous emissions monitoring system). These include pneumatic NDIR (non-dispersive infrared) for CO and SO_2; pyrosensor NDIR for CO_2; chemiluminescence (cross-flow modulation) for NO_x; and a galvanic cell for O_2 measurements. A vacuum pump is used to extract the sample gas at a flow rate of 0.4 l/min from the top of the reactor and passes it through a silica gel box and a filter to remove moisture and particles. The response time (T_{90}) of the analyzer is less than 45 sec for NO_x, CO, O_2 and CO_2 and less than 240 sec for SO_2. The Horiba analyzer is equipped with a drain separator unit (DS-200) and an electronic cooler unit.

Two FTIR analyzers (Fourier Transform Infrared spectroscopy) are also used to measure the gas composition in the exhaust gas. They do sampling at the same point, which allows for comparing different measurements for these species: H_2O, CO_2, CO, NO, N_2O, NO_2, SO_2, NH_3, HCl, HF, CH_4, C_2H_6 and C_3H_8. The Gasmet DX-4000 FTIR analyzer incorporates a spectrometer, a temperature controlled sample cell and signal processing

electronics. The sample cell is heated up to 180 °C which ensures that the sample stays in gaseous phase even with high concentrations of condensable hydrocarbons. The measurement time is typically 60 sec and the spectrometer resolution is 4 cm^{-1} at a scan frequency of 10 scans/s. The sample cell has a multi-pass fixed path length of 5 m and a volume of 0.4 l. To measure O_2, an optional oxygen sensor, based on a ZrO_2 cell, is attached to the analyzer. In total it can measure C_2H_4, C_6H_{14}, CHOH, HCN and O_2 in addition to the abovementioned 13 gases.

A Bomem MB 9100 FTIR analyzer is also used, to measure common mutual species and C_4H_{10}. The measurement time is typically 80 sec. A large cell, operating at 176 °C and equipped with a 1 cm^{-1} spectral resolution detector, was handling the analyses. Generally FTIR measurements of NO may introduce significant uncertainties. However, the NO_x emissions reported in the results part are based on the Horiba analyzer, which is using chemiluminescence technique. The N_2O measurements were made by the FTIR analyzers, and the reported values were measured by the Gasmet FTIR. The Bomem FTIR showed N_2O values close to the values measured by the Gasmet FTIR.

The temperatures at different levels in the reactor are measured by means of thermocouples and are monitored continuously to control and protect the furnace operation. These thermocouples are used to set and control the temperatures of the air preheaters and the reactor wall heaters during heat-up and during experiments.

Bottom ash collected in the ash bin, is removed manually after each test. Unburned carbon in the bottom ash was measured after each experiment by weighting the ash before and after exposing it to a temperature of 550 °C for a period of 20 hours. The chemical composition of the bottom ash was determined by the ICP-AES and ICP-SFMS methods. The particle sizes and size distribution of the flue gas samples were measured by a 12 stage electrical low-pressure impactor (ELPI) in the range of 0.03-10 µm and were collected on aluminum plates. The plates were covered by a thin layer of Vaseline to provide a sticky surface. The chemical analyses of the samples were made by energy-dispersive X-ray analysis connected to a scanning electron microscope, SEM/EDX. The total mass of the particles on each plate was around 10-100 µg and the detected elements by the analysis were C, O, Na, Mg, Al, Si, P, S, Cl, K, Ca, Fe, Zn and Pb. However, the signals for several of the measured elements were interfacing with the matrix, as discussed in [Backman *et al.* 2011], therefore, the results of C, O and Al are excluded.

4.2.1 Data treatment

Since the fuels were fed as pellets of different sizes and the position of the pellets on the grate after feeding varied, natural variations in primary and secondary excess air ratios are achieved. Consequently, the mentioned situation makes it possible to experimentally derive the effect of primary excess air ratio on the NO_x reduction potential by staged air combustion. It should be noted that data treatment has been carried out in a cautious

manner to avoid non-reliable data. Significant transient effects are effectively eliminated by a filtering procedure while treating the experimental data.

All experiments were checked with respect to carbon and hydrogen balance using both the Horiba analyzer and the Gasmet FTIR. Data points which:

1. did not satisfy a maximum deviation between the calculated and measured levels of CO_2 and
2. were clearly influenced by fast transient conditions

were removed from the results. This is because these data points were not reliable or not representative respectively for a close to continuous and constant combustion process.

The data treatment for the FTIR to measure the nitrogen intermediate species present as minor compounds in a gas stream containing a wide variety of compounds, were checked manually. The sample line for this FTIR was cooled down in order to remove all compounds that could potentially harm the instrument due to condensation. For that reason all of the tars and most of the water were removed. NH_3 was checked in the spectral range 1180−1100 cm^{-1} and at a distinctive peak that should be located at 1626 cm^{-1}. Two different methods were developed for the prediction of NO: the measurement of the height of an undisturbed peak at the wave length 1875.6 cm^{-1} and the use of a PLS (Partial Least Square) model in the region of 1916−1895 cm^{-1}. The PLS model was compensated for interferences from CH_4, C_2H_4 and H_2O. Both methods were developed using NO levels generated by mixing a calibration gas containing NO (in N_2) with N_2 purity of 5.0. NO was calibrated for the range 0–350 ppm. Both methods yielded a NO concentration that was within a window of 5 % compared to each other. For the calculations used in this work, the data from the PLS model was used. The challenging work was however to develop a method for HCN. HCN in the FTIR spectrum is present in the narrow wavelength range of 3400−3200 cm^{-1}. This range also absorbs C_2H_2 and H_2O and no single peak can be used for the prediction of HCN. A PLS model was developed for HCN prediction in the range 3382−3350 cm^{-1} which also included the compensation of the above mentioned compounds. HCN was calibrated by using spectra with concentrations of 0−350 ppm. The quality of the model was checked by measuring the height of a single peak after the spectra was subtracted manually for the interference caused by C_2H_2 and H_2O. In order to do so, the prediction of the interfering compounds was performed prior to HCN. The subtraction was made using a function in the software that was provided with the FTIR. This process is time consuming and was only performed on selected spectra to make sure that the PLS model was performing satisfactorily. The difference between the two methods was similar in magnitude to the NO prediction.

4.3 Fuels

The biomasses that have been used for this work are selected from a wide range of different categories: demolition wood, straw, sewage sludge, peat, tops and branches, and wood pellets. The received biomass is pelletized with a pellet machine to get a similar shape and composition for all the experimental runs. Figure 4-5 shows the final pellets from some of the fuels and sewage sludge in its original shape. To ensure a homogeneous distribution, a large volume of fuel samples was shredded to sawdust size, followed by thorough mixing. Pellets were then made from these fine pieces. Hence, variation in the N-content is not regarded as a challenge in these experiments.

The type of biomass, the origin of it and the pre-treatment technology applied to it, are important parameters influencing the ultimate and proximate analysis of the biomass. For example drying can reduce the moisture content from 65% in virgin wood down to below 10% in wood pellets.

As mentioned earlier, fuel mixing can be used to regulate some fuel properties: chemically and physically. Blending biomass fuels with different physical/elemental properties can optimize heating value, moisture content, ash content/composition and the amount of volatile matters. Increasing moisture content, decreases heating value, ignition range and combustion temperature, and increases flue gas yields while higher volatile content results in an increased combustion rate and the combustion process needs to be controlled accordingly. To avoid agglomeration, formation of low-melting alkali silicate phases should be avoided. A high agglomeration temperature can be reached by reaction of alkali with S to form alkali sulfates, instead. In addition, higher content of Al, Si and Ca in the fuel and adding silicate minerals to the process is leading to products with high melting point.

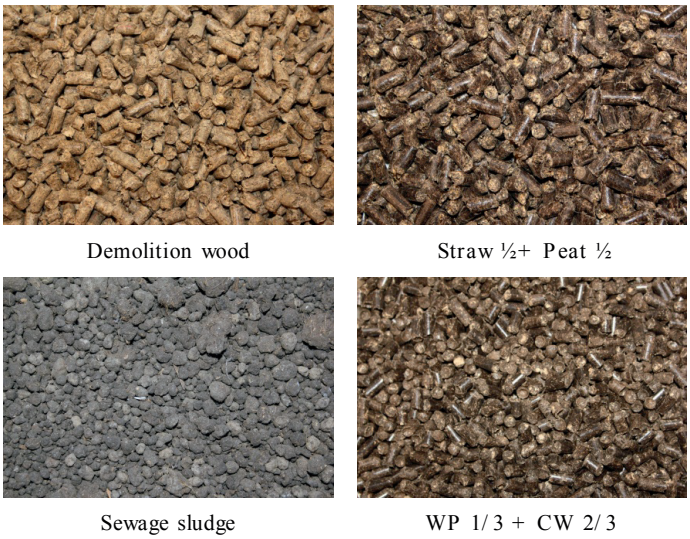

FIGURE 4-5: Some samples of the fuels and mixtures.

The proximate analyses of the present fuels are shown in Table 4-1 where the moisture content is measured during each experimental run. Moisture, VM and ash content are measured using ASTM E871 (50 g, 103±2 °C, 24 hr), ASTM E872 (1 g, 950 °C, 7 min) and ASTM D1102 (2 g, 580−600 °C, 4 hr) standards, respectively and the fixed carbon is calculated by difference to 100%. Three samples are analyzed from different parts of the pellets to get repeatable analyses, showing that the fuel was homogenous. Volatile matters for wood chips, bark and straw are normally in the range of 76−86, 70−77 and 70−81 wt%, respectively [Berndes *et al.* 2008], while for the DW it was 75.97%, as shown in Table 4-1.

TABLE 4-1: Proximate analysis of fuel pellets (wt%).

Pellets	Ash	Volatile matter	Fixed carbon	Moisture	HHV (MJ/kg)
Wood No.1 (WP§)	0.2	85.43	14.37	6.5	20.63
Demolition wood No.1 (DW§)	3.73	77.27	19	8.1	20.54
Coffee waste (CW)	5.8	76.17	18.07	17.53	22.2
½ WP§ + ½ DW§	1.97	81.35	16.69	6.78	20.62
½ WP§ + ½ CW	3	80.8	16.22	8.76	21.36
½ DW§ + ½ CW	4.77	76.72	18.54	12.72	21.24
2/3 WP§ + 1/3 CW	2.07	82.34	15.6	11.35	21.08
1/3 WP§ + 2/3 CW	3.93	79.26	16.84	8.02	21.55
1/3 WP§ + 1/3 DW§ + 1/3 CW	3.24	79.62	17.15	24.53	21.04
Demolition Wood No.2 (DW‡)	2.49	75.97	21.54	9.7–15	19.79
Wood No.2 (WP‡)	0.2	85.3	14.5	6.5	20.7
Branches and Tops (GG)	2.3	77	20.7	9.6	21.8
Straw	4.9	78.7	16.4	11.7	19.9
Sewage Sludge (SS)	35.6	56	8.5		21.1
Peat	10.3	65.4	24.3		22.9
WP‡ + GG 5%	0.4	84.6	15	14.4	20.8
WP‡ + GG 20%	0.6	83	16.5	14.4	20.9
WP‡ + GG 50%	1.3	80.7	18	11.8	21.2
Straw + GG 20%	4.4	77.9	17.7	13.8	20.4
Straw + GG 50%	3.6	77.5	18.9	11.8	20.9
Straw + SS 5%	6.3	77.6	16.1	12.8	20
Straw + SS 10%	7.9	76.6	15.5	15.4	20
Straw + SS 20%	11.8	73.6	14.6	9.4	20
Straw + Peat 5%	5.2	77.6	17.1	11.2	20
Straw + Peat 20%	5.9	77.1	17.1	14.4	20.3
Straw + Peat 50%	7.4	73.1	19.5	17.1	21.1

Table 4-2 shows the ultimate analysis (dry ash free) of the fuels and mixtures. All the samples have been dried in a vacuum exsiccator over phosphorus pentoxide prior to analysis. The determination of C/H/N/S is performed using an "EA 1108 CHNS-O" elemental analyzer. The method is adjusted for sample amounts of 2 to 10 mg and performs with an uncertainty within 0.3 wt% as required for confirmation of assumed chemical composition. The operation range covers the content from 100 to 0.1 wt%;

sulfur determination is in the concentration range of 1.0 down to at 0.01 wt% and the uncertainty is estimated to be 0.02 wt% for C/N/S/Cl. The nitrogen content, which is the most important element in this study, is in the range of 0.11−7.02%. The common nitrogen range for fuels such as wood, straw, peat, sewage sludge and coal is 0.03−1, 0.3−1.5, 0.5−2.5, 2.5−6.5 and 0.5−2.5 wt%, respectively [Glarborg *et al.* 2003].

TABLE 4-2: Ultimate analysis of fuel pellets (wt% dry ash free basis).

Pellets	**C**	**H**	**O**	**N**	**S**	**Cl**
Wood No.1 (WP[§])	51.22	6.07	42.54	0.14	0.03	0.02
Demolition wood No.1 (DW[§])	50.59	6.09	41.65	1.59	0.075	0.113
Coffee waste (CW)	52.9	6.47	37.64	2.8	0.187	0.038
½ WP[§] + ½ DW[§]	50.91	6.08	42.11	0.85	0.052	0.065
½ WP[§] + ½ CW	51.98	6.25	40.33	1.34	0.101	0.028
½ DW[§] + ½ CW	52.01	6.06	39.21	2.58	0.137	0.085
2/3 WP[§] + 1/3 CW	51.93	6.06	40.8	1.14	0.08	0.027
1/3 WP[§] + 2/3 CW	52.79	6.04	38.68	2.35	0.141	0.036
1/3 WP[§] + 1/3 DW[§] + 1/3 CW	51.72	6.07	40.45	1.67	0.097	0.061
Demolition Wood No.2 (DW[‡])	48.45	6.37	44.11	1.06	0.02	0.05
Wood No.2 (WP[‡])	51.4	6.1	42.4	0.11	0.05	0.02
Branches and Tops (GG)	53.4	6.2	39.9	0.43	0.12	0.04
Straw	49.5	6.1	43.6	0.5	0.21	0.1
Sewage Sludge (SS)	48.9	7.4	34.6	7.02	2.07	0.1
Peat	56	6.1	35	2.6	0.34	0.02
WP[‡] + GG 5%	51.5	6.1	42.3	0.12	0.06	0.02
WP[‡] + GG 20%	51.7	6.1	41.9	0.17	0.07	0.02
WP[‡] + GG 50%	52.3	6.1	41.2	0.27	0.09	0.03
Straw + GG 20%	50.3	6.2	42.8	0.48	0.2	0.09
Straw + GG 50%	51.5	6.2	41.7	0.46	0.17	0.07
Straw + SS 5%	49.5	6.2	43.3	0.72	0.28	0.1
Straw + SS 10%	49.5	6.2	43	0.94	0.34	0.1
Straw + SS 20%	49.4	6.3	42.3	1.42	0.47	0.1
Straw + Peat 5%	49.8	6.1	43.3	0.58	0.22	0.1
Straw + Peat 20%	50.5	6.1	42.3	0.82	0.23	0.09
Straw + Peat 50%	52.2	6.1	40	1.39	0.27	0.06

Table 4-3 shows the composition of the main ash constituents for the different straw mixtures with other problematic fuels.

TABLE 4-3: Main Elements in Ash (wt%, db; Zn and Pb are in mg/kg (db)).

	Si	**Al**	**Ca**	**Fe**	**K**	**Mg**	**Mn**	**Na**	**P**	**Ti**	**Zn**	**Pb**
Straw + GG 20%	1.06	0.01	0.39	0.01	0.7	0.07	0.01	0.02	0.08	-	18.6	0.49
Straw + GG 50%	0.73	0.01	0.47	0.01	0.55	0.07	0.03	0.02	0.06	-	41.3	0.73
GG	0.24	0.02	0.65	0.02	0.28	0.05	0.07	0.03	0.05	-	77.3	0.94
Straw + SS 10%	1.59	0.15	0.64	0.59	0.76	0.12	0.01	0.03	0.44	0.01	85.7	2.45
Straw + SS 20%	1.82	0.32	0.96	1.24	0.71	0.17	0.01	0.05	0.85	0.03	171	4.52
Straw + Peat 20%	1.5	0.1	0.52	0.1	0.75	0.09	0.01	0.02	0.1	-	6.7	0.59
Straw + Peat 50%	1.94	0.38	0.69	0.29	0.52	0.09	0.01	0.07	0.08	0.01	9.14	1.8

4.4 Experimental procedure

Experiments are performed for non-staged and staged air combustion. All the experiments are performed at a constant temperature of 850 °C, except for the case with varying temperature where four different temperatures are selected; 850, 900, 950 and 1000 °C. During each experiment, the temperature is kept constant for the reactor, and primary air and secondary air are kept at the mentioned values. All the sampling devices are calibrated each day, before starting the experiments. Also Gasmet FTIR calibration was performed daily by means of background spectra.

Pellets with a diameter of 6 mm and a length of 10−15 mm are fed by the automatic feeding system. The fuel feeding rate is set to 400 g/hr. To have a precise composition of the fuel, during each run, three different samples at three different times are taken from the fuel feeding system to analyze the moisture content.

The total excess air ratio for non-staged combustion is set to 1.6; however, the variation in the fuel feeding rate allows capturing a total excess air ratio range of 1.2−3, making it possible to see emission trends as a function of total excess air ratio. Each experiment has been carried out for at least two hours at stable operating conditions.

For the staged air combustion experiments, the total excess air ratio is also set to 1.6, while the primary excess air ratio is set to 0.8, which means that 50% of the total air is fed at each stage. The air flow has been held constant during the experiments. However, the variations in the fuel feeding rate cause natural variations in primary and secondary excess air ratios, since the fuel was fed as pellets and, depending on the length of the pellets and the position of the pellets on the grate after feeding, natural variations in the excess air ratio occurred. Therefore, the mentioned situation makes it possible to experimentally derive the effect of variations in the primary excess air ratio on the NO_x

reduction potential by staged air combustion. Data treatment has been carried out in a cautious manner to avoid non-reliable data. Significant transient effects are effectively eliminated by a filtering procedure while treating the experimental data. This filtering procedure requires that the change in the excess air ratio per second is less than 0.01; otherwise, the complete measured dataset at the current time is omitted in the final results.

For studying the effect of fuels and their blends on emissions, particulates, ash related problems and corrosion some risky biomass and a series of their mixtures are studied. Thermodynamic calculations are used to optimize the fuel mixtures based on the four main inorganic elements: Al, Si, Ca and S [Becidan *et al.* 2011]. The selected biomasses are problematic fuels: straw, peat and sewage sludge; where the reference fuel is straw. All the experiments are done under air-staged condition to reduce the NO_x emission primarily.

Chapter 5

Modeling

In this chapter, a brief introduction is given to the modeling approach that has been used in this study for biomass combustion, a two-stage model, and reduction of reaction mechanisms.

5.1 Reactor model

As combustion is the most common way of extracting energy from biomass, modeling and simulations of combustors are of great interest for the community. A number of investigations have been carried out to characterize the chemical kinetics of the combustion process of solid fuels such as coal and biomass [Glarborg *et al.* 1992; Hori *et al.* 1998; Pedersen *et al.* 1998; Coda Zabetta *et al.* 2000; Skreiberg *et al.* 2004b; Coda Zabetta and Hupa 2008; Ranzi *et al.* 2008; Andersen *et al.* 2009; Hansen and Glarborg 2010b].

To study the effect of staged air combustion and combined fuel- and air-staging, a detailed chemical kinetics mechanism is applied to a reactor model which constitutes of a sequence of *ideal* reactors. The chemical model which is used consists of a comprehensive reaction system for the formation of nitrogen oxides in combustion. This includes both

the kinetics related to NO_x formation via the formation of hydrogen cyanide (HCN) [Dagaut *et al.* 2008], and ammonia chemistry [Skreiberg *et al.* 2004b] under fuel rich conditions and moderate temperatures which is important to capture the situation at the second fuel stage. The reactor is modeled by a set of connected ideal 0-D reactors; plug flow reactors (PFR) to mimic the combustion chamber and capture the combustion zones. Sequences of 0-D models are common in reactor simulations when the main focus is on details of the chemical processes rather than the physical processes, such as transport and mixing [Løvås *et al.* 2004]. Simulations are performed for a set of different running conditions of the reactor. This includes variations of overall excess air ratio of 1.0, 1.5, 2.0, 2.5 and 3.0; primary excess air ratio, ranging from 0 to 3.0; the composition of the fuel (effect of fuel-N content) with different fuel-N content level of 100, 300 and 1000 ppm in the pyrolysis gas, and reactor temperature of 700, 850 and 1000 °C. All the simulations are done at isothermal conditions.

The pyrolysis gas composition which is used for the present model, is based on the average values from pyrolysis experiments [Chan 1983], and includes seven species (excluding fuel-N content) with the molar concentration as stated in Table 5-1.

TABLE 5-1: Pyrolysis gas composition.

Species	CO	CO_2	CH_4	C_2H_2	C_2H_6	C_2H_4	H_2O
Vol%	44.74	26.61	8.93	0.16	1.11	2.02	16.43

A small amount of N-species is added to the above stated fuel gas composition. N-species in the pyrolysis gas is considered to be a combination of NH_3 and HCN. The ratio between ammonia and hydrogen cyanide (HCN/NH_3) is a function of temperature, increasing from 0.3 at 700 °C to 1.0 at 1000 °C [Hansson *et al.* 2004]. Therefore, the ratio for 850 °C is 0.65 assuming a linear variation.

The kinetics mechanism which is selected for the gas phase reactions inside the reactors is an updated version of the mechanisms developed by the combustion group at DTU [Mendiara and Glarborg 2009a; Mendiara and Glarborg 2009b; Tian *et al.* 2009]. It is called the master-C/H/O/N mechanism, involving 81 species and 703 reactions (1401 reactions in total; forward and backward). For modeling of the described reactors and to apply the chemical mechanism, the DARS software package is used [DARS 2011].

Figure 5-1-(A) shows the principle of the air staging scenario. For air staging, a combination of two plug flow reactors is used in the modeling. The first reactor has a diameter, a length and an inlet gas velocity of 100 mm, 1.5 m and 1.5 m/s, respectively. The second reactor has the same diameter as the first, but with a length of 0.5 m and an inlet gas velocity of 0.5 m/s. Each reactor has a residence time of 1 sec.

Similar to staged air combustion, the fuel staging geometry is modeled according to Figure 5-1-(B). For combined air- and fuel staging, a combination of three plug flow

reactor is used. The first and second reactors have a diameter, a length and an inlet gas velocity of 100 mm, 0.75 m and 1.5 m/s, respectively. The third PFR operates with the same conditions as the second PFR in the air staging scenario. The second stage for the fuel injection accounts for 30% of the total fuel.

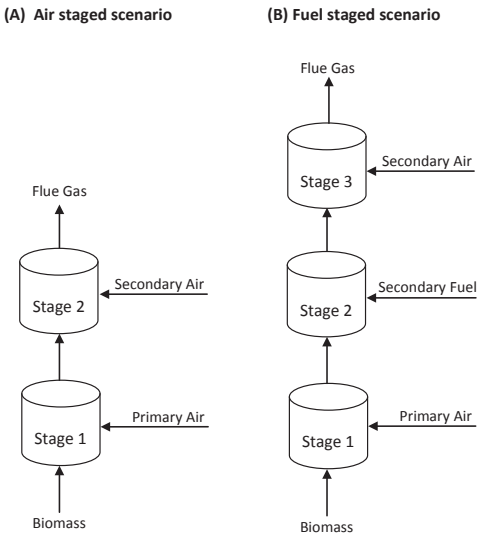

FIGURE 5-1: Reactors setup for staged combustion.

The input for the first reactor is the pyrolysis gas as stated in Table 5-1, adding NH_3, HCN, and air (21% O_2; 79% N_2) with an amount which is determined by the primary excess air ratio and the overall excess air ratio. Input for the next reactor is the flue gas from the previous reactor, plus the amounts of air or fuel (whether the stage is a fuel stage or an air stage) remaining of the total amount.

All results in this study concerning emissions from NO_x, CO, C_xH_y and N_2O are reported as the corrected values to 11% of O_2 in the dry-basis flue gas, to remove the effect of various degrees of dilution. Also to have a better view of how much of the initial N in the fuel is converted to molecular nitrogen; the TFN/Fuel-N ratio is used. TFN (total fixed nitrogen) is the total mass of nitrogen in the flue gas, (all gases coming out from the last reactor except for N_2), while fuel-N is the total mass of nitrogen in the input gas, excluding the N_2 content of the air input.

Discussions on the obtained results from this study are presented in Paper VII. The results show good consistency with the reduction level achieved in experiments.

5.2 Mechanism reduction

Studying the combustion of biomass due to its complex composition, having C, H, O, N, S, Cl and other minor and trace elements in the chemical composition, needs special attention with respect to emissions. The chemical mechanism should contain a wide range of species and therefore a large number of reactions to be able to perform a precise modeling analysis of biomass combustion reactors. On the other hand, to perform a complete CFD analysis, all the phenomena, including fluid flow, heat transfer and chemical kinetics should be modeled at the same time. Hence, implementing a complex and detailed mechanism into a CFD simulation is not always feasible due to expected long computational time and restricted hardware resources. Consequently, simplifying the computations by reducing the description of the chemical kinetics without loss of accuracy is an important task.

5.2.1 Reaction flow analysis

There are several ways to simplify the chemical model. A common procedure is to identify the major reaction paths by performing an element flux analysis, referred to as a reaction flow analysis [Warnatz *et al.* 2006]. It can be performed in any reaction system easily. In Figure 5-2, thick lines show reactions which are more probable, transferring most of the mass from the reactant to the product side.

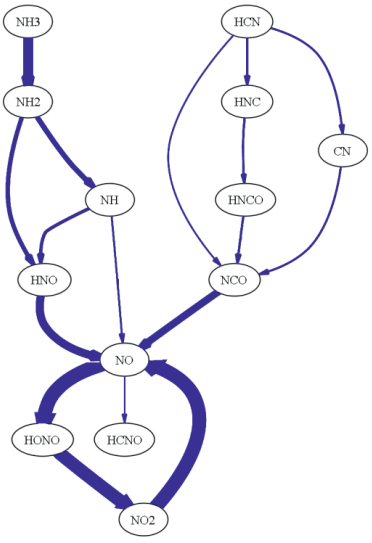

FIGURE 5-2: A sample reaction flow path diagram for nitrogen.

This type of analysis will enable the removal of the minor paths which are deemed not important for the reliable prediction of the significant combustion parameters, such as

temperature and major emissions. Mass flow of a specific atom from one species to another is determined from the following equation during a combustion process, where flow of element a from species j to species i is given by $F^a_{i,j}$ [DARS 2011]. This flow is integrated over time.

$$F^a_{i,j} = \int_{t=0}^{t_f} \left(\sum_{R=1}^{N_R} r_R(t) \left(v'_{jR} v''_{iR} - v''_{jR} v'_{iR} \right) \frac{n^a_j n^a_i}{\Delta n^a_R} \right) dt \qquad (5\text{-}1)$$

t is time, t_f is final reaction time, R is reaction number, N_R is total number of reactions involving element a, $r_R(t)$ is reaction rate, n^a_i is the number of a atoms in species i, v'_{iR} is the left hand side coefficient of species i in reaction R, v''_{iR} is the right hand side coefficient of species i in reaction R, and Δn^a_R is the total flow of atom a in reaction R; calculated by the following formula.

$$\Delta n^a_R = \sum_{k=1}^{N_s} n^a_k \left(v''_{kR} - v'_{kR} \right) \qquad (5\text{-}2)$$

where N_s is the total number of species in the mechanism.

5.2.2 Sensitivity analysis

In a sensitivity analysis, effects of species and reactions on specified parameters, e.g. temperature, are determined. In this way, reactions or species with low sensitivity on the target parameter can be ignored.

Sensitivity of a reaction, S^r, is defined as how much the target variable, Y, is changed when we apply 1% change to the Arrhenius coefficient, A_R.

$$S^r_{Y,R} = 0.01\, A_R \frac{\partial Y}{\partial A_R} \qquad (5\text{-}3)$$

Sensitivity of a species, S^s, is based on the same concept with 1% change in the concentration of species i, c_i.

$$S^s_{Y,j} = \frac{1}{0.01 c_i} \frac{dY}{d\alpha_i} \qquad (5\text{-}4)$$

where α_i is the error term for species concentration.

$$\alpha_i = 1 + \varepsilon_i; \qquad \varepsilon_i \prec\prec 1 \qquad (5\text{-}5)$$

A species which is only involved in minor flows can be very important in a short period of time. This species would be set as a redundant in the reaction flow analysis, while it

has a large effect on the reaction chain. Sensitivity analysis, however, is able to detect the importance of these species.

5.2.3 Necessity analysis

As explained in the previous sections, flow analysis has some limitations. However, the reaction flow analysis is usually combined with a sensitivity analysis to ensure that important species involved in only minor reaction flows are indeed kept in the model [Tomlin *et al.* 1997]. Necessity analysis is an improved reduction method, combining sensitivity and flow analysis.

In this method, a number of species such as NO_x, CO, and SO_x are defined as the target species, i.e., species of high importance as combustion products, beside other necessary targets such as temperature. The analysis aims at finding which species and reactions are necessary for the correct prediction of formation of the defined gases at the defined temperature condition. A list of necessary species can also be predefined by the user (species such as main reactants and products). This method is especially beneficial when the modeling aim is to study emissions from combustion processes [Løvås *et al.* 2004]. The necessity of species i is given by an index I_i, derived from the following equation:

$$I_i = \max\left\{I_j p^a_{i,j}, I_j c^a_{i,j}, I_i; j = \left[1, N_s\right], a = \left[1, N_a\right]\right\} \tag{5-6}$$

where the initial necessity value is calculated by:

$$I_{i,0} = \max\left\{\frac{S^s_{j,i}}{\max\left(S^s_{j,k}\right)_{k=\{1,N_s\}}}, B_i\right\} \tag{5-7}$$

N_a and N_s are number of atoms and species respectively, $S^s_{j,i}$ is the species sensitivity of species i, and B_i is 1 if species i is a user-defined necessary species and is 0 if not.

$p^a_{i,j}$ and $c^a_{i,j}$ are the reaction flow parameters and give the flow rate of element a by production of species i from species j and consumption from species i to species j, as defined below:

$$p^a_{i,j} = \frac{\int_{t=0}^{t_1}\left(\sum_{R=1}^{N_R} r_R\left(t\right) n^a_i \nu'_{jR}\nu''_{iR}\frac{1}{\Delta n^a_R}\right)dt}{\int_{t=0}^{t_1}\left(\sum_{R=1}^{N_R} r_R \nu'_{jR}\right)dt} \tag{5-8}$$

$$c_{i,j}^{a} = \frac{\int_{t=0}^{t_1} \left(\sum_{R=1}^{N_R} r_R(t)\, n_i^a v'_{jR} v''_{iR} \frac{1}{\Delta n_R^a} \right) dt}{\int_{t=0}^{t_1} \left(\sum_{R=1}^{N_R} r_R v''_{jR} \right) dt} \qquad (5\text{-}9)$$

5.2.4 Lifetime analysis

A further reduction is possible based on mathematical transformation of the chemical system based on a time scale analysis [Tomlin *et al.* 1997]. The underlying assumption is that many chemical reactions occur at time scales much shorter than the physical processes governing the system. The identification of reactions that are unimportant for both the fast and slow parts of the mechanisms enables that these can be treated in less detail by the numerical solver without considerable loss of accuracy, hence saving computational time. However, these methods require either a tabulation of the fast subspace or a separate treatment of the short lived species in the solver [Tomlin *et al.* 1997; Løvås 2002]. The time scale in a life time analysis is defined by;

$$\tau_i = \frac{1}{\partial \omega_i / \partial c_i} = \frac{c_i}{\sum_{j=1}^{N_R} \left(v'_{i,j} - v''_{i,j} \right)} v'_{i,k} r'_k \qquad (5\text{-}10)$$

where ω_i is concentration source term for species *i*. Lifetime analysis gives a good basis for steady state reduction.

5.3 Methodology

A detailed mechanism for biomass volatile oxidation has been the subject for a reaction flow and sensitivity analysis in order to generate a strongly reduced skeletal model in the last part of this study. The selected detailed mechanism contains 81 species and 703 elementary reactions. This mechanism includes C, H, O, and N in the structure while S, Cl, and the other trace elements are not included in the reaction flows. The mechanism has been used for predicting emissions from varying types of biomass sources [Skreiberg *et al.* 2004a; Skreiberg *et al.* 2004b; Mendiara and Glarborg 2009a; Tian *et al.* 2009]. It has furthermore been modified and extended over a period of time, and the latest version has been optimized only recently [Hansen and Glarborg 2010a; Klippenstein *et al.* 2011]. The mechanism is developed for the use in general solid fuel combustion systems, and the radical scheme is applicable for fuels ranging from bituminous coal to biomass. It should be noted that the present study only considers gas phase reactions as the chemical model in question does not include multi-phase reactions (solid to gas). The full treatment of

conversion from solid state to gas phase species will require extensive modeling including heat and mass transfer between the states, which is outside the scope of this work. Furthermore, a major section of the biomass furnace contains only gas phase species in a turbulent flow field. Hence, reduced chemical models for this section of the furnace are of great importance. Furthermore, to the knowledge of the authors, reduced mechanisms for oxidation of biomass volatiles is almost non-existent.

The modeling is done at a reactor temperature of 700−1400 °C, a residence time of 1, 0.1, 0.01 and 0.001 s, and an excess air ratio of 0.8−3.3 (equivalence ratio of $\varphi = 0.3 - 1.2$). For all the simulations isothermal condition is applied to a single PSR. For the model input, only the gas phase processes are considered and the primary (pyrolysis) gas is taken as the initial fuel mixture with the composition as shown in Table 5-2 [Becidan *et al.* 2007b; Houshfar *et al.* 2010a]. The values in Table 5-2 are averages for fiberboard (composed of spruce and pine) and pine wood pellets based on experimental data from the literature.

TABLE 5-2: Pyrolysis gas composition (vol%).

H_2	H_2O	CH_4	C_2H_2	C_2H_4	C_2H_6	CO	CO_2
14.45	8.22	11.73	0.23	2.88	1.58	39.14	21.77

The total fuel-N content is considered to be 1000 ppm which is typically valid for high nitrogen containing fuels, and here the selected gas composition for the model input is selected to have almost 2 wt% nitrogen in the original fuel. The HCN/NH_3 ratio is 0.65 based on a study on different types of biomass (whey protein, soya beans, yellow peas, shea, and bark) which showed that the HCN/NH_3 ratio is not significantly correlated with fuel O/N ratio, although it is slightly a function of temperature [Hansson *et al.* 2004]. The thermodynamic and transport properties have been taken from the CHEMKIN thermodynamic and transport databases [Kee *et al.* 1986; Kee *et al.* 1987].

H_2, N_2, H_2O, C_2H_2, C_2H_4, C_2H_6, NH_3, HCN, CO, CO_2, CH_4, O_2 are assumed as the necessary species and the necessity analysis targets are set to NO, NO_2, O_2, H_2O, and temperature. The necessity target species are selected so to carefully capture the NO_x concentration in the flue gas by the reduced mechanism. Since the final results are compared at the same flue gas condition (dry flue gas and 11% O_2 in the flow) to remove the effect of various degrees of dilution, O_2 and H_2O are also considered as they may have a small effect on the final results, and a true comparison of the NO_x level can be made for all cases. Reaction flow analysis is also used to check the flows of species at different conditions.

Three mechanisms are developed for different temperature ranges. The first reduced mechanism contains much fewer reactions and chemical species, i.e., 35 species and 198

reactions, corresponding to 72% reduction in the number of reactions and, therefore, improving the computational time considerably. Two more reduced mechanisms are also proposed for the high and low temperature range with 26 and 52 species, respectively. Further results and discussions are presented in Paper VI.

Chapter 6

Conclusions and Further Work

6.1 Concluding remarks

In this thesis, two-stage combustion technology has been used in a unique reactor setup in order to obtain maximum NO_x reduction with regard to various operational parameters. A detailed chemical kinetics model is then introduced for two-stage combustion and finally a reduced mechanism is developed for prediction of NO_x emissions in biomass combustion. Studies have also been carried out on corrosion related issues for high ash content fuels.

6.1.1 NO_x reduction

6.1.1.1 Fuel mixing and air ratio: Paper I, Paper III, and Paper IV

In this set of studies, we investigated NO_x, and N_2O, emissions for different biomass fuels and fuel mixtures thereof as pellets both with and without air staging in a grate fired multifuel reactor at a constant reactor set point temperature of 850 °C. The fuels investigated are wood, demolition wood, coffee waste, straw, tops and branches, sewage sludge, peat, and selected mixtures of these. The unburnt species' concentration (CO and C_xH_y) was very low in all cases due to the good combustion conditions.

A large NO_x reduction potential, up to 91% and corresponding to less than 20 ppm NO_x at 11% O_2 for a fuel containing about 3 wt% fuel-N, using air staging was found at the optimum primary excess air ratio. However, the reduction level depended on the excess air ratio at the first stage. An optimum primary excess air ratio of about 0.9 was found for the reactor in the primary zone (fuel rich condition). However, low ash melting characteristics of some of the fuels, particularly straw, caused this value to be somewhat higher due to sintering on the fuel grate.

The effect on N_2O, however, is adverse at the selected set point temperature and the optimum primary excess air ratio for NO_x reduction, with an increase in the N_2O emission level of up to 635%. The NO_x emission level increases with increasing fuel-N content, while the conversion factor for fuel-N to NO_x decreases with increasing fuel-N content. Fuel mixing has a positive influence on the NO_x emission level, but a negative influence on the overall conversion factor for fuel-N to NO_x and N_2O. The general conclusion is that air-staging can be effectively used in a grate combustion reactor in order to reduce NO_x emissions. Wood pellets with the lowest nitrogen content showed less reduction potential, while a blend of peat and sewage sludge, which had high fuel-N content, only converted about 2% of the fuel-N to NO_x and N_2O, the rest being converted directly to N_2, and a minor part remained in the ash.

Sewage sludge, having low VM and high ash content, is suggested as a favorable fuel to be blended with straw, showing high NO_x reduction and low fuel-N conversion. Grot, however, with high VM and low ash content, did not show desirable NO_x reduction and also made the combustion more unstable. The reduction potential for grot and sewage sludge mixtures was about 50% and 80%, respectively.

It is also found that fuel type influences the flue gas composition, especially the SO_x and NO_x levels depending on the fuel S and N levels. Further, higher probability of corrosion is expected in a plant fuelling forest residues compared to virgin wood, due to higher alkali content of the fuel. Air staging reduces HCl emissions somewhat, but does not have a clear effect on SO_x. Fuel mixing increases the small particles (aerosols at a range of 0.04−0.1 µm) emission in staged experiments, a behavior that is not noticed during experiments without air staging.

6.1.1.2 Temperature effect: Paper II

Experiments are carried out on demolition wood pellets showing that primary excess air ratio is the most important parameter which can be optimized for maximum conversion of fuel-N to N_2, hence reducing the NO_x level. The effect of two-stage combustion of biomass is significant for reduction of NO_x emission levels. Staged air combustion can reduce the emission level by 50−75% in average, and up to 85% at the optimum conditions. The maximum NO_x reduction happens when the primary air is injected at a primary excess air ratio of 0.8−0.95 and the total excess air ratio is 1.6−1.9 for staged air

combustion. The average N_2O level increase for the different temperatures is 75−1660%, but with a low amount of N_2O at high temperatures.

The NO_x emission level is not affected significantly by the reactor temperature neither in non-staged nor staged air combustion when temperatures are kept below 1000 °C in the reactor. Yet, the effect of temperature on the N_2O level is considerable. As expected, at high temperatures, N_2O emissions almost disappear. The results point to that the effects of moderate temperature and staged air combustion are counteractive for N_2O, meaning a negative influence on N_2O for staged air combustion. Therefore, to minimize N_2O emissions and reduce emissions of unburnt, temperatures of above 900 °C are beneficial for staged air combustion.

The C_xH_y emission level is almost independent of the combustion condition (staged air combustion or non-staged combustion), and is below 4 ppm at 11% O_2 in dry flue gas. CO emissions increase for staged air combustion compared to non-staged combustion by a factor of about 1.5 at a given temperature. Increasing temperature decreases the CO emission level in the whole temperature range of 850−1000 °C.

6.1.1.3 Modeling and mechanism reduction: Paper VI and Paper VII

The model based on ideal reactors showed that air- and fuel staging has considerable effect on NO_x reduction if an optimum primary excess air ratio is selected for the primary combustion zone, in agreement with what we have found in the experimental section. A NO_x reduction of up to 76% is achieved in the best case scenario. It is also shown that the potential of NO_x reduction is sensitive to other parameters such as: temperature, overall excess air ratio and fuel-N content. Increasing fuel-N content increases the NO_x reduction potential. Higher temperature gives lower emissions of CO and C_xH_y.

A set of three reduced mechanisms have been developed for biomass volatile oxidation. The chemical kinetics mechanism for biomass combustion is very sensitive to the combustion conditions and should be treated carefully in order to get correct results, and particularly the given temperature range has to be considered carefully when choosing the level of reduction. Furthermore, variations in temperature, excess air ratio, and residence time showed large effects on the NO_x level.

The reduced mechanisms have 52 species and 430 reactions, 35 species and 198 reactions, and 26 species and 91 reactions (compared with 81 species and 703 reactions in the detailed mechanism) applicable for a low, medium and high temperature range, respectively. However, even the intermediately reduced mechanism minimized the size of the detailed mechanism by almost 70% corresponding almost to the same amount of reduction in the time needed for such modeling or simulation works. The reduced mechanisms predict concentrations of NO_x very close to those of the complete mechanism in the range of reaction conditions of interest. In general it is found that for temperatures above 800 °C and excess air ratios of above 1.5 the reduced models give acceptable NO_x

results corresponding to errors less than 10%, although the very low residence time conditions have more narrow satisfactory range.

Additionally, a close to linear relationship is found between the reduction degree and the computational savings, which is reasonable taking into account the highly optimized solver used in this work and the already short calculation times associated with the PSR. Higher computational savings should be expected for less optimized solvers and for CFD applications.

6.1.2 Ash related problems

6.1.2.1 Fuel mixing: Paper VIII

Tree tops and branches, sewage sludge, and peat were mixed with straw to abate Cl-induced corrosion during combustion. The goal was to capture alkali metals in the bottom or fly ash, i.e., preventing the formation of corrosive alkali chlorides and promoting the formation of noncorrosive gaseous hydrogen chloride. The chemical composition of bottom ash and selected sub-micrometer particles in the flue gas were analyzed. The relative corrosion risk of the different fuel mixtures was classified on the basis of a careful observation of the obtained data. The following conclusions are drawn:

- The different fuel mixtures had a wide variation in the ash composition, which made the interpretation of the combustion results possible relative to the type and amount of the supplements used.
- Although the heterogeneous fuel was fed in a semi-continuous manner to the reactor, the measured combustion parameters showed good control over the process, where results were found to be consistent relative to time variation.
- The particle load in the flue gas was strongly influenced by sewage sludge, where a 10% addition resulted in a 65% decrease in the particle concentration in the flue gas compared to the fuel mixture of straw and 20 wt% grot. The reference experiment with pure straw could not be used as a baseline because of sintering problems, which rendered this experiment impossible to run in a reliable way. Grot, on the other hand, was not good as a fuel additive with straw because the aerosol load was influenced negatively at increased addition. Peat had a positive effect on decreasing the particle load, although an addition of 50% was needed to obtain similar results to the 20% sludge addition.
- The potential of chlorine corrosion could be best predicted through the results of the chemical composition of the aerosols. The grot addition was deemed to have an insignificant effect on reducing the alkali chloride concentration in the flue gas. Peat was found to contribute to a reduced corrosion environment only when highly supplemented to straw (50 wt%). The higher zinc concentration at this level of peat addition may reduce the overall effect gained in the reduced content

of alkali chlorides. The sewage sludge addition was very effective at reducing the alkali chlorides at 10% addition and almost eliminating them at 20% addition.

- The chlorine and sulfur distribution were calculated for all of the experiments and showed consistency with the other results concerning the corrosion risk, emphasizing the quality of the experiments.

6.1.2.2 Thermodynamics modeling: Paper IX

Different mixtures of peat and sewage sludge with straw were analyzed thermodynamically to obtain a mixture with the lowest formation of corrosive alkali chlorides during straw combustion.

The calculations confirm the corrosive alkali chloride reduction abilities of both biomass fuels as reported in the literature but also provide further information especially concerning threshold values (addition levels at which virtually no corrosion is predicted to happen): straw with 25 wt% sewage sludge or with 75 wt% peat. If straw is to be the main fuel, the 75 wt% value for peat is not possible, but if peat is the main fuel, it can be said that 25 wt% straw can be co-combusted without the formation of a significant amount of corrosive alkali chlorides. Experimental campaigns usually include no more than two–three mixtures, and therefore, no accurate threshold value can be proposed.

The mechanisms responsible for the disappearance of alkali chlorides are also recognized. The analyses indicate that the chemical elements preventing the formation of corrosive alkali chlorides vary with the additional fuel concentration, an important fact never mentioned in the literature to our knowledge. Attempts were made to use fuel molar ratios to further discuss these effects, but the complexity of the systems makes it difficult to draw clear conclusions. However, the practical implications of such a result are crucial; it is likely that, in a real system, local elemental concentrations (together with operating parameters, such as temperature and excess air ratio) will vary with time and space because of fuel and (fuel and air) distribution heterogeneities. This means that several mechanisms will simultaneously be responsible for eliminating corrosive alkali chlorides but also that the overall picture is not a static one. This may explain the enduring fact that most of the available experimental results are confusing, contradictory, and installation-specific.

S, Ca–S, or Al–Si is known to be the chemical elements reacting with alkalis during co-combustion of straw with sewage sludge or peat. The fact that some reactions are deemed impossible thermodynamically may indicate that the involved chemical compounds are only interacting with alkalis through adsorption, a physical process that cannot be studied by thermodynamic analysis. Combining experimental and modeling results leads to a more accurate and complete picture of the situation.

The trends for Pb and Zn chlorides are different from that of alkali chlorides because they are predicted to be found in higher concentrations in most mixtures compared to the pure fuels.

6.2 Recommendations for future work

For future studies the followings are suggested:

- ✓ Further research should be done on a wider range of fuels and fuel mixtures, including for example different types of waste (hazardous waste, clinical waste, and agricultural residues), local Norwegian wood and forest residues, etc.
- ✓ Future work should focus on getting more experimental results and measurements from the primary zone, especially for nitrogen containing species (NH_3, HCN, HNCO, and NO).
- ✓ It is recommended to carry out experimental campaigns on the effect of oxygen enriched atmosphere with O_2/N_2 and O_2/CO_2 atmospheres.
- ✓ Further improvement to the reactor, in order to modify and optimize the effect of the secondary air injection location, can be the scope of future studies.
- ✓ An improvement of the grate design, in order to optimize the effect of fuel staging on the NO_x reduction level is also recommended.
- ✓ A complete CFD modeling of the reactor, including reaction kinetics, heat and mass transfer, and hydrodynamics could be performed in order to compare the real reactor results with the developed model.
- ✓ For CFD modeling, a more compact reaction mechanism is desired to be developed for a narrow range of operating conditions, i.e. temperature, excess air ratio, etc.
- ✓ The developed mechanism should be tested and verified for a wider range of pyrolysis gas, i.e. to cover more fuels with different compositions.
- ✓ To understand the underlying kinetic behavior responsible for these trends, one needs to perform a careful reaction path and sensitivity analysis of the chemical system for a wide range of conditions, including fuel rich conditions. This could be part of future work also including the effect of turbulent mixing in the reactor.
- ✓ Thermodynamics modeling: Further work should focus on the influence of operating parameters, especially the influence of temperature, excess air ratio, and modes of occurrence of key elements.

- ✓ Due to the ash melting problems on the grate with straw mixtures, effect of flue gas recirculation should be the focus of further research for the low ash melting fuels.

Bibliography

Aho, M. and J. Silvennoinen (2004). "Preventing chlorine deposition on heat transfer surfaces with aluminium-silicon rich biomass residue and additive", *Fuel* 83(10): 1299-1305.

Aho, M., P. Yrjas, R. Taipale, M. Hupa and J. Silvennoinen (2010). "Reduction of superheater corrosion by co-firing risky biomass with sewage sludge", *Fuel* 89(9): 2376-2386.

Åmand, L. E., B. Leckner, D. Eskilsson and C. Tullin (2006). "Deposits on heat transfer tubes during co-cornbustion of biofuels and sewage sludge", *Fuel* 85(10-11): 1313-1322.

Andersen, J., P. A. Jensen, S. L. Hvid and P. Glarborg (2009). "Experimental and Numerical Investigation of Gas-Phase Freeboard Combustion. Part 2: Fuel NO Formation", *Energy & Fuels* 23(12): 5783-5791.

Anuar, S. H. and H. M. Keener (1995). Environmental performance of air staged combustor with flue gas recirculation to burn coal/biomass. *1995 ASAE annual international meeting*. Chicago, IL (United States).

Backman, R., R. A. Khalil, D. Todorović, Ø. Skreiberg, M. Becidan, F. Goile, A. Skreiberg and L. Sørum (2011). "The effect of peat ash addition to demolition wood on the formation of alkali, lead and zinc compounds at staged combustion conditions", *Fuel Processing Technology* doi: 10.1016/j.fuproc.2011.04.035.

Barnes, F., J. Bromly, T. Edwards and R. Mandyczewsky (1988). "NO_x emissions from radiant gas burners", *Journal of the Institute of Energy* 61(449): 184-188.

Bartels, M., W. G. Lin, J. Nijenhuis, F. Kapteijn and J. R. van Ommen (2008). "Agglomeration in fluidized beds at high temperatures: Mechanisms, detection and prevention", *Progress in Energy and Combustion Science* 34(5): 633-666.

Bauer, R., M. Gölles, T. Brunner, N. Dourdoumas and I. Obernberger (2010). "Modelling of grate combustion in a medium scale biomass furnace for control purposes", *Biomass & Bioenergy* 34(4): 417-427.

Becidan, M., Ø. Skreiberg and J. E. Hustad (2007a). "NO_x and N_2O Precursors (NH_3 and HCN) in Pyrolysis of Biomass Residues", *Energy & Fuels* 21(2): 1173-1180.

Becidan, M., Ø. Skreiberg and J. E. Hustad (2007b). "Products distribution and gas release in pyrolysis of thermally thick biomass residues samples", *Journal of Analytical and Applied Pyrolysis* 78(1): 207-213.

Becidan, M., L. Sørum and D. Lindberg (2010). "Impact of Municipal Solid Waste (MSW) Quality on the Behavior of Alkali Metals and Trace Elements during Combustion: A Thermodynamic Equilibrium Analysis", *Energy & Fuels* 24(6): 3446-3455.

Becidan, M., E. Houshfar, R. A. Khalil, Ø. Skreiberg, T. Løvås and L. Sørum (2011). "Optimal mixtures to reduce the formation of corrosive compounds during straw combustion: a thermodynamic analysis", *Energy & Fuels* 25(7): 3223–3234.

Berge, G. and K. B. Mellem (2009). "Kommunale avløp—Ressursinnsats, utslipp, rensing og slamdisponering 2008. Gebyrer 2009", *Statistics Norway*, Oslo, Norway.

Berndes, G., L. Baxter, P. Coombes, J. Delcarte, A. Evald, H. Hartmann, M. Jansen, J. Koppejan, W. Livingston, S. van Loo, S. Madrali, B. Moghtaderi, E. Nägele, T. Nussbaumer, I. Obernberger, H. Oravainen, F. Preto, Ø. Skreiberg, C. Tullin and G. Thek (2008). *The Handbook of Biomass Combustion and Co-firing*. London, Earthscan.

Bianchini, A., M. Pellegrini and C. Saccani (2009). "Hot waste-to-energy flue gas treatment using an integrated fluidised bed reactor", *Waste Management* 29(4): 1313-1319.

Biomass Energy Centre (2012). "*Fuel prices per kWh (excluding VAT)*", Retrieved 2012-02-08, from http://www.biomassenergycentre.org.uk/.

Boman, C., E. r. Pettersson, R. Westerholm, D. Boström and A. Nordin (2011). "Stove Performance and Emission Characteristics in Residential Wood Log and Pellet Combustion, Part 1: Pellet Stoves", *Energy & Fuels* 25(1): 307-314.

Boström, D., A. Grimm, C. Boman, E. Björnbom and M. Öhman (2009). "Influence of Kaolin and Calcite Additives on Ash Transformations in Small-Scale Combustion of Oat", *Energy & Fuels* 23(10): 5184-5190.

Bridgwater, A. V. (1990). "A survey of thermochemical biomass processing activities", *Biomass* 22(1–4): 279-292.

Bridgwater, A. V. (2003). "Renewable fuels and chemicals by thermal processing of biomass", *Chemical Engineering Journal* 91(2–3): 87-102.

Brunner, P. H. and H. Mönch (1986). "The flux of metals through municipal solid waste incinerators", *Waste Management & Research* 4(1): 105-119.

Chan, W. C. R. (1983). *Analysis of chemical and physical processes during the pyrolysis of large biomass pellets*. PhD PhD Thesis, University of Washington.

Chen, S. L., J. M. McCarthy, W. D. Clark, M. P. Heap, W. R. Seeker and D. W. Pershing (1988). "Bench and pilot scale process evaluation of reburning for in-

furnace NO_x reduction", *Symposium (International) on Combustion* 21(1): 1159-1169.

Climate and Pollution Agency (2011). from www.miljostatus.no.

ClimateTechWiki (2012). from http://climatetechwiki.org/technology/small-chp.

Coda, B., M. Aho, R. Berger and K. R. G. Hein (2001). "Behavior of Chlorine and Enrichment of Risky Elements in Bubbling Fluidized Bed Combustion of Biomass and Waste Assisted by Additives", *Energy & Fuels* 15(3): 680-690.

Coda Zabetta, E., P. Kilpinen, M. Hupa, K. Ståhl, J. Leppälahti, M. Cannon and J. Nieminen (2000). "Kinetic Modeling Study on the Potential of Staged Combustion in Gas Turbines for the Reduction of Nitrogen Oxide Emissions from Biomass IGCC Plants", *Energy & Fuels* 14(4): 751-761.

Coda Zabetta, E. and M. Hupa (2008). "A detailed kinetic mechanism including methanol and nitrogen pollutants relevant to the gas-phase combustion and pyrolysis of biomass-derived fuels", *Combustion and Flame* 152(1-2): 14-27.

Cremer, M., D. Wang, J. Bradley and D. Thompson (2003). "Staged Low NOx Combustion Systems for Coal Fired Boilers and Corrosion", *Praxair Technology, Inc.*

Dagaut, P., P. Glarborg and M. U. Alzueta (2008). "The oxidation of hydrogen cyanide and related chemistry", *Progress in Energy and Combustion Science* 34(1): 1-46.

DARS (2011). DARS - Software for Digital Analysis of Reactive Systems. *Available from: http://www.diganars.com/*. Delaware, USA, DigAnaRS.

Davidsson, K. O., L. E. Åmand, A. L. Elled and B. Leckner (2007a). "Effect of cofiring coal and biofuel with sewage sludge on alkali problems in a circulating fluidized bed boiler", *Energy & Fuels* 21(6): 3180-3188.

Davidsson, K. O., B. M. Steenari and D. Eskilsson (2007b). "Kaolin Addition during Biomass Combustion in a 35 MW Circulating Fluidized-Bed Boiler", *Energy & Fuels* 21(4): 1959-1966.

Davidsson, K. O., L. E. Åmand, B. M. Steenari, A. L. Elled, D. Eskilsson and B. Leckner (2008). "Countermeasures against alkali-related problems during combustion of biomass in a circulating fluidized bed boiler", *Chemical Engineering Science* 63(21): 5314-5329.

Dayton, D. C., B. M. Jenkins, S. Q. Turn, R. R. Bakker, R. B. Williams, D. Belle-Oudry and L. M. Hill (1999). "Release of Inorganic Constituents from Leached Biomass during Thermal Conversion", *Energy & Fuels* 13(4): 860-870.

Elled, A.-L., K. O. Davidsson and L.-E. Åmand (2010). "Sewage sludge as a deposit inhibitor when co-fired with high potassium fuels", *Biomass & Bioenergy* 34(11): 1546-1554.

Elled, A. L., L. E. Åmand, B. Leckner and B. A. Andersson (2006). "Influence of phosphorus on sulphur capture during co-firing of sewage sludge with wood or bark in a fluidised bed", *Fuel* 85(12-13): 1671-1678.

Fenimore, C. P. (1971). "Formation of nitric oxide in premixed hydrocarbon flames", *Symposium (International) on Combustion* 13(1): 373-380.

Fossum, M. (2002). *Biomass gasification: combustion of gas mixtures.* PhD Thesis, Norwegian University of Science and Technology.

FVM (2008). "Fuelling Future Energy Needs—The Agricultural Contribution", *The Danish Ministry of Food, Agriculture and Fisheries*, Copenhagen, Denmark.

Glarborg, P., N. I. Lilleheie, S. Byggstøyl, B. F. Magnussen, P. Kilpinen and M. Hupa (1992). "A reduced mechanism for nitrogen chemistry in methane combustion", *Symposium (International) on Combustion* 24(1): 889-898.

Glarborg, P., D. Kubel, K. Dam-Johansen, H.-M. Chiang and J. W. Bozzelli (1996). "Impact of SO2 and NO on CO oxidation under post-flame conditions", *International Journal of Chemical Kinetics* 28(10): 773-790.

Glarborg, P., A. D. Jensen and J. E. Johnsson (2003). "Fuel nitrogen conversion in solid fuel fired systems", *Progress in Energy and Combustion Science* 29(2): 89-113.

Hämäläinen, J. P., M. J. Aho and J. L. Tummavuori (1994). "Formation of nitrogen oxides from fuel-N through HCN and NH_3: a model-compound study", *Fuel* 73(12): 1894-1898.

Hansen, S. and P. Glarborg (2010a). "Simplified Model for Reburning Chemistry", *Energy & Fuels* 24(8): 4185-4192.

Hansen, S. and P. Glarborg (2010b). "A Simplified Model for Volatile-N Oxidation", *Energy & Fuels* 24(5): 2883-2890.

Hansson, K.-M., J. Samuelsson, C. Tullin and L.-E. Åmand (2004). "Formation of HNCO, HCN, and NH_3 from the pyrolysis of bark and nitrogen-containing model compounds", *Combustion and Flame* 137(3): 265-277.

Hayashi, J. i., T. Hirama, R. Okawa, M. Taniguchi, H. Hosoda, K. Morishita, C. Z. Li and T. Chiba (2002). "Kinetic relationship between NO/N_2O reduction and O_2 consumption during flue-gas recycling coal combustion in a bubbling fluidized-bed", *Fuel* 81(9): 1179-1188.

Hori, M., N. Matsunaga, N. Marinov, P. William and W. Charles (1998). "An experimental and kinetic calculation of the promotion effect of hydrocarbons on

the NO-NO_2 conversion in a flow reactor", *Symposium (International) on Combustion* 27(1): 389-396.

Hosoda, H., T. Hirama, N. Azuma, K. Kuramoto, J.-i. Hayashi and T. Chiba (1998). "NO_x and N_2O Emission in Bubbling Fluidized-Bed Coal Combustion with Oxygen and Recycled Flue Gas: Macroscopic Characteristics of Their Formation and Reduction", *Energy & Fuels* 12(1): 102-108.

Houshfar, E., T. Løvås and Ø. Skreiberg (2010a). "Detailed chemical kinetics modeling of NOx reduction in combined staged fuel and staged air combustion of biomass", *18th European Biomass Conference & Exhibition (EU BC&E)*, Lyon, France.

Houshfar, E., Ø. Skreiberg and T. Løvås (2010b). Emission Control through Primary Measures in Biomass Combustion. *The Renewable Energy Research Conference*. Trondheim, Norway.

Houshfar, E., Ø. Skreiberg and T. Løvås (2011a). NOx emission reduction by staged combustion in a grate fired multi-fuel reactor. *General Section Meeting of the Scandinavian-Nordic Section of the Combustion Institute (SNCI 2011)*. Trondheim, Norway.

Houshfar, E., Ø. Skreiberg, T. Løvås, D. Todorović and L. Sørum (2011b). "Effect of excess air ratio and temperature on NOx emission from grate combustion of biomass in the staged air combustion scenario", *Energy & Fuels* 25(10): 4643–4654.

Houshfar, E., R. A. Khalil, T. Løvås and Ø. Skreiberg (2012a). "Enhanced NO_x reduction by combined staged air and flue gas recirculation in biomass grate combustion", *Energy & Fuels* 26(5): 2003-2011.

Houshfar, E., T. Løvås and Ø. Skreiberg (2012b). "Experimental investigation on NO_x reduction by primary measures in biomass combustion: straw, peat, sewage sludge, forest residues, and wood pellets", *Energies* 5(2): 270-290.

Houshfar, E., J. Sandquist, W. Musinguzi, R. A. Khalil, M. Becidan, Ø. Skreiberg, F. Goile, T. Løvås and L. Sørum (2012c). "Combustion Properties of Norwegian Biomass: Wood Chips and Forest Residues", *Applied Mechanics and Materials* 110-116: 4564-4568.

Houshfar, E., Ø. Skreiberg, D. Todorović, A. Skreiberg, T. Løvås, A. Jovović and L. Sørum (2012d). "NO_x emission reduction by staged combustion in grate combustion of biomass fuels and fuel mixtures", *Fuel* (doi: 10.1016/j.fuel.2012.03.044).

Hu, Y. Q., N. Kobayashi and M. Hasatani (2003). "Effects of coal properties on recycled-NO_x reduction in coal combustion with O_2/recycled flue gas", *Energy Conversion and Management* 44(14): 2331-2340.

IEA Clean Coal Centre (2012). "*Pulverised coal combustion (PCC)*", from http://www.iea-coal.org.uk/site/2010/database-section/ccts/pulverised-coal-combustion-pcc?

IEA report (2008). "Energy Technology Perspectives, Scenarios and Strategies to 2050", *International Energy Agency*.

IEA report (2009). "World Energy Outlook 2009", *International Energy Agency*, Paris.

IEA report (2010). "Energy Technology Perspectives 2010, Scenarios and Strategies to 2050", *International Energy Agency*, Paris, France.

IEA task (2012). "*Bioenergy Task 34 for Pyrolysis*", Retrieved 2012-02-09, from http://www.pyne.co.uk.

IPCC (2007). "Contribution of Working Group III to the Fourth Assessment Report of the Intergovernmental Panel on Climate Change - Mitigation of Climate Change", Cambridge University Press, Cambridge, United Kingdom and New York, NY, USA.

Jenkins, B. M., L. L. Baxter and T. R. Miles (1998). "Combustion properties of biomass", *Fuel Processing Technology* 54(1-3): 17-46.

Johansson, L. S., B. Leckner, L. Gustavsson, D. Cooper, C. Tullin and A. Potter (2004). "Emission characteristics of modern and old-type residential boilers fired with wood logs and wood pellets", *Atmospheric Environment* 38(25): 4183-4195.

Johnston, H. S. (1992). "Atmospheric ozone", *Annual review of physical chemistry* 43(1): 1-31.

KanEnergi (2007). "Biomasse—Nok til alle gode formål?", Sandvika, Norway.

Kassman, H., L. Bafver and L. E. Åmand (2010). "The importance of SO_2 and SO_3 for sulphation of gaseous KCl - An experimental investigation in a biomass fired CFB boiler", *Combustion and Flame* 157(9): 1649-1657.

Kazanc, F., R. Khatami, P. Manoel Crnkovic and Y. A. Levendis (2011). "Emissions of NO_x and SO_2 from Coals of Various Ranks, Bagasse, and Coal-Bagasse Blends Burning in O_2/N_2 and O_2/CO_2 Environments", *Energy & Fuels* 25(7): 2850-2861.

Kee, R. J., G. Dixon-Lewis, J. Warnatz, M. E. Coltrin and J. A. Miller (1986). "The Chemkin Transport Database".

Kee, R. J., F. M. Rupley and J. A. Miller (1987). "The Chemkin Thermodynamic Database".

Khan, A. A., W. de Jong, P. J. Jansens and H. Spliethoff (2009). "Biomass combustion in fluidized bed boilers: Potential problems and remedies", *Fuel Processing Technology* 90(1): 21-50.

Kicherer, A., H. Spliethoff, H. Maier and K. R. G. Hein (1994). "The effect of different reburning fuels on NO_x-reduction", *Fuel* 73(9): 1443-1446.

Kilpinen, P. and M. Hupa (1991). "Homogeneous N_2O chemistry at fluidized bed combustion conditions: A kinetic modeling study", *Combustion and Flame* 85(1-2): 94-104.

Kilpinen, P., P. Glarborg and M. Hupa (1992). "Reburning chemistry: a kinetic modeling study", *Industrial & Engineering Chemistry Research* 31(6): 1477-1490.

Klippenstein, S. J., L. B. Harding, P. Glarborg and J. A. Miller (2011). "The role of NNH in NO formation and control", *Combustion and Flame* 158(4): 774-789.

Knudsen, J. N., P. A. Jensen and K. Dam-Johansen (2004). "Transformation and Release to the Gas Phase of Cl, K, and S during Combustion of Annual Biomass", *Energy & Fuels* 18(5): 1385-1399.

Kolb, T., P. Jansohn and W. Leuckel (1989). "Reduction of NO_x emission in turbulent combustion by fuel-staging/effects of mixing and stoichiometry in the reduction zone", *Symposium (International) on Combustion* 22(1): 1193-1203.

Kramlich, J. C., R. K. Nihart, S. L. Chen, D. W. Pershing and M. P. Heap (1982). "Behavior of N_2O in Staged Pulverized Coal Combustion", *Combustion and Flame* 48(1): 101-104.

KRAV (2008). "*http://www.sintef.no/Projectweb/KRAV/*".

Kühnemuth, D., F. Normann, K. Andersson, F. Johnsson and B. Leckner (2011). "Reburning of Nitric Oxide in Oxy-Fuel Firing—The Influence of Combustion Conditions", *Energy & Fuels* 25(2): 624-631.

Lang, T., P. A. Jensen and J. N. Knudsen (2006). "The Effects of Ca-Based Sorbents on Sulfur Retention in Bottom Ash from Grate-Fired Annual Biomass", *Energy & Fuels* 20(2): 796-806.

Laryea-Goldsmith, R. (2010). *Concurrent combustion of biomass and municipal solid waste*. PhD Thesis, Cranfield University.

Lin, W., P. A. Jensen and A. D. Jensen (2009). "Biomass Suspension Combustion: Effect of Two-Stage Combustion on NO_x Emissions in a Laboratory-Scale Swirl Burner", *Energy & Fuels* 23(3): 1398-1405.

Liu, H., Y. Yuan, H. Yao, S. Dong, T. Ando and K. Okazaki (2011). "Factors Affecting NO Reduction during O_2/CO_2 Combustion", *Energy & Fuels* 25(6): 2487-2492.

Liuzzo, G., N. Verdone and M. Bravi (2007). "The benefits of flue gas recirculation in waste incineration", *Waste Management* 27(1): 106-116.

Løvås, T. (2002). *Automatic reduction procedures for chemical mechanisms in reactive systems*. PhD, Lund Institute of Technology.

Løvås, T., D. Nilsson and F. Mauss (2004). "Development of Reduced Chemical Mechanisms for Nitrogen Containing Fuels", *International Journal of Energy for a Clean Environment* 5(3): 295-308.

Lundholm, K., A. Nordin, M. Ohman and D. Bostrom (2005). "Reduced bed agglomeration by co-combustion biomass with peat fuels in a fluidized bed", *Energy & Fuels* 19(6): 2273-2278.

Luo, S. Y., B. Xiao, Z. Q. Hu, S. M. Liu and Y. W. Guan (2009). "Experimental study on oxygen-enriched combustion of biomass micro fuel", *Energy* 34(11): 1880-1884.

Mahmoudi, S., J. Baeyens and J. P. K. Seville (2010). "NO_x formation and selective non-catalytic reduction (SNCR) in a fluidized bed combustor of biomass", *Biomass & Bioenergy* 34(9): 1393-1409.

Malte, P. and D. Pratt (1975). "Measurement of atomic oxygen and nitrogen oxides in jet-stirred combustion", Elsevier.

Mendiara, T. and P. Glarborg (2009a). "Ammonia chemistry in oxy-fuel combustion of methane", *Combustion and Flame* 156(10): 1937-1949.

Mendiara, T. and P. Glarborg (2009b). "Reburn Chemistry in Oxy-fuel Combustion of Methane", *Energy & Fuels* 23(7): 3565-3572.

Mereb, J. B. and J. O. L. Wendt (1994). "Air Staging and Reburning Mechanisms for NO_x Abatement in a Laboratory Coal Combustor", *Fuel* 73(7): 1020-1026.

Mohan, D., C. U. Pittman and P. H. Steele (2006). "Pyrolysis of Wood/Biomass for Bio-oil: A Critical Review", *Energy & Fuels* 20(3): 848-889.

Munir, S., W. Nimmo and B. M. Gibbs (2010). "Co-combustion of Agricultural Residues with Coal: Turning Waste into Energy", *Energy & Fuels* 24(3): 2146-2153.

Nedland, K. T. (2005). "Statusrapport for bruk av avløpsslam—Endringer siden år 2000", *Aquateam, Norsk Vannteknologisk Senter A/S*, Oslo, Norway.

Nielsen, H. P., F. J. Frandsen and K. Dam-Johansen (1999). "Lab-Scale Investigations of High-Temperature Corrosion Phenomena in Straw-Fired Boilers", *Energy & Fuels* 13(6): 1114-1121.

Nielsen, H. P., F. J. Frandsen, K. Dam-Johansen and L. L. Baxter (2000). "The implications of chlorine-associated corrosion on the operation of biomass-fired boilers", *Progress in Energy and Combustion Science* 26(3): 283-298.

Nimmo, W., S. S. Daood and B. M. Gibbs (2010). "The effect of O_2 enrichment on NO_x formation in biomass co-fired pulverised coal combustion", *Fuel* 89(10): 2945-2952.

Normann, F., K. Andersson, F. Johnsson and B. Leckner (2010). "Reburning in Oxy-Fuel Combustion: A Parametric Study of the Combustion Chemistry", *Industrial & Engineering Chemistry Research* 49(19): 9088-9094.

Normann, F., K. Andersson, F. Johnsson and B. Leckner (2011). "NO_x reburning in oxy-fuel combustion: A comparison between solid and gaseous fuels", *International Journal of Greenhouse Gas Control* 5(Supplement 1): S120-S126.

Nussbaumer, T. (1996). "Primary and secondary measures for the reduction of nitric oxide emissions from biomass combustion", *Developments in Thermochemical Biomass Conversion*, Banff, Canada, Blackie Academic & Professional.

Nussbaumer, T. (2003). "Combustion and co-combustion of biomass: fundamentals, technologies, and primary measures for emission reduction", *Energy & Fuels* 17(6): 1510-1521.

Obernberger, I. (1998). "Decentralized biomass combustion: state of the art and future development", *Biomass & Bioenergy* 14(1): 33-56.

Obernberger, I., T. Brunner and G. Bärnthaler (2006). "Chemical properties of solid biofuels--significance and impact", *Biomass & Bioenergy* 30(11): 973-982.

Okazaki, K. and T. Ando (1997). "NO_x reduction mechanism in coal combustion with recycled CO_2", *Energy* 22(2-3): 207-215.

Pedersen, L. S., P. Glarborg and K. Dam-Johansen (1998). "A Reduced Reaction Scheme for Volatile Nitrogen Conversion in Coal Combustion", *Combustion Science and Technology* 131(1&6): 193-223.

Pershing, D. W. and E. E. Berkau (1974). The Chemistry of Nitrogen Oxides and Control through Combustion Modifications. *Pollution Control and Energy Needs*. R. M. Jimeson and R. S. Spindt. Washington, DC, American Chemical Society. 127**:** 218-240.

Pettersson, A. (2008). *Characterisation of fuels and fly ashes from co-combustion of biofuels and waste fuels in a fluidised bed boiler—A phosphorus and alkali perspective*. PhD Thesis, Chalmers University of Technology.

Pettersson, A., M. Zevenhoven, B. M. Steenari and L. E. Åmand (2008). "Application of chemical fractionation methods for characterisation of biofuels, waste derived fuels and CFB co-combustion fly ashes", *Fuel* 87(15-16): 3183-3193.

Pommer, L., M. Ohman, D. Bostrom, J. Burvall, R. Backman, I. Olofsson and A. Nordin (2009). "Mechanisms Behind the Positive Effects on Bed Agglomeration and Deposit Formation Combusting Forest Residue with Peat Additives in Fluidized Beds", *Energy & Fuels* 23: 4245-4253.

Ranzi, E., A. Cuoci, T. Faravelli, A. Frassoldati, G. Migliavacca, S. Pierucci and S. Sommariva (2008). "Chemical kinetics of biomass pyrolysis", *Energy & Fuels* 22(6): 4292-4300.

Ravishankara, A. R., J. S. Daniel and R. W. Portmann (2009). "Nitrous Oxide (N_2O): The Dominant Ozone-Depleting Substance Emitted in the 21st Century", *Science* 326(5949): 123-125.

Ren, Q., C. Zhao, X. Wu, C. Liang, X. Chen, J. Shen and Z. Wang (2010). "Formation of NO_x precursors during wheat straw pyrolysis and gasification with O_2 and CO_2", *Fuel* 89(5): 1064-1069.

Riedl, R., J. Dahl, I. Obernberger and M. Narodoslawsky (1999). "Corrosion in fire tube boilers of biomass combustion plants", *China International Corrosion Control Conference '99, paper Nr.90129*, Beijing, China.

Roesler, J. F., R. A. Yetter and F. L. Dryer (1995). "Kinetic interactions of CO, NO_x, and HCI emissions in postcombustion gases", *Combustion and Flame* 100(3): 495-504.

Royal Dutch Shell plc (2008). "Shell energy scenarios to 2050", http://www-static.shell.com/static/public/downloads/brochures/corporate_pkg/scenarios/shell_energy_scenarios_2050.pdf.

Salour, D., B. M. Jenkins, M. Vafaei and M. Kayhanian (1993). "Control of in-bed agglomeration by fuel blending in a pilot scale straw and wood fueled AFBC", *Biomass & Bioenergy* 4(2): 117-133.

Salzmann, R. and T. Nussbaumer (2001). "Fuel Staging for NO_x Reduction in Biomass Combustion: Experiments and Modeling", *Energy & Fuels* 15(3): 575-582.

Seinfeld, J. (1986). Atmospheric Chemistry and Physics of Air Pollution, 738 pp, John Wiley and Sons, New York.

Skreiberg, Ø., P. Glarborg, A. D. Jensen and K. Dam-Johansen (1997). "Kinetic NO_x modelling and experimental results from single wood particle combustion", *Fuel* 76(7): 671-682.

Skreiberg, Ø., M. Becidan, J. E. Hustad and R. E. Mitchell (2004a). "Detailed chemical kinetics modelling of NO_x reduction by staged air combustion at moderate temperatures", *The Science in Thermal and Chemical Biomass Conversion Conference*, Victoria, BC, Canada, CPL Press.

Skreiberg, Ø., P. Kilpinen and P. Glarborg (2004b). "Ammonia chemistry below 1400 K under fuel-rich conditions in a flow reactor", *Combustion and Flame* 136(4): 501-518.

Sørum, L., Ø. Skreiberg, P. Glarborg, A. Jensen and K. Dam-Johansen (2001). "Formation of NO from combustion of volatiles from municipal solid wastes", *Combustion and Flame* 124(1-2): 195-212.

Spliethoff, H., W. Scheurer and K. R. G. Hein (2000). "Effect of co-combustion of sewage sludge and biomass on emissions and heavy metals behaviour", *Process Safety and Environmental Protection* 78(B1): 33-39.

Steenari, B. M. and O. Lindqvist (1999). "Fly ash characteristics in co-combustion of wood with coal, oil or peat", *Fuel* 78(4): 479-488.

Steenari, B. M., A. Lundberg, H. Pettersson, M. Wilewska-Bien and D. Andersson (2009). "Investigation of Ash Sintering during Combustion of Agricultural Residues and the Effect of Additives", *Energy & Fuels* 23: 5655-5662.

Strahle, W. C. (1993). *An Introduction to Combustion*, CRC.

Stubenberger, G., R. Scharler, S. Zahirovic and I. Obernberger (2008). "Experimental investigation of nitrogen species release from different solid biomass fuels as a basis for release models", *Fuel* 87(6): 793-806.

Suvarnakuta, P., S. Patumsawad and S. Kerdsuwan (2010). "Experimental Study on Preheated Air and Flue Gas Recirculation in Solid Waste Incineration", *Energy Sources, Part A: Recovery, Utilization, and Environmental Effects* 32(14): 1362-1377.

Svoboda, K., M. Pohořelý and M. Hartman (2003). "Effects of Operating Conditions and Dusty Fuel on the NO_x, N_2O, and CO Emissions in PFB Co-combustion of Coal and Wood", *Energy & Fuels* 17(4): 1091-1099.

Tariq, A. S. and M. R. I. Purvis (1996). "NO_x emissions and thermal efficiencies of small scale biomass-fuelled combustion plant with reference to process industries in a developing country", *International Journal of Energy Research* 20(1): 41-55.

Teknisk Ukeblad (2011). "*Alt om energi fra TU.no*", from http://energilink.tu.no/no.

Tian, Z., Y. Li, L. Zhang, P. Glarborg and F. Qi (2009). "An experimental and kinetic modeling study of premixed $NH_3/CH_4/O_2$/Ar flames at low pressure", *Combustion and Flame* 156(7): 1413-1426.

Tissari, J., O. Sippula, J. Kouki, K. Vuorio and J. Jokiniemi (2008). "Fine particle and gas emissions from the combustion of agricultural fuels fired in a 20 kW burner", *Energy & Fuels* 22(3): 2033-2042.

Tomlin, A. S., T. Turányi and M. J. Pilling (1997). Chapter 4 Mathematical tools for the construction, investigation and reduction of combustion mechanisms. *Comprehensive Chemical Kinetics*. M. J. Pilling, Elsevier. Volume 35**:** 293-437.

Trømborg, E., T. F. Bolkesjø and B. Solberg (2008). "Biomass market and trade in Norway: Status and future prospects", *Biomass and Bioenergy* 32(8): 660-671.

Turns, S. R. (1996). *An Introduction to Combustion: Concepts and Applications*, McGraw-Hill New York.

Uhlig, C. and E. Fjelldal (2005). "Torv til strø og talle i Nord-Norge. Grønn Kunnskap e", *Planteforsk*, Lofthus, Norway.

UNDP (2000). "World Energy Assessment: Energy and the Challenge of Sustainability - Part III: are sustainable futures possible?", http://www.undp.org/energy/weapub2000.htm.

Vamvuka, D., D. Zografos and G. Alevizos (2008). "Control methods for mitigating biomass ash-related problems in fluidized beds", *Bioresource Technology* 99(9): 3534-3544.

Van Gerven, T., H. Cooreman, K. Imbrechts, K. Hindrix and C. Vandecasteele (2007). "Extraction of heavy metals from municipal solid waste incinerator (MSWI) bottom ash with organic solutions", *Journal of Hazardous Materials* 140(1-2): 376-381.

Vassilev, S. V., D. Baxter, L. K. Andersen and C. G. Vassileva (2010). "An overview of the chemical composition of biomass", *Fuel* 89(5): 913-933.

Wargadalam, V. J., G. Loffler, F. Winter and H. Hofbauer (2000). "Homogeneous formation of NO and N_2O from the oxidation of HCN and NH_3 at 600-1000 °C", *Combustion and Flame* 120(4): 465-478.

Warnatz, J., U. Maas and R. W. Dibble (2006). *Combustion: physical and chemical fundamentals, modeling and simulation, experiments, pollutant formation*, Springer Verlag.

Warnecke, R. (2000). "Gasification of biomass: comparison of fixed bed and fluidized bed gasifier", *Biomass & Bioenergy* 18(6): 489-497.

WEC (2007). "Deciding the Future: Energy Policy Scenarios to 2050 - Promoting the sustainable supply and use of energy for the greatest benefit of all", *World Energy Council*, London, United Kingdom, 2012-02-07, from http://www.worldenergy.org/documents/scenarios_study_online.pdf.

Wei, X., U. Schnell, X. Han and K. R. G. Hein (2004). "Interactions of CO, HCl, and SOx in pulverised coal flames", *Fuel* 83(9): 1227-1233.

Wendt, J. O. L., C. V. Sternling and M. A. Matovich (1973). "Reduction of sulfur trioxide and nitrogen oxides by secondary fuel injection", *Symposium (International) on Combustion* 14(1): 897-904.

Wendt, J. O. L., D. W. Pershing, J. W. Lee and J. W. Glass (1979). "Pulverized coal combustion: NO_x formation mechanisms under fuel rich and staged combustion conditions", *Symposium (International) on Combustion* 17(1): 77-87.

Wendt, J. O. L., A. C. Bose and K. M. Dannecker (1987). "Mechanisms Governing the Fate of Coal Nitrogen during the Staged Combustion of High and Low Rank Pulverized Coals", *Abstracts of Papers of the American Chemical Society* 193: 98-Envr.

Wünning, J. A. and J. G. Wünning (1997). "Flameless oxidation to reduce thermal NO-formation", *Progress in Energy and Combustion Science* 23(1): 81-94.

Yin, C., L. A. Rosendahl and S. K. Kaer (2008). "Grate-firing of biomass for heat and power production", *Progress in Energy and Combustion Science* 34(6): 725-754.

Zabetta, E. C., M. Hupa and K. Saviharju (2005). "Reducing NOx Emissions Using Fuel Staging, Air Staging, and Selective Noncatalytic Reduction in Synergy", *Industrial & Engineering Chemistry Research* 44(13): 4552-4561.

Zhou, H., A. D. Jensen, P. Glarborg and A. Kavaliauskas (2006). "Formation and reduction of nitric oxide in fixed-bed combustion of straw", *Fuel* 85(5-6): 705-716.

Paper I

Combustion properties of Norwegian biomass: wood chips and forest residues

E. Houshfar, J. Sandquist, W. Musinguzi, R.A. Khalil, M. Becidan, Ø. Skreiberg, F. Goile, T. Løvås, L. Sørum

Applied Mechanics and Materials, Volume 110–116, pp. 4564–4568, 2012

Is not included due to copyright

Paper II

Effect of excess air ratio and temperature on NO_x emission from grate combustion of biomass in the staged air combustion scenario

E. Houshfar, Ø. Skreiberg, T. Løvås, D. Todorović, L. Sørum

Energy & Fuels, 25 (10), pp. 4643–4654, 2011

---

energy&fuels

ARTICLE

pubs.acs.org/EF

Effect of Excess Air Ratio and Temperature on NOx Emission from Grate Combustion of Biomass in the Staged Air Combustion Scenario

Ehsan Houshfar,*[,†] Øyvind Skreiberg,[‡] Terese Løvås,[†] Dušan Todorović,[§] and Lars Sørum[‡]

[†]Norwegian University of Science and Technology (NTNU), Department of Energy and Process Engineering, Kolbjørn Hejes vei 1B, NO-7491 Trondheim, Norway

[‡]SINTEF Energy Research, Postboks 4761 Sluppen, NO-7465 Trondheim, Norway

[§]University of Belgrade, Faculty of Mechanical Engineering, Kraljice Marije 16, 11000 Belgrade, Serbia

ABSTRACT: The combustion of biomass, in this case demolition wood, has been investigated in a grate combustion multifuel reactor. In this work a temperature range of 850−1000 °C is applied both for staged air combustion and nonstaged combustion of biomass to investigate the effects of these parameters on the emission levels of NOx, N_2O, CO, hydrocarbons (C_xH_y) and different other components. The composition of the flue gas is measured by four advanced continuous gas analyzers including gas chromatograph (GC), two Fourier transform infrared (FTIR) analyzers, and a conventional multispecies gas analyzer with fast response time. The experiments show the effects of staged air combustion, compared to nonstaged combustion, on the emission levels clearly. A NOx reduction of up to 85% is reached with staged air combustion. An optimum primary excess air ratio of 0.8−0.95 is found as a minimizing parameter for the NOx emissions for staged air combustion. Air staging has, however, a negative effect on N_2O emissions. Even though the trends show a very small reduction in the NOx level as temperature increases in nonstaged combustion, the effect of temperature is not significant for NOx and C_xH_y, neither in staged air combustion or nonstaged combustion, while it has a great influence on the N_2O and CO emissions, with decreasing levels with increasing temperature.

1. INTRODUCTION

Because of environmental problems and a significant decrease in the reserves of fossil fuels, the interest in using renewable energy carriers has become more and more widespread in recent decades. Figure 1 shows the share of different energy resources used by end users in the world in 2008.[1] Biomass, which is almost a CO_2-neutral carbon-based renewable energy source, is cheaper to utilize compared to the other sources of renewable energy, especially in the case of cofiring and combined heat and power (CHP) applications.[2] Thermal conversion of biomass, including combustion, gasification, and pyrolysis, is the most common method of extracting energy from biomass. Among the three mentioned technologies, combustion, which has been used for a long time as a source of heat for residential purposes, remains the leading technology also in recent years.

Life cycle analyses show that the most important environmental issue regarding emissions from wood combustion is NOx, contributing to almost 40% of the total emissions, including NOx, PM10, CO_2, SO_X, NH_3, CH_4, nonmethane volatile organic compounds (NMVOC), residues, and others.[3] The basis for this comparison is in relation to expected environmental impact points (EIP) of the specific emission according to the ecological scarcity method, applied for heating with wood chips. However, it is evident that the given data from any LCA analysis depends strongly on the valuation of the greenhouse gas effect since the ranking changes significantly as a result of the different CO_2 impacts of the fuels.[4] In this respect, much effort has been done to characterize biomass and reduce NOx emissions from the combustion of biomass and other solid fuels.[5,6] Two major approaches exist for NOx reduction, primary measures and secondary measures. The main difference is that primary measures prevent formation of NOx emissions, while secondary measures clean these emissions after their formation. Modifications to fuel properties and the combustion chamber and improvements to combustion technologies are examples of primary measures. One of the most important and widely used measures to reduce NOx in solid fuels combustion is staged combustion. Staged combustion, including staged air combustion and staged fuel combustion, can give a NOx reduction in the range of 50−80%.[4,7−10] The purpose of staged air combustion is to add primary air at a less than stoichiometric ratio, in order to devolatilize the volatile fraction of the fuel, resulting in a fuel gas consisting mainly of CO, H_2, C_xH_y, H_2O, CO_2, and N_2 and also small amounts of NH_3, HCN, and NOx from the fuel nitrogen content. If sufficient oxygen exists in the first stage, the fuel nitrogen intermediates will be converted to NOx (mainly NO), but shortage of oxygen will cause NO to act as an oxidant for CO, CH_4, HCN, and NH_i (with $i = 0, 1, 2, 3$) in the reduction zone, hence to reduce the nitrogen in NO and NH_i to molecular nitrogen, i.e., N_2, in reactions such as $NO + NH_2 = N_2 + H_2O$ or $NO + CO = CO_2 + 0.5N_2$.[4,11−13] NH_3 and HCN form in the pyrolysis stage of combustion depending on the temperature and fuel type, where ammonia is believed to be the most important N-species in the combustion of biomass, while HCN is more important for high-rank coals.[14−16] Ammonia that is formed in this stage is converted to radicals of NH_i. At high temperatures and fuel lean combustion, these radicals will be converted to NO, while at fuel rich conditions, N_2 will be the main product.[17] Thereafter sufficient air is added in the second

Received: May 13, 2011
Revised: August 24, 2011
Published: August 29, 2011

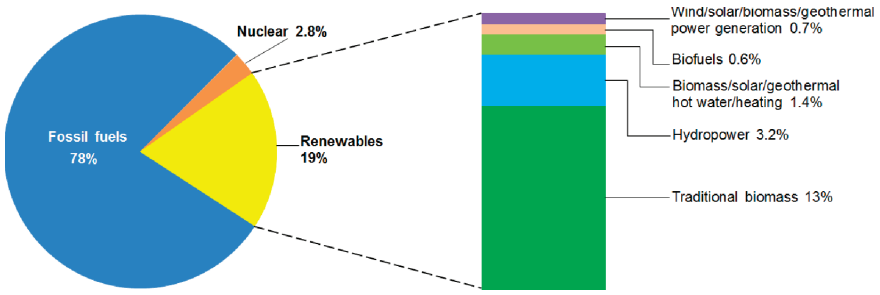

Figure 1. Renewable energy share of global final energy consumption, 2008.[1].

stage to ensure a good burnout and low emission levels from incomplete combustion.

The effect of excess air ratio, residence time, and temperature has previously been studied for a single wood particle in batch combustion, showing dependency of the NO level with excess air ratio and temperature simultaneously.[18] Also, previous work showed the effect of fuel type and cocombustion of biomass with natural gas on NO emissions when using two-stage combustion.[19] Fuel-N content and the conversion rate of NOx precursors (NH_3 and HCN) to NOx have been experimentally and numerically investigated for different solid biomass.[20−23]

Combined staged (CS) technology[10] is a method of NOx reduction including reburning, staged air combustion (AS), staged fuel combustion (FS), and selective noncatalytic reduction (SNCR).[24−26] Combined staged technology starts to reduce NOx emissions where the other methods are not sufficient. Studies showed that CS is more effective for NOx reduction, especially in the temperature range of 1000−1400 °C.[10] For temperatures below 850 °C, higher N_2O, lower NOx, and slightly higher CO emissions are reported for cocombustion of coal and woody biomass.[27] Another technique of primary measures for NOx reduction in biomass combustion is flue gas recirculation (FGR) which basically increases the total mass flux of the gases and decreases the temperature and the partial pressure of oxygen in the mixture.[28] It is proposed that in fixed-bed combustion of straw, the effect of FGR on NO reduction could be considerable.[29]

The present study aims to investigate the effect of temperature on the emission level, especially NOx, for a selected type of biomass, demolition wood (DW). Combustion of DW as a type of wood residue represents a large source of alternative energy, in addition to the fact that a waste disposal problem will also be solved. DW originates from many sources; therefore, it contains normally different undesirable components such as metals, paints, plastics, etc., which will raise the environmental impact of DW. Especially, the high nitrogen content, compared to wood, is the focus in this study. A series of experiments have been carried out for conventional combustion (nonstaged) and staged air combustion to study the effect of temperature variations, combustion technology, and excess air ratio. The work is a part of a wider study which has been carried out in the same reactor, investigating different operating parameters and fuels.[30]

In the next section a brief explanation of the experimental setup and test procedures is presented and the sampling devices and methodologies are described. Thereafter, the results are presented and discussed with respect to different variables, and finally conclusions are given.

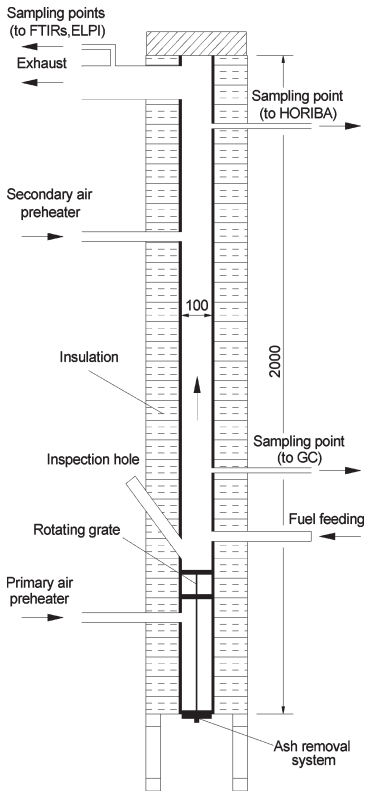

Figure 2. Schematic drawing of the reactor (the sizes are given in millimeters).

2. EXPERIMENTAL SECTION

2.1. Reactor Specifications. The reactor is shown in Figure 2. The reactor is installed vertically and has a total height of 2 m. The inner diameter is 100 mm. The reactor is made of ceramic material (alumina based) and has two reactor tube sections, each 1 m high. A rotating grate, with two grate levels, is placed 0.4 m from the bottom of the reactor, which means that the combustion zone is 1.6 m high. The two grate levels are 10 cm apart and there are rotating blades on each level that moves the unburnt fuel particles on the grates and from the upper grate to the second grate and from the second grate to the ash bin through a

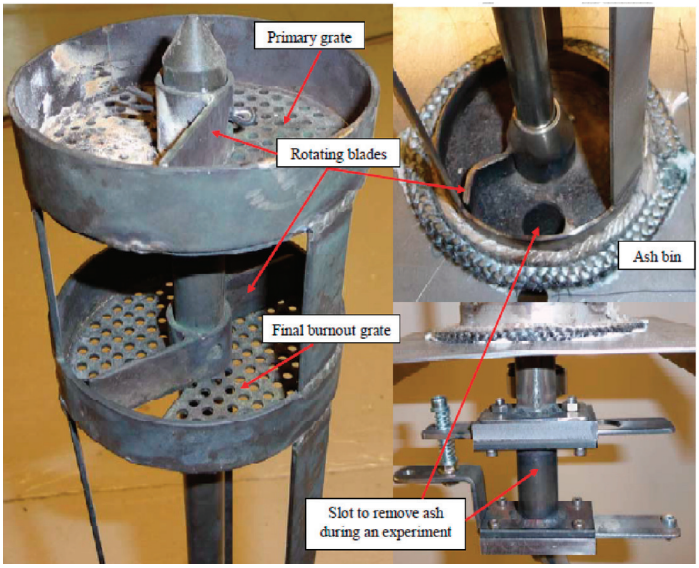

Figure 3. Design of two grates and ash bin.

slot in the grates. The rotational speed of the blades is about 3 min per revolution, which means that the residence time of each pellet on the grates is up to about 6 min, totally. This ensures complete burnout of the particles/char at the lower grate and that the ashes can be collected in the bottom of the reactor, i.e., in the ash bin. The grates and the ash bin are shown in Figure 3. A view glass is located just above of the upper grate to be able to see the combustion zone from the outside. The residence time of the fuel in the reactor is high, and the gas in the reactor has very low flow velocity (0.04−0.07 m/s). The secondary combustion zone ensures a residence time of several seconds and is hence in fact comparable to conventional combustion systems. According to the given reactor dimensions and velocity, the residence time for the primary zone (90 cm) is 13−23 s and for the secondary zone (70 cm) 10−18 s, giving a total residence time of 23−41 s. The outer surface of the reactor is insulated, and the reactor heating system has an effect of 16 kW, composed of four identical electric heaters with a height of 0.5 m.

The reactor can be heated up to 1300 °C, and the fuel feeding rate can be up to 0.5 kg/h. A pneumatic-vibration based feeding system is installed to ensure automatic fuel feeding at a set rate. Pellets are fed by a water-cooled moving piston into the reactor and immediately fall down on the upper grate. Air can be fed to the reactor in three stages (below the lower grate, above the upper grate (two inlets), and at one level higher up (two inlets)), up to 120 NL/min, totally. Five preheaters are installed, one for each air inlet stream, to heat the feeding air to the reactor temperature before entering the reactor. The air flow rate is controlled by mass flow controllers via a PC.

2.2. Sampling and Measurements. As shown in Figure 4, gas is extracted in four places to carry out analysis and further measurements. The flue gas composition is measured by means of three gas analyzers. In case of staged air combustion, a gas chromatograph (GC) is used to measure the gases in the primary section. The GC is sampling between the first and the second combustion stage and is a Varian CP-4900 Micro-GC. Sampling for the GC is made through an 8 mm diameter stainless steel probe, and the gas is passed through an ice bath to ensure removal of water, particles, and tars, in addition to reducing the temperature to an acceptable level for the GC. The sampling condition

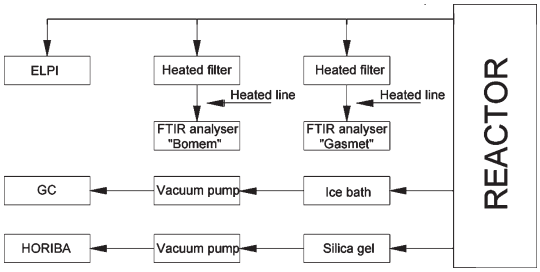

Figure 4. Schematic diagram of the sampling line.

is noncondensing gas of 0−40 °C and the maximum sample pressure is 200 kPa. The GC is equipped with two dual-channel micromachined thermal conductivity detectors (TCD), with a detection limit of 1 ppm for WCOT (wall-coated open-tubular) columns. The WCOT column is a column in which the liquid stationary phase is coated on the essentially unmodified smooth inner wall of the tube. The sample flow rate is 1 L/min and the sampling time interval is 2 min. Argon and helium are used in two columns, 10 and 20 m long, respectively. The first column measures CH_4, CO_2, $C_2H_2 + C_2H_4$, and C_2H_6 while the second column measures H_2, O_2, N_2, CH_4, and CO.

A Horiba multispecies gas analyzer PG-250 is sampling from the top of the reactor. It is capable of measuring five components, NOx, SO_2, CO, CO_2, and O_2, with the same methods used by a permanent continuous emissions monitoring system (CEMS). These include pneumatic nondispersive infrared (NDIR) for CO and SO_2, pyrosensor NDIR for CO_2, chemiluminescence (crossflow modulation) for NOx, and a galvanic cell for O_2 measurements. A vacuum pump is used to extract the sample gas at a flow rate of 0.4 L/min from the top of the reactor and passes it through a silica gel box and a filter to remove moisture and particles. The response time (T_{90}) of the analyzer is less than 45 s for NOx, CO, O_2, and CO_2 and less than 240 s for SO_2. The

dx.doi.org/10.1021/ef200714d |*Energy Fuels* 2011, 25, 4643–4654

Horiba analyzer is equipped with a drain separator unit (DS-200) and an electronic cooler unit.

Two Fourier transform infrared spectroscopy (FTIR) analyzers are also used to measure the gas composition in the exhaust gas. They do sampling at the same point, which allows for comparing different measurements for these species: H_2O, CO_2, CO, NO, N_2O, NO_2, SO_2, NH_3, HCl, HF, CH_4, C_2H_6, and C_3H_8. The Gasmet DX-4000 FTIR analyzer incorporates a spectrometer, a temperature controlled sample cell, and signal processing electronics. The sample cell is heated up to 180 °C which ensures that the sample stays in the gaseous phase even with high concentrations of condensable hydrocarbons. The measurement time is typically 60 s ,and the spectrometer resolution is 4 cm^{-1} at a scan frequency of 10 scans/s. The sample cell has a multipass fixed path length of 5 m and a volume of 0.4 L. To measure O_2, an optional oxygen sensor, based on a ZrO_2 cell, is attached to the analyzer. In total it can measure C_2H_4, C_6H_{14}, CHOH, HCN, and O_2 in addition to the above-mentioned 13 gases.

A Bomem MB 9100 FTIR analyzer is also used to measure common mutual species and C_4H_{10}. The measurement time is typically 80 s. A large cell, operating at 176 °C and equipped with a 1 cm^{-1} spectral resolution detector, was handling the analyses. Generally FTIR measurements of NO may introduce significant uncertainties. However, the NOx emissions reported in the results part are based on the Horiba analyzer, which is using the chemiluminescence technique. The N_2O measurements were made by the FTIR analyzers, and the reported values were measured by the Gasmet FTIR. The Bomem FTIR showed N_2O values close to the values measured by the Gasmet FTIR.

The temperatures at different levels in the reactor are measured by means of thermocouples and are monitored continuously to control and protect the furnace operation. These thermocouples are used to set and control the temperatures of the air preheaters and the reactor wall heaters during heat-up and during the experiment.

2.3. Experimental Procedures. Experiments are performed for nonstaged and staged air combustion. Four different temperatures are selected, 850, 900, 950, and 1000 °C. During each experiment, the temperature is kept constant for the reactor, primary air, and secondary air at the mentioned values. All the sampling devices are calibrated each day, before starting the experiments. Also the Gasmet FTIR calibration was performed daily by means of background spectra.

Pellets with a diameter of 6 mm and a length of 10−15 mm are fed by the automatic feeding system. The fuel feeding rate is set to 400 g/h. To have a precise composition of the fuel, during each run, three different samples at three different times are taken from the fuel feeding system to analyze the moisture content.

The total excess air ratio for nonstaged combustion is set to 1.6; however, the variation in the fuel feeding rate allows capturing a total excess air ratio range of 1.2−3, making it possible to see emission trends as a function of total excess air ratio. Each experiment has been carried out for at least 2 h at stable operating conditions.

For the staged air combustion experiments, the total excess air ratio is also set to 1.6, while the primary excess air ratio is set to 0.8, which means that 50% of the total air is fed at each stage. The air flow has been held constant during the experiments. However the variations in the fuel feeding rate cause natural variations in primary and secondary excess air ratios, since the fuel was fed as pellets and, depending on the length of the pellets and the position of the pellets on the grate after feeding, natural variations in the excess air ratio occurred. Therefore the mentioned situation makes it possible to experimentally derive the effect of variations in the primary excess air ratio on the NOx reduction potential by staged air combustion. Data treatment has been carried out in a cautious manner to avoid nonreliable data. Significant transient effects are effectively eliminated by a filtering procedure while treating the experimental data. This filtering procedure requires that the change in the excess air ratio per second is less than 0.01; otherwise, the complete measured data set at the current time is omitted in the final results.

Table 1. Proximate Analysis of DW Pellets (wt %)

pellets	ash (dry basis)	volatile (dry basis)	fixed carbon (dry basis)	moisture (wet basis)
demolition wood (DW)	2.49	75.97	21.54	9.68−14.97

Table 2. Ultimate Analysis of DW Pellets (wt % Dry Ash Free Basis)

pellets	C	H	O	N	S	Cl
demolition wood (DW)	48.45	6.37	44.11	1.06	0.02	0.05

2.4. Fuel Characteristics. The biomass that has been used for the present work is classified as demolition wood (DW). The received biomass is pelletized with a pellet machine to get a similar shape and composition for all the experimental runs. To ensure a homogeneous distribution, a large volume of demolition wood was shredded to sawdust size, followed by thorough mixing. Pellets were then made from these fine pieces. Hence, variation in the N-content is not regarded as a challenge in these experiments. The type of biomass, the origin of it, and the pretreatment technology applied to it are important parameters influencing the ultimate and proximate analysis of the biomass. For example, drying can reduce the moisture content from 65% in virgin wood down to below 10% in wood pellets. The proximate analysis of the present fuel is shown in Table 1, where the moisture content is measured during each experimental run. Moisture, VM, and ash content are measured using ASTM E871 (50 g, 103 ± 2 °C, 24 h), ASTM E872 (1 g, 950 °C, 7 min), and ASTM D1102 (2 g, 580−600 °C, 4 h) standards, respectively, and the fixed carbon is calculated by the difference to 100%. Three samples are analyzed from different parts of the pellets to get repeatable analyses, showing that the fuel was homogeneous. Volatile matters for wood chips, bark, and straw are normally in the range of 76−86, 70−77, and 70−81 wt %, respectively,[31] while for the DW it was 75.97%, as shown in Table 1.

Table 2 shows the DW ultimate analysis (dry ash free). All the samples have been dried in a vacuum exsiccator over phosphorus pentoxide prior to analysis. The determination of C/H/N/S is performed using the "EA 1108 CHNS-O" by Carlo Erba Instruments elemental analyzer. The method is adjusted for sample amounts of 2−10 mg and performs with an uncertainty within 0.3 wt % as required for confirmation of assumed chemical composition. The operation range covers the content from 100 to 0.1 wt %; sulfur determination is in the concentration range of 1.0 down to 0.01 wt % and the uncertainty is estimated to be 0.02 wt % for C/N/S/Cl. The nitrogen content, which is the most important element in this study is 1.06%, while for wood, straw, peat, sewage sludge, and coal it is 0.03−1, 0.3−1.5, 0.5−2.5, 2.5−6.5, and 0.5−2.5 wt %, respectively.[32]

3. RESULTS AND DISCUSSION

3.1. Accuracy of the Results and Combustion Quality. In order to establish the accuracy of the measured results, the total carbon balance is needed to quantify the measured values compared to expected analytical values. The carbon balance for one of the experiments, at 1000 °C for staged air combustion, is shown in Figure 5. This figure shows the results from the start time until the end of the experiment. However, it should be noted that the first and very last section of the data has not been considered in the final data for further treatment, since these parts are typical transient periods, outside of the stable run

period. The calculated values for CO_2, based on the carbon content in the fuel and the measured volume percentage of oxygen and CO in the flue gas, is very close to the measured values for CO_2 for each sampling interval and hence the deviation is sufficiently close to zero. In the case of a large deviation between measured and calculated values, the data set is removed from further treatment, since it could be from an unstable or transient period. Therefore the carbon balance for the presented set of results is in good order. All the experiments at the different temperatures, with and without staging air, show the same good results for the CO_2 deviation. Emission level of C_xH_y and CO for both staged and nonstaged combustion is shown in Figure 6. For C_xH_y, both staged air combustion and nonstaged combustion show the same emission level, typically below 4 ppm at 11% O_2 in dry flue gas. Here low values for C_xH_y and CO emissions, respectively, below 5 and 50 ppm shows good mixing conditions and residence times in line with modern industrial scale boilers.[33] Emissions of gaseous hydrocarbon compounds and CO are a result of incomplete combustion. Favorable combustion leads to small emissions of hydrocarbons because the organic material burns out. Large emissions of hydrocarbons indicate unsatisfactory combustion conditions and probably soot emissions. Large boilers are generally operated at an appropriate oxygen concentration, temperature, and residence time and consequently are under favorable combustion conditions. Particles originating from incomplete combustion are few or none and can be decreased in modern boiler types by 180 times,[21,34,35] and in the advanced wood furnaces, CO emissions of 10−20 mg/m^3 can be reached, depending on the temperature and selection of the optimum excess air ratio.[4] At 900 and 950 °C, some values up to 10 ppm C_xH_y are visible for nonstaged combustion, which originate from the sets of data from the period where the actual stable experiment had not been started, which means that in the stable run, the C_xH_y for both 900 and 950 °C still is 1 to 3 ppm. The C_xH_y emission level is slowly increasing with excess air ratio

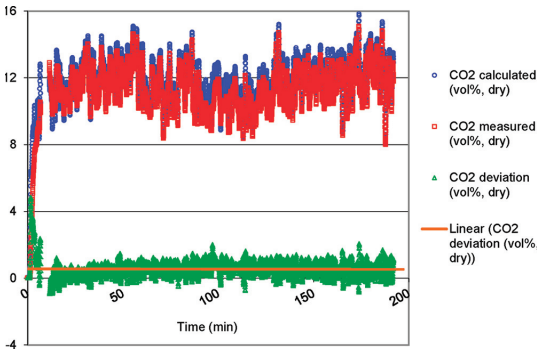

Figure 5. CO_2 deviation based on calculated and measured values from the Horiba gas analyzer for one set of the experiments; 1000 °C, staged air combustion.

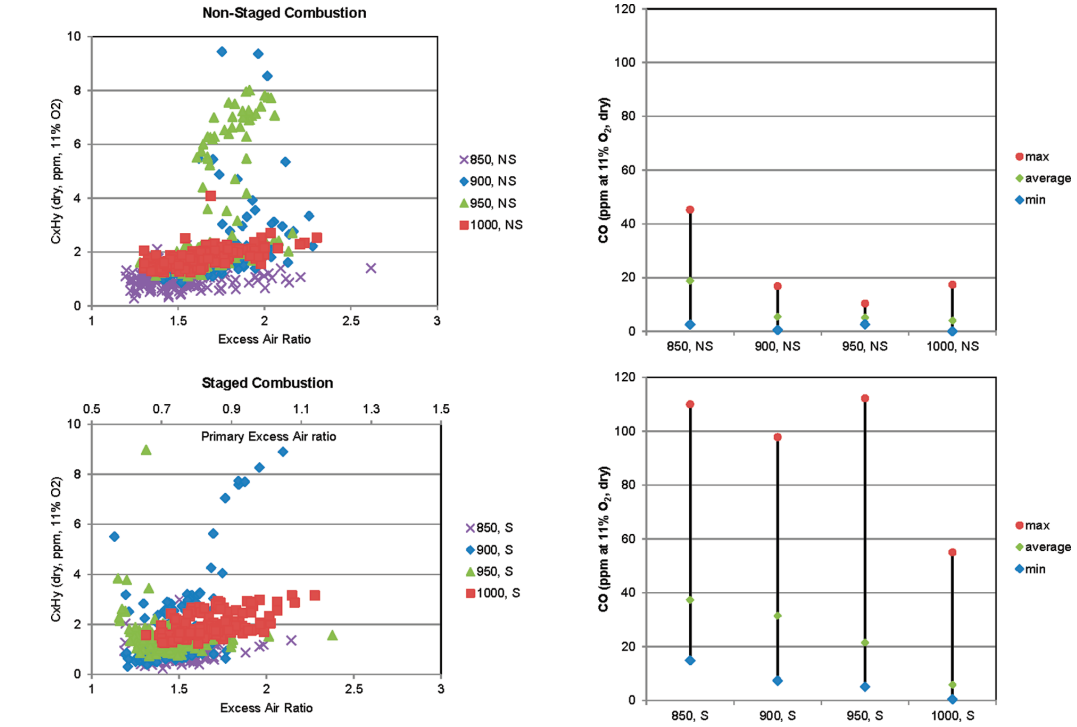

Figure 6. (Left) C_xH_y as ppm corrected to 11% O_2 in dry flue gas for staged air combustion and nonstaged combustion as a function of excess air ratio at the different temperature levels. (Right) Average, minimum, and maximum value of CO as ppm corrected to 11% O_2 in dry flue gas for staged air combustion (S) and nonstaged combustion (NS) at the different temperature levels.

dx.doi.org/10.1021/ef200714d |*Energy Fuels* 2011, 25, 4643–4654

for both staged air combustion and nonstaged combustion. The influence of excess air ratio is small, but the C_xH_y emission level is a direct function of the excess air ratio, and the minimum C_xH_y emission is taking place at the lowest total excess air ratio.

For nonstaged combustion, the temperature has an inverse effect on the C_xH_y emission levels. The lowest emissions occur at 850 °C, while at 900, 950, and 1000 °C the temperature has no effect. For staged air combustion, the effect of temperature is more visible than for nonstaged combustion. Here the effect of temperature is still low, but it is clearly possible to observe an increase in emission levels with increasing temperature in the lower graph. The observed increase of C_xH_y may be due to a higher release of gaseous hydrocarbons from the fuel at higher temperatures, where the pyrolysis process is intensified by temperature and the formation of hydrocarbons are increased.[36] Detailed experimental and thermodynamic studies on particulate emissions from this multifuel reactor to investigate particle size distribution and chemical composition of fly/bottom ash is extensively discussed recently.[37,38] The effect of temperature on CO is the same as for N_2O. As shown in Figure 6, increasing temperature decreases the CO level, while staged air combustion has a negative effect on CO. The former effect is due to a more complete oxidation of CO, forming CO_2. However, with air staging, the low stoichiometric ratio in the first stage cause the oxidation route to be less effective, so the emission of CO rises. The staged air combustion results indicate an increase of 99−482% for CO for staged air combustion, while the mean CO levels are about a factor of two increased.

Emissions of gaseous hydrocarbon compounds and CO are a result of incomplete combustion. Large emissions of CO indicate unsatisfactory combustion conditions. In the present case, higher excess air ratio (more oxygen available) will lead to an almost complete combustion (heated reactor, i.e., temperature not influenced by the excess air ratio). Consequently, the maximum CO level corresponds to the lowest excess air ratio or the more fuel rich condition. In the staged combustion experiments, because of the under-stoichiometric condition in the first stage, a large amount of unburnt species (including CO) will be formed in the primary stage. The burnout of the unburnt species should take place in the second stage. If necessary air is available in the burnout zone, the CO level will be very low; if not the CO level will be high. So the higher deviation for CO emission in the staged combustion is a result of the variations in secondary excess air ratio, where more fuel rich conditions in the secondary stage can, combined with not perfect mixing of fuel gas and secondary air, cause higher fluctuations in the CO level.

3.2. NOx Emissions: Effect of Excess Air Ratio and Air Staging. Skreiberg et al.[39] showed that the fuel-N conversion to NOx is strongly dependent on the excess air ratio and that it increases with increasing excess air. However, in this study we investigate further the effect of temperature on this dependency. Figure 7 shows the effect of temperature on the NOx emission level (ppm at 11% O_2 in dry flue gas) for both staged air combustion and nonstaged combustion of DW at 850, 900, 950, and 1000 °C. NO_2 was typically below 1 ppm for the staged and nonstaged experiments which is within the measurement error ranges for the analyzers (Gasmet and Bomem FTIRs) for NO_2, except for one case at 900 °C for staged-air combustion, where a NO_2 level of up to 3 ppm is measured. Consequently, we have not found any clear relation between NO_2 and temperature in the investigated temperature range. The upper graph for nonstaged combustion shows an increasing trend for NOx when the excess air ratio is increasing. This corresponds with the findings of Skreiberg et al.[39] The NOx level for these cases, at all temperatures, varies from 75 to 200 ppm at 11% O_2 in dry flue gas. However, this graph also indicates that temperature variations have almost no effect on the NOx emission level. All the data for the different temperatures are included, showing that they are in the same range for the same excess air ratio and temperature. This indicates that the temperatures are, as expected, too low for thermal NOx formation. According to the literature, thermal NOx formation in different biomass combustion systems starts at temperatures above 1400 °C.[8,40]

The lower graph, which shows the same information for staged air combustion of DW, is distinctively different from that of nonstaged combustion. Here an optimum excess air ratio exists for each combustion temperature. The NOx results are here plotted as a function of overall excess air ratio while the corresponding primary excess air ratio (half of the overall excess air ratio) is given on the upper *x*-axis for staged combustion. GC measurements were carried out to analyze the composition of the primary gas, but they can only provide an indicative value for the primary excess air ratio and not with a sufficient time resolution. The main point is to use total excess air ratio as an indicative value to show the effect of variations in the primary excess air ratio on the NOx reduction degree, and this was effectively achieved with the experimental setup, the measurements carried out, and the data treatment procedures employed. The NOx emission level is ranging from 25 to 120 ppm at 11% O_2 in dry flue gas. This range points out that the emission level by staged air combustion of DW decreases by a factor of 2−4, corresponding to 50−75% NOx reduction compared to nonstaged combustion. In the optimum case, i.e., at an excess air ratio of 1.6−1.9, the NOx reduction is 85%. This corresponds to an optimum primary excess air ratio of 0.8−0.95. Again, the effect of temperature is very low, as was the case for nonstaged combustion, and all temperatures show the same trend. First an increase occurs in the NOx level with an increasing excess air ratio up to approximately 1.5, and from this point the NOx level is decreasing until the excess air ratio approaches 2. A further increase in the excess air ratio will cause the NOx level to start increasing again. This effect is due to the increase of available air both in the primary and secondary zone, which causes the first stage not to be in a fuel-rich condition, as was explained in the Introduction. This will increase the TFN/Fuel-N ratio, hence lowering the NOx reduction potential, where total fixed nitrogen (TFN) is the total mass of nitrogen in the flue gas (all N containing gases coming out from the reactor except for N_2), and Fuel-N is the total mass of nitrogen in the fuel.[41] The concentration of NH_3 and HCN was very low in the flue gas after a long residence time, typically below 1 ppm, which was within the measurement error range of the analyzers for these species.

Figure 8 shows the effect of temperature on N_2O emissions at different excess air ratios. The upper graph clearly shows that in the case of nonstaged combustion, the N_2O emission level is not a function of the excess air ratio. However, the effect of temperature on the N_2O emission level is significant in nonstaged combustion. The maximum N_2O emission level is seen at the lowest temperature, i.e., 850 °C. Increasing the temperature with just 50 °C will decrease N_2O from 4.8 to 0.9 ppm (mean value), which corresponds to 80% reduction. The same trend has been found for N_2O formation for temperatures above 750 °C in the literature, where reduction of NO has a significant effect on the production of N_2O.[42,43] The production of N_2O is mainly

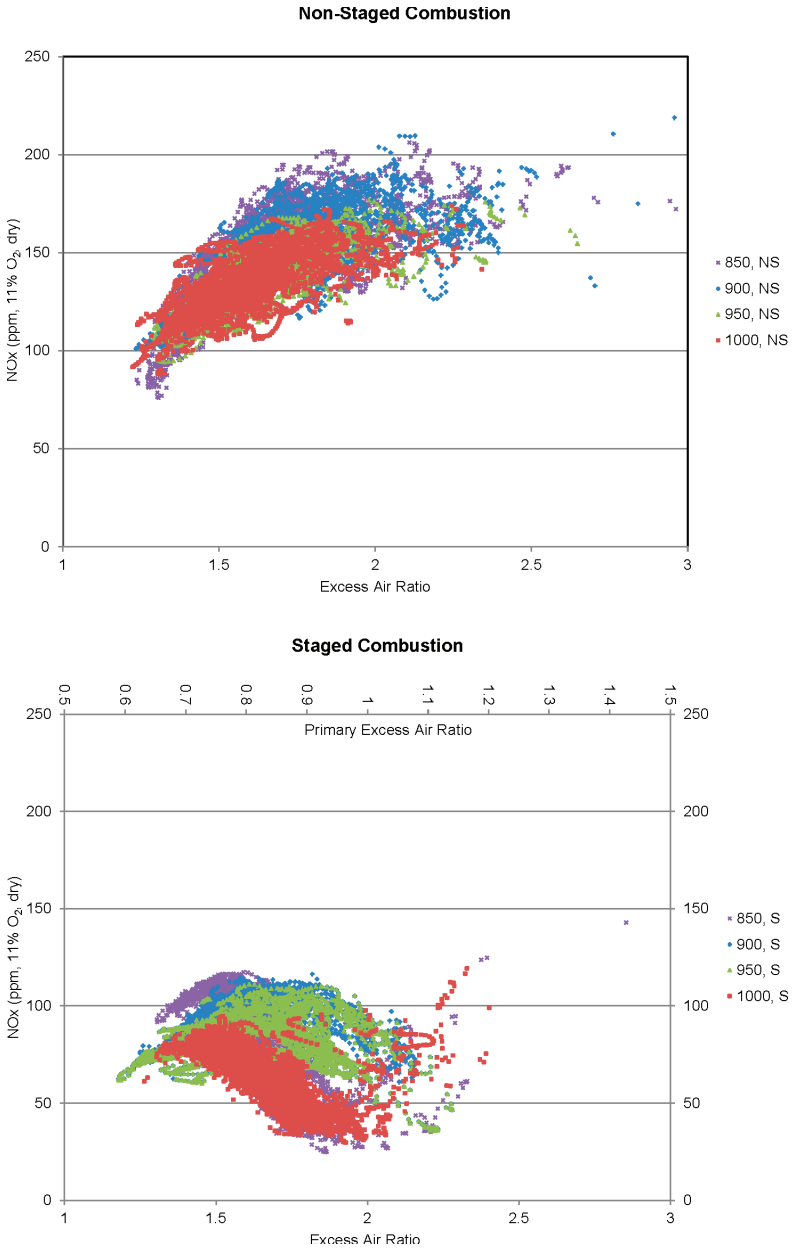

Figure 7. NOx as ppm corrected to 11% O_2 in the dry flue gas for staged air combustion and nonstaged combustion as a function of excess air ratio at the different temperature levels.

from the reaction of NO + NCO and NO + NH, so N_2O is mainly reduced by thermal decomposition. HCN and NH_3 either can reduce to N_2O and N_2 or oxidize to NO. At the higher temperature, the oxidation route becomes more dominant; therefore, having a low amount of N_2O is predicted.[11,42] The staged air combustion experiments show higher values of N_2O for the same conditions. At the optimum excess air ratio for NOx reduction, the increase in N_2O emission compared to nonstaged combustion is almost 120%.

3.3. Temperature Influence on NOx and N_2O Emission Levels. As discussed in sections 3.2 and 3.3, the effect of temperature on the NOx emission level is small in the investigated temperature range of 850−1000 °C. However, with the extraction of the maximum and minimum levels for each

dx.doi.org/10.1021/ef200714d |*Energy Fuels* 2011, 25, 4643–4654

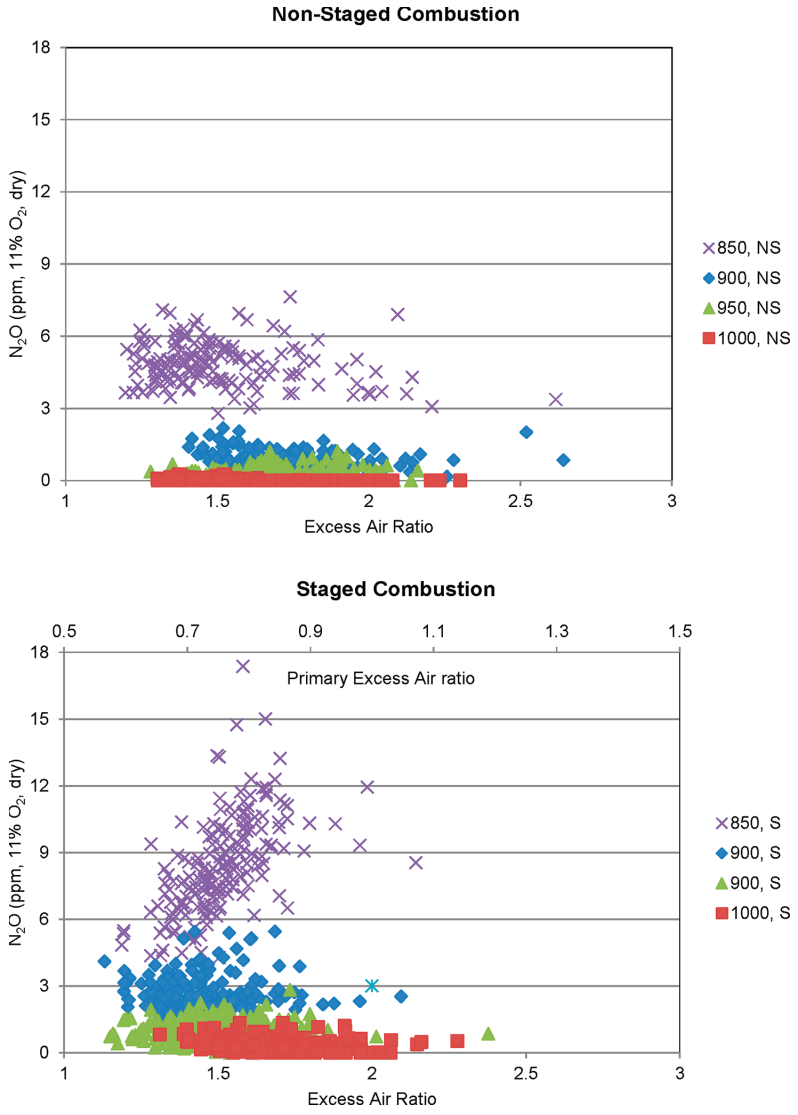

Figure 8. N_2O as ppm corrected to 11% O_2 in the flue gas for staged air combustion and nonstaged combustion as a function of excess air ratio at the different temperature levels.

temperature, some important trends can be established. Figure 9 shows mean, maximum, and minimum NOx emission level (ppm at 11% O_2 in dry flue gas) for nonstaged (NS) and staged air (S) combustion of DW in the mentioned temperature range. The average (mean value for different excess air ratios over a period of time) is remaining constant at the different temperatures, at almost 150 ppm for nonstaged combustion. The maximum, mean, and minimum values are at the highest level for 900 °C in the nonstaged experiments. NOx at staged air combustion seems not to be a function of temperature either. The average value is on the order of 80 ppm at 11% O_2 in dry flue gas and the highest mean value is seen at 900 and 950 °C. It is interesting to note that in both cases the spread between the highest and lowest values are higher in the lower end of the temperature range. The lower amount of NOx at 1000 °C needs more clarification. Considering the optimum primary excess air ratio as the key point for minimizing the NOx emission, we can see that at 1000 °C most of the time the reactor was running in the optimum excess air ratio range (see Figure 7). This resulted in a lower average NOx value (for a complete run). At 900 and 950 °C, in spite of our efforts to operate at optimum conditions, the primary excess air ratio has also been slightly lower than the optimum range (0.8−0.95) for the experiment. Hence, the higher average value at 900 and 950 °C corresponds to a lower average primary excess air ratio.

dx.doi.org/10.1021/ef200714d |*Energy Fuels* 2011, 25, 4643–4654

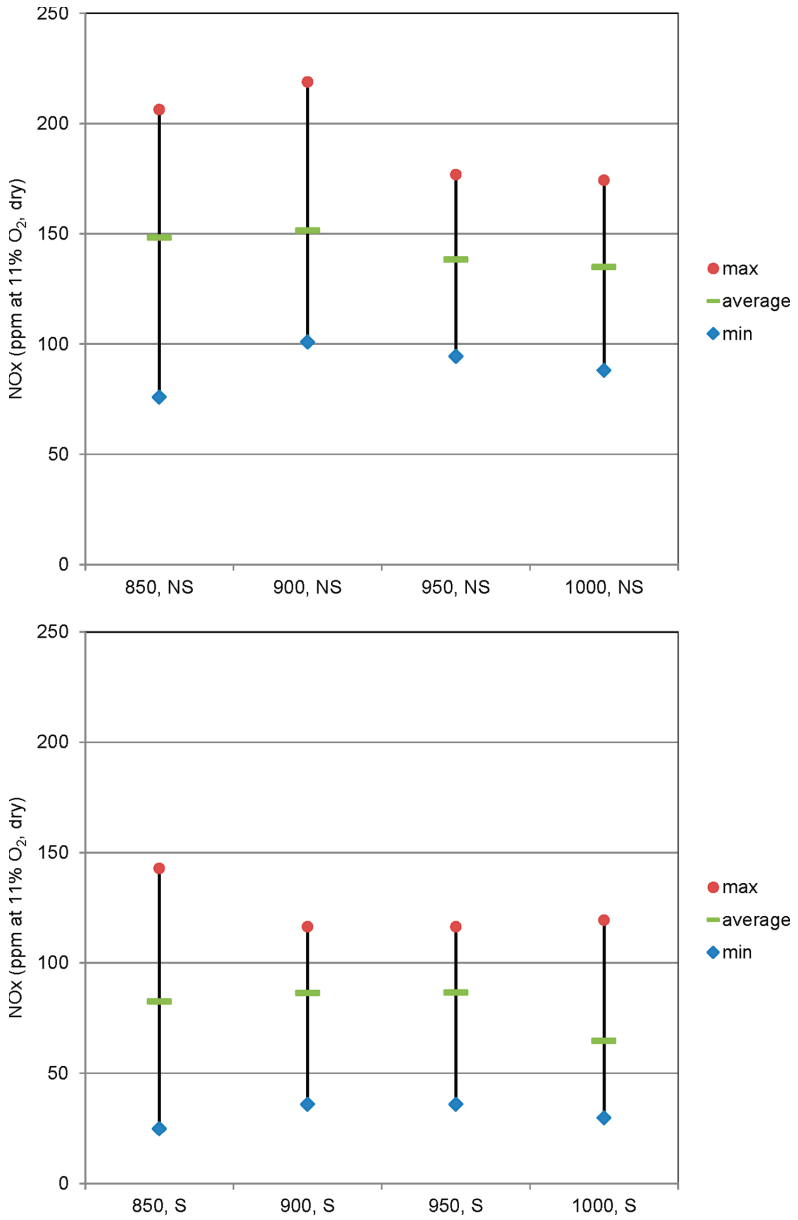

Figure 9. Average, minimum, and maximum value of NOx as ppm corrected to 11% O_2 in dry flue gas for staged air combustion (S) and nonstaged combustion (NS) at the different temperature levels.

N_2O has a different behavior in relation to temperature, showing similar values for staged air combustion and nonstaged combustion. However, temperature has a great influence on mean, maximum, and minimum N_2O levels, shown in Figure 10. They decrease significantly with increasing temperature, and for high temperatures the N_2O level is almost negligible. Yet again the spread between maximum and minimum values are higher in the lower end of the temperature range. Previous studies shows that the main precursor for N_2O formation is HCN oxidation,[12,44] while N_2O destruction is mainly by the reaction of $N_2O + H = N_2 + OH$.[45] At the high temperatures, the destruction reaction with H radicals is faster and also the HCN oxidation reaction tends to NO formation instead of N_2O. This mechanism causes the N_2O level to be very low at higher temperatures.

3.4. Effect of Stoichiometry, Temperature, and Residence Time on TFN/Fuel-N. In addition to the reactor temperature,

dx.doi.org/10.1021/ef200714d |*Energy Fuels* 2011, 25, 4643–4654

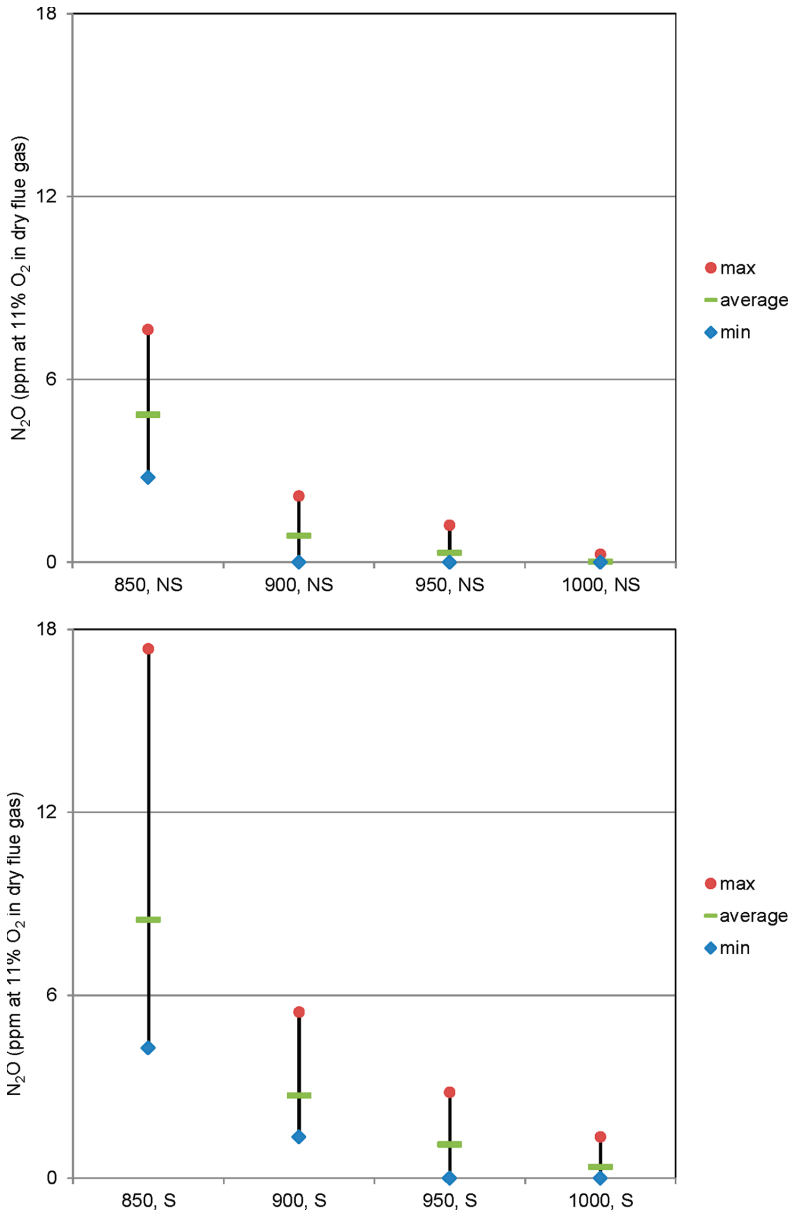

Figure 10. Average, minimum, and maximum value of N_2O as ppm corrected to 11% O_2 in dry flue gas for staged air combustion (S) and nonstaged combustion (NS) at the different temperature levels.

primary excess air ratio, fuel-N content, differences in residence times, and mixing conditions may also have an effect on the fuel nitrogen conversion. The optimum condition for maximum conversion of fuel-N to molecular nitrogen, N_2, is highly affected by the mentioned parameters. However, since only one fuel was tested, the primary excess air ratio is the only important variable in addition to the potential temperature effect regarding the NOx emission level. The NOx/Fuel-N and TFN/Fuel-N ratios, as shown in Figure 11, were checked and showed good consistency, always well below unity,[8] since the values for TFN (TFN = NO + NO_2 + $2N_2O$ + HCN + NH_3) is calculated after complete burnout where the residence time has been several seconds. Residence time in the reduction zone is of importance for nitrogen conversion, however up to a certain value, beyond which it does not significantly influence TFN/Fuel-N.[18,46] In this work, the residence time is well above the expected needed time

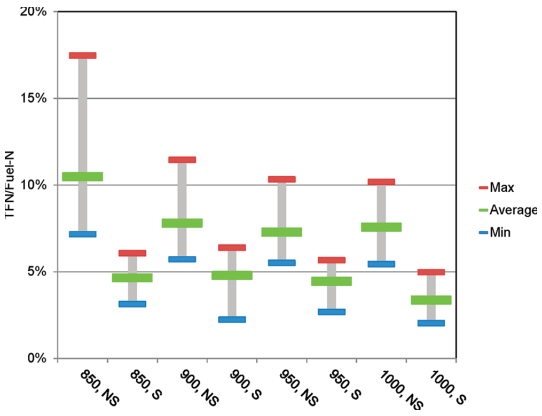

Figure 11. Average, minimum and maximum values of TFN/Fuel-N for staged air combustion (S) and nonstaged combustion (NS) at the different temperature levels.

(below 2 s) and, hence, the results are not influenced by the residence time. After the reduction zone, the combustion is completed by injection of the secondary air. Of course, good mixing of secondary air and the combustible gases are important. In average, a large amount of the TFN is composed of NOx (96%) and is varying between 81 and 100% depending on the temperature and the combustion scenario. Therefore the mentioned values in the last figure, Figure 11, can be regarded as approximate values for NOx/Fuel-N.

4. CONCLUSIONS

From the experimental studies carried out in the present work, using demolition wood pellets as fuel, the following conclusions can be drawn: The primary excess air ratio is the most important parameter which can be optimized for maximum conversion of fuel-N to N_2, hence reducing the NOx level. The effect of two-stage combustion of biomass is significant for reduction of NOx emission levels. Staged air combustion, in this case, can reduce the emission level by 50−75% and even up to 85% at the optimum conditions. The maximum NOx reduction happens when the primary air is injected at a primary excess air ratio of 0.8−0.95 and the total excess air ratio is 1.6−1.9 for staged air combustion. The experiments show that also the total excess air ratio has an important effect on the NOx emission.

The N_2O level has an inverse effect for staged air combustion, i.e., increasing for staged air combustion. The average N_2O level increase for the different temperatures is 75−1660% but with a low amount of N_2O at high temperatures.

However, the experimental results show that the NOx emission level is not affected significantly by temperature neither in nonstaged or staged air combustion when temperatures are kept below 1000 °C in the reactor. Yet, the effect of temperature on the N_2O level is considerable. This study shows, as expected, that at high temperatures, N_2O emissions almost disappear. The results point to that the effects of temperature and staged air combustion are counteractive for N_2O, meaning a negative influence on N_2O for staged air combustion and a desirable N_2O reduction effect with increasing temperature. Therefore to minimize N_2O emissions and reduce emissions of unburnt, temperatures of above 900 °C are beneficial.

Hydrocarbons emission, C_xH_y, is almost independent of the combustion condition whether it is staged air combustion or nonstaged combustion. In both cases, the emission levels of hydrocarbons are below 4 ppm at 11% O_2 in dry flue gas. CO emissions increase for staged air combustion compared to nonstaged combustion by a factor of about 1.5 at a given temperature. Increasing temperature decreases the CO emission level in the whole temperature range of 850−1000 °C.

AUTHOR INFORMATION

Corresponding Author

*E-mail: ehsan.houshfar@ntnu.no. Phone: +47-73593896. Fax: +47-73593580.

ACKNOWLEDGMENT

This research work was performed as part of the Bioenergy Innovation Centre (CenBio), which is funded by the Research Council of Norway, 19 Norwegian industry partners, and 7 R&D institutes, and as a part of the competence building project KRAV, funded by the Research Council of Norway, 5 Norwegian industry partners, and SINTEF Energy Research.

REFERENCES

(1) REN21. *Renewables 2010 Global Status Report*, Paris, REN21 Secretariat, 2010.

(2) Rodrigues, M.; Faaij, A. P. C.; Walter, A. Techno-economic analysis of co-fired biomass integrated gasification/combined cycle systems with inclusion of economies of scale. *Energy* **2003**, *28* (12), 1229–1258.

(3) Kessler, F. M.; Knechtle, N.; Frischknecht, R. *Heizenergie aus Heizöl, Erdgas oder Holz*; Umwelt Schrift Nr. 315; Bern, 2000.

(4) Nussbaumer, T. Combustion and co-combustion of biomass: fundamentals, technologies, and primary measures for emission reduction. *Energy Fuels* **2003**, *17* (6), 1510–1521.

(5) Miller, J. A.; Bowman, C. T. Mechanism and modeling of nitrogen chemistry in combustion. *Prog. Energy Combust. Sci.* **1989**, *15* (4), 287–338.

(6) Jenkins, B. M.; Baxter, L. L.; Miles, T. R. Combustion properties of biomass. *Fuel Process. Technol.* **1998**, *54* (1−3), 17–46.

(7) Houshfar, E.; Løvås, T.; Skreiberg, Ø. Detailed chemical kinetics modeling of NOx reduction in combined staged fuel and staged air combustion of biomass. *18th European Biomass Conference & Exhibition (EU BC&E)*, Lyon, France, 2010; pp 1128−1132.

(8) Salzmann, R.; Nussbaumer, T. Fuel Staging for NOx Reduction in Biomass Combustion: Experiments and Modeling. *Energy Fuels* **2001**, *15* (3), 575–582.

(9) Kicherer, A.; Spliethoff, H.; Maier, H.; Hein, K. R. G. The effect of different reburning fuels on NOx-reduction. *Fuel* **1994**, *73* (9), 1443–1446.

(10) Zabetta, E. C.; Hupa, M.; Saviharju, K. Reducing NOx Emissions Using Fuel Staging, Air Staging, and Selective Noncatalytic Reduction in Synergy. *Ind. Eng. Chem. Res.* **2005**, *44* (13), 4552–4561.

(11) Skreiberg, Ø.; Kilpinen, P.; Glarborg, P. Ammonia chemistry below 1400 K under fuel-rich conditions in a flow reactor. *Combust. Flame* **2004**, *136* (4), 501–518.

(12) Kilpinen, P.; Hupa, M. Homogeneous N2O chemistry at fluidized bed combustion conditions: A kinetic modeling study. *Combust. Flame* **1991**, *85* (1−2), 94–104.

(13) Kilpinen, P.; Glarborg, P.; Hupa, M. Reburning chemistry: a kinetic modeling study. *Ind. Eng. Chem. Res.* **1992**, *31* (6), 1477–1490.

(14) Hämäläinen, J. P.; Aho, M. J.; Tummavuori, J. L. Formation of nitrogen oxides from fuel-N through HCN and NH3: a model-compound study. *Fuel* **1994**, *73* (12), 1894–1898.

(15) Becidan, M.; Skreiberg, Ø.; Hustad, J. E. NOx and N2O Precursors (NH3 and HCN) in Pyrolysis of Biomass Residues. *Energy Fuels* **2007**, *21* (2), 1173–1180.

(16) Hansson, K.-M.; Samuelsson, J.; Tullin, C.; Åmand, L.-E. Formation of HNCO, HCN, and NH3 from the pyrolysis of bark and nitrogen-containing model compounds. *Combust. Flame* **2004**, *137* (3), 265–277.

(17) Nussbaumer, T. Primary and secondary measures for the reduction of nitric oxide emissions from biomass combustion. In *Developments in Thermochemical Biomass Conversion*, Banff, Canada, 1996; Bridgwater, A. V.; Boocock, D. G. B., Eds. Blackie Academic & Professional: 1997; pp 1447−1461.

(18) Skreiberg, Ø.; Glarborg, P.; Jensen, A. D.; Dam-Johansen, K. Kinetic NOx modelling and experimental results from single wood particle combustion. *Fuel* **1997**, *76* (7), 671–682.

(19) Lin, W.; Jensen, P. A.; Jensen, A. D. Biomass Suspension Combustion: Effect of Two-Stage Combustion on NOx Emissions in a Laboratory-Scale Swirl Burner. *Energy Fuels* **2009**, *23* (3), 1398–1405.

(20) Stubenberger, G.; Scharler, R.; Zahirovic, S.; Obernberger, I. Experimental investigation of nitrogen species release from different solid biomass fuels as a basis for release models. *Fuel* **2008**, *87* (6), 793–806.

(21) Johansson, L. S.; Leckner, B.; Gustavsson, L.; Cooper, D.; Tullin, C.; Potter, A. Emission characteristics of modern and old-type residential boilers fired with wood logs and wood pellets. *Atmos. Environ.* **2004**, *38* (25), 4183–4195.

(22) Dagaut, P.; Glarborg, P.; Alzueta, M. U. The oxidation of hydrogen cyanide and related chemistry. *Prog. Energy Combust. Sci.* **2008**, *34* (1), 1–46.

(23) Sørum, L.; Skreiberg, Ø.; Glarborg, P.; Jensen, A.; Dam-Johansen, K. Formation of NO from combustion of volatiles from municipal solid wastes. *Combust. Flame* **2001**, *124* (1−2), 195–212.

(24) Wendt, J. O. L.; Sternling, C. V.; Matovich, M. A. Reduction of sulfur trioxide and nitrogen oxides by secondary fuel injection. *Symp. (Int.) Combust.* **1973**, *14* (1), 897–904.

(25) Chen, S. L.; McCarthy, J. M.; Clark, W. D.; Heap, M. P.; Seeker, W. R.; Pershing, D. W. Bench and pilot scale process evaluation of reburning for in-furnace NOx reduction. *Symp. (Int.) Combust.* **1988**, *21* (1), 1159–1169.

(26) Pershing, D, W.; Berkau, E, E., The Chemistry of Nitrogen Oxides and Control through Combustion Modifications. In *Pollution Control and Energy Needs*, Jimeson, R. M.; Spindt, R. S., Eds.; American Chemical Society: Washington, DC, 1974; Vol. 127, pp 218−240.

(27) Svoboda, K.; Pohořelý, M.; Hartman, M. Effects of Operating Conditions and Dusty Fuel on the NOx, N2O, and CO Emissions in PFB Co-combustion of Coal and Wood. *Energy Fuels* **2003**, *17* (4), 1091–1099.

(28) Bauer, R.; Gölles, M.; Brunner, T.; Dourdoumas, N.; Obernberger, I. Modelling of grate combustion in a medium scale biomass furnace for control purposes. *Biomass Bioenergy* **2010**, *34* (4), 417–427.

(29) Zhou, H.; Jensen, A. D.; Glarborg, P.; Kavaliauskas, A. Formation and reduction of nitric oxide in fixed-bed combustion of straw. *Fuel* **2006**, *85* (5−6), 705–716.

(30) Houshfar, E.; Skreiberg, Ø.; Todorović, D.; Skreiberg, A.; Løvås, T.; Jović, A.; Sørum, L. NOx emission reduction by staged combustion in grate combustion of biomass fuels and fuel mixtures. *Fuel* **2011**, submitted for publication.

(31) Berndes, G.; Baxter, L.; Coombes, P.; Delcarte, J.; Evald, A.; Hartmann, H.; Jansen, M.; Koppejan, J.; Livingston, W.; Loo, S. v.; Madrali, S.; Moghtaderi, B.; Nägele, E.; Nussbaumer, T.; Obernberger, I.; Oravainen, H.; Preto, F.; Skreiberg, Ø.; Tullin, C.; Thek, G. *The Handbook of Biomass Combustion and Co-firing*; Earthscan: London, 2008.

(32) Glarborg, P.; Jensen, A. D.; Johnsson, J. E. Fuel nitrogen conversion in solid fuel fired systems. *Prog. Energy Combust. Sci.* **2003**, *29* (2), 89–113.

(33) Nussbaumer, T. *Biomass Combustion in Europe Overview on Technologies and Regulations*; Report 08-03; prepared by Verenum Switzerland for New York State Energy Research and Development Authority: Albany, NY, 2008.

(34) Johansson, L. S.; Tullin, C.; Leckner, B.; Sjövall, P. Particle emissions from biomass combustion in small combustors. *Biomass Bioenergy* **2003**, *25* (4), 435–446.

(35) Eskilsson, D.; Rönnbäck, M.; Samuelsson, J.; Tullin, C. Optimisation of efficiency and emissions in pellet burners. *Biomass Bioenergy* **2004**, *27* (6), 541–546.

(36) Kozinski, J. A.; Saade, R. Effect of biomass burning on the formation of soot particles and heavy hydrocarbons. An experimental study. *Fuel* **1998**, *77* (4), 225–237.

(37) Becidan, M. l.; Houshfar, E.; Khalil, R. A.; Skreiberg, Ø.; Løvås, T.; Sørum, L. Optimal mixtures to reduce the formation of corrosive compounds during straw combustion: a thermodynamic analysis. *Energy Fuels* **2011**, *25* (7), 3223–3234.

(38) Khalil, R. A.; Houshfar, E.; Musinguzi, W.; Becidan, M.; Skreiberg, Ø.; Goile, F.; Løvås, T.; Sørum, L. Experimental investigation on corrosion abatement in straw combustion by fuel-mixing. *Energy Fuels* **2011**, *25* (6), 2687–2695.

(39) Skreiberg, Ø.; Hustad, J. E.; Karlsvik, E. Empirical NOx-modelling and experimental results from wood stove combustion. In *Developments in Thermochemical Biomass Conversion*, Banff, Canada, 1996; Bridgwater, A. V.; Boocock, D. G. B., Eds. Blackie Academic & Professional: London, UK, 1997; pp 1462−1478.

(40) Mahmoudi, S.; Baeyens, J.; Seville, J. P. K. NOx formation and selective non-catalytic reduction (SNCR) in a fluidized bed combustor of biomass. *Biomass Bioenergy* **2010**, *34* (9), 1393–1409.

(41) Skreiberg, Ø.; Becidan, M.; Hustad, J. E.; Mitchell, R. E. Detailed chemical kinetics modelling of NOx reduction by staged air combustion at moderate temperatures. In *The Science in Thermal and Chemical Biomass Conversion Conference*, Victoria, BC, Canada, 2004, Bridgwater, A. V., Boocock, D. G. B., Eds. CPL Press: Newbury, Berkshire, UK, 2006, pp 40−54.

(42) Kristensen, P. G.; Glarborg, P.; Dam-Johansen, K. Nitrogen chemistry during burnout in fuel-staged combustion. *Combust. Flame* **1996**, *107* (3), 211–222.

(43) Liu, H.; Gibbs, B. M. Modelling of NO and N2O emissions from biomass-fired circulating fluidized bed combustors. *Fuel* **2002**, *81* (3), 271–280.

(44) Aho, M. J.; Hämäläinen, J. P.; Tummavuori, J. L. Importance of solid fuel properties to nitrogen oxide formation through HCN and NH3 in small particle combustion. *Combust. Flame* **1993**, *95* (1−2), 22–30.

(45) Winter, F.; Wartha, C.; Hofbauer, H. NO and N2O formation during the combustion of wood, straw, malt waste and peat. *Bioresour. Technol.* **1999**, *70* (1), 39–49.

(46) Padinger, R.; Leckner, B.; Åmand, L.-E.; Thunman, H.; Ghirelli, F.; Nussbaumer, T.; Good, J.; Hassler, P.; Salzmann, R.; Winter, F.; Wartha, C.; Löffler, G.; Wargadalam, V. J.; Hofbauer, H.; Saastamoinen, J.; Oravainen, H.; Heiskanen, V. P.; Hämäläinen, J. P.; Taipale, R.; Bilbao, R.; Alzueta, M. U.; Millera, A.; Oliva, M.; Ibáñez, J. C.; Kilpinen, P. Reduction of nitrogen oxide emissions from wood chip grate furnaces, Final report for the EU-JOULE III project JOR3-CT96-0059, *1st World Conference on Biomass for Energy and Industry*, Sevilla, Spain, 2000, Kyritsis, S., Beenackers, A. A. A. M., Helm, P., Grassi, A., Chiaramonti, D., Eds.; James & James (Science Publishers) Ltd.: Sevilla, Spain, 2000; pp 1457−1463.

Paper III

NO_x emission reduction by staged combustion in grate combustion of biomass fuels and fuel mixtures

E. Houshfar, Ø. Skreiberg, D. Todorović, A. Skreiberg, T. Løvås, A. Jovović, L. Sørum

Fuel, In press, 2012

doi: 10.1016/j.fuel.2012.03.044

Is not included due to copyright

Paper IV

Experimental investigation on NO_x reduction by primary measures in biomass combustion: straw, peat, sewage sludge, forest residues, and wood pellets

E. Houshfar, T. Løvås, Ø. Skreiberg

Energies, 5 (2), pp. 270–290, 2012

Energies **2012**, *5*, 270-290; doi:10.3390/en5020270

OPEN ACCESS

energies

ISSN 1996-1073

www.mdpi.com/journal/energies

Article

Experimental Investigation on NO_x Reduction by Primary Measures in Biomass Combustion: Straw, Peat, Sewage Sludge, Forest Residues and Wood Pellets

Ehsan Houshfar [1,*], Terese Løvås [1] and Øyvind Skreiberg [2]

[1] Department of Energy and Process Engineering, Norwegian University of Science and Technology (NTNU), Kolbjørn Hejes Vei 1B, Trondheim NO-7491, Norway; E-Mail: terese.lovas@ntnu.no

[2] SINTEF Energy Research, Trondheim NO-7465, Norway; E-Mail: oyvind.skreiberg@sintef.no

* Author to whom correspondence should be addressed; E-Mail: ehsan.houshfar@ntnu.no; Tel.: +47-73593896; Fax: +47-73593580.

Received: 6 December 2011; in revised form: 29 January 2012 / Accepted: 1 February 2012 / Published: 8 February 2012

Abstract: An experimental investigation was carried out to study the NO_x formation and reduction by primary measures for five types of biomass (straw, peat, sewage sludge, forest residues/Grot, and wood pellets) and their mixtures. To minimize the NO_x level in biomass-fired boilers, combustion experiments were performed in a laboratory scale multifuel fixed grate reactor using staged air combustion. Flue gas was extracted to measure final levels of CO, CO_2, C_xH_y, O_2, NO, NO_2, N_2O, and other species. The fuel gas compositions between the first and second stage were also monitored. The experiments showed good combustion quality with very low concentrations of unburnt species in the flue gas. Under optimum conditions, a NO_x reduction of 50–80% was achieved, where the highest reduction represents the case with the highest fuel-N content. The NO_x emission levels were very sensitive to the primary excess air ratio and an optimum value for primary excess air ratio was seen at about 0.9. Conversion of fuel nitrogen to NO_x showed great dependency on the initial fuel-N content, where the blend with the highest nitrogen content had lowest conversion rate. Between 1–25% of the fuel-N content is converted to NO_x depending on the fuel blend and excess air ratio. Sewage sludge is suggested as a favorable fuel to be blended with straw. It resulted in a higher NO_x reduction and low fuel-N conversion to NO_x. Tops and branches did not show desirable NO_x reduction and made the combustion also more unstable. N_2O emissions were very low, typically below 5 ppm at 11% O_2 in the dry flue gas, except for mixtures with high nitrogen content, where values up to 20 ppm were observed. The presented results are part of a larger study on

problematic fuels, also considering ash content and corrosive compounds which have been discussed elsewhere.

Keywords: biomass mixtures; combustion; NO_x; staged air; wood; straw; peat; sewage sludge

1. Introduction

According to the analysis carried out by the European Renewable Energy Council, the EU aims for a 100% renewable energy future by 2050, where biomass will potentially supply about 36% of the total European primary energy consumption, while the potential for many developing countries is higher since the resources are larger in such areas [1]. Biomass, with large resources around the World, which contains carbon in its structure, is almost a CO_2-neutral fuel. Combustion is the conventional way of extracting energy from biomass to produce heat, electricity or combined heat and power (CHP). Biomass can also be converted to synthetic natural gas or liquid fuels like methanol in order to be used in the transportation sector [2,3]. As a carbon- and nitrogen-containing fuel, combustion of biomass is nevertheless associated with emissions of harmful pollutants. Emissions from a biomass combustion process are normally divided into three groups [4,5]:

(1) incomplete combustion products or unburnt species: CO, C_xH_y, …
(2) complete combustion emissions: CO_2, H_2O, NO_x, …
(3) bottom ash and fly ash

In large industrial boilers, particles from incomplete combustion are generally low due to favorable combustion conditions [6]. However for each type of biomass, based on the source, characteristics and chemical composition, special care should be taken with certain emissions and residues as they can cause environmental problems [7]. For example sewage sludge needs consideration regarding the high ash content and the problems regarding ash removal from the reactor. Parallel studies on the same fuel batch show that straw needs care due to a low ash melting temperature and high alkali content which may cause damage to the tubes and walls via agglomeration, corrosion, deposition and fouling [8]. This was confirmed by others for varying types of reactors [9,10]. Furthermore, peat, sewage sludge and straw have all high nitrogen contents that results in a high NO_x emission level [11–14]. It is difficult to reduce all the mentioned pollutants simultaneously. There is e.g., a trade-off between NO_x emissions and unburnt hydrocarbons and carbon monoxide. Hence decreasing one may result in increases in another [15]. Furthermore nitrogen oxides (NO_x = NO + NO_2 + NO_3) were classified as an indirect greenhouse gas in the Kyoto Protocol, by producing ozone via photochemical reactions in the atmosphere. The impact of NO_x emissions on global warming, acid rain, and formation of toxic chemicals should therefore be controlled.

Formation of NO_x ocurrs through four different processes: thermal NO_x (Zeldovich mechanism), N_2O-intermediate mechanism, prompt NO (Fenimore mechanism), and fuel-N conversion [11,16]. In solid fuels fired systems, fuel-NO accounts for more than 80% of the total NO_x and NO_x is mainly produced by conversion of volatile nitrogen-containing species such as NH_3 and HCN, while

remaining char-N oxidation in the reactor bed accounts for a minor part of the total NO [11,17–22]. In addition, thermal NO_x formation becomes important at temperatures above 1400 °C, which is far from the typical temperature range (800–1200 °C) of biomass combustion systems [16,23,24]. Experimental investigations are needed to characterize the release of nitrogen containing species from different solid biomass fuels to establish input for CFD modeling studies [25]. Figure 1 shows the conversion path for fuel-nitrogen in a conventional biomass combustion system.

Figure 1. Simple fuel nitrogen conversion path diagram.

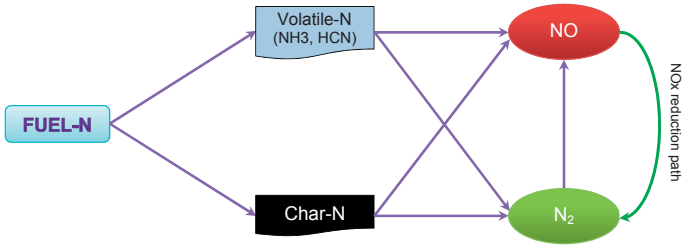

The parameters that affect NO_x formation and reduction potential are residence time, temperature, excess air ratio, fuel-N content, and mixing condition [26–29]. Temperature has the least influence on NO_x formation as mentioned earlier due to relatively low temperature range of typical biomass combustion [26]. Note still that it is proved that reburning during oxy-combustion is more sensitive to temperature [30]. Also, NO_x precursors, *i.e.*, ammonia and hydrogen cyanide, are very sensitive to temperature and the HCN/NH_3 ratio increases with increasing temperature [31–33].

Major technologies to reduce the NO_x emissions, based on the fuel composition and combustion system are divided into two categories: primary measures and secondary measures [34]. Primary measures reduce the emissions within the combustion chamber or before fuel feeding, so the formation of NO_x will be prevented as much as possible before the flue gases leave the reactor. These measures include staged air and staged fuel combustion, modification to the fuel composition by fuel blending, co-combustion, improvements to the combustion chamber, flue gas recirculation, fuel pretreatment, *etc.* [4,35–44]. e.g., the use of biomass/coal cofiring has become more interesting due to the increased environmental performance of energy production from solid fuels at a moderate cost. Generally the sulfur content of biomass is lower than that of coal, so the SO_x emissions from coal/biomass cofiring will be lowered since the sulfur content of the fuels blend has a lower level. Furthermore a reduction in NO_x emissions is predicted in cofiring plants as the mixture has lower nitrogen content [45].

Secondary measures are used to remove the formed emissions from the flue gas, where selective catalytic reduction (SCR) and selective non-catalytic reduction (SNCR) are the most well-known secondary technologies and can reduce the NO_x level up to 90%. However, the operation range and the overall economics of the plant should be considered before applying such costly methods [16,41,46,47]. Therefore, for small biomass combustion reactors, only primary reduction techniques are considered used in a feasible way. Air staging is most interesting in this respect due to its rather simple application and high NO_x reduction potential. In an air staged scenario, the total air is divided and fed to the reactor in two stages. The majority of fuel-N is converted to HCN, NO and NH_3 in the first stage

where the primary excess air ratio is kept lower than, but close to, stoichiometric conditions. Thereafter, the remaining air is added to the reactor in the second stage. Ammonia is converted to NH_i and may form NO if fuel lean conditions exist in the second stage [48]. However, due to the under-stoichiometric condition in the second stage, HCN and NH_i radicals react with NO to form N_2 responsible for the NO_x reduction [27]. Hence, keeping the primary excess air ratio at an optimum value is the key to minimize NO_x in staged air combustion.

Staged air combustion is widely applied in biomass combustion applications, both on the small scale and the large scale. Fuel staging follows a concept similar to air staging, but with addition of the fuel to the reactor in two stages. Some researchers tried to use a *combination* of the methods. Such combined staging (CS) was developed by Zabetta *et al.* [41] who used staged air, staged fuel and selective noncatalytic reduction (SNCR), and differs from other approaches since it pursues the reduction of NO_x via HCN as the key intermediate. The application of CS method is relative for the small burner or very fast engines where the residence time is too short to reach the maximum reduction from the simple staging technique. In addition, it needs more modification to the burner and is therefore costly. The reactor setup used in this study, however, has a long residence time which allows the maximum reduction via air staging.

In this work, experiments were performed in a fixed grate small scale multifuel reactor in order to investigate the NO_x emissions. The reactor has the possibility to facilitate both fuel and air staging, of which the latter has been the focus in this work. The fuels used in the present study are problematic fuels regarding ash related issues and corrosive content which make the combustion process complicated in large scale boilers. The ash related issues have been studied for the same batch of fuels and are presented and discussed elsewhere [8,49]. Furthermore, the selected biomasses cover a relatively broad range of nitrogen content and include straw, sewage sludge, peat, wood pellets, and tops and branches. Hence, the effect of initial fuel-N content on the conversion rate of nitrogen to NO_x is also investigated and discussed. Additional studies are needed on branches and tops due to a large resource potential in Northern Europe. Particularly it is necessary to investigate the emission levels from blends of fuels, and the effect this has on the expected optimum NO_x reduction potential by staged air combustion.

2. Materials and Methods

2.1. Sample Preparation

Five types of biomass and mixtures thereof were investigated to provide a wide basis for understanding emissions based on fuel characteristic. The selected fuels for this study were straw, sewage sludge, peat, virgin wood and forest residues (tops and branches) which had nitrogen content of 0.11–7.02 wt%. All fuels were pelletized to 6 mm diameter. Wood pellets and forest residues were obtained from Norwegian sources. Forest residues were collected from southern Norway, from stands with poor site quality. Peat was provided by Eidsiva Bioenergi AS. Sewage sludge and straw were provided through the SciToBiCom ERA-net by respectively Bioenergy2020+ (Austria) and DTU (Denmark). The wood pellet samples are hereby named WP, the forest residue samples GG (or Grot), and the Sewage Sludge samples SS, and so on. To prepare the fuel mixtures, the original fuels were

first grinded and then mixed and pelletized in a lab-scale pellet machine. Proximate and ultimate analyses were carried out both for the pure fuels and the mixtures. The results of the analyses are given in Table 1 and Table 2. ASTM E871, ASTM E872 and ASTM D1102 were used to measure moisture content, volatile matter and ash content of the fuels respectively and fixed carbon was obtained by difference to 100%.

Table 1. Ultimate analyses of the samples, wt% daf (dry, ash free).

	C	H	O	N	S	Cl
WP	51.4	6.1	42.4	0.11	0.05	0.02
GG	53.4	6.2	39.9	0.43	0.12	0.04
Straw	49.5	6.1	43.6	0.50	0.21	0.10
SS	48.9	7.4	34.6	7.02	2.07	0.10
Peat	56.0	6.1	35.0	2.60	0.34	0.02
WP + GG 5%	51.5	6.1	42.3	0.12	0.06	0.02
WP + GG 20%	51.7	6.1	41.9	0.17	0.07	0.02
WP + GG 50%	52.3	6.1	41.2	0.27	0.09	0.03
Straw + GG 20%	50.3	6.2	42.8	0.48	0.20	0.09
Straw + GG 50%	51.5	6.2	41.7	0.46	0.17	0.07
Straw + SS 5%	49.5	6.2	43.3	0.72	0.28	0.10
Straw + SS 10%	49.5	6.2	43.0	0.94	0.34	0.10
Straw + SS 20%	49.4	6.3	42.3	1.42	0.47	0.10
Straw + Peat 5%	49.8	6.1	43.3	0.58	0.22	0.10
Straw + Peat 20%	50.5	6.1	42.3	0.82	0.23	0.09
Straw + Peat 50%	52.2	6.1	40.0	1.39	0.27	0.06

Table 2. Proximate analyses of the samples (wt%, dry).

	VM	Fixed Carbon	Ash	Moisture (wet base)	HHV (MJ/kg)
WP	85.3	14.5	0.2	6.5	20.7
GG	77.0	20.7	2.3	9.6	21.8
Straw	78.7	16.4	4.9	11.7	19.9
SS	56.0	8.5	35.6	□	21.1
Peat	65.4	24.3	10.3	□	22.9
WP + GG 5%	84.6	15.0	0.4	14.4	20.8
WP + GG 20%	83.0	16.5	0.6	14.4	20.9
WP + GG 50%	80.7	18.0	1.3	11.8	21.2
Straw + GG 20%	77.9	17.7	4.4	13.8	20.4
Straw + GG 50%	77.5	18.9	3.6	11.8	20.9
Straw + SS 5%	77.6	16.1	6.3	12.8	20.0
Straw + SS 10%	76.6	15.5	7.9	15.4	20.0
Straw + SS 20%	73.6	14.6	11.8	9.4	20.0
Straw + Peat 5%	77.6	17.1	5.2	11.2	20.0
Straw + Peat 20%	77.1	17.1	5.9	14.4	20.3
Straw + Peat 50%	73.1	19.5	7.4	17.1	21.1

The mixtures were selected based on thermodynamic analyses to minimize the formation of corrosive components in the reactor and the results regarding corrosion abatement as presented and discussed in the earlier publications [8,49].

Small deviations (not presented) between the measured (Table 2) and calculated values exist for the composition of the mixture samples, which are probably due to the higher measurement uncertainties in the lowest measurement range [50]. This is discussed further in the Results section.

2.2. Experimental Setup

The combustion tests were carried out in SINTEF Energy Research's multifuel reactor, which is an electrically heated high temperature reactor. A schematic drawing is presented in Figure 2. The reactor has a ceramic inner tube with a diameter of 100 mm and a length of 2 m. The vertical tube consists of two 1 m long ceramic tubes connected with a ceramic socket. The ceramic tubes are made of non-porous and non-catalytic alumina.

Figure 2. Schematic of the multifuel reactor.

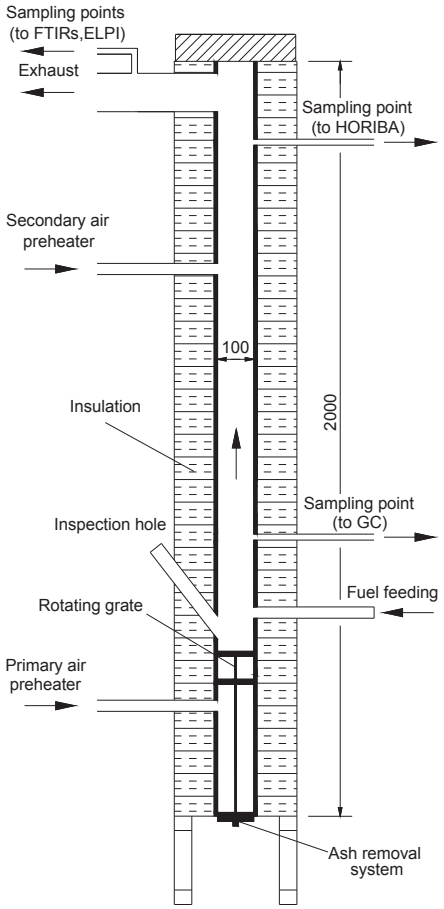

The reaction section, located above the grate, is 1.6 m long, while the section below the grate is 0.4 m long. The heating system is fitted inside the insulation shell and consists of four separate 0.5 m high heating zones of 4 kW each (16 kW in total) that enclose the ceramic tubes. The top and bottom of the reactor are insulated, but not heated, and both include detachable and insulated plates. The lower part of the multifuel reactor is the section containing the grate, which has two levels (10 cm apart), a primary grate and a final burnout grate and an ash collection system with an ash bin. The grate and the ash bin are both made of Inconel. The reactor setup thus combines two possible reduction technologies simultaneously, staged air and staged fuel combustion. The 2-level grate may give a possible fuel staging effect. The inlet air is preheated to the reactor temperature in external preheaters. The primary air is added under the grate (underfire air) and the secondary air is added above the grate (overfire air). The air flow is controlled by high precision digital mass flow controllers. The temperature inside the reactor is measured at several points. Furthermore, additional thermo-couples are used to control and protect the heating elements of the reactor from overheating. The preheating units have separate control systems. The temperatures are also monitored in the flue gas channel with four K-type thermocouples.

2.3. Gas Sampling

The flue gas composition, both at the reactor exit and in the primary zone, is continuously monitored. A schematic diagram of the sampling lines is shown in Figure 3.

Figure 3. Schematic diagram of the sampling lines.

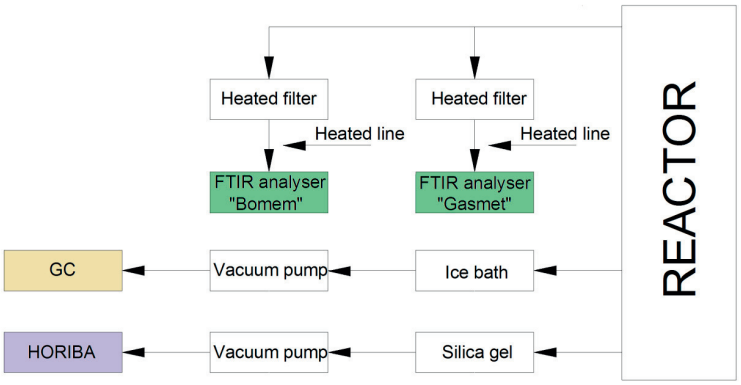

For gas analysis in the primary zone, a Varian CP-4900 micro gas chromatograph (GC) was used. A stainless steel probe with an outside diameter (OD) of 10 mm and an inner diameter (ID) of 8 mm was used for the gas sampling. The sampled gas passed first through a tar, water and particle ice-cooled trap consisting of a steel container filled with glass wool and with a glass microfiber paper filter. The sampling gas flow was about 1 L/min. The GC was equipped with two Thermal Conductivity Detectors (TCDs) with a detection limit of 1 ppm, and double injectors, each connected to a separate column. The first column was a 10 m long PoraPLOT Q-type, with an inner diameter of 0.25 mm and a 10 μm film thickness produced by Varian Inc., and uses helium as carrier gas. This column was used for the separation of CO_2, CH_4, C_2H_2 + C_2H_4 and C_2H_6. The second column was a 20 m long

CP-MolSieve 5A PLOT, with an inner diameter of 0.25 mm and a 30 μm film thickness produced by Varian Inc., and used argon as carrier gas in order to be able to detect H_2. This column was able to quantify H_2, O_2, N_2, CH_4 and CO. The GC had a sampling time interval of approximately two minutes.

The exhaust gases were quantified online with a Gasmet DX-4000 Fourier transform infrared (FTIR) spectrometer which was equipped with an integrated ZrO_2/O_2-analyzer, and a Mercury Cadmium Telluride (MCT) detector and had a maximum resolution of 4 cm^{-1}. The sampling line and cell were heated to 180 °C. The cell volume was 0.4 L and the optical path length was 5 m. The FTIR was used to quantify H_2O, CO_2, CO, NO, N_2O, NO_2, SO_2, NH_3, HCl, HF, CH_4, C_2H_6, C_2H_4, C_3H_8, C_6H_{14}, CHOH, HCN and O_2. Extracted gases were passing through heated filters and heated lines, before reaching the FTIR. A stainless steel probe with an OD of 10 mm and an ID of 8 mm was used for sampling. The sampling position was located in the stack. The second FTIR spectrometer was a Bomem MB9100, which takes samples from a position near the first FTIR. This analyzer was used to measure all the species mentioned for Gasmet in addition to C_4H_{10}. The analyses was done by a large cell heated to 176 °C with a 1 cm^{-1} spectral resolution detector and with a measurement time interval of 80 s.

Flue gas samples were also extracted through a sampling point near the top of the reactor. An Inconel probe with 6 mm OD and 4 mm ID was used for sampling. The gas first passed through silica gel and was thereafter led to a HORIBA analyzer using a vacuum pump. The sampling rate was 0.4 L/min. The HORIBA PG-250 is a portable gas analyzer that can simultaneously measure up to five separate gas components. The HORIBA PG-250 uses non-dispersive infrared (NDIR) absorption to quantify CO, SO_2 and CO_2, cross-modulation ordinary pressure chemiluminescence to measure NO_x, and a galvanized Zr cell for O_2 measurements. The sampling unit comprises a filter, a mist catcher, a pump, an electronic cooling unit, and an NO_2 to NO converter.

Bottom ash collected in the ash bin was removed manually after each test. Unburnt carbon in the bottom ash was measured after each experiment by weighing the ash before and after exposing it to a temperature of 550 °C for a period of 20 h.

2.4. Experimental Procedure

The experimental matrix is given in Table 3. The experiments were carried out with pellets of 6 mm diameter from five biomass fuels and mixes of these, all in air staging mode. Only isothermal experiments were performed with a reactor temperature of 850 °C. The total excess air ratio was about 1.6, and the primary excess air ratio was about 0.8, however due to small variations in the fuel feeding rate, a range of excess air ratios was obtained during stable period of the experiments.

The fuel pellets were fed automatically from a fuel container located over a water-cooled piston. The perfectly sealed piston transported the fuel into the reactor and the pellets fell on the upper grate, thereafter the piston quickly returned to its starting position and the process was repeated. The feeding frequency was set to approximately 6–7 seconds, based on the fuel density and pellets size distribution, to ensure a fuel feeding rate of about 400 g/h.

Table 3. The experimental matrix.

Experiment No.	Fuel 1	Fuel 2	Fuel 2 in the mixture (wt%)
1	Wood Pellet	-	-
2	Wood Pellet	Grot	5%
3	Wood Pellet	Grot	20%
4	Wood Pellet	Grot	50%
5	Grot	-	-
6	Straw	Grot	20%
7	Straw	Grot	50%
8	Straw	Sewage Sludge	5%
9	Straw	Sewage Sludge	10%
10	Straw	Sewage Sludge	20%
11	Straw	Peat	5%
12	Straw	Peat	20%
13	Straw	Peat	50%

The pellets were mainly combusted on the upper (primary) grate. Then the pellets were gradually moved to a slot leading to the second (final burnout) grate by means of rotating blades. Each grate had two rotating blades rotating slowly around and completing a circle in around three minutes. Final burnout took place on the lower grate before the ash is moved to the ash bin. At the bottom of the ash bin another rotating blade moved the ash into an ash tube. The gas residence time between the grate levels was in the range of 1–2 s. and the total residence time of fuel gases in the reactor was 25–50 s, due to the very low flow velocity (0.03–0.07 m/s).

3. Results and Discussion

The carbon and hydrogen balance as a function of total excess air ratio for one of the experiments (mixture of straw 50% + peat 50%) is shown in Figure 4. As shown, the deviation between the measured and calculated values is in the range of ±2%, so the experimental measurements are reliable with low uncertainty. The same trend was seen for all the other experiments (results not presented).

Combustion quality was also checked for all experiments with regard to unburnt species. The concentration of CO and C_xH_y (as ppm at 11% O_2 in the dry flue gas) is shown in Figure 5 for the experiment with "straw 80% + grot 20%". Due to the relatively long residence times (25–50 s), good mixing and high temperatures, the amounts of CO and unburnt hydrocarbons were very low. For the other mixtures CO and C_xH_y were below 50 ppm and 5 ppm at 11% O_2 in dry flue gas, respectively. Hence, in all experiments the combustion can be considered complete under the given conditions. This is important to ensure that measurements of fuel-N originating NO_x are representative for what may be expected under normal and efficient running conditions.

Figure 4. Carbon and hydrogen balance check: CO_2 and H_2O concentration and measured deviation for the experiment with "Straw 50% + Peat 50%".

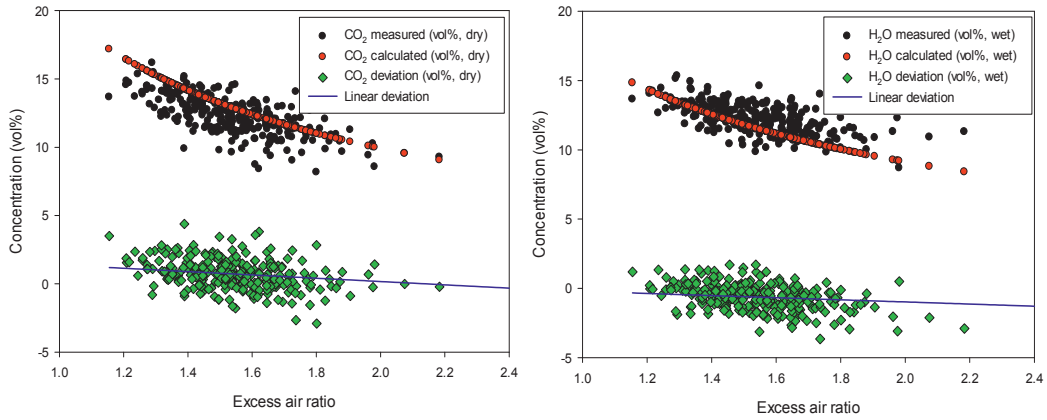

Figure 5. Unburnt gases (CO and C_xH_y): concentration as ppm at 11% O_2 in dry flue gas for the experiment with "Straw 80% + Grot 20%".

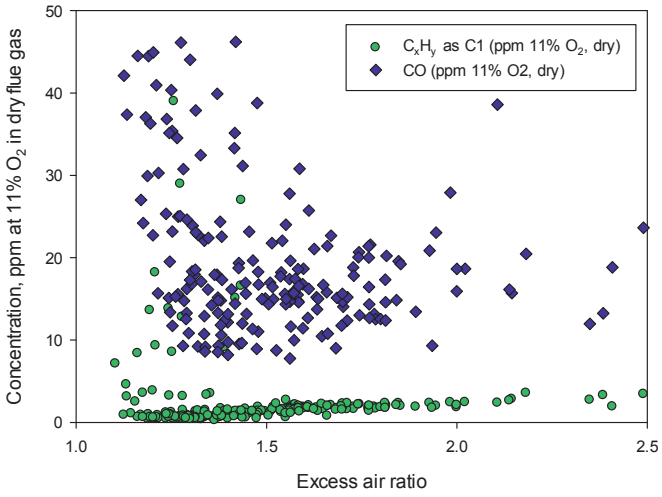

3.1. NO_x Reduction in Air Staged Combustion

The experiments revealed the NO_x reduction potential with staged air combustion. The primary excess air ratio was the key influencing factor for NO_x reduction in the set of experiments, where the results were especially relevant for a grate-furnace. In Figures 6–9 the effect of primary excess air ratio for different mixtures of straw, peat, sewage sludge, forest residues and wood pellets are compared.

Figure 6. Influence of the primary excess air ratio on the NO_x emissions from "straw + peat" mixtures for air staging (temperature: 850 °C, NO_x as ppm in dry flue gas at 11% O_2).

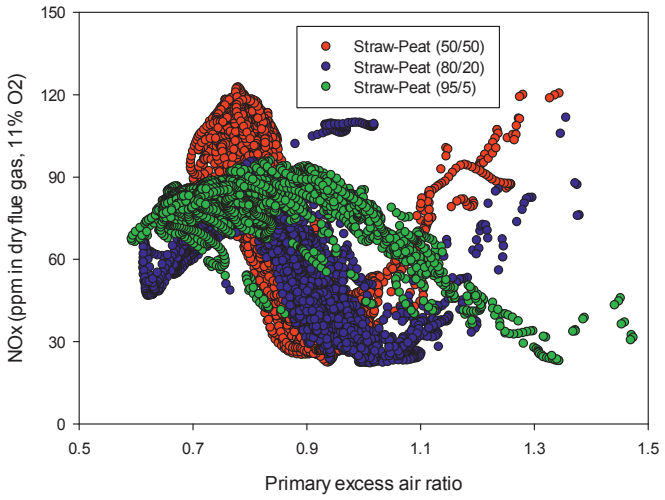

Figure 7. Influence of the primary excess air ratio on the NO_x emissions from "straw + sewage sludge" mixtures for air staging (temperature: 850 °C, NO_x as ppm in dry flue gas at 11% O_2).

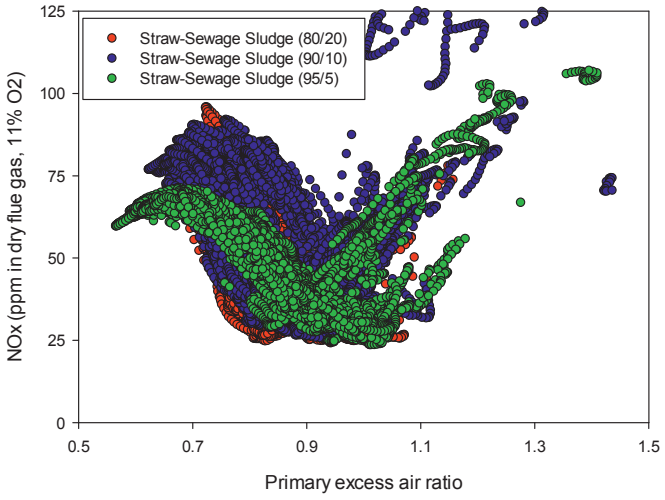

Figure 8. Influence of the primary excess air ratio on the NO_x emissions from "straw + tops and branches" mixtures for air staging at a temperature of 850 °C.

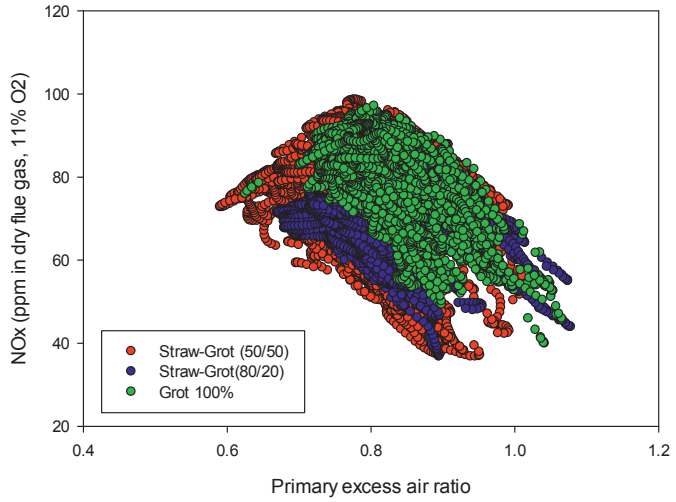

Figure 9. Influence of the primary excess air ratio on the NO_x emissions from "wood pellet + tops and branches" mixtures at a temperature of 850 °C.

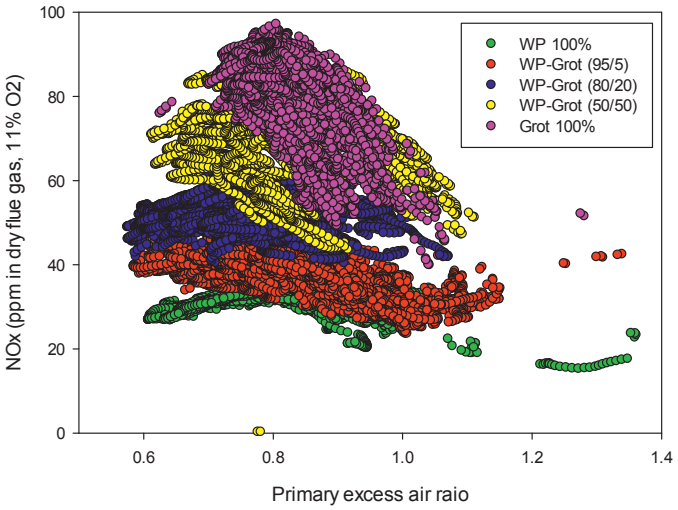

The NO_x level was clearly reduced when the primary excess air ratio increased up to about 1. An optimum reduction was found for almost all the experiments at a primary excess air ratio close to 0.9. The optimum primary excess air ratio for combustion of "straw 95% + peat 5%" was however found around 1.3 as seen in Figure 6 which is high for typical values of optimum primary excess. This needs some more clarifications. In this experiment, because of a high share of straw in the mixture, the ash melting temperature for the fuel blend was low, and 5 wt% peat did not improve the ash melting behavior of straw. Hence, during the running of the reactor, sintering happened on the grate, which caused the air slots on the grates to be filled with melted ash. In this case the actual "available oxygen"

for the fuel in the reactor was clearly lower than the amount of air which was fed to the reactor. Therefore the real primary excess air ratio for the case "straw 95% + peat 5%" may be regarded as a value closer to the other experiments, *i.e.*, 0.9–0.95. Similar problems were also observed for "straw 80% + peat 20%", which explains that the optimum point is shifted toward an excess air ratio of 1, by the same interpretation. This issue is of course related to the design of the reactor. However, as it is not uncommon with such fuel grates in a conventional combustor, low ash melting properties for certain fuels [9] should be considered when designing for optimum combustion of biomass.

The reduction in NO_x level for the staged air experiments was found to start from a primary excess air ratio of about 0.7 and continue to the highest reduction on the excess air ratio of about 0.9. However, further increase in the excess air ratio increased again the NO_x emissions. This can be explained by the staged combustion effect. In the first stage, primary air was added for devolatilization of the volatile fraction of the fuel, which forms a fuel gas composed of mainly CO, H_2, C_xH_y, H_2O, CO_2 and N_2. In addition, supplying less air than stoichiometric condition in a range of 0.7–0.9 causes the volatile-N fraction to form nitrogen containing NO_x precursors. Therefore, small amounts of NH_3, HCN, HOCN and NO will be produced depending on the fuel nitrogen content, temperature and other operating conditions. In the second stage, sufficient air is fed to the reactor to ensure final burnout of emissions from incomplete combustion, e.g., CO, C_xH_y. Adding the remaining air in the second stage creates the path for NO reduction, where NO_x act as an oxidant agent for the other N-containing species and also products of incomplete combustion (NH_2, NH_3, CO, CH_4, …) in reactions such as:

$$NO + NH_2 \rightarrow N_2 + H_2O \quad \text{(R1)}$$

$$NO + CH_4 \rightarrow 1/2N_2 + CO + 2H_2 \quad \text{(R2)}$$

In the regions where the injected primary air is very low, the oxygen will not be sufficient for NO formation and just NH_i and HCN will appear in the first stage from the fuel nitrogen. Following that, in the second stage, the remaining secondary air provides more than enough O_2, so the formation of NO from its precursors' oxidation will be elevated following the reaction:

$$NH_i + O_2 \rightarrow NO + \ldots \quad \text{(R3)}$$

In contrast, when the primary excess air increases above 1, excess oxygen in the first stage will cause the oxidation of all pyrolysis gases. Therefore much more NO will appear while no sufficient NH_i exists for the second stage to minimize the NO emissions via the reduction path, reaction (1), resulting in a raised NO emission level in the flue gas.

The results of staged air combustion of wood pellet and forest residues mixtures are presented in Figure 9. For better comparison, the results from pure wood and 100% grot are also included in the graph. Grot shows higher NO_x emissions which are due to its higher nitrogen content. The NO_x reduction is also limited to 40–50% for WP at the optimum excess air ratio. It is important to note that the NO_x reduction potential depends greatly on the fuel nitrogen content. A reduction of 50–80% is observed for the experiments where 80% reduction corresponds to the experiment with highest nitrogen content in the fuel blend, *i.e.*, "straw 50% + peat 50%". This will be discussed further below.

3.2. Effect of Fuel-N Content on N-Conversion: NO_x

For comparison purposes and to evaluate the conversion of the fuel nitrogen to NO_x, the ratio NO_x/Fuel-N is generally used. This ratio is obtained by dividing the total amount of nitrogen that exists in the measured NO_x in the flue gas by the nitrogen content of the biomass input. The major part of NO_x was by far composed of NO for the set of experiments at the given conditions.

NO_x/Fuel-N results are presented in Figure 10 for the fuels and mixtures at different stoichiometric ratios. It is shown that the nitrogen conversion level depends greatly on the fuel nitrogen content. The mixtures with wood pellets, which have the lowest fuel-N content, revealed high conversion of nitrogen to NO_x, while mixtures with peat converted considerably less nitrogen to NO_x.

Figure 10. Fuel-N conversion and the effect of fuel-N content.

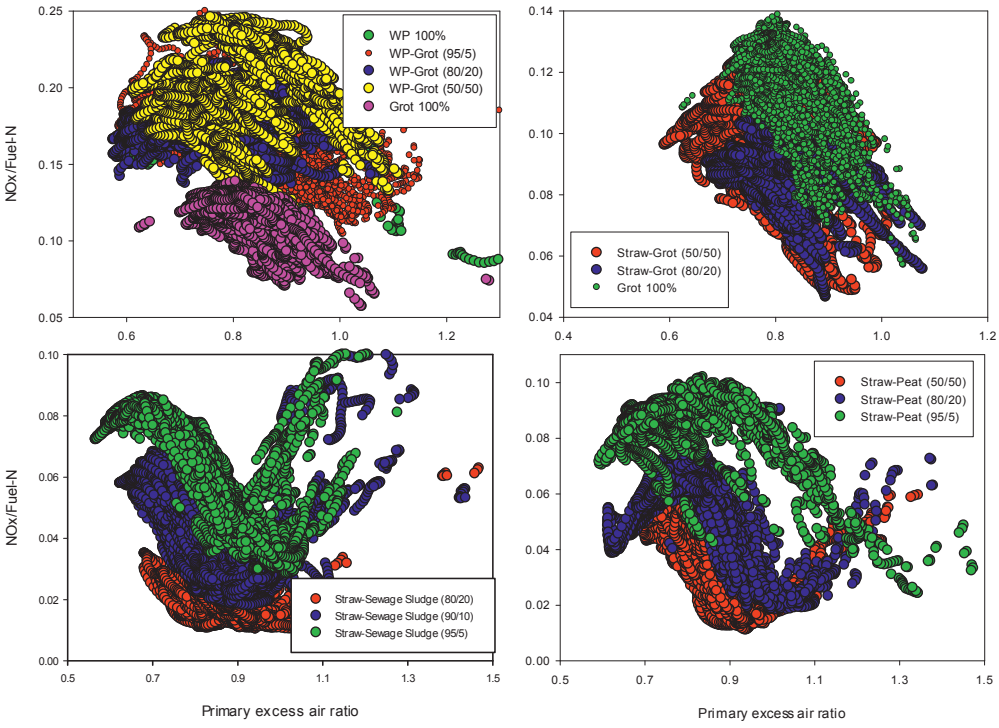

The plot in Figure 11 summarizes the conversion rate of fuel nitrogen to NO_x with respect to the investigated fuels nitrogen content. The results are derived from the combustion at the optimum condition, *i.e.*, primary excess air ratio of 0.9–0.95. Therefore this graph shows the minimum potential fuel-N conversion to NO_x in the grate reactor. However, the trend for other excess air ratios is the same, where the fuels and blends with high nitrogen content typically convert only 2% of the fuel-N to NO_x.

Figure 11. Influence of fuel-N content on the conversion to NO_x.

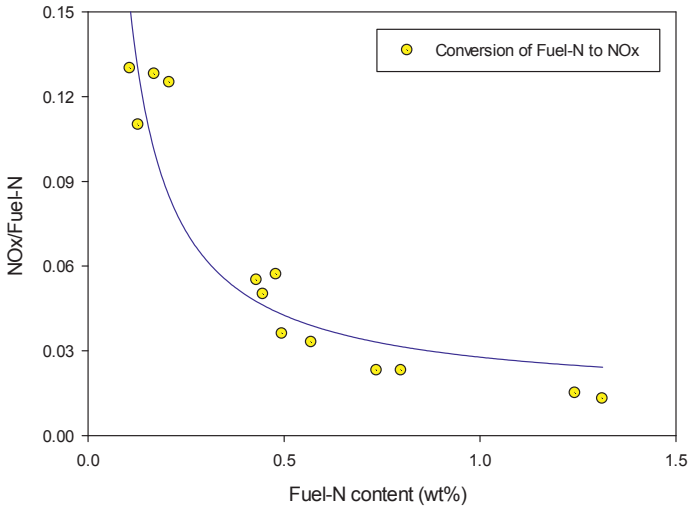

3.3. Effect of Fuel-N Content on N-Conversion: N_2O

The N_2O concentration in the flue gas is shown in Figure 12. Nitrous oxide emissions are typically low, below 5 ppm at 11% O_2 in the dry flue gas. However, it should be noticed that the N_2O level for a number of experiments with high nitrogen content in the fuel was up to 25 ppm. The N_2O concentration increased with primary excess air ratio. Unburnt species such as CO and CH_4 that are reductive agents for NO_x, as discussed earlier, have proven to promote the fuel-N conversion to N_2O in high excess air ratios [51]. Therefore, the conditions which are in general favorable for NO_x reduction result in more N_2O formation.

Figure 12. Effect of the primary excess air ratio on the N_2O emissions at a temperature of 850 °C.

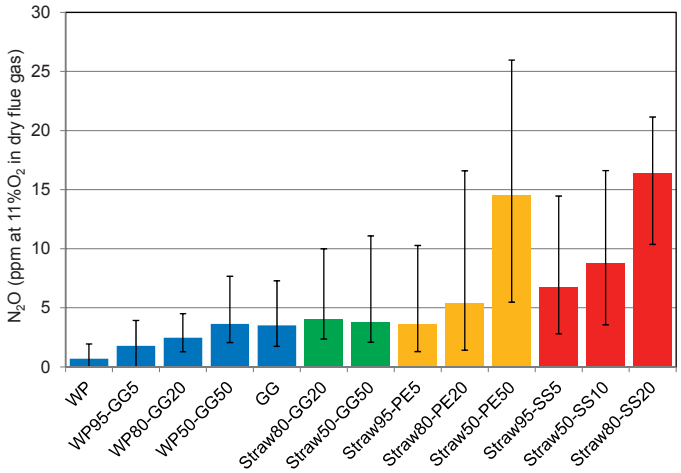

3.4. Effect of Fuel Type on NO_x

Figure 13 presents the yields of the main unburnt gases in the primary zone. CO, H_2 and CH_4 were measured by a GC. The proximate analysis of the fuels reveals that the five original fuels are very different from each other, especially regarding ash content and volatile matters. The volatile matter (VM) contents of the selected original fuels ranged from around 56 to 85 wt% (dry basis) with ash contents from 0.2 to about 36 wt%. Wood pellets have the lowest ash and highest VM, while the highest ash and lowest VM belongs to sewage sludge. However, the volatile content of GG and straw are quite close to each other, even though straw has two times higher ash content. Obviously, the volatiles are very important for the nitrogen release and especially for the share of char or volatile nitrogen content, which finally affect the NO_x reduction path. Ash elemental composition should also be considered in a fuel type discussion, since elements such as calcium can act as catalyst to reduce nitrogen oxides [52]. Addition of fuels with higher volatile content would result in higher NO_x reduction, since the availability of radical species necessary for NO reduction is higher in the combustion zone. This is related to the reaction mechanism which is explained in the previous section, reactions R1-R3.

Figure 13. Level of main unburnt species in the primary zone for different fuels and mixtures.

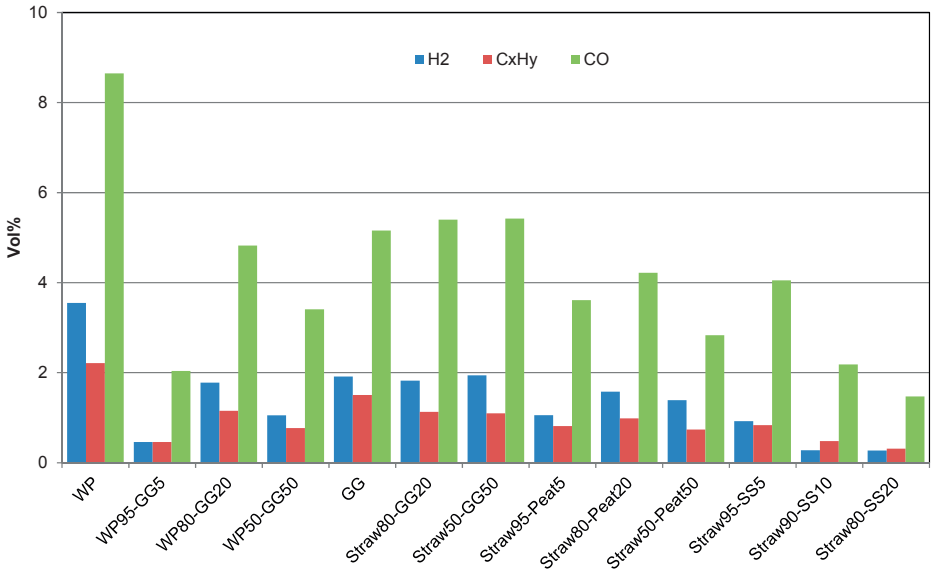

On the other hand, release of char nitrogen is affected by particles residence time, size of pellets and the amount of inorganic elements, where the latter is being determined by the fuel type [11]. Due to the special design of our reactor (two level grate), the potential effect of volatile species interaction with the char matrix should also be considered as a potential significant factor. Straw mixtures with 20% GG, peat and SS give the following results: blending with GG gives the highest VM and the lowest Ca in the mixture. Contrary, the mixture of straw with SS has the lowest VM and the highest Ca. There is a competition between the explained mechanism for nitrogen release and reduction. Although GG has

higher volatile content and release a higher amount of volatile species according to Figure 13, the minimum NO_x emission and NO_x/Fuel-N for Straw + GG20 is significantly higher than for the other two blends. The NO_x reduction potential was also in the lowest range for this GG mixture, around 50%. Hence, it is suggested that GG is not a good selection to be blended with straw in order to reduce fuel-NO_x emissions. However, peat and SS showed a higher NO_x reduction (75–80%) with a minimum NO_x level of about 20–25 ppm at 11% O_2 in dry flue gas. Figure 13 shows lower volatiles amounts from SS mixtures compared to peat mixtures, so it seems that the effect of the reduction reaction R2 has been minimal in this case compared to other mechanisms. Finally, sewage sludge gives the lowest fuel-N conversion to NO_x compared to the other mixtures which makes this fuel a proper blend for straw combustion. It is suggested that SS addition to straw leads to increased mineral matters on the grate, hence resulting in catalytic activities of ash elements leading to NO_x reduction by CO or CH_4. However, further investigations are required to quantify the effect of the mentioned mechanism solely.

4. Conclusions

The present study demonstrated that air-staging can be effectively used in a grate combustion reactor in order to reduce the NO_x emissions. Furthermore, staged air combustion for different biomass fuels and in particular mixtures of the selected fuels were investigated. Staged air combustion reduced the NO_x emissions significantly. However, the reduction level depended on the stoichiometric ratio of the first stage. An optimum primary excess air ratio of about 0.9 was found for the reactor in the primary zone (fuel rich condition). However, low ash melting characteristics of some of the fuels, particularly straw, caused this value to be somewhat higher due to sintering on the fuel grate. The NO_x level was reduced with 50–80% based on the fuel type. Mixtures with high nitrogen content showed higher reduction potential while wood pellets with the lowest nitrogen content showed less reduction. The unburnt species' concentration (CO and C_xH_y) was very low in all cases due to the good combustion quality. Regarding fuel-N conversion to NO_x, this depends on the nitrogen content of the biomass. The fuels with lower nitrogen content showed a higher conversion of fuel-N to NO_x, while a blend of peat and sewage sludge, which had high fuel-N content, only converted about 2% of the fuel-N, the rest being converted directly to N_2, and a minor part remained in ash. SS, having low VM and high ash content, is suggested as a favorable fuel to be blended with straw, showing high NO_x reduction and low fuel-N conversion. GG, however, with high VM and low ash content, did not show desirable NO_x reduction and also made the combustion more unstable. The reduction potential for GG and SS mixtures was about 50% and 80%, respectively.

Acknowledgments

The authors wish to acknowledge the financial support from the Research Council of Norway and a number of industrial partners through the project KRAV ("Enabling small scale biomass CHP in Norway"). We also thank Bioenergy2020+ and DTU for providing fuels through SciToBiCom ERA-net Bioenergy project.

References

1. Zervos, A.; Lins, C.; Muth, J. *RE-Thinking 2050*; European Renewable Energy Council, Renewable Energy House: Brussels, Belgium, 2010.
2. Borgwardt, R.H. Methanol production from biomass and natural gas as transportation fuel. *Ind. Eng. Chem. Res.* **1998**, *37*, 3760–3767.
3. Jurascik, M.; Sues, A.; Ptasinski, K.J. Exergetic evaluation and improvement of biomass-to-synthetic natural gas conversion. *Energy Environ. Sci.* **2009**, *2*, 791–801.
4. Nussbaumer, T. Combustion and co-combustion of biomass: Fundamentals, technologies, and primary measures for emission reduction. *Energy Fuels* **2003**, *17*, 1510–1521.
5. Khan, A.A.; de Jong, W.; Jansens, P.J.; Spliethoff, H. Biomass combustion in fluidized bed boilers: Potential problems and remedies. *Fuel Process. Technol.* **2009**, *90*, 21–50.
6. Johansson, L.S.; Tullin, C.; Leckner, B.; Sjövall, P. Particle emissions from biomass combustion in small combustors. *Biomass Bioenergy* **2003**, *25*, 435–446.
7. Obernberger, I.; Brunner, T.; Bärnthaler, G. Chemical properties of solid biofuels--significance and impact. *Biomass Bioenergy* **2006**, *30*, 973–982.
8. Khalil, R.A.; Houshfar, E.; Musinguzi, W.; Becidan, M.; Skreiberg, Ø.; Goile, F.; Løvås, T.; Sørum, L. Experimental investigation on corrosion abatement in straw combustion by fuel-mixing. *Energy Fuels* **2011**, *25*, 2687–2695.
9. Nielsen, H.P.; Frandsen, F.J.; Dam-Johansen, K. Lab-scale investigations of high-temperature corrosion phenomena in straw-fired boilers. *Energy Fuels* **1999**, *13*, 1114–1121.
10. Thy, P.; Jenkins, B.M.; Williams, R.B.; Lesher, C.E.; Bakker, R.R. Bed agglomeration in fluidized combustor fueled by wood and rice straw blends. *Fuel Process. Technol.* **2010**, *91*, 1464–1485.
11. Glarborg, P.; Jensen, A.D.; Johnsson, J.E. Fuel nitrogen conversion in solid fuel fired systems. *Prog. Energy Combust. Sci.* **2003**, *29*, 89–113.
12. Ren, Q.; Zhao, C.; Duan, L.; Chen, X. NO formation during agricultural straw combustion. *Bioresour. Technol.* **2011**, *102*, 7211–7217.
13. Giuntoli, J.; de Jong, W.; Verkooijen, A.H.M.; Piotrowska, P.; Zevenhoven, M.; Hupa, M. Combustion characteristics of biomass residues and biowastes: Fate of fuel nitrogen. *Energy Fuels* **2010**, *24*, 5309–5319.
14. Aho, M. Pyrolysis and combustion of peat and wood as single particles and as a layer. *J. Anal. Appl. Pyrolysis* **1987**, *11*, 149–162.
15. Eskilsson, D.; Rönnbäck, M.; Samuelsson, J.; Tullin, C. Optimisation of efficiency and emissions in pellet burners. *Biomass Bioenergy* **2004**, *27*, 541–546.
16. Mahmoudi, S.; Baeyens, J.; Seville, J.P.K. NO_x formation and selective non-catalytic reduction (SNCR) in a fluidized bed combustor of biomass. *Biomass Bioenergy* **2010**, *34*, 1393–1409.
17. Permchart, W.; Kouprianov, V.I. Emission performance and combustion efficiency of a conical fluidized-bed combustor firing various biomass fuels. *Bioresour. Technol.* **2004**, *92*, 83–91.
18. Qian, F.P.; Chyang, C.S.; Huang, K.S.; Tso, J. Combustion and NO emission of high nitrogen content biomass in a pilot-scale vortexing fluidized bed combustor. *Bioresour. Technol.* **2011**, *102*, 1892–1898.

19. Winter, F.; Wartha, C.; Hofbauer, H. NO and N_2O formation during the combustion of wood, straw, malt waste and peat. *Bioresour. Technol.* **1999**, *70*, 39–49.
20. Aho, M.J.; Hämäläinen, J.P.; Tummavuori, J.L. Importance of solid fuel properties to nitrogen oxide formation through HCN and NH_3 in small particle combustion. *Combust. Flame* **1993**, *95*, 22–30.
21. Hämäläinen, J.P.; Aho, M.J.; Tummavuori, J.L. Formation of nitrogen oxides from fuel-N through HCN and NH_3: a model-compound study. *Fuel* **1994**, *73*, 1894–1898.
22. Hämäläinen, J.P.; Aho, M.J. Effect of fuel composition on the conversion of volatile solid fuel-N to N_2O and NO. *Fuel* **1995**, *74*, 1922–1924.
23. Salzmann, R.; Nussbaumer, T. Fuel staging for NO_x reduction in biomass combustion: Experiments and modeling. *Energy Fuels* **2001**, *15*, 575–582.
24. Lopes, M.H.; Gulyurtlu, I.; Cabrita, I. Control of pollutants during FBC combustion of sewage sludge. *Ind. Eng. Chem. Res.* **2004**, *43*, 5540–5547.
25. Stubenberger, G.; Scharler, R.; Zahirovic, S.; Obernberger, I. Experimental investigation of nitrogen species release from different solid biomass fuels as a basis for release models. *Fuel* **2008**, *87*, 793–806.
26. Houshfar, E.; Skreiberg, Ø.; Løvås, T.; Todorović, D.; Sørum, L. Effect of excess air ratio and temperature on NO_x emission from grate combustion of biomass in the staged air combustion scenario. *Energy Fuels* **2011**, *25*, 4643–4654.
27. Skreiberg, Ø.; Glarborg, P.; Jensen, A.D.; Dam-Johansen, K. Kinetic NO_x modelling and experimental results from single wood particle combustion. *Fuel* **1997**, *76*, 671–682.
28. Kolb, T.; Jansohn, P.; Leuckel, W. Reduction of NO_x emission in turbulent combustion by fuel-staging/effects of mixing and stoichiometry in the reduction zone. *Symp. (Int.) Combust.* **1989**, *22*, 1193–1203.
29. Jenkins, B.M.; Baxter, L.L.; Miles, T.R. Combustion properties of biomass. *Fuel Process. Technol.* **1998**, *54*, 17–46.
30. Normann, F.; Andersson, K.; Johnsson, F.; Leckner, B. NO_x reburning in oxy-fuel combustion: A comparison between solid and gaseous fuels. *Int. J. Greenhouse Gas Control* **2011**, *5*, S120–S126.
31. Hansson, K.-M.; Samuelsson, J.; Tullin, C.; Åmand, L.-E. Formation of HNCO, HCN, and NH_3 from the pyrolysis of bark and nitrogen-containing model compounds. *Combust. Flame* **2004**, *137*, 265–277.
32. Ren, Q.; Zhao, C.; Wu, X.; Liang, C.; Chen, X.; Shen, J.; Wang, Z. Formation of NO_x precursors during wheat straw pyrolysis and gasification with O_2 and CO_2. *Fuel* **2010**, *89*, 1064–1069.
33. Becidan, M.; Skreiberg, Ø.; Hustad, J.E. NO_x and N_2O precursors (NH_3 and HCN) in pyrolysis of biomass residues. *Energy Fuels* **2007**, *21*, 1173–1180.
34. Berndes, G.; Baxter, L.; Coombes, P.; Delcarte, J.; Evald, A.; Hartmann, H.; Jansen, M.; Koppejan, J.; Livingston, W.; van Loo, S.; *et al*. *The Handbook of Biomass Combustion and Co-Firing*; Earthscan: London, UK, 2008.

35. Padinger, R.; Leckner, B.; Åmand, L.-E.; Thunman, H.; Ghirelli, F.; Nussbaumer, T.; Good, J.; Hassler, P.; Salzmann, R.; Winter, F.; *et al*. Reduction of Nitrogen Oxide Emissions from Wood Chip Grate Furnaces — Final Report for the EU-JOULE III Project JOR3-CT96-0059. In *Proceedings of 1st World Conference on Biomass for Energy and Industry*, Sevilla, Spain, 5–9 June 2000; Kyritsis, S., Beenackers, A.A.A.M., Helm, P., Grassi, A., Chiaramonti, D., Eds.; James & James (Science Publishers) Ltd.: Sevilla, Spain, 2000; pp. 1457–1463.
36. Padinger, R. NO_x Reduction of Biomass Combustion by Optimized Combustion Chamber Design and Combustion Control. In *Progress in Thermochemical Biomass Conversion*; Blackwell Science Ltd.: Hoboken, NJ, USA, 2008; pp. 918–928.
37. Kicherer, A.; Spliethoff, H.; Maier, H.; Hein, K.R.G. The effect of different reburning fuels on NO_x-reduction. *Fuel* **1994**, *73*, 1443–1446.
38. Kristensen, P.G.; Glarborg, P.; Dam-Johansen, K. Nitrogen chemistry during burnout in fuel-staged combustion. *Combust. Flame* **1996**, *107*, 211–222.
39. Weissinger, A.; Obernberger, I.; Scharler, R. NO_x Reduction in Biomass Grate Furnaces by Primary Measures — Evaluation by Means of Lab-Scale Experiments and Chemical Kinetic Simulation Compared with Experimental Results and CFD Calculations of Pilot-Scale Plants. In *Proceedings of 6th European Conference on Industrial Furnaces and Boilers*, Estoril, Portugal, 2–5 April 2002.
40. Svoboda, K.; Pohořelý, M.; Hartman, M. Effects of operating conditions and dusty fuel on the NO_x, N_2O, and CO emissions in PFB co-combustion of coal and wood. *Energy Fuels* **2003**, *17*, 1091–1099.
41. Zabetta, E.C.; Hupa, M.; Saviharju, K. Reducing NO_x emissions using fuel staging, air Staging, and selective noncatalytic reduction in synergy. *Ind. Eng. Chem. Res.* **2005**, *44*, 4552–4561.
42. Ghani, W.A.W.A.K.; Alias, A.B.; Savory, R.M.; Cliffe, K.R. Co-combustion of agricultural residues with coal in a fluidised bed combustor. *Waste Manag.* **2009**, *29*, 767–773.
43. Lin, W.; Jensen, P.A.; Jensen, A.D. Biomass suspension combustion: Effect of two-stage combustion on NO_x emissions in a laboratory-scale swirl burner. *Energy Fuels* **2009**, *23*, 1398–1405.
44. Houshfar, E.; Løvås, T.; Skreiberg, Ø. Detailed Chemical Kinetics Modeling of NO_x Reduction in Combined Staged Fuel and Staged Air Combustion of Biomass. In *Proceedings of 18th European Biomass Conference & Exhibition (EU BC&E)*, Lyon, France, 3–7 May 2010; pp. 1128–1132.
45. Baxter, L. Biomass-coal co-combustion: opportunity for affordable renewable energy. *Fuel* **2005**, *84*, 1295–1302.
46. Coda Zabetta, E.; Hupa, M. A detailed kinetic mechanism including methanol and nitrogen pollutants relevant to the gas-phase combustion and pyrolysis of biomass-derived fuels. *Combust. Flame* **2008**, *152*, 14–27.
47. Røjel, H.; Jensen, A.; Glarborg, P.; Dam-Johansen, K. Mixing effects in the selective noncatalytic reduction of NO. *Ind. Eng. Chem. Res.* **2000**, *39*, 3221–3232.
48. Nussbaumer, T. *Biomass Combustion in Europe Overview on Technologies and Regulations*; Report 08-03. Available online: http://www.nyserda.ny.gov/en/Publications/Research-and-Development/~/media/Files/Publications/Research/Biomass%20Solar%20Wind/08-03_Biomass-Combustion-in-Europe.ashx (access on 6 February 2012).

49. Becidan, M.; Houshfar, E.; Khalil, R.A.; Skreiberg, Ø.; Løvås, T.; Sørum, L. Optimal mixtures to reduce the formation of corrosive compounds during straw combustion: A thermodynamic analysis. *Energy Fuels* **2011**, *25*, 3223–3234.
50. Thy, P.; Esbensen, K.H.; Jenkins, B.M. On representative sampling and reliable chemical characterization in thermal biomass conversion studies. *Biomass Bioenergy* **2009**, *33*, 1513–1519.
51. Jiang, X.; Huang, X.; Liu, J.; Han, X. NO_x Emission of fine- and superfine- pulverized coal combustion in O_2/CO_2 atmosphere. *Energy Fuels* **2010**, *24*, 6307–6313.
52. Lissianski, V.V.; Zamansky, V.M.; Maly, P.M. Effect of metal-containing additives on NO_x reduction in combustion and reburning. *Combust. Flame* **2001**, *125*, 1118–1127.

Paper V

Enhanced NO_x reduction by combined staged air and flue gas recirculation in biomass grate combustion

E. Houshfar, R.A. Khalil, T. Løvås, Ø. Skreiberg

Energy & Fuels, 26 (5), pp. 3003–3011, 2012

---

energy&fuels

Article

pubs.acs.org/EF

Enhanced NO_x Reduction by Combined Staged Air and Flue Gas Recirculation in Biomass Grate Combustion

Ehsan Houshfar,*[,†] Roger A. Khalil,[‡] Terese Løvås,[†] and Øyvind Skreiberg[‡]

[†]Norwegian University of Science and Technology (NTNU), Department of Energy and Process Engineering, NO-7491, Trondheim, Norway

[‡]SINTEF Energy Research, Department of Thermal Energy, NO-7465, Trondheim, Norway

ABSTRACT: Flue gas recirculation (FGR) is a conventional means of reducing NO_x emissions that involves lowering the peak flame temperature and reducing the oxygen concentration in the combustion region. Staged air combustion is also an effective means of NO_x reduction, especially in biomass combustion. This article reports results on NO_x emissions in a set of experiments combining FGR and staged air combustion in a grate-fired laboratory-scale reactor. Two different compositions of the recirculated flue gas were used: CO_2 and CO_2 + NO. The CO_2 concentration varied between 0−8 vol % of the total inlet flow rate and the NO concentration varied between 0 and 64 ppm. Two different FGR locations were also tested: above and below the grate. The results are compared with a reference experiment performed without FGR. The NO_x reduction level from staged air combustion at the optimal primary excess air ratio is ∼70%, while employing FGR can reduce the NO_x emissions by an additional 5%−10%. The optimal primary excess air ratio range is 0.9−1. However, FGR more effectively reduces NO_x when employed outside of the optimum primary excess air ratio range, i.e., excess air ratios higher than 1 and less than 0.9. The experiments with FGR located above the grate exhibit higher reduction potential, while FGR located below the grate produces decreased reduction. The recycled-NO conversion factor, which gives a measure of maximal FGR efficiency, at the maximum point, is nearly 100% when FGR is applied below the grate and is 85%−100% in the case of recirculation above the grate.

INTRODUCTION

According to recent findings, the CO_2 concentration in the atmosphere should not be higher than 350 ppm.[1] This limit was surpassed in 1988 and measurements taken in November 2011 found a CO_2 concentration of 390 ppm.[2] Biomass can provide an easily accessible source of renewable energy that is almost CO_2-neutral.

Almost all types of biomass contain nitrogen-bound compounds, which makes thermal conversion a challenge, with regard to NO_x formation. Typical nitrogen contents vary from below 0.1 wt % in wood to 7 wt % in sewage sludge. Demolition wood, which is the fuel used in this study, is an inexpensive source of fuel that is even more challenging to combust, because of its relatively high nitrogen content, which results in high NO_x emissions. NO_x contributes to environmental problems such as acid rain, smog formation, and ozone depletion. Therefore, many countries enforce strict regulations on NO_x emissions from power plants and other combustion systems.

NO_x Reduction. There are numerous well-established methods that can be applied to reduce the nitrogen oxides emissions from biomass combustion. These methods are categorized as primary and secondary measures based on the location and time of application inside the reactor. Staged air, staged fuel combustion, and flue gas recirculation (FGR) are the most common primary measures and effectively reduce NO_x emissions inside the furnace. For a better understanding of the NO_x formation and reduction, processes such as pyrolysis, tar and char combustion, and connected nitrogen conversion should be considered.[3]

The staged-air combustion reduction mechanism and the related chemistry have been extensively described elsewhere.[4−9] The important species and intermediates for NO_x formation and reduction are NH_3, HCN, NO, and HNCO.[10−14]

Fuel-N Conversion. The reaction mechanism for fuel-N conversion, the main source of NO_x in biomass combustion, is fairly well understood. The contribution of the fuel NO_x to the total NO_x in solid fuel combustion is shown to be greater than 75%−80%, with the rest originating mainly from the thermal NO_x mechanism.[7,15−18] The share of fuel-N to NO_x is even higher in biomass combustion, in which the reactor temperature is relatively low, compared to that of coal combustion.[7] Note that thermal NO_x formation becomes important at temperatures above 1300−1400 °C, which is generally relevant to, e.g., pulverized fuel combustion. However, in our grate furnace, all experiments are carried out at a constant temperature of 850 °C. We also note that, even in the flame region (primary zone), the temperature is below the range within which thermal NO_x is formed. The positive effect that temperature exerts on NO decomposition in the fuel-rich primary zone is reduced because of increased NO formation in the secondary stage caused by secondary air addition.[19]

Biomass, on the other hand, contains considerable amounts of fuel nitrogen, which promotes the formation of fuel NO_x during combustion. Therefore, it is important to understand that FGR in biomass combustion may not be as effective as it is in the combustion of natural gas or oil. However, it has been

Received: February 2, 2012
Revised: April 7, 2012
Published: April 9, 2012

proven that air staging and FGR are effective NO_x reduction methods for high-nitrogen-content fuels.[20] The nitrogen conversion path includes char and volatiles, and the proportion of each depends on the temperature and fuel type.

The released intermediate NO_x species, HCN and NH_3, can be converted to NO through oxidation reactions via amines (mostly NH-type radicals) or reduced to N_2, depending on the stoichiometric conditions, temperature, residence time, etc.[7,10]

The residence time is one of the important parameters in NO_x formation/reduction. Up to a certain point, an increased residence time in the primary stage will enhance the NO_x reduction potential. In this work, the residence time is well above the expected required time (<2 s);[19] thus, the results are not influenced by the residence time. The residence time in the primary zone (90 cm) of the reactor in this study is 13−23 s.

Flue Gas Recirculation (FGR). FGR is most likely one of the oldest NO_x reduction measures used in oil and gas combustion. The employment of FGR in grate-fired coal combustion has also exhibited a considerable NO_x reduction potential.[21] The main advantage of FGR and staged combustion is that they can be applied in existing boilers with low cost and few modifications to the furnace, while the implementation of secondary measures such as selective noncatalytic reduction (SNCR) and especially selective catalytic reduction (SCR) is generally more costly.

NO_x reduction through FGR is achieved because:

(1) the recirculated flue gas acts as an inert gas containing mainly CO_2, H_2O, a low level of O_2, and N_2. When mixed with the combustion air, it lowers the temperature in the flame region and, hence, reduces thermal NO_x formation;
(2) by mixing the flue gas with the combustion air, the oxygen availability in the reaction zone is reduced, which consequently affects the NO_x formation chemistry; and
(3) the residence time of the recirculated NO_x is increased by allowing it to go through the combustion zone a second time.

The high concentration of CO_2 caused by FGR is known to influence the formation of H/O/OH radicals, which play a critical role in NO_x emissions.[22] In the mentioned study, the concentration of H/O/OH radicals with elevated CO_2 concentration is different in the reburning zone and the burnout zone. Generally, in the first stage (i.e., the reburning zone), the higher CO_2 content results in reduced radical formation, while the radical formation is increased in the burnout zone. On the other hand, the relative order of the quantity of radicals is H > OH > O in O_2/N_2 combustion, while in O_2/CO_2 combustion, it changes to OH > O > H.[22] In addition to the effects of FGR on the actual residence time and the radical formation mechanisms, a higher CO_2 concentration in the inlet oxidant may enhance char nitrogen conversion.[23]

The effect of oxygen enrichment has been studied primarily in coal combustion and co-combustion systems.[24−26] Recent investigations have also been carried out with O_2/CO_2 as oxidants rather than oxygen-enriched air.[27] This study showed that, in coal combustion, the fuel-N to NO conversion factor decreased as the CO_2 concentration increased in the presence of coal. The authors also stated that the interaction of fuel-N with recycled NO caused the conversion ratio to decrease as the NO concentration increased in the recycled gas and that the global conversion factor depends on the excess air ratio; these findings are consistent with the present investigation. Reburning of recirculated NO from the flue gas has also been studied using propane in a burner to avoid fuel-N and heterogeneity effects.[28] Those experiments showed that the reduction potential of reburning is lower in oxy-fuel (high O_2 concentration in the inlet oxidant) than in air combustion, and applying FGR to oxy-fuel combustion systems increased the total NO reduction.

Combustion of different types of coal in an electrically heated combustor with recycling ratios of 0.2−0.4 showed a recycled-NO reduction of 60%−80% at equivalence ratios of ∼1.4, while the reduction was less at low recycling ratios.[29,30] The effects of CO_2 concentration, recycled NO_x, and interactions between the fuel-N and the recycled NO_x on NO_x emission have been studied in coal combustion with recycled CO_2, and a 50%−80% reduction of recycled NO in the furnace was found.[31]

Many studies have also been performed in waste combustion plants, because of the higher nitrogen content of waste. Bianchini et al.[32] performed a study on a fluidized-bed reactor (FBR) with 60% recirculation of hot flue gas. Their study included temperature effects and showed that FGR can reduce NO_x emissions up to 30% in waste-to-energy plants. A NO_x reduction of up to 20% was also achieved in a waste incineration plant using an FGR ratio of ∼25%.[33] Investigations of high-temperature air combustion in the incineration of solid waste also demonstrated that NO_x emission was reduced by 28%−38% when FGR was used to decrease the oxygen concentration.[34]

In this study, a *combination* of staged-air combustion and flue gas recirculation was applied to a grate-fired laboratory-scale reactor to mitigate NO_x emissions. As stated above, these measures have known effects when applied individually. However, staged combustion has a known optimum effect within a rather narrow window of excess air ratios. In the present work, we address how this effect can be modified by including FGR. The experiments performed provided important data for assessing the effect of combined staged-air combustion and FGR on NO_x formation in the combustion of demolition wood, a fuel that contains a relatively high nitrogen concentration. The parameters that have been investigated in this study are (1) the amount of recirculated flue gas, (2) the recirculated flue gas composition, and (3) the point of flue gas introduction inside the reactor.

■ EXPERIMENTAL SETUP AND PROCEDURE

The Multifuel Reactor. The SINTEF Energy Research's grate-fired laboratory-scale multifuel reactor was used to carry out the combustion tests. This reactor is an electrically heated high-temperature reactor. Figure 1 shows a schematic drawing of the reactor. The reactor has a ceramic inner tube with a diameter of 100 mm and a length of 2 m. The vertical tube consists of two ceramic tubes 1 m in length connected by a ceramic socket. The ceramic tubes are made of nonporous and noncatalytic alumina. A more-detailed description of the reactor can be found in a recent study by Khalil et al.[35] The reaction section, located above the grate, is 1.6 m long, while the section below the grate is 0.4 m long. The reactor is fitted with a unique two-level grate system, as shown in Figure 2, which allows for two-stage fuel burning. Its function will be described in more detail in the next section. As shown in the photo, the blades are designed to keep the pellets on both grates (upper and lower level) for the same amount of time, i.e., the blades rotate at the same speed at both grates. The heating system fits inside the insulation shell and consists of four separate heating zones.

Figure 3 shows the sampling lines for gas concentration measurements. The gas concentration in the primary stage (NO, HCN, NH_3, ...) is measured by a Fourier transform infrared (FTIR)

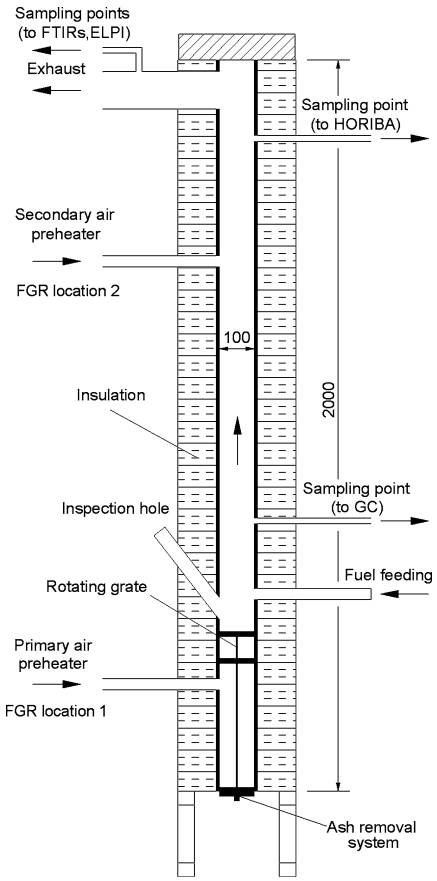

Figure 1. Schematic drawing of the reactor.

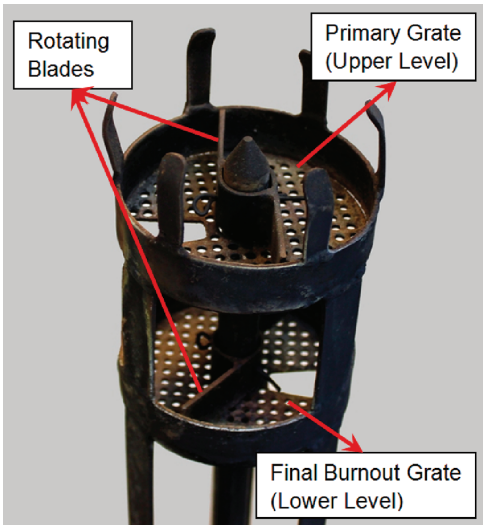

Figure 2. The design of the two-level grate.

analyzer using a suction probe located 25 cm above the grate. NO_x measurement in the flue gas is performed by both a continuous gas analyzer and another FTIR analyzer at the top of the reactor, where the burned gases leave the reactor. Extended descriptions of the sampling devices and measurement techniques have been provided elsewhere.[5]

Experimental Procedures. The experimental matrix is presented in Table 1. The experiments were carried out using 6-mm-diameter pellets of demolition wood and in two modes: (1) experiments using FGR in the primary zone, and (2) experiments using FGR in the secondary zone. Recirculated flue gas was either mixed with primary air and fed to the reactor ca. 30 cm below the grate, or mixed with secondary air before being fed to the reactor ca. 90 cm above the grate. These two FGR modes are used to obtain more information about the NO_x emission levels and the reduction potential of FGR, as each mode results in different chemistry inside of the reactor. The obtained results can be used as a basis for improved design and operation of larger scale combustion systems. Most of the available studies on FGR used CO_2 as the recirculated flue gas. However, we also included nitrogen oxide in the flow, similar to how FGR is used in an industrial boiler. Each case was carried out with two different recirculated flue gases: CO_2 only and CO_2 + NO. Only isothermal experiments were performed, and the reactor temperature was 850 °C. Experiment 5 is considered to be the reference experiment and is performed only with air (i.e., without any flue gas recirculation). The total excess air ratio was ∼1.6, and the primary excess air ratio was ∼0.8. The excess air ratio (λ) is defined as the ratio between the air-to-fuel ratio at the measurement time (A/F) and the stoichiometric air-to-fuel ratio ($(A/F)_{stoic}$). Hence, $\lambda < 1$ indicates fuel-rich conditions. The stoichiometric condition is defined using the fuel composition (ultimate analysis).

The proximate and ultimate analyses are shown in Table 2. The demolition wood (DW) has a relatively high nitrogen content of 1.06 wt %. However, the sulfur and chlorine contents of the fuel are very low, and DW can be regarded as a relatively safe fuel, in terms of Cl-related corrosion issues, compared to, e.g., agricultural residues or waste. The ash content of DW is higher than that of virgin wood and requires an ash collection and disposal system for proper handling in a combustion plant.

The fuel pellets are fed automatically from a fuel container located above a water-cooled piston. The piston transports the fuel into the reactor, and the pellets fall down on the upper grate, after which the piston quickly returns to its starting position and the process is repeated. The feeding frequency was set to ∼6−7 s, which produced a feeding rate of ∼400 g/h. The piston frequency was carefully calibrated prior to each experiment.

The pellets were primarily combusted on the upper (primary) grate. The pellets were then gradually moved to a slot leading to the second (final burnout) grate by means of rotating blades. Each grate has two blades rotating slowly, which complete a circle within ∼3 min. Final burnout takes place on the lower grate before the ash is moved to the ash bin through another rotating blade. The gas residence time between the grate levels is in the range of 1−2 s, and the total residence time of the fuel gases in the reactor is ∼25−50 s, because of a low flow velocity.

As mentioned earlier and shown in Figure 3, two FTIRs were used in this experimental work. The challenge with the one located just above the grate is to measure the intermediate nitrogen species present as minor compounds in a gas stream containing a wide variety of compounds that vary substantially in time. This system is difficult to measure using an automated method and must be checked manually. The sample line for this FTIR was cooled to remove all compounds that could potentially harm the instrument due to condensation. Thus, all of the tar and most of the water were removed. NH_3 was measured over the spectral range of 1180−1100 cm^{-1} and at a distinctive peak that should be located at 1626 cm^{-1}. Two different methods were developed for measuring the NO content: the measurement of the height of an undisturbed peak at the wavelength of 1875.6 cm^{-1} and the use of a PLS (Partial Least Squares) model in the region of 1916−1895 cm^{-1}. The PLS model was corrected for interference from CH_4, C_2H_4, and H_2O. Both methods were developed using NO levels

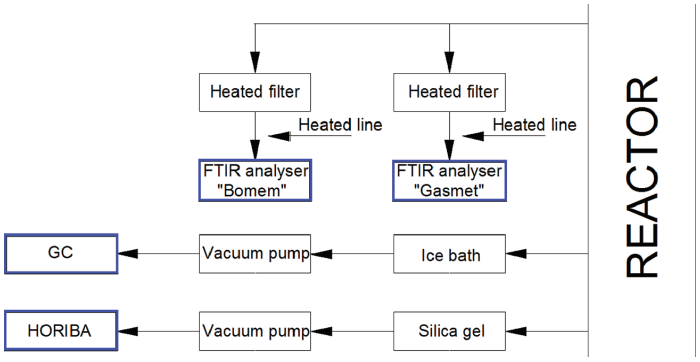

Figure 3. Schematic diagram of the sampling lines.

Table 1. The Experimental Matrix

	FGR location	CO_2 (vol % of total air flow)	NO (ppm in total air flow)
1	primary zone	2.4	
2	primary zone	3.3	
3	primary zone	5.9	
4	primary zone	6.7	
5	**reference experiment**		
6	secondary zone	2.5	
7	secondary zone	4.6	
8	secondary zone	6.4	
9	secondary zone	8.0	
10	primary zone	3.9	17
11	primary zone	3.7	28
12	primary zone	3.9	41
13	secondary zone	4.4	19
14	secondary zone	4.4	47
15	secondary zone	4.5	64

generated by mixing a calibration gas containing NO (in N_2) with N_2 purity of 5.0. The NO content was calibrated within the range of 0−350 ppm and the two methods yielded NO concentrations that were within 5% of each other. The data from the PLS model was used for the calculations shown in this work. The challenge, however, was to develop a method for measuring the HCN content. HCN in the FTIR spectrum is present in the narrow wavelength range of 3400−3200 cm^{-1}. This range also absorbs C_2H_2 and H_2O, and no single peak can be used to measure the HCN content. A PLS model was developed for HCN prediction in the range of 3382−3350 cm^{-1}, which also included corrections for the above-mentioned compounds. The HCN content was calibrated using spectra with concentrations between 0 and 350 ppm. The quality of the model was checked by measuring the height of a single peak after the interference spectra of C_2H_2 and H_2O were subtracted. To do so, the concentrations of these interfering compounds were predicted prior to the HCN content. The subtraction was performed using a function in the software that was provided with the FTIR analysis. This process is time-consuming and was only performed on selected spectra to ensure that the PLS model was performing satisfactorily. The difference between the two methods was similar in magnitude to the difference in the NO predictions.

The experiments were carried out using the following parametric variations:

(1) CO_2 recirculation at different concentrations, relative to the combustion air;
(2) CO_2/NO recirculation at different concentrations, relative to the combustion air; and
(3) for each of the above methods, two recirculation locations were investigated: below the grate and ∼90 cm above the grate.

RESULTS AND DISCUSSION

In this section, the observed results from the experiments are presented.

As mentioned earlier, NO_x precursors in the primary zone (above the top grate) were detected and quantified using FTIR spectroscopy. In all of the experiments, the concentration of ammonia (NH_3) was below the detectable limit. It seems that the conditions under which these experiments were performed favored the formation or survival of HCN and NO in the region where the samples were taken for analysis. In addition, the FTIR analyzer used a suction probe located 25 cm above the grate. This distance corresponds to several seconds of residence time above the fuel pellets, which is more than enough time for NH_3 to be fully converted to other intermediate N-species, including HCN, or N_2,[36,37] while further reactions are limited by the very low remnant radical pool. When secondary air is added, some further reduction of the remaining intermediate N-species to N_2 will occur, while the remainder will be converted primarily to NO.

CO_2 Recirculation. Figure 4 shows NO_x emission levels in the flue gas at different excess air ratios for all of the experiments performed with recirculation of CO_2 alone. The maximum NO_x emissions for the different experiments were in the range of 90−115 ppm (11 vol % O_2 in dry flue gas) for low excess air ratios (ca. 0.7) and were reduced to as low as 30 ppm for an excess air ratio close to 1. The right graph demonstrates that the addition of CO_2 has a positive effect on NO_x reduction

Table 2. Fuel Proximate and Ultimate Analysis

	Proximate Analysis (wt % on dry basis)				Ultimate Analysis (wt % on dry ash-free basis)					
pellet	ash	volatile matter	fixed carbon	moisture (wet basis)	C	H	O	N	S	Cl
demolition wood, DW	2.18	75.97	21.85	10.58	48.45	6.37	44.11	1.06	0.02	0.05

dx.doi.org/10.1021/ef300199g | *Energy Fuels* 2012, 26, 3003−3011

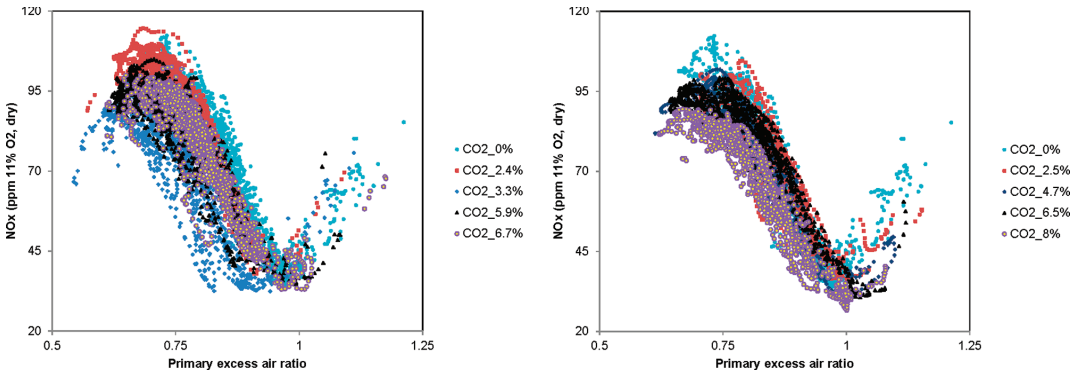

Figure 4. Effects of primary excess air ratio and amount of CO_2 in the inlet oxidant on the NO_x emissions: (left) CO_2 below the grate and (right) CO_2 above the grate.

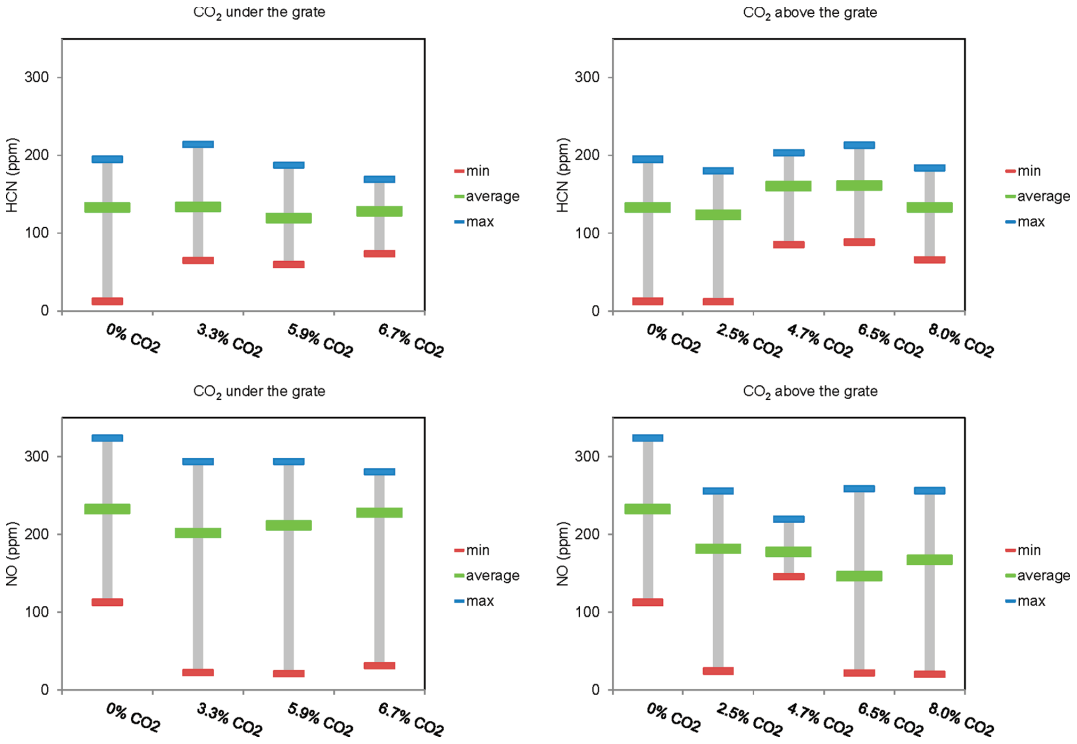

Figure 5. Effects of CO_2 in the inlet oxidant on the NO and HCN levels in the primary zone: (left) CO_2 below the grate and (right) CO_2 above the grate.

above the grate. The left graph presents the same trend below the grate but with more widely scattered data points. The reverse effect is observed in the case of 3.3% CO_2, which could originate from the combustion instabilities in the mentioned experiment. Because of the desired reduction chemistry in the first stage, the primary air should be supplied to the reactor to create reducing conditions and thus maximize NO_x reduction. Compared to the reference experiment, in which no CO_2 recirculation was employed, the NO_x concentration was more strongly reduced at increased amounts of CO_2 recirculation. However, it should be noted that the reduction due to FGR is much lower than that of air staging. The total reduction at the optimal condition is ~70%, while CO_2 recirculation provides an additional reduction of 5%−10%, depending on the amount of recirculated CO_2. The CO_2 addition lowers the local temperature (electrically heated reactor) due to the increased heat capacity of the flue gas and lowers the O_2 concentration inside the reactor, which, in return, decreases the formation of nitrogen oxides. A long residence time in the primary (reduction) zone ensures a low NO_x emission level at the

dx.doi.org/10.1021/ef300199g | *Energy Fuels* 2012, 26, 3003−3011

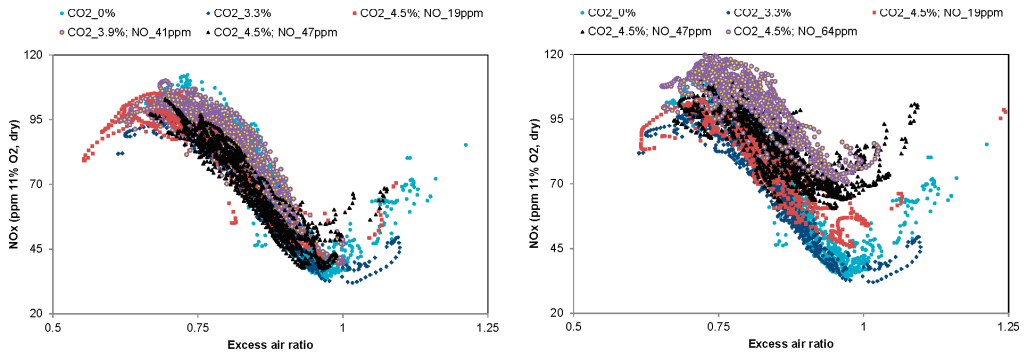

Figure 6. Effects of the primary excess air ratio and amounts of CO_2 and NO in the inlet oxidant on the NO_x emissions: (left) CO_2 + NO below the grate and (right) CO_2 + NO above the grate.

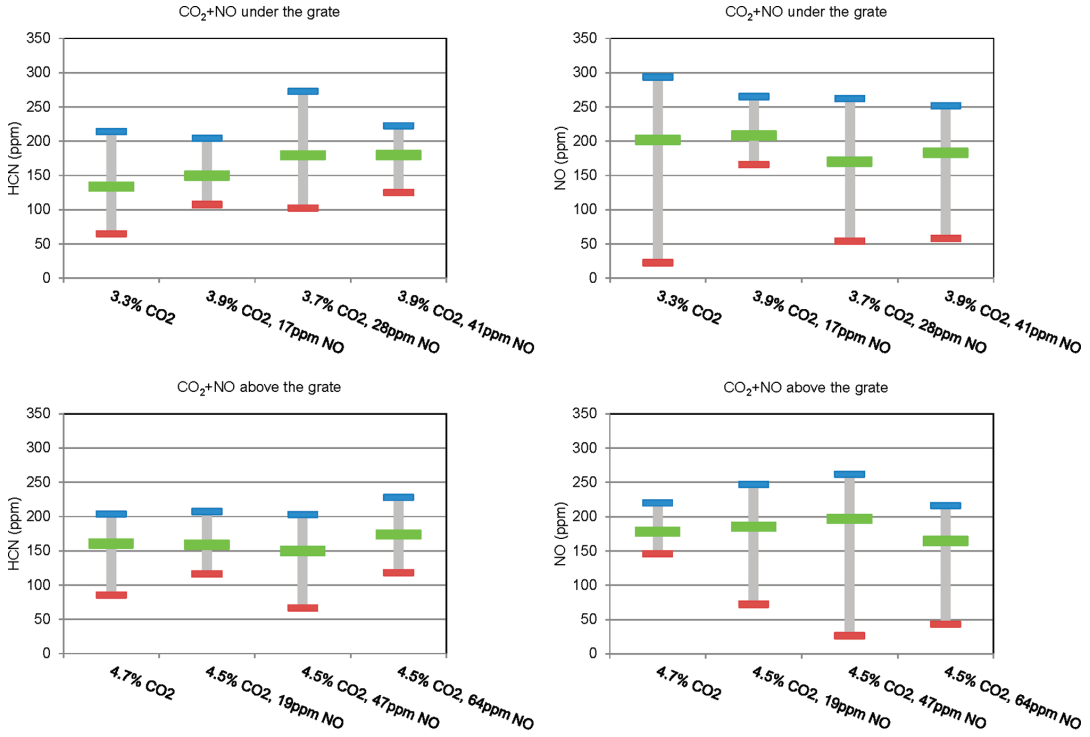

Figure 7. Effects of CO_2/NO in the inlet oxidant on the NO and HCN levels in the primary zone: (left) CO_2 + NO below the grate and (right) CO_2 + NO above the grate.

optimum primary excess air ratio, i.e., a very high reduction level. Therefore, the additional effect of the second method, FGR, is minimal at the optimum primary excess air ratio, as explained in the Introduction section.

The FGR position also has a clear effect on the NO_x emissions. The left graph in Figure 4 shows that the additional CO_2 in the primary zone (i.e., below the grate) contributes to NO_x reduction over a wide range of excess air ratios. However, at the optimum excess air ratio, the effect of FGR is minimal. The widely scattered results in this graph may be due to unstable combustion conditions, while FGR above the grate keeps the combustion quite stable. The right graph presents the same results with CO_2 recirculated above the grate, and the reduction level is clearly visible and higher even at the optimum primary excess air ratio. For instance, at a low primary excess air ratio of ca. 0.7, the maximum NO_x emission level at the highest FGR ratio is reduced by ~20% from the reference experiment in the case of FGR above the grate. Under the same conditions, FGR below the grate reduces the NO_x emission level by 25%. The CO_2 concentration in the flue gas can be calculated as follows:

dx.doi.org/10.1021/ef300199g | *Energy Fuels* 2012, 26, 3003–3011

$$\beta = \frac{\alpha\gamma}{1+\gamma} \quad (1)$$

where α is the CO_2 concentration in the flue gas, β the inlet CO_2 concentration, and γ the FGR ratio.

The gas concentration measurement in the primary zone which is carried out using FTIR spectroscopy, reveals the effects of different CO_2 recirculation levels on the formation of NO_x precursors. Figure 5 shows the minimum, maximum, and average concentrations of HCN (in ppm) in the upper graphs. The HCN content exhibits a weak tendency to decrease with increasing CO_2 recirculation at the injection point above the grate, with the exception of the points 2.5% to 4.7% above the grate. Further studies using more FGR ratios (CO_2 levels) between 2.5 and 5.0% are required to clarify this issue. Please note that max and min values do not correspond to uncertainties; instead, these are the measured maximum and minimum values at the different excess air ratios tested for each experiment. The difference between the average HCN levels at different FGR ratios and CO_2 injection points compared to the reference experiment is minimal. The measured concentration of NO in the primary zone above the grate is presented in the lower graphs of Figure 5. In this case, the decreasing tendency of the NO concentration with increasing CO_2 is clearly visible up to a certain CO_2 percentage. For the experiments with CO_2 injection above the grate, the NO concentration decreases as the CO_2 recirculation increases up to 6.5%. However, the NO concentration in the recirculation gas did not continue to decrease once the CO_2 concentration increased above 2.5% CO_2. More investigations are required in future work to clarify this behavior.

CO_2 + NO Recirculation. The effect of the primary excess air ratio and the amount of NO recirculation is shown in Figure 6. The left graph presents the NO_x emission in the flue gas for the experiments applying FGR below the grate. In this case, the NO_x emission levels are very similar to those presented above, which demonstrates that the NO_x emission levels are unaffected by the increased NO concentration in the recirculated gas. This finding indicates that the NO that is returned to the reactor undergoes complete conversion. The elementary reactions that reduce the NO introduced into the reactor are heterogeneous reactions with char on the bed or homogeneous reactions with volatiles in the gas phase. The corresponding reactions are suggested[29] to be the direct conversion of NO to N_2 through NO ⇔ N_2 and NO ⇔ N_2O, including the elementary reaction N_2O + (CO) ⇔ N_2 + CO_2. The right graph shows the same scenario with FGR located above the grate. In this case, the NO_x emission levels in the flue gas increase as the NO concentration in the recycled gas increases. The data in the right graph demonstrate the existence of a distinct minimum in the NO_x emission levels within a primary excess air ratio range of 0.9−1 for all cases. This holds true even though the optimal minimum differs as a function of the CO_2/NO concentration in the recycled gas. The mentioned excess air ratio has been shown to be optimal in several experimental campaigns performed on different fuels and under different operating conditions.[4,5,9,38] These results show that the excess air ratio that achieves the optimum NO_x reduction for the reactor design used in the current study is ∼0.9−0.95. This finding is in agreement with the modeling and kinetics studies on NO_x reduction by fuel or air staging, which also find that the optimal excess air ratio is close to 1.[39,40]

Figure 7 presents the HCN and NO concentrations above the grate, close to the devolatilization zone. The experimental data suggest that the average HCN concentration above the grate increases as the NO concentration in the recirculated flue gas increases when the FGR is located below the grate. This trend may be due to the higher level of available fixed nitrogen and increased conversion of char nitrogen. However, the HCN concentration does not exhibit a clear dependency on the FGR ratio when FGR is located above the grate. The average NO concentration also does not exhibit a clear trend. It is also important to note that the maximum NO values decrease as the NO concentration in the inlet flow increases (Figure 7, right graph). This result can explain the higher HCN concentration in the corresponding cases.

The HCN and NO concentrations in the primary zone for the experiments employing FGR in the secondary zone are presented in the bottom graphs of Figure 7. The average HCN and NO concentrations (150−175 ppm and 160−195 ppm, respectively) are quite constant. With FGR located in the secondary zone (above the grate), the possible effects of the recirculated CO_2 and NO on char-N conversion are avoided. In addition, the volatile N-species very near the fuel bed and just above the pellets are unaffected by the FGR, gases because the secondary air feeding point is placed at a somewhat higher position. Therefore, there is no interaction between the fuel bed and the recycled flue gas, and the reaction mechanism at the bed does not change compared to the reference case, which leads to the relatively constant concentrations of intermediate species in this case.

To characterize the effect of FGR on NO_x emissions, a new parameter is introduced: the recycled-NO conversion factor (η_{NO}). Figure 8 shows the influence of FGR on the recycled-NO reduction for experiments run with FGR located below the grate (top graph) and above the grate (bottom graph). The recycled-NO conversion factor is defined based on the NO_x emission level, consisting of mainly NO, in the flue gas compared to that of the reference experiment where only staged air combustion is applied to the reactor. Therefore, this quantity provides a measure of FGR effectiveness; a NO conversion factor of 1 corresponds to maximum reduction of the recycled NO.

$$\eta_{NO} = \frac{NO_{\text{ppm in inlet air}} - (NOx_{\text{in NO + CO}_2\text{ case}} - NOx_{\text{in CO}_2\text{ case}})}{NO_{\text{ppm in inlet air}}} \quad (2)$$

The upper graph indicates that when FGR is located in the primary zone, all of the recirculated NO can be converted to N_2. The maximum values shown in Figure 8 indicate 100% NO reduction is achieved in all experiments with FGR below the grate. The average values also indicate a considerable NO_x reduction of 60%−100%. The lower graph presents the same results with FGR located above the grate, with a maximum NO_x reduction of 85%−100% and an average reduction of 54%−66%. The reduction potential is higher with FGR located below the grate than above the grate, because of the lower residence time of the inlet NO under reducing conditions when it is supplied to the reactor in the secondary zone, in addition to the different heterogeneous kinetics available for NO and char nitrogen conversion.

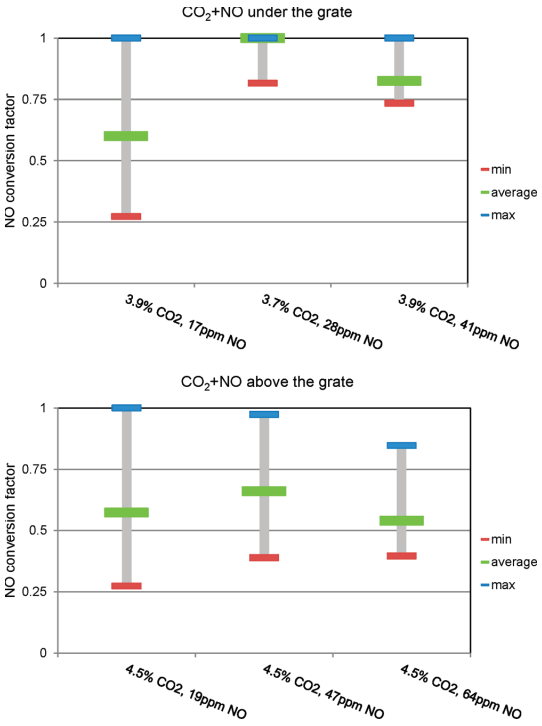

Figure 8. NO conversion factor: (top) CO_2 + NO below the grate and (bottom) CO_2 + NO above the grate.

CONCLUSIONS

In this study, experiments on combustion of demolition wood are performed in a laboratory-scale reactor. The most important findings were the following:

- The optimum air distribution that maximized the NO_x reduction level was a primary excess air ratio of ~0.9−1 for all experiments, regardless of the flue gas recirculation (FGR) ratio and the NO concentration in the inlet gas.
- The NO_x reduction level from staged air combustion at the optimum primary excess air ratio was ~70%.
- Applying FGR to the reactor allows NO_x to be reduced by ~75%−80% under the optimum combustion condition, i.e., 5%−10% more than the reduction without FGR.
- The results show that the NO_x reduction level depends heavily on the stoichiometric conditions in the primary (reduction) zone. The effectiveness of FGR is higher outside of the optimum range of excess air ratios.
- The experiments employing FGR in the secondary zone exhibit higher reduction potential, while FGR in the primary zone gives lower reduction. The recycled NO-conversion factor at the maximum point is almost 100% for FGR below the grate and 85%−100% for FGR above the grate.

AUTHOR INFORMATION

Corresponding Author

*E-mail: ehsan.houshfar@ntnu.no.

Notes

The authors declare no competing financial interest.

ACKNOWLEDGMENTS

The financial support through the KRAV project funded by SINTEF Energy Research, the Research Council of Norway, and industrial partners is greatly acknowledged.

REFERENCES

(1) Hansen, J.; Sato, M.; Kharecha, P.; Beerling, D.; Berner, R.; Masson-Delmotte, V.; Pagani, M.; Raymo, M.; Royer, D. L.; Zachos, J. C. Target Atmospheric CO_2: Where Should Humanity Aim? *Open Atmos. Sci. J.* **2008**, *2*, 217−231.

(2) Mauna Loa Observatory, Scripps Institution of Oceanography. http://co2now.org/, accessed December 2011.

(3) Zhou, H.; Jensen, A. D.; Glarborg, P.; Kavaliauskas, A. Formation and reduction of nitric oxide in fixed-bed combustion of straw. *Fuel* **2006**, *85* (5−6), 705−716.

(4) Houshfar, E.; Skreiberg, Ø.; Todorović, D.; Skreiberg, A.; Løvås, T.; Jovović, A.; Sørum, L. NO_x emission reduction by staged combustion in grate combustion of biomass fuels and fuel mixtures. *Fuel* **2012**, DOI: 10.1016/j.fuel.2012.03.044.

(5) Houshfar, E.; Skreiberg, Ø.; Løvås, T.; Todorović, D.; Sørum, L. Effect of excess air ratio and temperature on NO*x* emission from grate combustion of biomass in the staged air combustion scenario. *Energy Fuels* **2011**, *25* (10), 4643−4654.

(6) Houshfar, E.; Skreiberg, Ø.; Glarborg, P.; Løvås, T. Reduced chemical kinetics mechanisms for NO_x emission prediction in biomass combustion. *Int. J. Chem. Kinet.* **2012**, *44* (4), 219−231.

(7) Glarborg, P.; Jensen, A. D.; Johnsson, J. E. Fuel nitrogen conversion in solid fuel fired systems. *Prog. Energy Combust. Sci.* **2003**, *29* (2), 89−113.

(8) Salzmann, R.; Nussbaumer, T. Fuel Staging for NO_x Reduction in Biomass Combustion: Experiments and Modeling. *Energy Fuels* **2001**, *15* (3), 575−582.

(9) Houshfar, E.; Løvås, T.; Skreiberg, Ø. Experimental investigation on NO_x reduction by primary measures in biomass combustion: Straw, peat, sewage sludge, forest residues, and wood pellets. *Energies* **2012**, *5* (2), 270−290.

(10) Skreiberg, Ø.; Kilpinen, P.; Glarborg, P. Ammonia chemistry below 1400 K under fuel-rich conditions in a flow reactor. *Combust. Flame* **2004**, *136* (4), 501−518.

(11) Sørum, L.; Skreiberg, Ø.; Glarborg, P.; Jensen, A.; Dam-Johansen, K. Formation of NO from combustion of volatiles from municipal solid wastes. *Combust. Flame* **2001**, *124* (1−2), 195−212.

(12) Becidan, M.; Skreiberg, Ø.; Hustad, J. E. NO_x and N_2O Precursors (NH_3 and HCN) in Pyrolysis of Biomass Residues. *Energy Fuels* **2007**, *21* (2), 1173−1180.

(13) Hansson, K.-M.; Samuelsson, J.; Tullin, C.; Åmand, L.-E. Formation of HNCO, HCN, and NH_3 from the pyrolysis of bark and nitrogen-containing model compounds. *Combust. Flame* **2004**, *137* (3), 265−277.

(14) Hämäläinen, J. P.; Aho, M. J.; Tummavuori, J. L. Formation of nitrogen oxides from fuel-N through HCN and NH_3: A model-compound study. *Fuel* **1994**, 73 (12), 1894−1898.

(15) Courtemanche, B.; Levendis, Y. A. A laboratory study on the NO, NO_2, SO_2, CO and CO_2 emissions from the combustion of pulverized coal, municipal waste plastics and tires. *Fuel* **1998**, *77* (3), 183−196.

(16) Wendt, J. O. L.; Pershing, D. W.; Lee, J. W.; Glass, J. W. Pulverized coal combustion: NO_x formation mechanisms under fuel rich and staged combustion conditions. *Symp. (Int.) Combust.* **1979**, *17* (1), 77−87.

(17) Pershing, D. W.; Wendt, J. O. L. Relative Contributions of Volatile Nitrogen and Char Nitrogen to NO*x* Emissions from Pulverized Coal Flames. *Ind. Eng. Chem. Process Des. Dev.* **1979**, *18* (1), 60−67.

(18) Pershing, D. W.; Wendt, J. O. L. *Pulverized coal combustion: The influence of flame temperature and coal composition on thermal and fuel NOx*; Elsevier: Amsterdam, 1977; pp 389−399.
(19) Spliethoff, H.; Greul, U.; Rüdiger, H.; Hein, K. R. G. Basic effects on NO_x emissions in air staging and reburning at a bench-scale test facility. *Fuel* **1996**, *75* (5), 560−564.
(20) Anuar, S. H.; Keener, H. M. Environmental performance of air staged combustor with flue gas recirculation to burn coal/biomass. Presented at the *1995 ASAE Annual International Meeting*, Chicago, IL, 1995.
(21) Li, X.; Jianmin, G.; Guangbo, Z.; Laifu, Z.; Zhifeng, Z.; Shaohua, W. The Influence of Flue Gas Recirculation on the Formation of NO*x* in the Process of Coal Grate-Fired. In *2011 International Conference on Intelligent Computation Technology and Automation (ICICTA)*, March 28−29, 2011; pp 901−904.
(22) Normann, F.; Andersson, K.; Johnsson, F.; Leckner, B. Reburning in Oxy-Fuel Combustion: A Parametric Study of the Combustion Chemistry. *Ind. Eng. Chem. Res.* **2010**, *49* (19), 9088−9094.
(23) Hosoda, H.; Hirama, T.; Azuma, N.; Kuramoto, K.; Hayashi, J.-i.; Chiba, T. NO_x and N_2O Emission in Bubbling Fluidized-Bed Coal Combustion with Oxygen and Recycled Flue Gas: Macroscopic Characteristics of Their Formation and Reduction. *Energy Fuels* **1998**, *12* (1), 102−108.
(24) Luo, S. Y.; Xiao, B.; Hu, Z. Q.; Liu, S. M.; Guan, Y. W. Experimental study on oxygen-enriched combustion of biomass micro fuel. *Energy* **2009**, *34* (11), 1880−1884.
(25) Kazanc, F.; Khatami, R.; Manoel Crnkovic, P.; Levendis, Y. A. Emissions of NO_x and SO_2 from Coals of Various Ranks, Bagasse, and Coal-Bagasse Blends Burning in O_2/N_2 and O_2/CO_2 Environments. *Energy Fuels* **2011**, *25* (7), 2850−2861.
(26) Nimmo, W.; Daood, S. S.; Gibbs, B. M. The effect of O_2 enrichment on NO_x formation in biomass co-fired pulverised coal combustion. *Fuel* **2010**, *89* (10), 2945−2952.
(27) Liu, H.; Yuan, Y.; Yao, H.; Dong, S.; Ando, T.; Okazaki, K. Factors Affecting NO Reduction during O_2/CO_2 Combustion. *Energy Fuels* **2011**, *25* (6), 2487−2492.
(28) Kühnemuth, D.; Normann, F.; Andersson, K.; Johnsson, F.; Leckner, B. Reburning of Nitric Oxide in Oxy-Fuel Firing—The Influence of Combustion Conditions. *Energy Fuels* **2011**, *25* (2), 624−631.
(29) Hayashi, J. i.; Hirama, T.; Okawa, R.; Taniguchi, M.; Hosoda, H.; Morishita, K.; Li, C. Z.; Chiba, T. Kinetic relationship between NO/N_2O reduction and O_2 consumption during flue-gas recycling coal combustion in a bubbling fluidized-bed. *Fuel* **2002**, *81* (9), 1179−1188.
(30) Hu, Y. Q.; Kobayashi, N.; Hasatani, M. Effects of coal properties on recycled-NO_x reduction in coal combustion with O_2/recycled flue gas. *Energy Convers. Manage.* **2003**, *44* (14), 2331−2340.
(31) Okazaki, K.; Ando, T. NO_x reduction mechanism in coal combustion with recycled CO_2. *Energy* **1997**, *22* (2−3), 207−215.
(32) Bianchini, A.; Pellegrini, M.; Saccani, C. Hot waste-to-energy flue gas treatment using an integrated fluidised bed reactor. *Waste Manage.* **2009**, *29* (4), 1313−1319.
(33) Liuzzo, G.; Verdone, N.; Bravi, M. The benefits of flue gas recirculation in waste incineration. *Waste Manage.* **2007**, *27* (1), 106−116.
(34) Suvarnakuta, P.; Patumsawad, S.; Kerdsuwan, S. Experimental Study on Preheated Air and Flue Gas Recirculation in Solid Waste Incineration. *Energy Sources, Part A* **2010**, *32* (14), 1362−1377.
(35) Khalil, R. A.; Houshfar, E.; Musinguzi, W.; Becidan, M.; Skreiberg, Ø.; Goile, F.; Løvås, T.; Sørum, L. Experimental investigation on corrosion abatement in straw combustion by fuel-mixing. *Energy Fuels* **2011**, *25* (6), 2687−2695.
(36) Orikasa, H.; Matsuoka, K.; Kyotani, T.; Tomita, A. HCN and N_2 formation mechanism during NO/char reaction. *Proc. Combust. Inst.* **2002**, *29* (2), 2283−2289.
(37) Leppälahti, J.; Koljonen, T. Nitrogen evolution from coal, peat and wood during gasification: Literature review. *Fuel Process. Technol.* **1995**, *43* (1), 1−45.
(38) Houshfar, E.; Sandquist, J.; Musinguzi, W.; Khalil, R. A.; Becidan, M.; Skreiberg, Ø.; Goile, F.; Løvås, T.; Sørum, L. Combustion Properties of Norwegian Biomass: Wood Chips and Forest Residues. *Appl. Mech. Mater.* **2012**, *110−116*, 4564−4568.
(39) Skreiberg, Ø.; Glarborg, P.; Jensen, A. D.; Dam-Johansen, K. Kinetic NO_x modelling and experimental results from single wood particle combustion. *Fuel* **1997**, *76* (7), 671−682.
(40) Houshfar, E.; Løvås, T.; Skreiberg, Ø. Detailed chemical kinetics modeling of NOx reduction in combined staged fuel and staged air combustion of biomass. In *18th European Biomass Conference & Exhibition (EU BC&E)*, Lyon, France, 2010; pp 1128−1132.

Paper VI

Reduced chemical kinetics mechanisms for NO_x emission prediction in biomass combustion

E. Houshfar, Ø. Skreiberg, P. Glarborg, T. Løvås

International Journal of Chemical Kinetics, 44 (4), pp. 219–231, 2012

Is not included due to copyright

Paper VII

Detailed chemical kinetics modeling of NO_x reduction in combined staged fuel and staged air combustion of biomass

E. Houshfar, T. Løvås, Ø. Skreiberg

Proceedings of 18th European Biomass Conference & Exhibition (EU BC&E), Lyon, France, May 3–7, 2010

doi: 10.5071/18thEUBCE2010-VP2.4.4

Is not included due to copyright

Paper VIII

Experimental investigation on corrosion abatement in straw combustion by fuel-mixing

R.A. Khalil, E. Houshfar, W. Musinguzi, M. Becidan, Ø. Skreiberg, F. Goile, T. Løvås, L. Sørum

Energy & Fuels, 25 (6), pp. 2687–2695, 2011

---

energy&fuels

ARTICLE

pubs.acs.org/EF

Experimental Investigation on Corrosion Abatement in Straw Combustion by Fuel Mixing

Roger A. Khalil,*[,†] Ehsan Houshfar,[‡] Wilson Musinguzi,[‡] Michaël Becidan,[†] Øyvind Skreiberg,[†] Franziska Goile,[†] Terese Løvås,[‡] and Lars Sørum[†]

[†]Department of Energy Processes, SINTEF Energy Research, NO-7465 Trondheim, Norway

[‡]Department of Energy and Process Engineering, Norwegian University of Science and Technology (NTNU), NO-7491 Trondheim, Norway

ABSTRACT: In an attempt to minimize corrosion in biomass-fired boilers, combustion experiments were performed using binary mixtures of straw with peat, sewage sludge, or grot (branches and treetops). The mixing ratios were carefully selected using literature and thermodynamic calculations. All mixtures were pelletized. The combustion experiments were performed in a laboratory-scale multi-fuel reactor. Extensive analytical analysis of the system included the gas concentration and particle size distribution in the flue gas, the elemental composition of the fuel, and the bottom ash and specific particle size fractions of fly ash. This allowed for the determination of the fate of the main corrosive compounds, in particular, chlorine. The corrosion risk associated with the three fuel mixtures was quite different. Grot was found to be a poor corrosion-reduction additive because of its marginal influence on the chlorine share in aerosols. Grot could not serve as an alternative fuel for co-firing with straw either because no dilution effect on the particle load was measured. Peat was found to reduce the corrosive compounds only at high peat additions (50 wt %). Sewage sludge was the best alternative for corrosion reduction because 10 wt % addition almost eliminated chlorine from the fly ash.

INTRODUCTION

According to the world energy outlook of the International Energy Agency (IEA), the total energy consumption in the world will increase by a rate of 1.5% per year until 2030.[1] Fossil fuels produce the major greenhouse gas, CO_2, when they are used for electricity or heat production. Biomass, which is already the main contributor to renewable energy, is expected to further increase its share in three key sectors: heat and power, transportation fuels, and production of bioproducts. Energy conversion from biomass is close to being CO_2-neutral; however, biomass use will most likely result in the emission of other types of pollutants. An increased number of biomass energy plants are looking into cutting down their costs using cheaper feedstock alternatives, i.e., herbaceous and agricultural biomass, energy crops, waste wood, municipal solid waste, etc. These types are usually continuously produced locally and are likely to be available within a reasonable vicinity of the power plant, which is quite advantageous in terms of fuel transport cost reduction. However, these types of feedstock usually have a higher ash content compared to wood, and in addition, they are composed of higher concentrations of problematic ash compounds. For example, straw (the main focus of this work) contains high quantities of chlorine and alkali metals. This combination creates severe corrosion problems in combustion systems. Straw is also known to cause slagging and fouling because of a relatively low ash melting temperature.[2] In fluidized-bed systems, low-temperature ash melting can also cause agglomeration of bed material, resulting in defluidization of the bed.[3]

Dependent upon the chemical composition of the ash, the products of combustion for chlorine are mainly hydrogen chloride (HCl), Cl_2, alkali chlorides (KCl and NaCl), and zinc and lead chlorides ($ZnCl_2$ and $PbCl_2$).[4] In the boiler section of the biomass combustion plants, especially at the surface of superheater tubes, the subsequent cooling of the flue gas results in the condensation of alkali chlorides.[5] In the same manner, zinc and lead chlorides may have a major corrosive effect in boilers because of their relatively lower melting temperature, in addition to their ability to form low-temperature eutectics that, in return, facilitate corrosive reactions furthermore.[6] HCl, on the other hand, plays part in the formation of polychlorinated dibenzo-*p*-dioxins (PCCDs) and polychlorinated dibenzofurans (PCDFs), which are halogenated organic compounds that are considered to be extremely toxic.[7] However, from a corrosion point of view, HCl is the favorable compound to produce because it is expected to escape the heat-exchange section without condensing. HCl can, in addition, be easily removed from the flue gas through sorption (dry or in activated carbon) or with scrubbers (using limestone).[8]

The importance of avoiding alkali chlorides in the boiler becomes clear when understanding the corrosion mechanism. High-temperature Cl-induced corrosion may be described as such: as metal chlorides condense on the iron surface, Cl_2 can be formed by chemical reactions with gaseous compounds. Cl_2 diffuses to the superheater tubes of the boiler and reacts with iron to form ferrous chloride ($FeCl_2$). Because of the high steam pressure, $FeCl_2$ migrates and evaporates toward the flue gas, where it reacts with oxygen and forms iron oxide. In this process, Cl_2 is regenerated and again ready to react with the iron surface.[4,7] The chlorine is therefore recycled to the metal surface, where it participates continuously with the iron stripping of the

Received: February 14, 2011
Revised: May 12, 2011
Published: May 12, 2011

Table 1. Proximate Analysis of the Different Fuels and Fuel Mixtures (wt %, db)[a]

	ash	volatile matter	fixed carbon	moisture	HHV (MJ/kg)
straw(80)G(20)	4.4	77.9	17.7	13.8	20.2
straw(50)G(50)	3.7	77.5	18.9	11.8	20.7
grot(100)	2.3	77.0	20.7	9.6	21.8
straw(90)S(10)	7.9	76.6	15.5	9.3	20.0
straw(80)S(20)	11.9	73.6	14.6	9.4	20.0
straw(80)P(20)	5.9	77.1	17.1	14.4	20.4
straw(50)P(50)	7.4	73.1	19.5	17.1	21.3

[a] In the first column, G, grot; S, sewage sludge; and P, peat.

superheater tubes. To reduce chlorine corrosion, several methods exist, although none of them can claim to completely remedy this problem. Corrosion reduction can be attained through (i) fuel leaching (washing of biomass to decrease the Cl content),[9] (ii) automated and continuous cleaning of boiler parts, (iii) coatings and corrosion-resistant materials, (iv) lower steam parameters, although this will result in reduced efficiency, or (v) modification of the elemental composition of the fuel by mixing different biomasses or using additives to alter the ash chemistry. The latter is actively researched because of the complexity of the chemistry involved. Among these studies, it is worth mentioning the work on biomass fuel mixing,[10−12] the co-firing of risky biomass with non-problematic fuels,[13−17] and the use of additives.[18−23] The aim is to capture the alkali metals through several possible paths and thereby prevent the formation of alkali chlorides. Different ash elements are capable of capturing alkalis, among these are aluminum silicates, phosphates, and sulfur. For sulfur, the reaction with alkali chlorides is possible with either SO_2 or SO_3 according to eqs 1 and 2 and where M could be either K or Na.

$$2MCl + SO_2 + H_2O + 1/2O_2 \rightarrow M_2SO_4 + 2HCl \quad (1)$$

$$2MCl + SO_3 + H_2O \rightarrow M_2SO_4 + 2HCl \quad (2)$$

Reaction 1 is very slow compared to the sulfation reaction (eq 2). This makes the formation of SO_3 the limiting step for the capture of alkalis.[5,24] SO_3 formation can happen in boilers through different sulfur sources, among these are SO_2, aluminum sulfate $[Al_2(SO_4)_3]$, iron sulfate $[Fe_2(SO_4)_3]$, and ammonium sulfate $[(NH_4)_2SO_4]$.[25] The so-called ChlorOut system developed and patented by Vattenfall uses a spraying solution of ammonium sulfate prior to the superheater section in the boiler as a means of alkali capture.[26] Phosphorus may also contribute to alkalis capture directly or by making sulfur more available through the formation of calcium phosphates because calcium would otherwise form calcium sulfate.[27,28] The dominating crystalline phases containing potassium and phosphorus have been identified as $CaK_2P_2O_7$ and $MgKPO_4$ in ash from combustion of cereal grains.[14,27] The aluminum silicate sources are many and will not be mentioned in details in this paper. Kaolin ($Al_2O_3 \cdot 2SiO_2 \cdot 2H_2O$) is an example of an additive based on aluminum silicate that can capture alkalis in both reducing and oxidizing atmospheres. Many different alkali aluminum silicates may be formed; i.e., leucite ($KAlSiO_6$) and kalsilite ($KAlSiO_4$) have been observed.[29]

Table 2. Elemental Composition of the Different Fuels and Fuel Mixtures (wt %, daf) in Addition to Cl and S (wt %, db)[a]

	C	H	O	N	S	Cl
straw(80)G(20)	50.2	6.1	42.8	0.48	0.20	0.17
straw(50)G(50)	51.4	6.1	41.7	0.46	0.17	0.12
grot(100)	53.4	6.2	39.9	0.43	0.12	0.04
straw(90)S(10)	49.4	6.2	42.9	0.93	0.34	0.19
straw(80)S(20)	49.3	6.3	42.3	1.40	0.47	0.19
straw(80)P(20)	50.7	6.1	41.9	0.89	0.24	0.17
straw(50)P(50)	52.6	6.1	39.4	1.51	0.27	0.11

[a] In the first column, G, grot; S, sewage sludge; and P, peat.

The complexity of the ash chemistry during combustion has led to the creation of several indices to quantify the corrosion risk. These indices take into account elements capable of capturing alkalis and relate it to the problematic elements or compounds in the fuel. For example, a S/Cl molar ratio of 4−6 is expected to decrease the mass flow of Cl in the fine fly ash, whereas S/Cl values lower than 2 are considered to give a high corrosion risk.[15,24] The excess of sulfur compared to alkalis is considered in the molar ratio $2S/(K + Na)$, while other forms of the same ratio incorporating Ca exist $[2S/(2Ca + K + Na)]$. Ca incorporation is of importance because it can form $CaSO_4$, thereby prohibiting sulfur from capturing alkali. Similar ratios exist emphasizing the aluminum silicate ability to capture alkalis.[14,30] As an example, the minimum suggested value for the $(Al + Si)/Cl$ molar ratio is 8−10 to avoid chlorine deposition on heat-exchange surfaces.[31] Although such indices are a practical tool for a general evaluation of the relative risk of chlorine-induced corrosion, the authors feeling is that these ratios should be used carefully and that they may not reflect precisely the real life corrosion risk.

In this work, the abatement of corrosion in straw combustion is studied. Peat and sewage sludge were chosen as fuel additions to straw because of their rich nature in sulfur and aluminum silicates. Grot was chosen as a fuel additive for two reasons: (i) to serve as a reference experiment to compare to the other additives because pure straw could not be used as a result of problems with slagging at the selected temperature and (ii) to check if it could serve as a dilution fuel to lower the concentration of unwanted compounds. The different fuels and the rate of mixing were carefully chosen based on the literature and thermodynamic calculations, with the sole purpose of minimizing the corrosion risk.

MATERIALS AND METHODS

Sample Preparation. The biomass fuels used in this experimental campaign were obtained from different sources. The straw and sewage sludge were acquired through the SciToBiCom ERA-net bioenergy scheme activity. Peat was provided by Eidsiva Bioenergi AS. In addition, a mixture of branches and tops (grot) was provided by The Norwegian Forest and Landscape Institute. The Norwegian word grot is hereafter used for the biomass fuel referred to as "branches and treetops". The fuels were grinded in a mill to produce a maximum particle size of 2−3 mm. The different fuels were mixed and pelletized in a laboratory-scale pellet machine. The produced pellets had a diameter of 6 mm and a length of 5−15 mm and were air-dried before they were used in experiments. Only binary mixtures were studied in this work. The compositions of the mixtures are shown in Table 1. For all tables and figures, the first bracketed number in the code word of each experiment

Table 3. Main Elements in Ash (wt %, db)[a]

Si	Al	Ca	Fe	K	Mg	Mn	Na	P	Ti	Zn	Pb
1.06	0.01	0.39	0.01	0.70	0.07	0.01	0.02	0.08		18.6	0.49
0.73	0.01	0.47	0.01	0.55	0.07	0.03	0.02	0.06		41.3	0.73
0.24	0.02	0.65	0.02	0.28	0.05	0.07	0.03	0.05		77.3	0.94
1.59	0.15	0.64	0.59	0.76	0.12	0.01	0.03	0.44	0.01	85.7	2.45
1.82	0.32	0.96	1.24	0.71	0.17	0.01	0.05	0.85	0.03	171	4.52
1.50	0.10	0.52	0.10	0.75	0.09	0.01	0.02	0.10		6.7	0.59
1.94	0.38	0.69	0.29	0.52	0.09	0.01	0.07	0.08	0.01	9.14	1.80

[a] The fuel sequence is the same as in the previous tables. Zn and Pb are in mg/kg (db).

Table 4. Corrosion Indicators for the Different Fuel Mixtures[a]

	S/Cl	2S/(K + Na)	(Al + Si)/(K + Na)	(Al + Si)/Cl
straw(80)G(20)	1.4	0.6	2.2	9.5
straw(50)G(50)	1.7	0.7	1.9	9.4
grot(100)	3.8	0.9	1.1	9.1
straw(90)S(10)	2.4	1.1	3.1	13.8
straw(80)S(20)	3.7	1.6	4.0	18.6
straw(80)P(20)	1.7	0.8	3.0	12.8
straw(50)P(50)	2.8	1.2	4.7	21.7

[a] In the first column, G, grot; S, sewage sludge; and P, peat.

represents the weight percent of straw, while the second number gives the percentage of the added fuel. S stands for sewage sludge; P stands for peat; and G stands for grot. The proximate analyses of the samples (Table 1) were carried out according to the standard methods ASTM E871, ASTM E872, and ASTM D1102. The fixed carbon was calculated by difference to 100%. The ultimate analysis and the higher heating value (HHV) (calculated on the basis of the elemental composition of the fuel) are presented in Table 2. A chemical analysis of the ash content of the primary fuel and all of the blends was determined by inductively coupled plasma−atomic emission spectrometry (ICP−AES) and inductively coupled plasma−sector field mass spectrometry (ICP−SFMS). Table 3 shows the composition of the main ash constituents for the different fuel mixtures, while Table 4 shows some corrosion indicator molar ratios for the respective fuels. In all mixtures, the S/Cl molar ratio is below 4 (Table 4), which is the lowest recommended ratio to avoid severe corrosion. The ratio 2S/(K + Na) for the different mixtures is between 0.6 and 1.6, which is also well below the recommended value of 4. The aluminum silicate ratios for the fuel mixtures also lie below recommended values. However, the indicators do not take into consideration the full complexity of the ash chemistry during combustion and should not be regarded as very reliable concerning corrosion abatement. A better predictive tool for the relative corrosion risk of the fuel mixtures used in this study is thermodynamic equilibrium calculations (not presented here). Such calculations for straw mixed with grot, sludge, or peat were performed for a mixing range of 5−95%. The mixing levels selected for the experimental campaign are based on these calculations as well as the literature, with the purpose of minimizing the formation of corrosive compounds in straw-fired boilers. The results of equilibrium calculations are discussed in detail in another paper.[32]

Experimental Setup. The experiments were carried out in an electrically heated laboratory-scale multi-fuel reactor. Its schematic drawing is presented in Figure 1. The setup used is able to generate close to identical conditions for the combustion of the different fuel mixtures, providing a good platform where the formation of corrosive

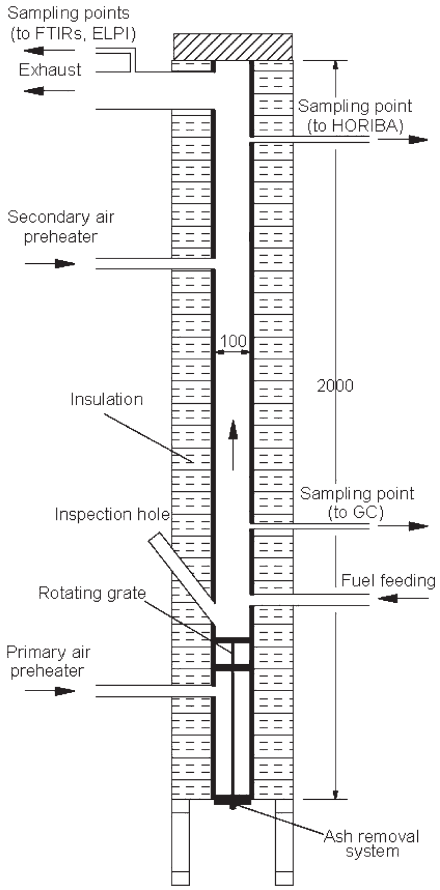

Figure 1. Schematic drawing of the laboratory reactor.

compounds from the different fuel mixtures could be easily compared. The reactor has a ceramic inner tube (100 mm diameter). The altogether 2 m high vertical tube consists of two 1 m ceramic tubes connected with a ceramic socket. The ceramic tubes are made of nonporous and noncatalytic alumina. The reaction section, located above the grate, is 1.6 m long, while the section below the grate is 0.4 m long. The reactor heating system is fitted inside the insulation shell and consists of four separate 0.5 m high heating zones of 4 kW each (16 kW in total) that enclose the ceramic tube. The combustion air is preheated to the reactor temperature by external preheaters. The primary air is added under the grate, and the secondary air is added above the grate. The distance between the grate and the secondary air supply is 865 mm, corresponding to a residence time of 19 s. The air flow is controlled by two high-precision digital mass flow controllers. The lower part of the multi-fuel reactor contains a two-grate system (10 cm apart): a primary grate and a final burnout grate, as well as an ash collection system. Both grates and the ash bin are made of Inconel. The two-level design of the grate also permits fuel staging. Both the reactor flue gas composition and the composition of the fuel gas after the primary zone, as well as the particle emission size distribution, were continuously monitored. A schematic diagram of the sampling lines is shown in Figure 2. For gas analysis in the primary zone, a micro gas chromatograph (GC) was used. The exhaust gases were quantified

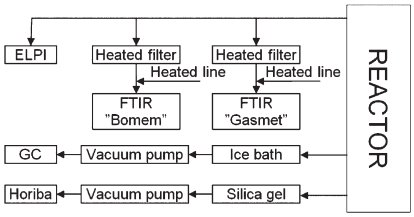

Figure 2. Schematic diagram of the sampling system.

online with two different Fourier transform infrared (FTIR) instruments and where the extracted gases were passing through heated filters and heated lines. To detect instabilities during combustion, an online gas analyzer with a fast response time was also deployed. A partial flow was taken through a sampling point near the top of the reactor. The analyzer is a portable stack gas analyzer that can simultaneously measure CO, SO_2, CO_2, O_2, and NO_x. The particle size distribution and concentration in the flue gas were measured by an electrical low-pressure impactor (ELPI). A partial stream of flue gas was collected through a stainless-steel probe located in the flue gas stack. The flue gas was then led through a double diluter system to the ELPI. The instrument is a real-time particle size analyzer for monitoring aerosol particle size distribution. The ELPI measures the airborne particle size distribution in the range of 0.03−10 μm with 12 stages and a time resolution of 1 s. The nominal air flow is 10 L/min, and the lowest stage pressure is 100 mbar. The ELPI operates at ambient temperature, while the gas sample is taken at a temperature of 110 °C. The dilution ratio is approximately 80, while the particle concentration in the diluted stream is about 3.9×10^5 particle/cm^3. The aerosol samples were collected on aluminum plates. The plates were covered by a thin layer of vaseline to provide a sticky surface. The chemical analyses of the samples were made by energy-dispersive X-ray analysis connected to a scanning electron microscope (SEM/EDX). The total mass of the particles on each plate was 10−100 μg. For each run, four plates with the particle sizes (D50%) of 0.093, 0.26, 0.611, and 1.59 μm were chosen for SEM/EDX analysis. Five EDX spot analyzes were selected from different locations on each plate. The elements detected by the analysis were C, O, Na, Mg, Al, Si, P, S, K, Ca, Cl, Fe, Zn, and Pb. After standard ZAF correction, the analysis was normalized to 100% by weight. The signals for carbon, oxygen, and aluminum cannot be used for quantitative information because their signals are disturbed by various experimental sources. The variation among the five analyses for each plate was negligible, indicating that the particles in the piles were homogeneous. The main components in the analyzed particles were K, S, Cl, and Na (Figure 6). On average, 80 wt % of the oxygen-free samples (excluding C and Al) consisted of these four elements. Zn and Pb constituted on average of 14 wt %, whereas the portion of the inert oxide-forming elements (Si, Ca, Fe, P, Mg, and Cr) was 6 wt %. P and Mg concentrations were very low in all samples. The portion of inert metals was considerably higher in the larger particles compared to the smaller fractions, indicating that the compounds of these metals (oxides) originate from the original fuel ash and have not originated from devolatilization. Lead and zinc are partly in oxide form and partly in salt form. The oxides are almost certainly ZnO and PbO. The salt part was made of sulfate and chloride of K, Na, Zn, and Pb. The crucial step of the data treatment was to estimate the compounds in which the elements were studied. This consideration was based on a recently published study on aerosol formation in combustion.[23] The assumptions regarding the speciation can be explained as follows: (i) Potassium and sodium are as chlorides or sulfates, because alkali is volatilized as hydroxides or chlorides and some of the alkali is sulfated at high temperatures. (ii) Silicon, calcium, iron, magnesium, and chromium

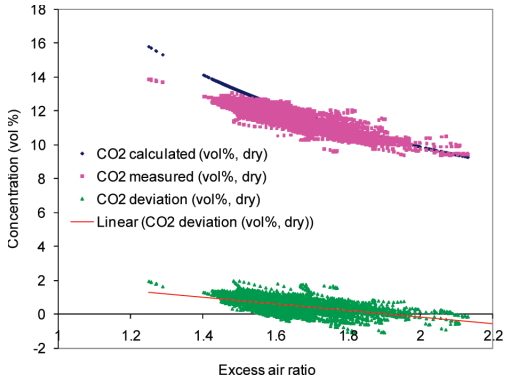

Figure 3. CO_2 concentration for the reference experiment with grot. A comparison between measured and calculated values.

are as oxides, because these are nonvolatile and these elements do not form sulfates or chlorides at higher temperatures (except Ca, which forms sulfate and phosphate, but in the present case, Ca content in the samples is low). (iii) Zinc and lead can both be as oxides and/or chlorides and sulfates. Two chemical fractions in the fly ash samples were then defined: an "inert" part constituted of high-melting insoluble oxides (SiO_2, CaO, Fe_2O_3, MgO, P_2O_5, Cr_2O_3, ZnO, and PbO) and a "salt" part consisting of low-melting water-soluble chlorides and sulfates (K, Na, Zn, Pb, Cl_2, and SO_4). The salt fraction is the one causing corrosion and deposition problems in the superheater area. It is evident that the salt part must have a balance between cations and anions. Thus, because the amount of Cl, S (as SO_4), K, and Na is known from chemical analysis of the fly ash samples, the portion of Zn and Pb can be determined by difference. The notation K_2, Na_2, and Cl_2 are used for consistency with $ZnCl_2$ and $PbCl_2$. "S" should be read as "SO_4".

Experimental Procedure. All experiments in this work were carried out employing staged air combustion and isothermal conditions. The reactor and the primary and secondary air inputs were preheated to 850 °C prior to the startup of the experiment. The pellets were fed semicontinuously from a rotating battery of fuel containers using a pneumatically driven piston. The feeding frequency was set to ensure a feeding rate of 400 g/h. The pellets are primarily combusted on the upper grate. The pellets are gradually moved to a slot leading to the second grate by rotating blades. Each grate has two rotating blades moving at a speed of 3 min/round. The final burnout takes place on the second grate before the ash is moved to a slot from where it falls into the ash bin. At the bottom of the ash bin another rotating blade moves the ash into an ash container. Because of minor variations in the pellet size, it was not possible to feed exactly the target rate of 400 g/h. Hence, the supply of primary air could not be regulated accurately to attain the set substoichiometric condition of 0.8, although the variations were within an acceptable range (0.7−0.9). The primary air supply was adjusted, so that the CO concentration from the primary zone was approximately 3%. The flow of the secondary air supply was adjusted to an overall excess air ratio of 1.6 in the stack.

RESULTS AND DISCUSSION

The amount of unburnt gas was very low (typically below 50 ppm CO at 11% O_2 in dry flue gas). However, during an initial stabilization period and short periods of high fluctuation in the fuel feeding, the excess air ratio deviated from the target value of 1.6. During such periods, the CO emission level increased to

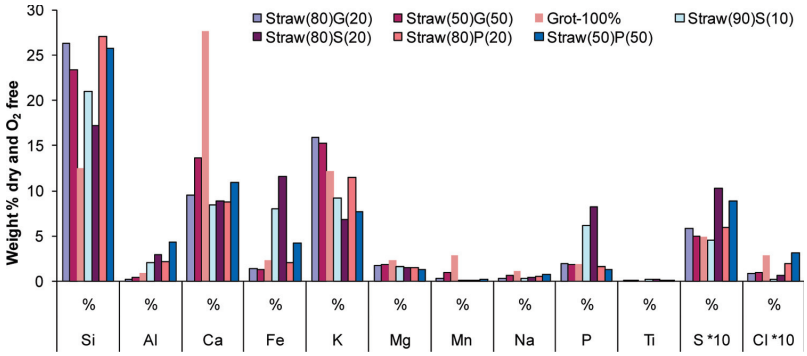

Figure 4. Major composition of bottom ash from all experiments (in the legend, G, grot; S, sewage sludge; and P, peat).

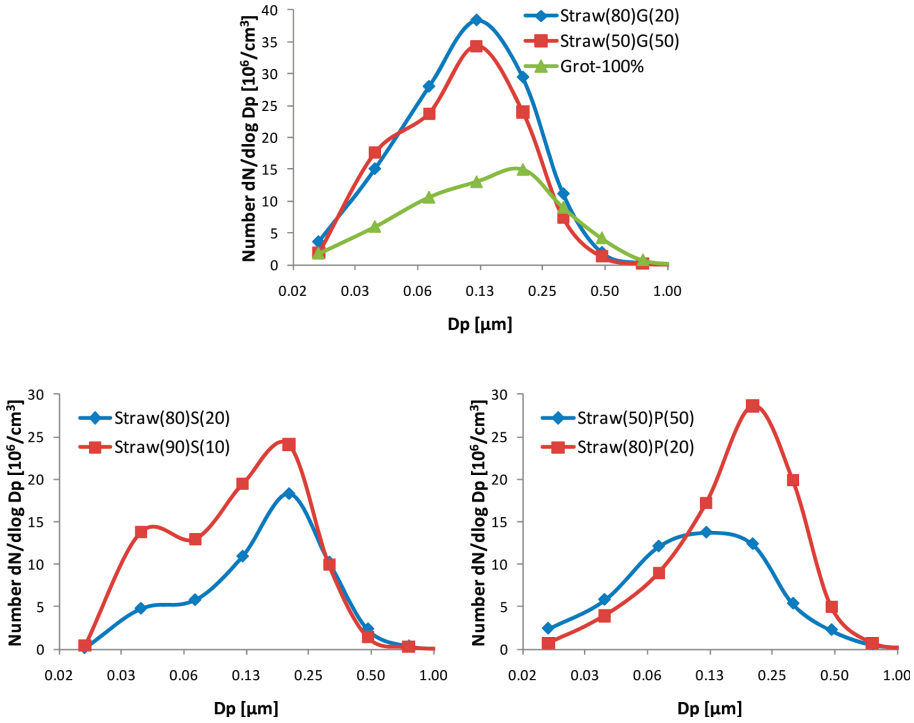

Figure 5. Particle size distribution in the fly ash (0−1 μm) for the three binary mixtures (in the legend, G, grot; S, sewage sludge; and P, peat).

typically 200 ppm at 11% O_2 in dry flue gas. The combined emission levels of hydrocarbons were typically below 5 ppm at 11% O_2 in dry flue gas. The accurate control of the fuel feed and the combustion air made it possible to check the carbon and hydrogen balance by calculating the CO_2 and H_2O concentration from the known fuel composition. The overall balance was corrected for the unburned carbon in the bottom ash (collected after the experiments) by weighting the ash before and after exposing it to a temperature of 550 °C for 20 h. The calculated carbon and hydrogen balances were used to remove outliers in the measured concentrations. Figure 3 shows the carbon balance as a function of the excess air ratio for the experiment with grot. The deviation between the calculated and measured value was within a 2% range; this was the case for all of the experiments performed in this study.

Bottom Ash Analysis. To assess the fate of key ash elements during biomass combustion and the possible effects of fuel mixing, the chemical composition of the bottom ash was determined by ICP−AES and ICP−SFMS. The concentrations of the most important elements are shown in Figure 4. A higher concentration of silicon and lower concentration of calcium for the straw mixtures are noticeable, as compared to the pure grot.

dx.doi.org/10.1021/ef200232r |*Energy Fuels* 2011, 25, 2687–2695

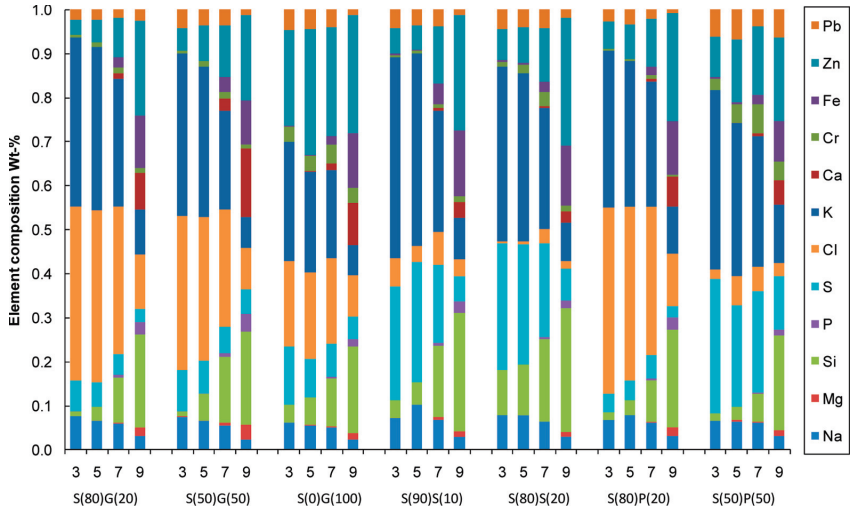

Figure 6. Elemental composition of the aerosols (the impactor stages 3, 5, 7, and 9) corresponding to the sizes 0.093, 0.26, 0.611, and 1.59 μm of the fly ash taken by the ELPI in the exhaust of the reactor, in weight percent for all of the experiments (G, grot; S, sewage sludge; and P, peat).

It is also worth mentioning that the concentration of sulfur and chlorine in the bottom ash is low, which stresses the fact that their volatilities during combustion are high. The bottom ash composition of the straw/sludge mixtures differs from the rest of the mixtures in their higher phosphorus and iron contents. The effect of the fuel interaction is not possible to determine from this figure alone; however, the effect of fuel mixtures of some important elements is discussed later in more detail.

Aerosol Size Distribution and Composition. The experiments with the straw/grot mixtures (top graph of Figure 5) give similar results for the particle concentration, producing a peak at a particle diameter of 0.12 μm. In comparison to experiments with pure grot, the peak concentration for the mixtures is more than doubled and lies close to $4 \times 10^7/\mathrm{cm}^3$. The peak concentration value is shifted toward larger particle diameters with pure grot compared to the straw/grot mixtures (from 0.12 to 0.20 μm). On the basis of the results of the fine particle emissions of the straw/grot mixtures, it can be concluded that grot may not be a proper fuel mixing choice for corrosion reduction in straw combustion for two reasons. First, grot does not appear to have any significant particle load reduction effect with straw. Second, it seems that not even a dilution effect is observed in the mixtures. This nonlinear effect indicates that the aerosol-forming chemistry is actually affected negatively by grot−straw interactions. A broader comparison to the combustion of 100% straw was unfortunately not possible because of severe problems with ash sintering on the grate, which prevented us from collecting reliable experimental results. The graph on the bottom left of Figure 5 represents the results with straw/sludge mixtures. The particle concentration for this series is significantly lower than for the straw/grot mixture and is close to the concentration of the pure grot experiment. Fewer problems related to chlorine corrosion from the sludge mixtures can be expected because sub-micrometer particles have high concentrations of alkali chlorides (in comparison to coarse particles). It is also interesting to point out that the shape of the curves appears to be bimodal, with the first peak at a particle size diameter of 0.04 μm and the second peak at a particle size diameter of 0.2 μm. The bimodal type of particle emission might be caused by different mechanisms of particle formation. The increase of the sewage sludge share from 10 to 20% in the straw substantially decreases the particle load in the flue gas. Most of the reduction occurs in the lower range of the particle size diameter and up to the point where the first peak is almost eliminated. The graph in the bottom right of Figure 5 shows the effect of peat addition on the particle load during straw/peat combustion. For 20% addition with straw, the particle concentration ranking is grot > peat > sewage sludge, and this classification can be said to directly reflect the corrosion reduction efficiency of these additional fuels to straw. For peat, an additional increase to 50% was able to further decrease the particle load. As opposed to the bimodal particle emission of the mixtures with sewage sludge, the emission profile for the peat mixtures is unimodal.

Figure 7 shows the resulting chemical compositions of selected aerosol fractions from the straw/grot experiments. The salt part is very rich in chlorides because over 70% of the salt metals are bound to chlorine for the 20% mixture. Increasing the grot share in the straw is slightly decreasing the chlorides and increasing the sulfates. For the experiment with pure grot, the salt metals are evenly distributed between chlorides and sulfates. It is also worth noticing that zinc chloride or sulfate is largely represented among the salts, and its concentration is increasing with an increasing particle size. The ratio between sodium and potassium is rather constant (1:2−3). However, in all of the mixtures, the portion of potassium decreases with an increasing particle size. For all experiments, lead is only present in marginal quantities. The chemical compositions of selected aerosol fractions for sewage sludge/peat mixtures are shown in Figure 8. For the sewage sludge mixtures, the chlorides are considerably reduced, as compared to grot addition at 10 wt %. Increasing the sludge to 20 wt % is almost completely eliminating chlorides from the aerosols. The results indicate that the smaller particles have fewer chlorides than the larger particles. The salt part

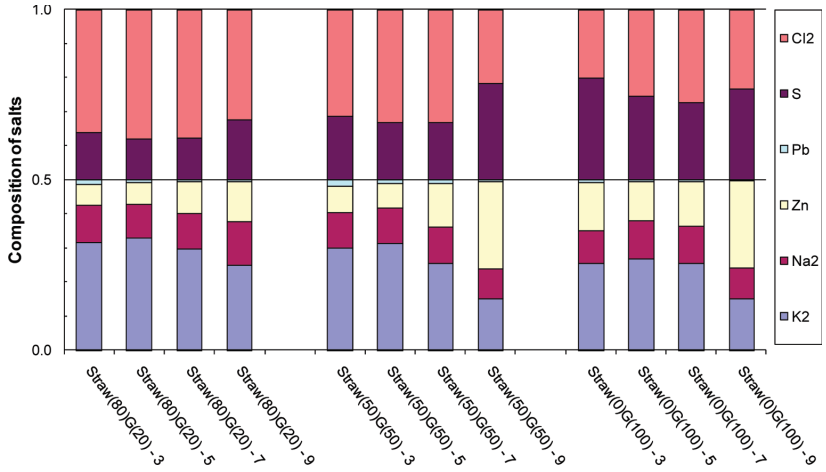

Figure 7. Chemical composition of the aerosols (impactor stages 3, 5, 7, and 9) corresponding to the sizes 0.093, 0.26, 0.611, and 1.59 μm of the fly ash taken by the ELPI in the exhaust of the reactor for the straw/grot (G) fuel mixtures.

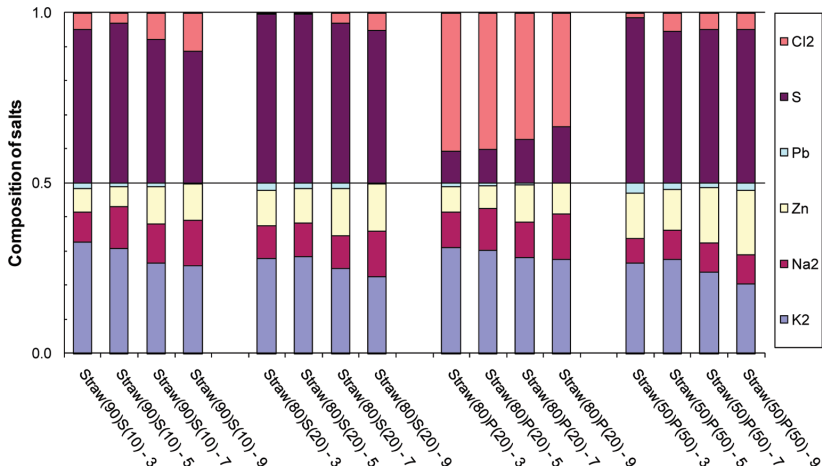

Figure 8. Chemical composition of the aerosols (impactor stages 3, 5, 7, and 9) corresponding to the sizes 0.093, 0.26, 0.611, and 1.59 μm of the fly ash taken by the ELPI in the exhaust of the reactor for the straw/sewage sludge (S) and the straw/peat (P) fuel mixtures.

consists of approximately 60% potassium sulfates, and the rest are equally distributed between zinc and sodium sulfates. With 20 wt % peat addition, the chlorides are dominating, much higher than for the 50% grot addition, but comparable to the 20% addition. For the experiment with 50% peat addition, the chlorides are dramatically reduced. The salt metal composition is more or less comparable to experiments with sludge addition. However, an increase in zinc and lead is noticed for the experiment with 50% peat addition. The greatly reduced chloride amounts at 50% peat addition might reduce the overall corrosion risk in boilers, but the higher Zn and Pb concentrations may lead to higher melt fractions in the aerosols, a factor which could significantly worsen the corrosion risk.

Fate of Chlorine. The chlorine distribution among the solid phase (bottom ash) and the gas phase is shown in Figure 9. This figure does not include the chlorine part found in the fly ash because only some impactor stages were analyzed. However, the amount of chlorine found in the fly ash is most likely very low and thus of little significance to the total Cl mass balance. HCl (gas) accounts for approximately 80% of the chlorine found in the fuel. Chlorine retained in the bottom ash after combustion is quite low for all experiments but increases with increased proportions of secondary fuel. The most noticeable chlorine retention can be seen for 50% peat addition, where 20% of the chlorine found in the mixture is retained in the bottom ash. About 20% of the Cl is unaccounted for because of experimental uncertainties, except for the 50% peat in straw experiment, where the unaccounted Cl value is below 10%.

Fate of Sulfur. A similar mass balance is presented in Figure 10 for sulfur. The results are somehow more scattered than the ones

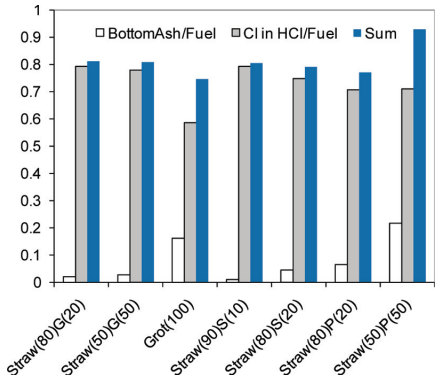

Figure 9. Chlorine distribution in the gas, the bottom ash, and (part of the) fly ash phase for all of the experiments (for the *x* axis, G, grot; S, sewage sludge; and P, peat).

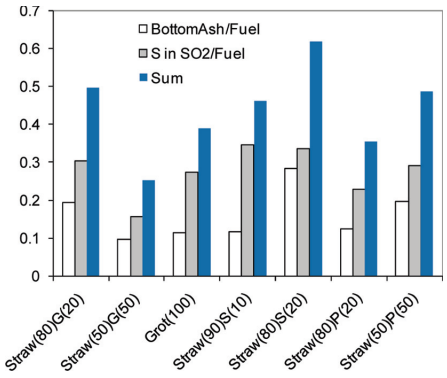

Figure 10. Sulfur distribution in the gas, the bottom ash, and (part of) the fly ash phase (for the *x* axis, G, grot; S, sewage sludge; and P, peat).

from the chlorine balance. The sulfur shares in the gas phase (as SO_2) and in the bottom ash are varying between 25 and 60%, as a function of the fuel mixtures. An increasing retention of sulfur in the bottom ash with increasing sludge and peat addition is clearly observed, while the opposite effect seems to occur with grot addition.

Potassium and Sodium Retention. As already mentioned, the combination of high contents of both alkali metals and chlorine in straw makes the combustion process very challenging. Preventing alkali chlorides from exiting the combustion chamber is regarded as the most effective measure for avoiding corrosion in boilers. Increased alkali capture in the bottom ash should therefore directly translate into a decreased corrosion risk. In Figure 11, the retention of potassium and sodium in the bottom ash relative to quantities in the raw fuel is presented. The results for potassium can be described as such: (1) K retention is about 80% or more for most of the experiments in this study; K can therefore be described as a moderate to nonvolatile compound. (2) Increasing proportions of added fuels improve K retention in the bottom ash to about 100% in two cases: 20% sewage sludge and 50% peat (with straw as the main fuel). Grot only increases K retention to about 90% at a 50% addition level. The trends of

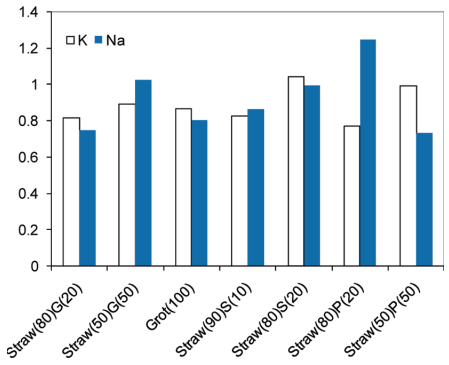

Figure 11. Potassium and sodium retention in the bottom ash for all of the experiments. (for the *x* axis, G, grot; S, sewage sludge; and P, peat).

sodium retention in the bottom ash are very similar to the potassium, except for peat addition, where opposite trends are observed. Sodium is usually omitted from discussions in scientific journals, mainly because it is present in lower quantities (see Table 3) in biomass, which make its effect on corrosion insignificant compared to potassium. The low concentration of sodium in the raw fuel could also explain the higher uncertainty in the mass balance calculation.

CONCLUSION

Several promising secondary fuels to be added to straw have been tested to abate Cl-induced corrosion straw during combustion. The goal was to capture alkali metals in the bottom or fly ash, i.e., preventing the formation of corrosive alkali chlorides and promoting the formation of noncorrosive gaseous hydrogen chloride. Three supplementary fuels were used: grot, sewage sludge, and peat. Binary mixtures with different mixing ratios were combusted in a multi-fuel laboratory reactor under controlled conditions: (1) The concentrations of the most relevant gaseous species were monitored. (2) The aerosol size distribution and the chemical composition of selected sub-micrometer particles in the flue gas were measured. (3) The chemical composition of the bottom ash and in the raw fuel mixtures was analyzed. The relative corrosion risk of the different fuel mixtures was classified on the basis of a careful observation of the measured data. The following conclusions are drawn: (i) The different fuel mixtures had a wide variation in the ash composition, which made the interpretation of the combustion results quite interesting relative to the type and amount of the supplements used. (ii) Although the heterogeneous fuel was fed in a semi-continuous manner to the reactor, the measured combustion parameters showed good control over the process, where results were found to be consistent relative to time variation. (iii) The particle load in the flue gas was strongly influenced by sewage sludge, where a 10% addition resulted in a 65% decrease in the particle concentration in the flue gas compared to the fuel mixture of straw and 20 wt % grot. The reference experiment with pure straw could not be used as a baseline because of sintering problems, which rendered this experiment impossible to run in a reliable way. Grot, on the other hand, was not good as a fuel additive with straw because the aerosol load was influenced negatively at increased addition. Peat had a positive effect on decreasing the particle load, although an addition of 50% was

needed to obtain similar results to the 20% sludge addition. (iv) The potential of chlorine corrosion could be best predicted through the results of the chemical composition of the aerosols. The grot addition was deemed to have an insignificant effect on reducing the alkali chloride concentration in the flue gas. Peat was found to contribute to a reduced corrosion environment only when highly supplemented to straw (50 wt %). The higher zinc concentration at this level of peat addition may reduce the overall effect gained in the reduced content of alkali chlorides. The sewage sludge addition was very effective at reducing the alkali chlorides at 10% addition and almost eliminating them at 20% addition. (v) The chlorine and sulfur distribution were calculated for all of the experiments and showed consistency with the other results concerning the corrosion risk, emphasizing the quality of the experiments.

AUTHOR INFORMATION

Corresponding Author

*E-mail: roger.a.khalil@sintef.no.

ACKNOWLEDGMENT

The work is financed by the Research Council of Norway and a number of industrial partners through the projects KRAV ("Enabling Small Scale Biomass CHP in Norway") and CenBio (Bioenergy Innovation Centre). We also thank BIOENERGY 2020+, Austria, and DTU, Denmark, for providing fuels and related fuel data through the SciToBiCom ERA-net.

REFERENCES

(1) International Energy Agency (IEA). *World Energy Outlook 2009*; IEA: Paris, France, 2009.

(2) Yin, C.; Rosendahl, L. A.; Kaer, S. K. *Prog. Energy Combust. Sci.* **2008**, *34* (6), 725–754.

(3) Coda, B.; Aho, M.; Berger, R.; Hein, K. R. G. *Energy Fuels* **2001**, *15* (3), 680–690.

(4) Nielsen, H. P.; Frandsen, F. J.; Dam-Johansen, K.; Baxter, L. L. *Prog. Energy Combust. Sci.* **2000**, *26* (3), 283–298.

(5) Davidsson, K. O.; Amand, L. E.; Steenari, B. M.; Elled, A. L.; Eskilsson, D.; Leckner, B. *Chem. Eng. Sci.* **2008**, *63* (21), 5314–5329.

(6) Becidan, M.; Sørum, L.; Lindberg, D. *Energy Fuels* **2010**, *24* (6), 3446–3455.

(7) Riedl, R.; Dahl, J.; Obernberger, I.; Narodoslawsky, M. Corrosion in fire tube boilers of biomass combustion plants. *Proceedings of the China International Corrosion Control Conference '99*; China Chemical Anticorrosion Technology Association (CCATA), Beijing, China, 1999; Paper 90129.

(8) Obernberger, I.; Brunner, T.; Bärnthaler, G. *Biomass Bioenergy* **2006**, *30* (11), 973–982.

(9) Dayton, D. C.; Jenkins, B. M.; Turn, S. Q.; Bakker, R. R.; Williams, R. B.; Belle-Oudry, D.; Hill, L. M. *Energy Fuels* **1999**, *13* (4), 860–870.

(10) Salour, D.; Jenkins, B. M.; Vafaei, M.; Kayhanian, M. *Biomass Bioenergy* **1993**, *4* (2), 117–133.

(11) Steenari, B. M.; Lindqvist, O. *Fuel* **1999**, *78* (4), 479–488.

(12) Pettersson, A.; Zevenhoven, M.; Steenari, B. M.; Amand, L. E. *Fuel* **2008**, *87* (15−16), 3183–3193.

(13) Munir, S.; Nimmo, W.; Gibbs, B. M. *Energy Fuels* **2010**, *24*, 2146–2153.

(14) Davidsson, K. O.; Amand, L. E.; Elled, A. L.; Leckner, B. *Energy Fuels* **2007**, *21* (6), 3180–3188.

(15) Aho, M.; Yrjas, P.; Taipale, R.; Hupa, M.; Silvennoinen, J. *Fuel* **2010**, *89* (9), 2376–2386.

(16) Spliethoff, H.; Scheurer, W.; Hein, K. R. G. *Process Saf. Environ. Prot.* **2000**, *78* (B1), 33–39.

(17) Lundholm, K.; Nordin, A.; Ohman, M.; Bostrom, D. *Energy Fuels* **2005**, *19* (6), 2273–2278.

(18) Davidsson, K. O.; Steenari, B. M.; Eskilsson, D. *Energy Fuels* **2007**, *21* (4), 1959–1966.

(19) Vamvuka, D.; Zografos, D.; Alevizos, G. *Bioresour. Technol.* **2008**, *99* (9), 3534–3544.

(20) Boström, D.; Grimm, A.; Boman, C.; Björnbom, E.; Öhman, M. *Energy Fuels* **2009**, *23* (10), 5184–5190.

(21) Bartels, M.; Lin, W. G.; Nijenhuis, J.; Kapteijn, F.; van Ommen, J. R. *Prog. Energy Combust. Sci.* **2008**, *34* (5), 633–666.

(22) Khalil, R.; Todorovic, D.; Skreiberg, Ø.; Becidan, M.; Backman, R.; Goile, F.; Skreiberg, A.; Sørum, L. The effect of kaolin on the combustion of demolition wood under well controlled conditions. *Waste Manage. Res.*, **2011**, manuscript submitted for publication.

(23) Backman, R.; Khalil, R.; Todorovic, D.; Skreiberg, Ø.; Becidan, M.; Goile, F.; Skreiberg, A.; Sørum, L. The effect of peat ash addition to demolition wood on the formation of alkali, lead and zinc compounds at staged combustion conditions. *Fuel Process. Technol.* **2011**10.1016/j.fuproc.2011.04.035.

(24) Kassman, H.; Bafver, L.; Amand, L. E. *Combust. Flame* **2010**, *157* (9), 1649–1657.

(25) Aho, M.; Vainikka, P.; Taipale, R.; Yrjas, P. *Fuel* **2008**, *87* (6), 647–654.

(26) Broström, M.; Kassman, H.; Helgesson, A.; Berg, M.; Andersson, C.; Backman, R.; Nordin, A. *Fuel Process. Technol.* **2007**, *88* (11−12), 1171–1177.

(27) Elled, A. L.; Amand, L. E.; Leckner, B.; Andersson, B. A. *Fuel* **2006**, *85* (12−13), 1671–1678.

(28) Grimm, A.; Skoglund, N.; Boström, D.; Öhman, M. *Energy Fuels* **2011**, *25*, 937–947.

(29) Elled, A.-L.; Davidsson, K. O.; Åmand, L.-E. *Biomass Bioenergy* **2010**, *34* (11), 1546–1554.

(30) Åmand, L. E.; Leckner, B.; Eskilsson, D.; Tullin, C. *Fuel* **2006**, *85* (10−11), 1313–1322.

(31) Aho, M.; Silvennoinen, J. *Fuel* **2004**, *83* (10), 1299–1305.

(32) Becidan, M.; Houshfar, E.; Khalil, R.; Skreiberg, Ø.; Sørum, L. Optimal biomass mixtures to reduce corrosion and deposition: A thermodynamic analysis. *Energy Fuels* **2011**, manuscript submitted for publication.

Paper IX

Optimal mixtures to reduce the formation of corrosive compounds during straw combustion: a thermodynamic analysis

M. Becidan, E. Houshfar, R.A. Khalil, Ø. Skreiberg, T. Løvås, L. Sørum

Energy & Fuels, 25 (7), pp. 3223–3234, 2011

---

energy&fuels

ARTICLE

pubs.acs.org/EF

Optimal Mixtures To Reduce the Formation of Corrosive Compounds during Straw Combustion: A Thermodynamic Analysis

Michaël Becidan,*[,†] Ehsan Houshfar,[‡] Roger A. Khalil,[†] Øyvind Skreiberg,[†] Terese Løvås,[‡] and Lars Sørum[†]

[†]Department of Energy Processes, SINTEF Energy Research, NO-7465 Trondheim, Norway

[‡]Department of Energy and Process Engineering, Norwegian University of Science and Technology (NTNU), NO-7491 Trondheim, Norway

ABSTRACT: The thermodynamic analysis carried out focuses on biomass mixing to reduce the formation of corrosive (mainly alkali) chlorides during straw combustion. The calculations confirm the reduction abilities of sewage sludge and peat and provide information on the addition levels at which no corrosive compounds are expected to form. The calculations provide insight into the mechanisms responsible for the disappearance of alkali chlorides. The mechanisms that can potentially take place are known (reaction with sulfur and reaction with or adsorption on aluminosilicates or other ash compounds). However, many aspects remain unclear, and calculations cast light on several of them. The main result obtained in this study is that, in a given binary mixture, the chemical elements involved in the decomposition of corrosive alkali chlorides (or preventing them from forming) change with the mixing proportions, an important fact never mentioned to our knowledge. The practical implications are significant: in a real system, local elemental concentrations will vary; this means that several mechanisms will simultaneously fight the formation of corrosive alkali compounds. This new result may explain why the experimental results from the literature are often confusing or even contradictory even for a given mixture; the overall chemical picture is not static. The chemical elements reacting with alkalis during co-combustion of straw with sewage sludge or peat are predicted to be S, Ca−S, and aluminosilicates.

INTRODUCTION

In the global race to increase the share of renewable energy, biomass is by large the prime contributor on a world basis and is developing rapidly. However, many biomasses have high alkali contents that may cause operational problems in thermal systems, especially Cl-induced corrosion. During combustion, Cl can be transported to and deposited on heat-exchange (mainly superheater) surfaces as gaseous alkali chlorides but also as condensed alkali chlorides found on fine and coarse fly ash particles. This Cl can then react with steel components, thereby destroying the metal structural integrity. Corrosion is not only responsible for a sizable fraction of the maintenance costs, it also causes unplanned shutdowns.

Several chemical elements are known to prevent Cl from reaching and depositing on heat-exchange surfaces. The main known beneficial elements include Al and Si (mainly as aluminosilicates) and S (mainly as sulfates). The main modes of action of aluminosilicates and sulfur are presented in reactions 1 and 2 (M = Na or K).[1,2]

R1: $Al_2O_3 \cdot xSiO_2(s) + 2MCl(g) + H_2O(g) \rightarrow M_2O \cdot Al_2O_3 \cdot xSiO_2(s) + 2HCl(g)$ (chemisorption).

R2: $SO_3(g) + 2MCl(g) + H_2O(g) \rightarrow 2HCl(g) + M_2SO_4(s)$ (sulfation).

R2 requires the formation of SO_3, the key component of fast sulfation. SO_3 can originate from the oxidation of sulfur or the decomposition of sulfates, with the latter being more effective.

A third (physical and not chemical) route is also possible.

R3: alkali and/or Cl are bound to the additive ash by van der Waals forces (i.e., absorption).

Furthermore, compounds such as Al, Si, Ca, P, Fe, and more generally "reactive" (i.e., available for reactions) ash compounds[3] are expected to affect alkali chemistries, but the mechanisms involved, either physical or chemical, are not clear.[4] The overall picture of corrosion reduction in real systems is therefore complex to describe in detail.

The corrosion reduction processes are either sequestrating alkali or alkali chlorides or forming alkali sulfates. Cl is either physically (by capture) or chemically (by forming HCl) prevented from depositing (by condensation as vapor or impaction as part of particles/aerosols).

The aforementioned elements may be introduced in the combustion system using dedicated additives, but an innovative solution is co-combustion of biomasses with high corrosion and biomass propensities with additional biomass fuels containing high concentrations of aluminosilicates and/or sulfur and/or other ash compounds. This will often be cheaper and allow for the safe and sound disposal of the secondary fuels. Such fuels include peat, sludge (sewage, pulp, digested, raw, etc.), and coal ash.

In this study, the co-combustion of straw with sewage sludge and peat is investigated. Straw is an agricultural byproduct from grains and oilseed crops. Straw is a high chlorine-, high potassium-, and high silica-containing biomass. The composition of straw makes it a fuel with both high corrosion and high deposition propensities. Extensive experience from Denmark confirms these challenges, but it does not prevent this country from combusting more than 1 million tons of straw annually in large straw-fired boilers and also farm plants, to produce about 5 TWh

Received: February 16, 2011
Revised: May 20, 2011
Published: June 01, 2011

bioenergy.[5] In the meantime, straw is almost completely unused for energy purposes in Norway and is often considered a waste. The annual potential for bioenergy from straw in Norway has been evaluated to 2.5 TWh.[6] Despite its challenges, straw is of interest because it is readily available and cheap because it is considered a largely useless residue today.

Sludge is a semi-solid mixture of particles and water left from industrial wastewater (in the pulp and paper industry, for example) or sewage treatment. About 100 000 tons of sewage sludge (total solids) recovered from treatment plants were reported as "disposed of" in 2008 in Norway.[7,8] While more than 80% are used for soil improvement, it is unclear how much (if any) is used to produce energy in thermal systems today. Even though biogas collection from the anaerobic fermentation of sewage sludge and its further use for energy production (CHP) is currently happening, no sewage sludge was combusted in Norway as of 2005 because of high costs and because the authorities have been restrictive in authorizing sewage sludge combustion because it is considered to be a valuable fertilizing agent (especially concerning the recycling of phosphorus).[9] However, the current fate of the remaining 20% (given as unknown, other, landfilling, or cover material in landfill sites) may be considered less sound than combustion with energy recovery, especially when sewage sludge is considered a valuable corrosion-fighting additive.

Peat[10,11] is an accumulation of partially decayed vegetal matter rich in humus and carbon. Its formation rate is slow, but it may still be exploited in a sustainable manner. Peat briquettes and pellets can be combusted in wood-burning stoves. The total Norwegian resources are evaluated to 5000 million cubic meters of raw peat,[10,11] equivalent to 700 million tons of crude oil or 300 million tons of coal. This corresponds to a total energetic value of 8000 TWh (for comparison, the net domestic end-use of energy in Norway in 2005 was 225 TWh, with half of it being electricity). Its annual growth (in Norway) is evaluated to an energy potential of 4−8 TWh. Contrary to countries such as Finland, these peat resources are almost completely unexploited today and, hence, offer a large energetic reservoir.

Despite the fact that the processes that may affect the corrosive alkali chloride formation appear to be known, more work is needed because results are often contradictory and installation-specific. The thermodynamic analysis carried out in this study focuses on various mixtures to reduce the formation of corrosive alkali chlorides during straw combustion. The 2-fold goal is to investigate (1) the alkali chloride reduction ability of peat and sewage sludge when co-combusted with straw and (2) the mechanism(s) eventually leading to changes in alkali chemistry (especially alkali chloride reduction) in the mixtures compared to straw alone. This study will provide basic knowledge about the thermodynamically preferred species for alkali and chloride during co-combustion of straw with either sewage sludge or peat compared to straw alone.

MODELING SECTION

The software package FactSage 6.1 is used for the thermodynamic equilibrium calculations. The calculations are carried out at 850 °C with an excess air ratio (λ) of about 1.6 for several mixtures of straw + sewage sludge and straw + peat (dry fuels). The study of the influence of the temperature, moisture content, air ratio, and chemical forms (also known as modes of occurrence) of the chemical elements are out of the scope of this paper: conditions typical of a biomass-fired grate chamber are chosen to provide an overall picture of the chemistry, and no limitation on the availability of chemical elements is imposed.

Even though thermodynamic equilibrium calculations are a unique tool to simultaneously handle multicomponent, multiphase chemical systems, limitations have to be considered when interpreting thermodynamic equilibrium results because kinetics and transport phenomena are not included. However, careful interpretation of the observed trends can help with the understanding of the underlying chemistry. Accordance as well as disagreement between calculations and experiments will provide much needed knowledge.

A custom-made database using data from FACT databases is used. This database is especially adapted to the study of high-temperature biomass combustion and includes 192 gases, 328 pure solids, and several solution phases. These phases are (FACT denomination): FToxid-SLAGA (liquid oxide), FTsalt-ACL_A (ss, rock salt structure: NaCl−KCl−$CaCl_2$); FTsalt-CSOB [$(Na, K)_2(CO_3, SO_4)$], and FTsalt-SALTF [liquid salt: $(Na, K)_{1,2}(Cl, OH, SO_4, CO_3, NO_3)$]. The 13 elements included in the calculations are C, H, O, S, N, Cl, Na, K, Pb, Zn, Si, Al, and Ca. The fuel composition (for the selected elements) and combustion air, used as input for the calculations, are given in Table 1.[12] Straw is a Cl- and K-rich biomass, while sewage sludge is especially rich in Ca, Al, and Si. Peat also contains significant amounts of Al, Si, and Ca but significantly less than sewage sludge. Some ash-forming elements are not included either because they are not of importance to alkali chemistry (Fe and Mg) or because of limited data (P), but no major effect on the overall thermodynamic trends is expected.

An efficient way to evaluate the relative corrosion risk associated with the gas phase evolving from the combustion chamber is by computing the amount of gaseous alkali chlorides formed because they are the main vessels of Cl in its journey to heat-exchange surfaces. The higher the amount of these gaseous alkali chlorides, the more corrosive the gas phase is considered to be.

Second, changes in speciation of alkali and chloride in the different mixtures will provide knowledge about the preferred pathway(s) involved in the reduction of corrosive alkali species as well as the ones not taking place.

RESULTS AND DISCUSSION

Fate of Alkali Chlorides. *Straw + Sewage Sludge Mixtures.* As indicated earlier, the amount of alkali chlorides generated during combustion is used to evaluate the overall Cl-induced corrosion risk. Figure 1 presents the results concerning both gaseous alkali chlorides in straw−sewage sludge mixtures. Potassium chloride is the main alkali by far, but looking at the different behaviors of potassium and sodium is of interest. It appears that digested, dewatered, and dried sewage sludge is a very efficient fuel for reducing the overall amount of alkali chloride generation during co-combustion with straw; a 2.5 wt % sewage sludge addition is enough to reduce alkali chlorides by almost 50%. The addition of 5−10 wt % sewage sludge causes a reduction of about two-thirds of the generated alkali chlorides according to the calculations. For a 25 wt % sewage sludge addition level, almost no corrosive alkali chlorides are formed. However, both alkalis do not react completely alike, a phenomena almost never discussed in the literature. The most remarkable comment concerning the mixtures is that the amount of sodium chloride does not decrease (and is even slightly increasing) below its 100% straw level before the proportion of sewage sludge added is higher than 5 wt %, while potassium chloride is decreasing sharply at low sewage sludge levels (i.e., below 5 wt %). Because the overall chemistry of the system is dependent upon both its composition and the elemental thermodynamic properties, it is difficult to give a clear explanation but it clearly shows that nonlinear effects are to be expected in complex

Table 1. Compositions of Fuels (100 g of Dry Fuel) and Combustion Air

straw[a]		sewage sludge[a,b]		peat[c]	
element	amount (g)	element	amount (g)	element	amount (g)
C	45.93	C	29.47	C	53.18
H	5.86	H	4.43	H	5.50
S	0.111	S	1.23	S	0.265
N	0.64	N	4.35	N	2.05
Cl	0.19	Cl	0.0841	Cl	0.0474
Al	0.0061	Al	1.68	Al	0.2642
Ca	0.433	Ca	3.54	Ca	0.5723
K	0.904	K	0.358	K	0.0372
Na	0.0114	Na	0.199	Na	0.0139
Si	1.4	Si	4.5	Si	0.9871
Zn	0.0008	Zn	0.0994	Zn	0.0061412
Pb	0.00004	Pb	0.00258	Pb	0.0011908
fuel O (by difference)	41.7	fuel O (by difference)	19.01	fuel O (by difference)	33.94
N_2 (air)	754	N_2 (air)	538	N_2 (air)	866
O_2 (air)	229	O_2 (air)	163	O_2 (air)	263

[a] Data from SciToBiCom ERA-net. [b] Digested, dewatered, and dried. [c] Data from ref 12.

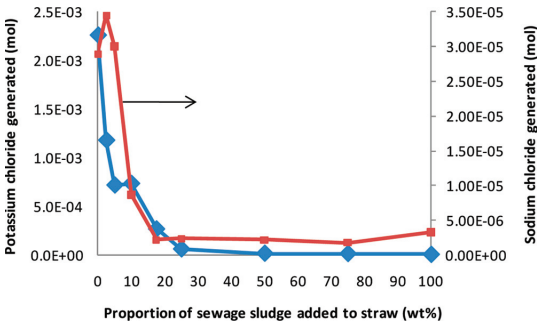

Figure 1. Alkali chloride formation during straw and sewage sludge co-combustion at different ratios. Total fuel weight = 100 g for all cases.

mixtures where multicomponent interactions are taking place. Furthermore, the almost identical potassium chloride levels at 5 and 10 wt % sewage sludge addition are surprising in light of the other results and are shortly discussed later. Apart from that, both alkalis exhibit pretty similar trends in the different mixtures.

In parallel, the proportion of Cl found as HCl is increasing with increasing amounts of sewage sludge; while 57% Cl forms HCl for straw, this percentage increases to more than 76% for a 2.5 wt % sewage sludge level, 85% for 5 wt % sewage sludge, and 98% for 25 wt % sewage sludge addition.

The thermodynamic results are in very good accordance with experimental results from the literature, where sewage sludge is co-combusted with different biomasses (and waste). Table 2[1−3,13−26] summarizes the main overall results from several experimental campaigns. The experimental studies report a decrease in the gaseous alkali chloride concentration. The decrease is usually described as important in most cases, with sewage sludge levels varying between 4 and 30 wt %. Alkali chlorides are described as "eliminated" or "removed" or their disappearance as "nearly total" for levels between 12 and 30 wt %; these results are very close to the results predicted by thermodynamic equilibrium analysis.

Experimental results (Table 2) from the literature (focusing on peat and sewage sludge) also reveal that this reduction is correlated with the following: (1) First, lower concentrations of fine particles[17,18,24] and higher concentrations of coarse particles[18] do not seem to increase deposition, but no explanation is proposed. (2) Second, the qualitative and quantitative properties of the deposits are affected; sewage sludge reduces the amount of deposited material,[1,17,18,25] as well as the amount of Cl and alkali deposited,[1,2,14,25] as predicted by the calculations. (3) Third, the resulting co-combustion fly ashes are enriched in trace elements originating from the sewage sludge,[16,24] a fact that might affect their final disposal.

Sewage sludge should be pretreated to ensure good chemical and physical properties as well as to promote interactions between ash-forming elements and reduce operational problems. Dried pellets are therefore recommended to facilitate feeding, mixing, and combustion[2,4,19,24] while avoiding excessive entrainment of unreacted material and disturbances by high water contents. This indicates that the highest co-combustion levels recommended by the calculations, about 25 wt %, may not be practical to attain because of feeding issues[19] as well as high drying costs. The corrosion and deposition reduction benefits should be carefully considered against these challenges. It is clear that combining and comparing experimental and modeling results lead to a more accurate and complete assessment of the situation.

Trace metal chlorides are of significance concerning the corrosion risk because they may form eutectics (mixtures with low melting points). This mixture will therefore be melted at superheater metal surface temperatures, and this may increase the corrosion rate on this surface because chemical reactions are faster in a liquid phase than with solid−solid reactions and because a molten phase provides an electrolyte or a pathway for ionic change transfer for electrochemical attack. Straw and sewage sludge actually produce almost the same amounts of $ZnCl_2$. The amounts of $ZnCl_2$ predicted to form are significantly

dx.doi.org/10.1021/ef2002475 |*Energy Fuels* 2011, 25, 3223–3234

Table 2. Co-combustion Experiments Involving Peat or Sewage Sludge: Overall Practical Results

reactor	mixtures	alkali chlorides and corrosion	deposit	bottom and fly ash and other comments	reference
12 MW CFB	23−30% sewage sludge, wood, and straw	chloride removed	no alkali, no Cl		13
12 MW CFB	67% wood, 21% straw, 12% sewage sludge	nearly total reduction of KCl	none on deposit probe		14
12 MW CFB	wood/straw (80/20% energy basis) + zeolites (amount?)	decreased KCl(g)		80% alkali in the bag filter (mostly stable forms)	15
12 MW CFB	55% wood pellets 21% straw pellets 24% sewage sludge	removed from the flue gas	Cl eliminated K reduced increased Al, Ca, S formation rate affected	increased total ash flows	1
12 MW CFB	wood pellets and municipal sewage sludge (16−39−52%)			ashes enriched in trace elements with increasing share of sewage sludge	16
12 MW CFB	wood pellets, waste wood, and sewage sludge (5−13%) and added ZnO, HCl		removed or considerably reduced	amount of sub-micrometer particles decreases radically	17
12 MW CFB	67% wood pellets, 20% straw pellets, 13% sewage sludge (reference: 80% wood, 20% straw)		low deposits	concentration of fine particles lowered and coarse particles increased	18
20 kW BFB	crushed fir bark pellets and crushed recycled fuel pellets from municipal and industrial solid waste treatment + 2 sludges (4−8% enb)	decreased alkali chloride concentration	decreased Cl deposition		2
75 MW CFB	waste: 30−50% household waste, 50−70% industrial waste + up to 20% sewage sludge	corrosion rate decreased by 80%		problems with sewage sludge feeding (pump) and high water content	19
20 kW BFB	bark and sewage sludge (0, 2, 4, 6, and 8% enb)		decreased K and Cl eliminated	ash flow doubled already at 4% enb	25
lab-scale grate reactor	straw with sewage sludge (10 and 20%)			Cl reduction in aerosols, aerosols load reduced, bottom ash enriched in K	24
"large-scale" CFB	main fuel: bark + cardboard, peat co-combustion (?%)	minor reduction of gaseous alkali chlorides	Cl in the deposit and deposit growth greatly reduced		20
52 MW CFB	30−40% wood, 60−70% peat			properties of the solid residues from mixtures cannot be predicted on the basis of the ash from each fuel	21
20 kW cereal burner	oat grains with 20% peat			increased emissions of ash compounds, probably because of the higher temperature	22
5 kW FB	pine and spruce bark from a sawmill + 5−10−30% peat			5% enough to prevent agglomeration	23
5 kW bench-scale FB	80% branches and tree tops + 20% peat (eight samples)		decreased levels of K and Cl, increased Si, S, Ca, Fe	reduced amounts of fine particles, increased number of coarse particles	3
lab-scale grate	straw with peat (20 and 50%)			Cl reduction in aerosols, aerosols load reduced, bottom ash enriched in K	24
lab-scale EFR	straw with peat (0, 10, 20, 30, ..., 100%) (peat with bark not presented)		nonlinear	increasing Cl/S ratios in the feed ash did not affect Cl/S in the deposit	26

dx.doi.org/10.1021/ef2002475 |Energy Fuels 2011, 25, 3223–3234

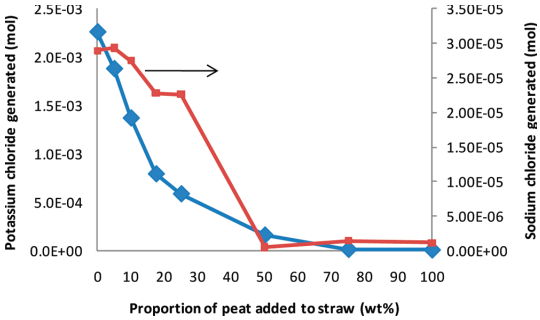

Figure 2. Alkali chloride formation during straw and peat co-combustion at different ratios. Total fuel weight = 100 g in all cases.

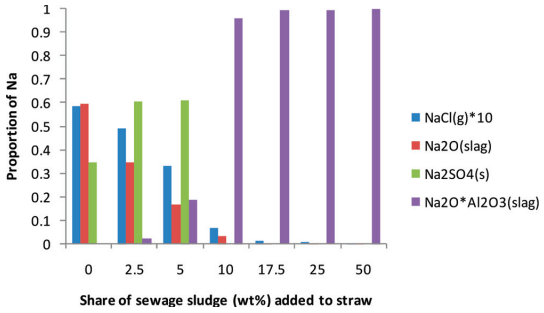

Figure 3. Na relative speciation as a function of the sewage sludge addition to straw.

higher in all of the mixtures studied than in the pure fuels, with a maximum of 2.04×10^{-5} mol at a 17.5 wt % sewage sludge addition level. $PbCl_2$ is produced in smaller amounts but exhibits the same trends. These behaviors are good examples of the complexity and variety of the interactions taking place in mixtures. It does not seem possible to solely achieve positive outcomes; both synergies and negative effects are to be expected. Hence, mixtures will have to be evaluated after careful assessment of a variety of advantages and disadvantages.

Straw + Peat Mixtures. Figure 2 presents the results concerning the formation of gaseous alkali chlorides in various straw−peat mixtures, with potassium chloride being the most important by far. Peat does not appear to be as efficient as sewage sludge because with an addition level of 10 wt %, peat gives a reduction of about 40% (for both alkalis combined) compared to more than 65% with 10 wt % sewage sludge addition. However, the addition of a fuel with high concentrations of S, Al, and Si (and other ash elements) has definitely positive effects when it comes to corrosive alkali chlorides according to thermodynamic analysis. Interestingly, while potassium chloride formation follows what can be described as an inverse exponential function with increasing peat addition (similar to the straw + sewage sludge mixtures), sodium chloride does not decrease significantly at first. Its level suddenly drops between 25 and 50 wt % peat addition. The amount of Na present in the different mixtures is rather stable because both fuels have similar Na concentrations (Table 1).

Similar to sewage sludge, Cl is predicted to increasingly form HCl when peat is co-fired; 57% Cl is found as HCl in straw combustion, but this percentage increases gradually to 71, 85, and 94% at the respective peat levels of 10, 25, and 50 wt %.

The threshold of 75 wt % peat to stop the formation of corrosive alkali chlorides is of course not realistic if straw is to be the main fuel. However, the peat resources in Norway (see the Introduction) allow peat to be considered as a potential main fuel. In this configuration, it can be said that it is safe to co-combust up to 25 wt % straw, a problematic fuel, with peat.

Within the experimental studies involving peat found in the literature (see Table 2), it is reported that co-combusting peat with various biomasses (only two studies involving straw and peat were found[24,26]) can reduce the Cl content of aerosols, which may deposit,[21,24] thereby reducing the Cl content of the deposits as well as the deposit growth rate.[20] However, only a single study provides information concerning the influence of peat on gaseous alkali chloride formation and reports that, while the Cl content is greatly reduced in deposits, only a minor reduction of alkali chlorides is observed in the gas phase.[20] Looking specifically at straw + peat mixtures,[26] it appears that the role of S in alkali chemistry might not be central but that other effects (Si−Al compounds) may take place. This complex situation shows the necessity for further investigation of the actual mechanisms possibly involved in the abatement of alkali chlorides. This will be the theme of the next section of this paper.

The observed results concerning fly ash emissions differ with the main fuel (Table 2). While some report lesser amounts of fine particles[3,24] and a greater number of coarse particles,[3] others observe increased emissions of PM_1 ash compounds.[22]

As with sewage sludge (see the previous section), $ZnCl_2$ formation is predicted to increase at first with peat addition (0−25 wt % levels) before decreasing. The amount of $ZnCl_2$ produced is not back to its 100% straw level until a peat addition of about 70 wt %. Because an addition level of 25 wt % can be seen as a maximum if peat is used as an additive, with straw being the main fuel, co-firing will surely worsen the situation when it comes to $ZnCl_2$ production. This phenomenon or more accurately an increase in Zn concentration in aerosols with increasing peat addition levels has been observed experimentally.[24] $PbCl_2$ is present at very small amounts but exhibits the same behavior. The specific and detailed fate of trace metals during co-firing is rarely discussed in the literature despite its importance.

Fate of Alkalis: Mechanistic Insights. *Straw + Sewage Sludge.* Na relative speciation during straw combustion is the following (in order of importance): Na_2O (Na in oxide/silicate slag, given as oxide in the thermodynamic model), $Na_2SO_4(s)$, and NaCl(g). How is Na chemistry influenced by increasing proportions of sewage sludge? Figure 3 summarizes the relative speciation of Na in different mixtures. Three different situations are predicted by the thermodynamic equilibrium calculations: (1) At 2.5 and 5 wt % sewage sludge addition, sulfation of Na is predominant; at 2.5%, about 60% Na is found as $Na_2SO_4(s)$ compared to 35% when no sewage sludge is present. (2) At 10 wt % sewage sludge addition, about 96% Na is forming $Na_2O \cdot Al_2O_3$(slag). (3) At 17.5 wt % sewage sludge addition and above, about 99% Na is found as $Na_2O \cdot Al_2O_3$(slag).

It appears therefore that, thermodynamically, different chemical elements are involved in alkali chloride reduction sequentially rather than simultaneously as a function of the sewage sludge addition. However, it can safely be said that, in real systems, both mechanisms will overlap, especially because operating conditions (concentrations of fuels but also temperature and excess air) will

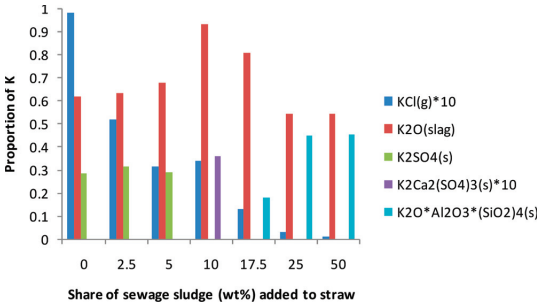

Figure 4. K relative speciation as a function of the sewage sludge addition to straw.

vary locally and change swiftly. This is especially relevant for systems where the mixing quality is not optimal. The fact that the simulations indicate that the predominant mechanism preventing the formation of corrosive alkali chlorides is dependent upon the concentration of the corrosion fighting additional fuel may, at least partly, explain the often confusing, conflicting, and installation-specific experimental results found in the experimental literature.

Initially, i.e., during straw combustion, K has a speciation very similar to Na; the three main compounds formed (in order of importance) are K_2O (K in oxide/silicate slag given as oxide in the thermodynamic model), $K_2SO_4(s)$, and KCl(g). Increasing sewage sludge fractions decrease KCl(g) both absolutely (amount) and relatively (percentage of total K). The thermodynamic equilibrium analysis accompanies this decrease in corrosive alkali chlorides and predicts the following (see Figure 4): (1) At 2.5 wt %, most of the disappearing KCl(g) is sulfated to $K_2SO_4(s)$. (2) At 5 wt %, a further decrease of KCl(g) is due to the formation of K_2O(slag). (3) At 10 wt %, $K_2Ca_2(SO_4)_3(s)$ is appearing as a new K compound, while $K_2SO_4(s)$ is not formed anymore. Ca is usually expected to promote alkali chloride formation by binding some S as $CaSO_4$, but it appears that the overall effect of Ca on alkali chemistry might be more complex. (4) From 17.5 wt %, leucite, $K_2O \cdot Al_2O_3 \cdot (SiO_2)_4(s)$, appears and its proportion increases with sewage sludge. At 25 and 50 wt % sewage sludge addition, about 45% K is found combined as solid aluminosilicate. In the meantime, no significant amounts of potassium sulfates (either with or without Ca) are formed above 5 wt % sewage sludge addition.

According to the thermodynamic analysis, the chemical elements "removing" gaseous alkali chlorides include aluminosilicate, S, and S together with Ca depending upon the addition level. Even though the overall alkali chloride reduction mechanism can be described as sequential for Na, it is interesting to notice that, in two instances, two chemical elements are simultaneously involved in alkali capture, Ca−S and Al−Si.

The amount of potassium chloride generated at 5 and 10 wt % addition levels are almost the same (there is actually a very slight increase when more sludge is added), and this is rather surprising in view of the other results. No clear explanation can be given. However, it should be noticed that the speciations of alkalis are quite different in these two mixtures; going from 5 to 10 wt % sewage sludge, alkali sulfates are decreasing dramatically, while $K_2Ca_2(SO_4)_3$ is appearing.

The overwhelming majority of experimental studies dealing with co-combustion of various biomasses solely discuss in terms of alkalis or K because it is the predominant alkali in problematic biomass fuels. However, thermodynamic analysis gives us the opportunity to look in detail at the behaviors of alkalis independently. The calculations actually show both similarities and differences between K and Na behaviors in the various mixtures investigated: (1) Both Na and K speciations are affected by co-combustion; their chlorides decrease with increasing shares of sewage sludge but do not follow the exact reduction pattern (see Figure 1). This may have important implications in fuels, where Na/K is not small, such as waste (MSW). (2) The elements involved in Na and K shift in speciation are changing with the addition levels. (3) Na and K are not affected to the same extent and by the same elements at a given sewage sludge addition level.

Molar ratios based on the fuel composition are often used in association to understand and/or attempt to predict general speciation trends and the underlying chemistry. This means that ratios may provide insight into the more (or less) probable reactions between given elements. Fuel molar ratios are also employed to determine the molar threshold values characterizing specific processes.

A total of 11 molar ratios are collected from the literature[1,2,13,17] and computed for the present calculations. Below is a list of these ratios and their interpretations (as described in the literature): (1) (Na + K)/(2S + Cl), quantifies the availability of Na and K to form other compounds than chlorides and sulfates; (2) (Al + Si)/(fuel Cl), maintained above 8−10, this will prevent the presence of Cl in deposits; (3) 2S/(Na + K), above 1, it will ensure that Cl content in deposits is kept negligible; (4) (Al + Si)/(K + Na), it is relevant when discussing the reactions of alkali with aluminum silicates; however, it does not cover all possible stoichiometries; (5) Al/(Na + K), no interpretation given; (6) S/Cl, high enough (above 4), sulfates dominate and deposits of KCl are absent; (7) Cl/(Na + K), formation of alkali chlorides; (8) S/(Ca + 2K + 2Na) (or 2S/(K + Na + 2Ca), to evaluate "excess S" and therewith SO_2 emissions; (9) Ca/S, if high, there will be significant $CaSO_4$ formation and, hence, less available S to alkalis; (10) Al/Cl, no interpretation given; and (11) Ca/(0.5Cl + S), should be kept above 5 to keep SO_2 emissions low.

The aforementioned ratios are focusing on (a) alkali chemistry because it is of prime importance for corrosion, (b) Cl chemistry because it is similarly central to the corrosion risk on heat-exchange surfaces, (c) S because sulfates are known to be related to chlorides and SO_2 emissions, (d) AlSi reaction with alkalis, and (e) Ca chemistry because it may promote the formation of corrosive alkali chlorides by binding some S as $CaSO_4$.

Figures 5 and 6 show all of the mentioned ratios for the straw−sewage sludge mixtures. What are the main (strongest) trends observed with these ratios concerning the corrosive and noncorrosive alkali compounds in mixtures containing increasing proportions of sewage sludge? In a system as complex as the one being studied here, interpretation may be difficult, because secondary effects might blur trends; as an example, two chemical elements involved in a given ratio might have their chemistries affected by a third one absent of this ratio.

However, when the interesting trends are isolated, it can be said that, as sewage sludge proportions are increasing: (1) S proportions compared to Cl are increasing, implying a shift from alkali chlorides to alkali sulfates with increasing sewage sludge proportions. It is observed at only very low sewage sludge additions because Al and Si are increasing at a far greater pace. (2) The Ca/S ratio is stable in most mixtures; there is always a

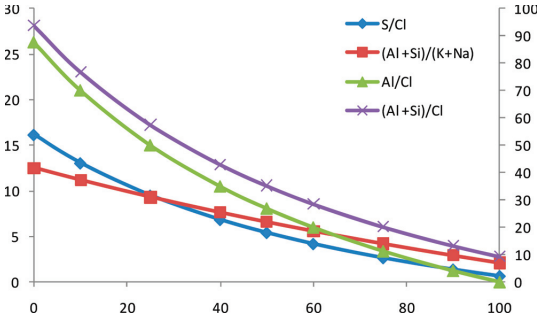

Figure 5. Molar ratios for straw + sewage sludge mixtures as a function of the straw proportion in percent (part 1 of 2). Right side *y* axis: (Al + Si)/Cl.

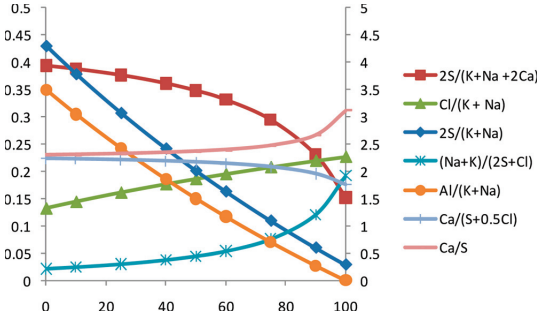

Figure 6. Molar ratios for straw + sewage sludge mixtures as a function of the straw proportion in percent (part 2 of 2). Right side *y* axis: Ca/S, Ca/(S + 0.5Cl), 2S/(K + Na), and Al/(K + Na).

large surplus of Ca. However, the amount of Ca is significantly larger in the 0−20 wt % sewage sludge range, and this can explain why Ca−S−alkali compounds are susceptible to exist in these mixtures.

It is important to keep in mind that many of these ratios are empirical and that, as such, they are only giving very general indications. As an example, three ratios claiming to assess the corrosion risk, namely, S/Cl, (Al + Si)/(fuel Cl), and 2S/(Na + K), are not yielding the same results for the studied system. According to these ratios, there will be no risk of Cl deposition and corrosion for mixtures containing no more than 60 wt %, no more than 75 wt %, or up to almost 100 wt %, straw, respectively. Hence, no consistent indication is obtained.

It is tempting to compute a myriad of ratios, especially ratios fitting the predicted speciation (with the appropriate stoichiometry) or including Na- and/or K-specific ratios. Various sensitivity studies were performed investigating this (calculated results are not presented here), but it was concluded that this is of limited interest because (1) it might be rather confusing (especially alkali-specific ratios because it is difficult to assess Na and K separately), (2) it would require an *a priori* knowledge of speciation, and (3) general ratios seem sufficient to detect the strongest speciation trends in most cases.

Even though experimental results provide some insight, they are not able to accurately describe and quantify the mechanism(s) of corrosive alkali chloride reduction during sewage sludge co-combustion. Adverbs such as "possibly", "partly",[1] or "most likely"[14] or diffuse terms such as "important", "strong contribution",[2] "one of these ways or a combination of them",[17] or "cannot be ruled out"[13] are used.

However, is there some kind of consensus? Five experimental studies discussing the mechanisms taking place during co-combustion of straw with sewage sludge (and often some wood) have been found (Table 3[1,2,13−15,17−19,25]). These experimental studies usually require extensive and advanced analytical analysis of the flue gas, the fly ash, and the bottom ash to determine the processes at work. The overall results can be summarized as such: (a) Aluminum silicates are capturing a large fraction (difficult to be more precise but most certainly the majority) of the alkali by reaction and/or adsorption. Alkali aluminum silicates will be mainly found in the bottom ash and in coarse particles (above 1 μm). (b) Sulfur may play a role, but no clear experimental proof has been obtained. This may be due to the fact that sulfation might actually take place in a variety of ways, i.e., as a gas phase reaction but also on solid surfaces/particles. (c) Other ash compounds (Ca, P, Fe, and Mg) are most likely involved in retaining alkalis by either reaction or adsorption on particles.

Some excerpts describing the mechanistic insights further are given in Table 3 (together with other studies involving sewage sludge but not straw). The somewhat lengthy (slightly edited) quotes presented in Table 3 convey the difficulty of describing and interpreting experimental results, as well as the uncertainties still existing.

Some important precisions, clarifications, and new conclusions have been obtained by the present analysis concerning the thermodynamically preferred pathways for alkalis speciation when straw is co-combusted with sewage sludge (in comparison to straw combustion). The most valuable result of this study is that the predominant mechanism contributing to the decomposition (or nonformation) of corrosive alkali chlorides will be affected by the concentration of sewage sludge. Because the proportion of sewage sludge may vary with time and space in real systems, so will the alkali chemistry; sulfation will be the main mechanism at low concentrations of additives (below 5 wt %). At higher sewage sludge levels, reaction with aluminosilicates will become the main mechanism. Interestingly, at intermediary levels (above 5 and below 17.5 wt % sewage sludge), K is predicted to form a calcium sulfate compound, confirming that other ash compounds might become involved in alkali chemistry. In real systems, because local concentration conditions may vary, all of these mechanisms will superimpose (i.e., take place simultaneously), effectively blurring any experimental results, especially when comparing different campaigns. This provides a very good explanation for the scattered, sometimes contradictory, and somewhat system-specific results obtained in experimental investigations. The overall makeup of mechanisms involved with a given fuel 1 + fuel 2 in a given plant is not a static one. The complexity of experimental campaigns results in the practical implementation and study of only very few mixtures, something that might explain the fact that the changing nature of alkali chemistry has not been reported or discussed thus far.

As previously mentioned, thermodynamic analysis has known limitations. It cannot provide data about physical processes, such as adsorption, heterogeneous condensation (gas on fly ash), the eroding effect of additional ash particles on deposits, or in-deposit reactions, but the overall trends observed thermodynamically both confirm as well as specify the experimental results (in areas such as Na−K differentiated behaviors) reported in the literature.

Table 3. Co-combustion Experiments Involving Sewage Sludge as Co-fuel: Mechanistic Considerations

reference	mechanistic remarks (no/little experimental basis)	mechanistic insights (on the basis of experimental results)
13[a]	sulfation of KCl cannot be ruled out as a parallel mechanism	Al−Si compounds are important for the capture of K because its removal as cyclone ash is correlated with inflow of Al
14[a]	sewage sludge probably provided ash-forming components, most likely aluminum silicates, iron compounds, and different phosphates, that worked favorably by immobilizing K, Na, and Cl	fly ashes from the combustion of fuel mixes with sewage sludge showed the presence of $KAlSi_3O_8$, $NaAlSi_3O_8$, and zeolite residues; thus, a binding of K in zeolites in combustion is indicated; the exact mechanism is not clear (but a laboratory investigation has been initiated to clarify this) most of the alkali was harder bound after combustion, which suggests that aluminum silicates had captured alkalis
15[a]		both SEM−EDX and XRD analysis confirmed the presence of non-soluble alkali−aluminum silicates, and this indicates that there is a capture of potassium in aluminum silicates in the combustion chamber
1[a]		the beneficial effects are due to partly the content of S in the sewage sludge and partly to the properties of the sewage sludge ash the results suggest that alkali chlorides were removed from the flue gas possibly by reaction with aluminum silicates or by adsorption on the increased amount of particles in the flue gas (crystalline phases containing K in cyclone ashes are identified with XRD)
18[a]		the lowest deposit growth occurred during co-combustion with sewage sludge when alkali reacts with (or is adsorbed by) an aluminum-containing compound, probably forming potassium−aluminum silicates, present as coarse particles
17	there may be at least four reasons for the beneficial impact of the additional fuel: (1) sulfur in the fuel may react with potassium, producing sulfate and gaseous hydrogen chloride, which are less harmful; (2) potassium chloride may be removed by condensation on fly ash particles added with the other fuel; (3) potassium in gaseous form may react with aluminosilicates provided by the additional fuel; and finally, (4) deposits may be mechanically removed by the increased ash flows caused by the additional fuel; in one of these ways or a combination of them, formation of deposits on tubes by KCl could be avoided or alleviated	the present data do not allow for a clear differentiation between the modes of disappearance of deposits; the results, supported by the references quoted, indicate that the reaction with aluminosilicates is the main mechanism
2		the alkali sulfates found in the fine fly ash confirmed the contribution of sulfation to alkali capture; however, the order of the sludges in alkali capture power indicated strong contribution of the aluminum silicate reaction the sludges have different "active" AlSi and S contents
19		results indicate that the effect of digested sewage sludge is connected to the conversion of alkali chlorides to the corresponding sulfates in the flue gas and in the deposits
25		interaction of potassium with Al silicates in the bed is a probable cause for the decrease of potassium in the deposits, while both sulfation of potassium chlorides and possibly also the alkali capture by Al silicates can weaken the deposition of Cl

[a] Involves straw and sewage sludge.

dx.doi.org/10.1021/ef2002475 |Energy Fuels 2011, 25, 3223–3234

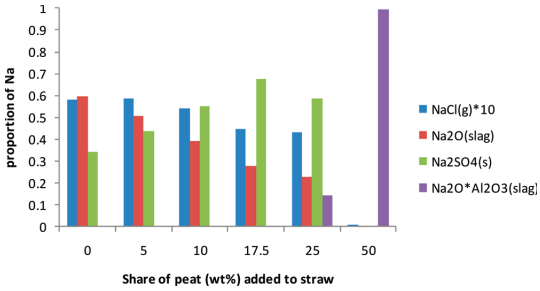

Figure 7. Na relative speciation as a function of the peat addition to straw.

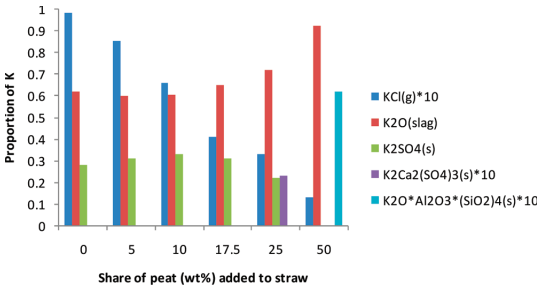

Figure 8. K relative speciation as a function of the peat addition to straw.

Straw + Peat. Peat is predicted to abate the formation of corrosive alkali chlorides during co-combustion with straw but not as efficiently as sewage sludge. Alkali chlorides can almost completely be removed, but this requires very high peat levels.

Na relative speciation in straw combustion is (in order of importance): Na_2O(slag), Na_2SO_4(s), and NaCl(g). Four behaviors have been predicted by thermodynamic equilibrium depending upon the amount of peat added (Figure 7): (1) The proportion of NaCl(g) is not affected at all by a 5 wt % addition of peat. (2) At 10 wt % peat addition, a slight reduction of NaCl(g) is observed; this is due to sulfation only. (3) At 17.5 wt % peat addition, sulfation is still the main mechanism explaining NaCl(g) reduction but $Na_2O \cdot Al_2O_3$(slag) is appearing and represents 0.26% Na. (4) At 25 wt % peat addition, NaCl(g) is further reduced. Two opposite trends are observed: sodium sulfate is still the main Na compound, but its proportion is decreasing (in comparison to 17.5 wt % peat addition but still more than in pure straw or all of the other mixtures), while the proportion of $Na_2O \cdot Al_2O_3$(slag) is increasing to reach 14.2% Na. (5) At 50 wt % peat addition and above, S is no more involved in alkali chemistry because 99.5% Na is predicted to form $Na_2O \cdot Al_2O_3$(slag).

During straw combustion, K is found as (in order of importance): K_2O(slag), K_2SO_4(s), and KCl(g). How is K chemistry affected by increasing peat levels? The calculations predict that (Figure 8): (1) At 5 and 10 wt % peat addition, the formation of sulfates rather than chlorides is slightly promoted in comparison to pure straw combustion. (2) At 17.5 wt % peat addition, the proportion of KCl(g) is decreasing further for the sole benefit of K_2O(slag). (3) At 25 wt % peat addition, the proportion of KCl(g) is decreasing further to the benefit of K_2O(slag) and $K_2Ca_2(SO_4)_3$(s). (4) At 50 wt % peat addition, K_2O(slag) is the predominant K compound, representing about 92.5% K present in the system but $K_2O \cdot Al_2O_3 \cdot (SiO_2)_4$(s) is also appearing (6.2% K). (5) At higher peat level addition (not presented in Figure 8), $K_2O \cdot Al_2O_3 \cdot (SiO_2)_4$ becomes the main K component; more than 83% K is found as aluminosilicates at a 75 wt % peat level.

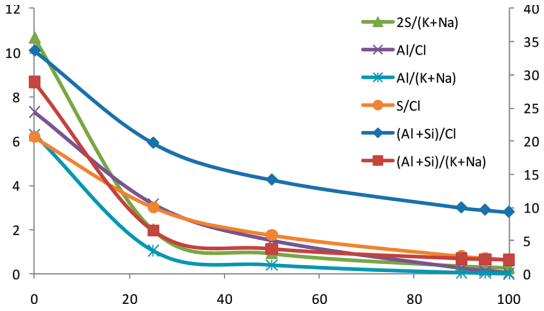

Figure 9. Molar ratios for straw + peat mixtures as a function of the straw proportion in percent (part 1 of 2). Right side *y* axis: (Al + Si)/Cl and (Al + Si)/(K + Na).

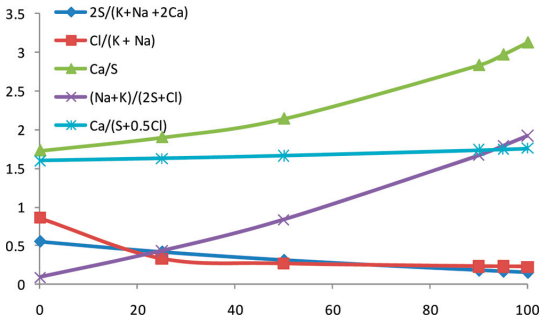

Figure 10. Molar ratios for straw + peat mixtures as a function of the straw proportion in percent (part 2 of 2).

Peat is globally less efficient than sewage sludge; i.e., higher shares of peat are necessary to affect alkali chemistry to the same extent as with sewage sludge.

Thermodynamic analysis provides insight into the different behaviors of Na and K. Such differentiation is difficult to attain experimentally especially in biomass systems, where the Na concentration is much smaller than the K concentration. The main features can be summarized as such: (1) at low peat addition levels, shifts in chemistry for both alkalis are mainly due to increased sulfation; (2) only K forms solid aluminosilicates; (3) Ca is only involved in the capture of K and not Na, but it is impossible to determine whether this is due to a non-affinity with Ca or a lack of it.

Figures 9 and 10 present molar fuel ratios used in the literature. All of the ratios presented in Figure 9 exhibit the same trend: an increase with increasing proportions of peat; this is translating the increasing importance of Al and Si but also S in the system, mainly at the detriment of Cl. Furthermore, in mixtures in which peat represents more than 60−70 wt %, the increasing slopes of the ratios are picking up significantly. This is in accordance with

dx.doi.org/10.1021/ef2002475 |*Energy Fuels* 2011, 25, 3223–3234

Table 4. Co-combustion Experiments Involving Peat as Co-fuel: Mechanistic Considerations

reference	mechanistic remarks (no/little experimental basis)	mechanistic insights (on the basis of experimental results)
23	agglomeration prevention mechanism: sulfur reacts with alkali metals, and the alkali sulfates are either elutriated up from the bed or prevent agglomeration by an increased melting temperature and a lowered viscosity (not proven but could not be excluded)	the mechanism of the agglomeration prevention varied between different peat fuels (SEM−EDS analysis of bed particles); the possible mechanisms are the minerals in the peat fuel retain alkali, which is then either elutriated up from the bed or captured in the bed calcium and other refractory elements increase the melting temperature and, thereby, counteract the melting of alkali; XRD analysis of the cyclone ashes indicted significant amounts of $KAlSi_3O_8$ and $K_2Ca(CO_3)_2$
3		the most likely explanation for the reduced potassium level in the inner layer (of bed particles) is (1) transference of potassium in the gas phase to a less reactive particular form via sorption and/or reaction with peat ash (containing calcium and silicon) and/or (2) formation of solid S-rich compounds when peat with high sulfur content was used; because almost no clay minerals were detected in the peat, the removal of potassium in the gas phase via sorption and reaction with clay minerals to less problematic potassium aluminosilicates were considered to be of less importance; aluminum, originally bound to humic substances in the peat, may possibly react with potassium to form potassium aluminates; however, this needs to be further investigated the effects on particle and deposit formation during co-combustion were reduced amounts of fine particles and an increased number of coarse particles; the mechanisms for the positive effects were a transfer and/or removal of potassium in the gas phase to a less reactive particular form via sorption and/or a reaction with the reactive peat ash (SiO_2 and CaO), which in most cases formed larger particles (>1 μm) containing calcium silicon and potassium the fact that there was no difference in the composition of crystalline phases (in coarse and fine particles) in combusted forest residue alone and when peat was added may be explained with the fact that the addition of peat did not change the particle formation chemistry but instead changed the amount of released/volatilized compounds during combustion in the fluidized bed when peat was added, the amount of calcium sulfate in the (coarse) particles generally increased and potassium chloride decreased, all according to XRD measurements; the addition of peat generally increased the fraction of silicon and iron in the particles and decreased the level of chlorine, sodium, phosphorus, and manganese coarse particle composition: quartz (dominant), potassium chloride, calcium sulfate, calcium carbonate/oxide, feldspars (microcline and albite), maghemite (Fe_2O_3), merwinite [$Ca_3Mg(SiO_4)_2$], biotite [$KMg_3-(Si_3Al)O_{10}(OH)_2$], and apatite fine particle composition: KCl and $K_2SO_4/K_3Na(SO_4)_2$; the crystalline fraction in the fine particles did not exhibit any significant differences when peat was added to the fuel
20	plausible processes: in-deposit reactions (no detail), erosion by peat ash and solid−gas sulfation	gas-phase sulfation not important
26[a]	possible alternative effects (to the interaction of Cl and S): Si−Al compounds and peat ash erosion effect	for peat−straw mixtures, it was concluded that the deposition behavior is governed by other mechanisms than the interaction of Cl and S

[a] Involves straw and peat.

the predicted results, indicating that it is not before above about 70 wt % peat addition that Al and Si are clearly dominating alkali chemistry.

Figure 10 does bring further insight into the systems studied; Ca is always in excess compared to S, indicating low SO_2 emissions but also explaining, at least partly, why sulfates never react with more than about a third of the alkalis.

As discussed earlier, alkali-specific ratios and ratios adapted to the predicted products could be employed but do not bring further insight in the present cases because strong elemental trends appear clearly.

When it comes to further discussing the actual mechanisms taking place by combining thermodynamic equilibrium and experimental campaigns, the main obstacle is that only one study

co-firing peat with straw (discussing deposition) was found.[26] Table 4[3,20,23,26] presents this study as well as experimental investigations involving three biomasses co-fired with peat: bark from pine and spruce from a sawmill, branches and tree tops from a young population of Norwegian spruce, and finally, bark together with cardboard (a high Cl-containing fuel). The mechanistic insights provided by the experiments involving straw and peat seem to indicate that the predominant mechanism preventing the formation of corrosive alkali chlorides is not involving S. The alternative processes mentioned are Al−Si compounds, but other elements should not be completely left out, as suggested by the other studies (not involving straw); for example, analysis of ashes shows that alkalis may react with or be adsorbed on so-called "reactive peat ash" (no clear explanation of the term "reactive" is given), with SiO_2 and CaO being mentioned.[3] Furthermore, the mechanisms affecting alkali chloride formation may depend upon the peat used because different peats will have significantly different elemental compositions and modes of occurrence for key elements; high available (i.e., available for reaction) S levels (compared to aluminosilicates) mean that sulfation of alkali chlorides will be the mechanism of predilection, while aluminum silicates will take over in the opposite case. However, the location where sulfation is taking place (gas-phase reaction, particle−gas reaction, or in-deposit sulfation) is not clear. The fundamental trends predicted by thermodynamic equilibrium clarify some of the aforementioned points; the predominant mechanism affecting alkali chemistry will depend upon the addition ratio of peat. Alkali chloride reduction can be attributed to the single or combined effect of S and aluminosilicates with the contribution from other ash compounds, with the importance of Ca being clearly predicted.

CONCLUSION

The thermodynamic analysis carried out in this study focuses on biomass mixtures to reduce the formation of corrosive alkali chlorides during straw combustion. The investigated aspects are (1) the reduction ability of peat and sewage sludge and (2) the elucidation of the mechanism(s) taking place.

The calculations confirm the corrosive alkali chloride reduction abilities of both biomass fuels as reported in the literature but also provide further information especially concerning threshold values (addition levels at which virtually no corrosion is predicted to happen): straw with 25 wt % sewage sludge or with 75 wt % peat. If straw is to be the main fuel, the 75 wt % value for peat is not realistic, but if peat is the main fuel, it can be said that 25 wt % straw can be co-combusted without the arising of a significant amount of corrosive alkali chlorides. Experimental campaigns usually include no more than two−three mixtures, and therefore, no accurate threshold value can be proposed.

The calculations also provide further insight into the mechanisms responsible for the disappearance of alkali chlorides. The main mechanisms that can potentially take place are known, but several key points remain unclear, including the predominant mechanism(s) in a given system, the importance of operation parameters (fuel mix composition, excess air ratio, and temperature), the exact mode(s) of a given reaction (gas−gas reaction, gas−solid reaction, etc.), the individual behaviors of Na and K, and the importance of physical processes (adsorption, erosion, etc.). The present calculations cast light on several of these aspects, with the main one being that the calculations indicate that the chemical elements preventing the formation of corrosive alkali chlorides vary with the additional fuel (here, peat or sewage sludge) concentration present in the system, an important fact never mentioned in the literature to our knowledge. It is believed to be due to the intertwined and nonlinear effects of thermodynamic properties and relative amounts of key chemical elements. Attempts were made to use fuel molar ratios to further discuss these effects, but the complexity of the systems makes it difficult to draw clearer conclusions. However, the practical implications of such a result are crucial; it is likely that, in a real system, local elemental concentrations (together with operating parameters, such as temperature and air ratio) will vary with time and space because of fuel and (fuel and air) distribution heterogeneities. This means that several mechanisms will simultaneously be responsible for eliminating corrosive alkali chlorides but also that the overall picture is not a static one. This may explain the enduring fact that most of the available experimental results are confusing, contradictory, and installation-specific.

The chemical elements reacting with alkalis during co-combustion of straw with sewage sludge or peat are predicted to be S, Ca−S, or Al−Si. The predicted compounds have been reported in the literature, bringing further weight to the additional knowledge attained by thermodynamic analysis. The fact that some reactions are deemed impossible thermodynamically may indicate that the involved chemical compounds are only interacting with alkalis through adsorption, a physical process that cannot be studied by thermodynamic analysis. Combining experimental and modeling results leads to a more accurate and complete picture of the situation.

Pb and Zn chlorides do not exhibit the same trends as alkali chlorides because they are predicted to be found in higher concentrations in most mixtures compared to pure fuels.

Further work should focus on the influence of operating parameters, especially the influence of temperature, air ratio, and modes of occurrence of key elements.

AUTHOR INFORMATION

Corresponding Author

*Telephone: (+47) 73-59-29-11. Fax: (+47) 73-59-28-89. E-mail: michael.becidan@sintef.no.

ACKNOWLEDGMENT

This work is part of the KRAV Project (Enabling Small-Scale Biomass CHP in Norway) supported by the Research Council of Norway. The financial support of the Bioenergy Innovation Centre (CenBio) is also acknowledged. The authors also thank BIOENERGY 2020+, Austria, and DTU, Denmark, for providing fuels and related fuel data through the SciToBiCom ERA-net. The first author wishes to thank Daniel Lindberg (Åbo Akademi, Finland) for the valuable input concerning the thermodynamic database.

REFERENCES

(1) Elled, A. L.; Davidsson, K. O.; Amand, L. E. Sewage sludge as a deposit inhibitor when co-fired with high potassium fuels. *Biomass Bioenergy* **2010**, *34* (11), 1546–1554.

(2) Aho, M.; Yrjas, P.; Taipale, R.; Hupa, M.; Silvennoinen, J. Reduction of superheater corrosion by co-firing risky biomass with sewage sludge. *Fuel* **2010**, *89* (9), 2376–2386.

(3) Pommer, L.; Ohman, M.; Bostrom, D.; Burvall, J.; Backman, R.; Olofsson, I.; Nordin, A. Mechanisms behind the positive effects on bed

agglomeration and deposit formation combusting forest residue with peat additives in fluidized beds. *Energy Fuels* **2009**, *23*, 4245–4253.

(4) Pettersson, A. Characterisation of fuels and fly ashes from co-combustion of biofuels and waste fuels in a fluidised bed boiler—A phosphorus and alkali perspective. Doctoral Thesis, Chalmers University of Technology, Göteborg, Sweden, 2008.

(5) The Danish Ministry of Food, Agriculture and Fisheries. *Fuelling Future Energy Needs—The Agricultural Contribution*; The Danish Ministry of Food, Agriculture and Fisheries: Copenhagen, Denmark, 2008.

(6) Bernhard, P.; Bugge, L. *Biomasse—Nok til alle gode formål?*; Kanenergi: Sandvika, Norway, 2007.

(7) Climate and Pollution Agency. www.miljostatus.no.

(8) Berge, G.; Mellem, K. B. *Kommunale avløp—Ressursinnsats, utslipp, rensing og slamdisponering 2008. Gebyrer 2009*; Statistics Norway: Oslo, Norway, 2009; 2009/49.

(9) Nedland, K. T. *Statusrapport for bruk av avløpsslam—Endringer siden år 2000*; Aquateam, Norsk Vannteknologisk Senter A/S: Oslo, Norway, 2005; 05-029.

(10) Ukeblad, T. *Alt om energi fra TU.no*; http://energilink.tu.no/no.

(11) Uhlig, C.; Fjelldal, E. Torv til strø og talle i Nord-Norge. *Grønn Kunnskap e*; Planteforsk: Lofthus, Norway, 2005; Vol. 9, pp 1−56.

(12) Strömberg, B. *Bränslehandboken - Handbook of Fuels*; Värmeforsk Service AB: Stockholm, Sweden, 2005.

(13) Davidsson, K. O.; Amand, L. E.; Elled, A. L.; Leckner, B. Effect of cofiring coal and biofuel with sewage sludge on alkali problems in a circulating fluidized bed boiler. *Energy Fuels* **2007**, *21* (6), 3180–3188.

(14) Pettersson, A.; Zevenhoven, M.; Steenari, B. M.; Amand, L. E. Application of chemical fractionation methods for characterisation of biofuels, waste derived fuels and CFB co-combustion fly ashes. *Fuel* **2008**, *87* (15−16), 3183–3193.

(15) Pettersson, A.; Amand, L. E.; Steenari, B. M. Chemical fractionation for the characterisation of fly ashes from co-combustion of biofuels using different methods for alkali reduction. *Fuel* **2009**, *88* (9), 1758–1772.

(16) Amand, L. E.; Leckner, B. Metal emissions from co-combustion of sewage sludge and coal/wood in fluidized bed. *Fuel* **2004**, *83* (13), 1803–1821.

(17) Amand, L. E.; Leckner, B.; Eskilsson, D.; Tullin, C. Deposits on heat transfer tubes during co-combustion of biofuels and sewage sludge. *Fuel* **2006**, *85* (10−11), 1313–1322.

(18) Johansson, L. S.; Leckner, B.; Tullin, C.; Amand, L. E.; Davidsson, K. Properties of particles in the fly ash of a biofuel-fired circulating fluidized bed (CFB) boiler. *Energy Fuels* **2008**, *22* (5), 3005–3015.

(19) Pettersson, J. Evaluation of different fuel additives' ability to master corrosion and deposition on steam superheaters in a waste fired CFB-boiler. *Consortium Materials Technology for Development and Demonstration of Thermal Energy Processes, KME*; Elforsk AB: Stockholm, Sweden, 2009; KME-411.

(20) Kassman, H.; Broström, M.; Berg, M.; Åmand, L.-E. Measures to reduce chlorine in deposits: Application in a large-scale circulating fluidised bed boiler firing biomass. *Fuel* **2011**, *90* (4), 1325–1334.

(21) Steenari, B. M.; Lindqvist, O. Fly ash characteristics in co-combustion of wood with coal, oil or peat. *Fuel* **1999**, *78* (4), 479–488.

(22) Tissari, J.; Sippula, O.; Kouki, J.; Vuorio, K.; Jokiniemi, J. Fine particle and gas emissions from the combustion of agricultural fuels fired in a 20 kW burner. *Energy Fuels* **2008**, *22* (3), 2033–2042.

(23) Lundholm, K.; Nordin, A.; Ohman, M.; Bostrom, D. Reduced bed agglomeration by co-combustion biomass with peat fuels in a fluidized bed. *Energy Fuels* **2005**, *19* (6), 2273–2278.

(24) Khalil, R. A.; Houshfar, E; Musinguzi, W.; Becidan, M.; Skreiberg, Ø.; Goile, F.; Løvås, T.; Sørum, L. Experimental investigation on corrosion abatement in straw combustion by fuel mixing. *Energy Fuels* **2011**10.1021/ef200232r.

(25) Yrjas, P.; Aho, M.; Zevenhoven, M.; Taipale, R.; Silvennoinen, J.; Hupa, M. Co-firing of sewage sludge with bark in a bench-scale bubbling fluidized bed—A study of deposits and emissions. *Proceedings of the 20th International Conference on Fluidized Bed Combustion*; Xi'an, China, 2009; pp 922−929.

(26) Theis, M.; Skrifvars, B. J.; Zevenhoven, M.; Hupa, M.; Tran, H. H. Fouling tendency of ash resulting from burning mixtures of biofuels. Part 2: Deposit chemistry. *Fuel* **2006**, *85* (14−15), 1992–2001.